Modelling the dryland agricultural systems of Q'a Shubayqa, Jordan

Ali Ben Mustapha

Thesis submitted to the University of Nottingham for the degree of

Doctor of Philosophy

April 2025

School of Geography

University of Nottingham

Abstract

This project investigates a rainfed agricultural system in the drylands of north-eastern Jordan. The study area, Q'a Shubayqa, is characterized by very low rainfall rates but supports a cereal-based mono-cropping system. Local farmers were surveyed to define the main components of the agricultural system and its limiting factors. Farmers confirmed that system productivity has been affected by climate change and severe weather events during the last three decades. Results of the farmer survey and remote sensing and climate data analyses have shown that growth and development of cultivated wheat and barley crops in Q'a Shubayqa mainly depend on seasonal flash-floods that occurs following winter rainfall in the south-western highlands of Syria. Hydrological SWAT modelling of the study area watershed, undertaken for a long-term period to quantify flood water has shown unstable patterns in terms of quantity and timing which would affect cereal planting dates. Historical grain yield simulations using genetic coefficients of the studied cultivars, that were derived in this study from observed data collected from different environments across Jordan and over different seasons, have shown that planting date is a limiting factor for both crop types. Using these DSATT models the impact of different climate change scenarios

through to 2100, on grain yield and grain filling period was investigated. Most of studied cultivars were sensitive to future climate change where grain yields decreased, and grain filling period reduced. The effect of high atmospheric CO_2 levels on grain yield was limited with a slight increasing but gain yield still below the grain yield baseline. The impacts of additional agricultural practices were evaluated when simulating grain yield under future climate change considering high atmospheric CO_2 levels and results showed that delayed planting date has decreased grain yield, however organic amendment positively affected grain production. Results suggest that wheat cultivar Hourani and barley cultivar Rum are less affected by climate change.

Acknowledgements

I would like to thank and express my sincere gratitude to my supervisors Professor Matthew Jones and Professor Sarah Metcalfe for their guidance, support, constructive feedback, encouragement, and outstanding academic support throughout the development of this thesis. My supervisors were always ready to provide advice and help. In addition, they supported me when I was facing critical personal challenges, they were very understanding. I was lucky to be supervised by these two distinguished scholars and I felt honoured that I was able to acquire knowledge under their supervision. I would like also to thank Dr Stephen Ramsden for being my 3rd supervisor during the early stage of the PhD.

I would like also to thank all the PalaeoRAS project team and the School of Geography staff for being very cooperative and for providing a convenient work environment. Special thanks to my collaborators in Jordan Dr Khaled Al-Masaeed and Dr Ahmad Al-Shdaifat. Many thanks for Dr. Ayed Al-Abdallat and Dr Faddel Ismail for being very supportive and for their collaboration.

Special thanks to my uncle who passed away last year, Professor Habib Ouerdiane, for inspiring and encouraging me. I would like to express my deep appreciation and love to my wife and my kids, Nour Ghalia and Haydar, for being with me during the hard times and for their patience. Finally, I would like to thank my mother and my father for supporting me all the time.

Contents

List of abbreviations

SDGs: sustainable development Goals

UN: United Nations

UNCCD: United Nations Convention to Combat Desertification

FAO: Food and Agriculture Organization

UNEP: United Nations Environment Programme

AI: Aridity Index

CPFR: Center for People, Food and Environment

mm/yr: millimetre/ year

m^3/yr: cubic metre/year

MENA: Middle East and North Africa

NDVI: Normalized Difference Vegetation Index

ICCD: Impact of Climate Change on Dryland project

WANA: West Asia and north Africa regions

FAOSTAT: Statistics Division of Food and Agriculture Organization

Yp: Potential yield

Yw: water-limited potential yield

Ya: actual farmers' yield

CO_2: Carbon dioxide

IT: Information Technology

ha: hectare

IFPO: French Institute of the Near East

Km: Kilometre

Km^2: Kilometre square

MWI: Ministry of Water and Irrigation

USDA: United States Department of Agriculture

Myr: Million year

DSJ: Department of Statistics in Jordan

MoA: Ministry of Agriculture

ACSAD: Arab Centre for Agricultural Research in Dry Lands

ICARDA: International Centre for Agricultural Research in the Dry Areas

Mm^3/yr: Million cubic meter/year

JMD: Jordanian Meteorological Department

MoEnv: Ministry of Environment

OAGCMs: Ocean-Atmosphere General Circulation Models

m: meter

km: kilometre

$CaCO_3$: Calcium carbonate

IWMI: International Water Management Institute

U.S $: United State Dollar

BP: Before Present

CHN elemental analyser: Carbon, Hydrogen and Nitrogen elemental analyser

EDTA: Ethylenediamine tetra-acetic Acid

SOM: Soil Organic Matter

mg/l: milligrams per litre

NARC: National Agricultural Research Centre (Jordan)

CCI: World Meteorological Organisation Commission on Climatology

CLIVAR: Climate Variability and Prediction

ETCCDI: Expert Team on Climate Change Detection and Indices

L5: Landsat 5

L8: Landsat 8

NDWI: The Normalized Difference Water Index

NIR: near-infrared spectrum

VIS: visible spectrum

GEE: Google Earth Engine

SWIR: short-wave infrared

m^3: cubic metre

R.S: Remote sensing

DSSAT: decision support system for agrotechnology transfer

ASL: Above See Level

DEFRA: Department for Environment, Food & Rural Affairs

GPS: Global Positioning System

AVHRR: Advanced Very High Resolution Radiometer

TIR: Thermal infrared

VNIR: Visible Near-infrared

CFMASK: Cloud Function Mask

LaSRC: Land Surface Reflectance Code

ECMWF: European Centre for Medium-Range Weather Forecasts

SWAT: Soil and Water Assessment Tool

AET: Actual Evapotranspiration

USDA-NRCS: USDA-Natural Resources Conservation Service

ICRISAT: International Crops Research Institute for the Semi-Arid Tropics

MDS: Minimum Data Set

CSM: Crop Simulation Model

UNFCCC: United Nations Framework Convention on Climate Change

CIMMYT: International Maize and Wheat Improvement centre

RMSE: Root mean square error

RMSEn: normalized Root mean square error

IPCC: Intergovernmental Panel on Climate Change

CMIP5: Coupled Model Intercomparison Project Phase 5

RCP: Representative Concentration Pathway

APSIM: Agricultural Production Systems sIMulator

Statement of the impact of COVID-19

Due to the COVID pandemic and international travel restrictions, field work for this project was postponed twice and the data collection processes were delayed. Given this, the initial plan was to work with in-country collaborators, to conduct the survey and collect data on my behalf, but the impact of COVID lockdowns within Jordan was also significant. People were not at work, which limited their access to information and there were restrictions on internal travel.

A decision was therefore made to focus on undertaking remote sensing dataset analyses and hydrological modelling as alternative approaches to defining the components of the agricultural system, its limiting factors, and to evaluate the impact of climate change on the agricultural cycle and crop production in Q'a Shubayqa. The focus has been on estimating and quantifying the main limiting component of the farming system, the water resource (water streamflow/floods).

Chapter 1: Research and Thesis Overview

1.1. Introduction

In 2015 all United Nations Member States adopted the 2030 Agenda for Sustainable Development, which includes 17 sustainable development Goals (SDGs) considered as an urgent call for action by all countries (developed and developing) in a global partnership. Among these goals we find the most important and difficult challenges faced by mankind, including Zero Hunger (goal 2) which involves promoting sustainable agriculture, supporting small scale farmers, and equal access to land, technology and markets as well as investment in infrastructure and technology to improve agricultural productivity (UN, 2015). Achieving this vital goal requires the global food system to deliver a nutritious diet for all Earth's population and should be based on sustainable food production systems that provide livelihoods for the farmers we rely on to produce our food while sustaining and building a resilient agroecosystem. The main two obstacles facing the achievement of the Zero Hunger goal are global population growth and climate change impacts on agriculture (food production) (Okello et al., 2021).

The most recent revision of the world population prospects conducted by the United Nations (2022) indicates that population on the planet will reach 9.7 billion by 2050 and the highest increases are estimated to be recorded in Sub-Saharan Africa, central and southern Asia, and eastern and south-eastern Asia. Most of these regions are developing countries with large expanses of drylands. The inhabitants of these areas are often rural communities of smallholder farmers mainly depending on their own land for food production. They are often considered vulnerable communities because of the relatively harsh climate conditions in these drylands, leading to uncertainty in cropping system productivity (Ahmed et al., 2022). Despite this, so-called drylands contain 44% of the world's croplands and 50% of world's livestock (UNCCD, 2011). These statistics, combined with the typical dryland farming practices, are evidence that smallholder farmers are capable of building sustainable, resilient agroecosystems and are able to adapt their agricultural management practices to environmental changes. However, the sustainability of these systems is at risk with population growth and climate change (Ahmed et al., 2022; FAO, 2011) putting more pressures on these systems.

Climate change is geographically heterogeneous and, as a result, creating adaptation approaches based on considering the specificity and the complexity of each individual system

is needed. The study area of this research, Q'a Shubayqa, is located in the northeast of Jordan ,within the Fertile crescent zone (Figure 1.1), where people have been practising dryland agriculture for thousands of years (Arranz-Otaegui et al., 2018; M. D. Jones et al., 2019). Q'a Shubayqa is a flat playa or dry lake, cut by several meandering wadi channels that brings flood water to the q'a from the Jabal Druz mountain in south Syria. The farming system productivity in this area mainly depends on these floods, that usually occur several times during the cropping season provide plant water needs by submerging cultivated lands. Climate change and alterations of weather patterns in Q'a Shubayqa and its surrounding area during the last decades have resulted in a dramatic decline in crop production, by affecting the environmental limiting factors of crop growth. Future climate change impact could be catastrophic especially for such vulnerable farming system located in fragile dryland areas (Ahmed et al., 2022).

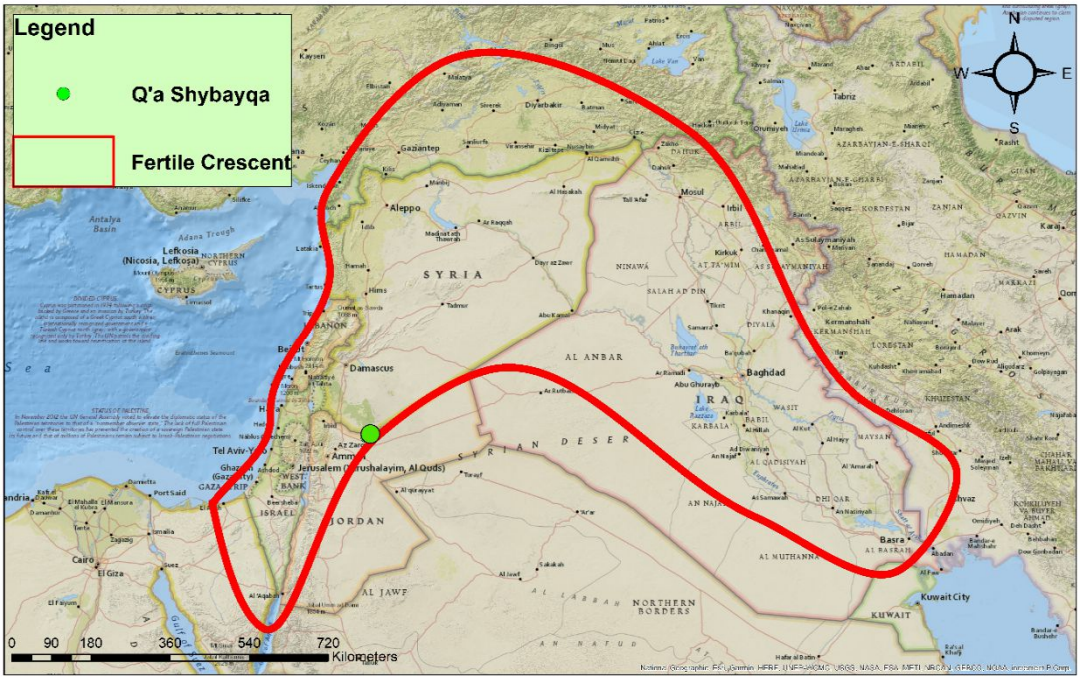

Figure 1.1: The study area location within the Fertile crescent

1.2. Thesis overview

Given the above this thesis aims to represent an overview about how climate change will affect Q'a Shubayqa agricultural system and its sustainability factors by undertaking a series of objectives, which build on each other, through the thesis chapters:

- Exploring the characteristics and specificities of the farming system in Q'a Shubayqa by defining its main components and limiting environmental factors (Chapter 3).
- Investigating historical climate change in Q'a Shubayqa and its impact on crop health (Chapter 4 and Chapter 5).
- Defining the main source(s) of water of the Shubayqa cropping system and understanding the specificities of the relevant hydrological system(s) (Chapter 5 and Chapter 6).
- Estimating traits and characteristics of the cultivated cereal genotypes in Q'a Shubayqa (Chapter 7)
- Evaluating the impact of historical and future climate change on crop yield in Shubayqa and if farming mitigation practices could reduce the potential negative impact of future climate change (Chapter 8).

Figure 1.2 represents the approaches and the relationship between models employed in this research. The following chapter (Chapter 2) provides some broader context for this work.

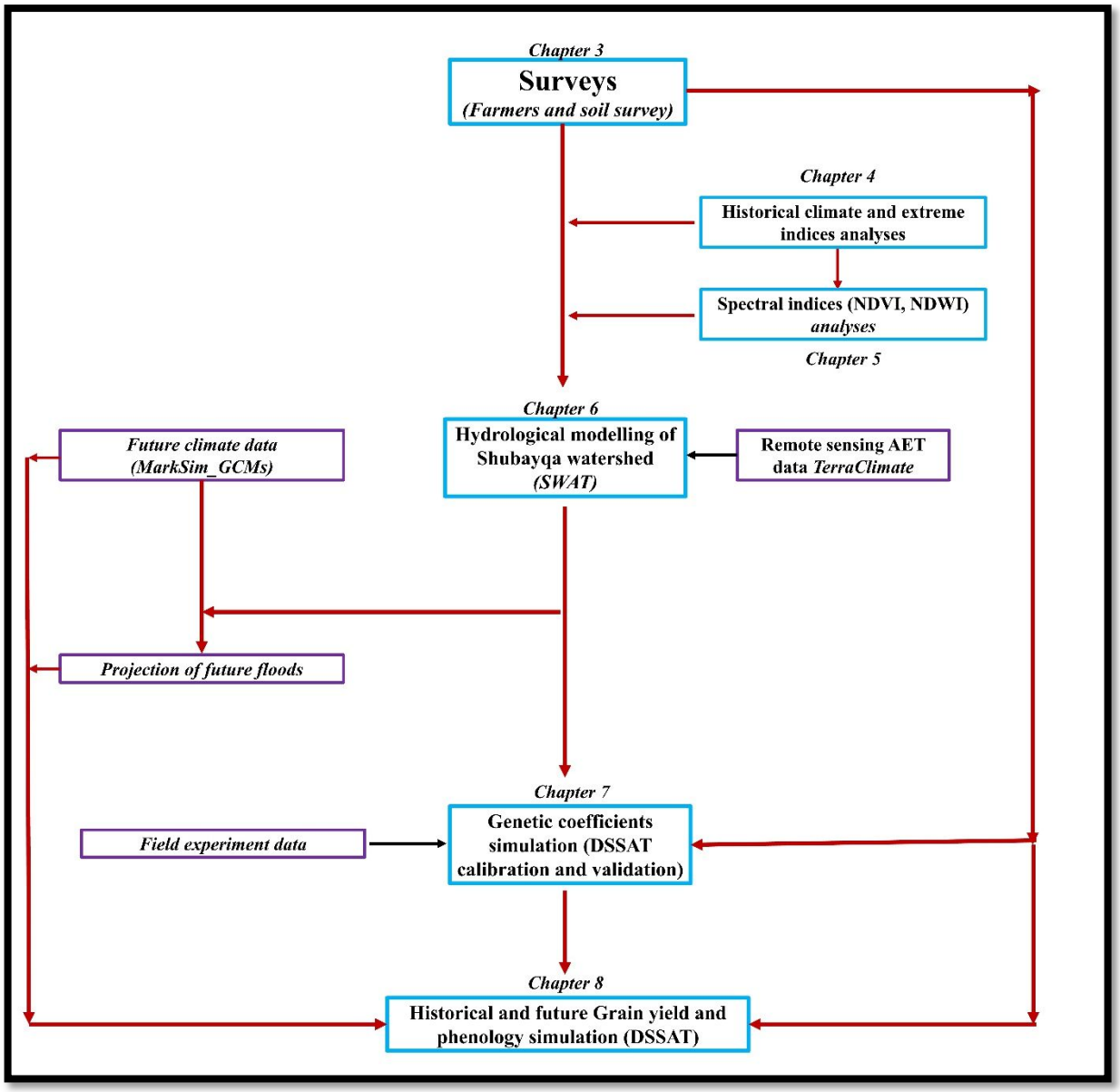

Figure 1.2: Schematic of the logic of the approach and the relationships among the models used in this research

Chapter 2: Drylands: environmental and agricultural specificities

2.1. Introduction

The defining characteristic of drylands is aridity, or water deficit. According to the United Nations Environment Programme (UNEP), dryland classifications are based on the aridity index (AI), which is the ratio between annual average precipitation and potential evapotranspiration, where drylands are areas with an AI of less than 0.65 and annual mean potential evapotranspiration is at least ~1.5 greater than annual mean precipitation. Drylands are found in most of the world's biomes and climatic areas and constitute 45% of the global land area (Figure 2.1). These are distributed over the west, east and southern Africa, Mediterranean coasts, south and southwestern Asia, western south America and most of Australia, and are inhabited by 2.1 billion people (UNCCD, 2011).

Drylands are divided, according to aridity level, into four classes (Safriel et al., 2005): 1) Dry sub-humid lands (18% of world's land surface) with a value between 0.5<AI<0.65, often naturally dominated by broad leaved savannah woodlands, tree canopies or covered by perennial grasses; 2) Semi-arid areas with AI between 0.2<AI<0.5 covering 20% of the land surface: 3) Arid lands that account for 7% of total world's land have an AI between 0.05<AI<0.2 and support minimal vegetation; 4) Hyper-arid lands with AI<0.05, considered as true desert, with no potential for agricultural production except where irrigation water is available.

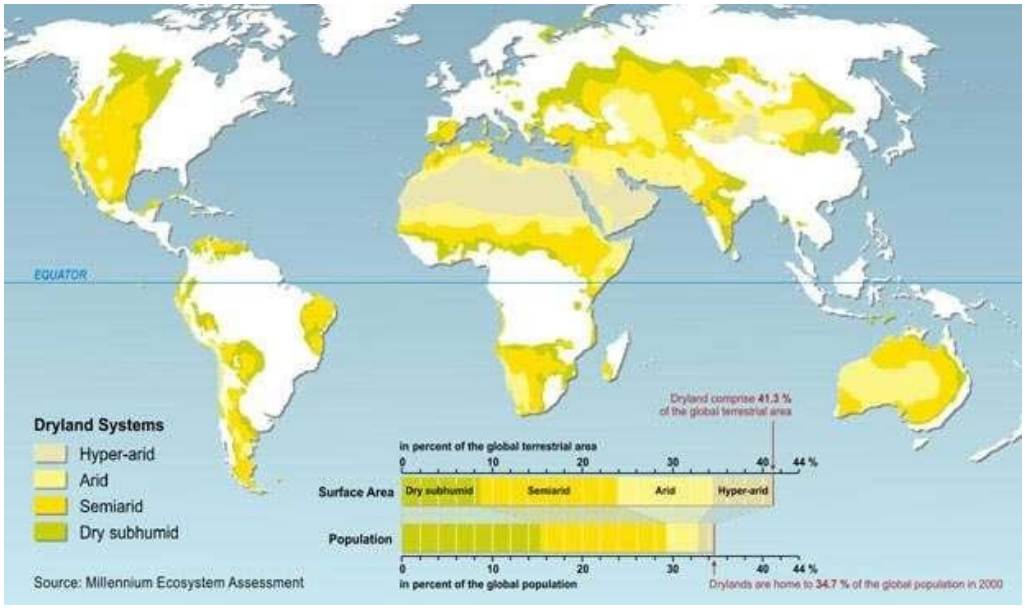

Figure 2.1: Global dryland distribution (Metternicht et al., 2015)

2.2. Dry land characteristics, importance and current issues

2.2.1. Overview

Rangelands and croplands jointly occupy around 90% of dryland areas and are often overlapping, producing an integrated agropastoral livelihood which provides much of the world's grain and livestock (UNCCD, 2011a). Drylands include some of the most productive areas, but also some of the most fragile, because of unstable conditions which can result in dramatic changes in ecology and subsequently in human well-being (UNCCD, 2011a). In addition, ecosystems in drylands are a major factor in global biophysical processes such as reflecting and absorbing solar radiation and maintaining the balance of atmospheric constituents (Folliott et al., 2002), besides their important role in minimising climate change through carbon storage in soils (Conant et al., 2001). Dryland soil organic reserves represent 27% of the global total (Safriel et al., 2005).

2.2.2. Climate

Drylands are characterised by high summer temperatures, high solar radiation intensity, due to the absence of clouds for over 70% of the year (Laity, 2009), low relative humidity rates, high interannual precipitation variability and high evapotranspiration rates. 50 to 100% of the yearly total precipitation amount in drylands falls at one time during the year, often as convective storms (Salameh and Bannayan, 1993). These large rainstorms cannot be absorbed because of abiotic factors including frequent Aridisols and Alfisols soil classes in dryland environments (CPFR, 1991), so water is often lost as runoff (Brooks et al., 2012). Otherwise, water from rainfall of low intensity is lost through evaporation, where 90% of the rainfall in such areas evaporates back into the atmosphere (Molden et al., 2007).

These climatic factors directly affect drylands characteristics and have shaped their ecosystems and biodiversity (Davies et al., 2016; UNCCD, 1994). In Jordan, recorded meteorological data over three decades (1985-2020) have shown that precipitation varies from less than 50 mm/yr in the south-eastern desert area of the country, to more than 650 mm/yr in the highlands and northern mountains (Chapter 3). This large difference, and resulting environmental gradients, is a common situation in drylands.

2.2.3. Geomorphology

The geomorphology of drylands is highly variable, but the main types of Earth's dryland geomorphology are:

Mountain-Basin regions where bedrock is exposed and having a high relative relief controlled by geology,

Piedmonts that are transitional areas between the uplands and lowlands where landforms including alluvial fans and pediments exist.

Stony deserts which have a low relative relief and structural plateaux with plains covered by stones. These are vegetation-free areas with a high density of coarse particles at the surface overlying a finer soil. Such geomorphology is found in the north basalt plateaux in Jordan (Bullard, 2005).

The fourth type mainly contain floodplains, dry lake basins and ephemeral rivers, these areas are often dry but during high intensity occasional rainfall storms of short duration, they can be inundated by large flows of water and sediments. These floods may be generated within the dryland (endogenic drainage) or from precipitation outside this dryland (allogenic drainage) but flow into it, such as in the study site of Q'a Shubayqa.

The final main type are sandy deserts, which comprise expansive areas with or without dune forms (Bullard, 2005), the former driven by typically windy conditions, that can also lead to frequent dust storms.

2.2.4. Biodiversity

Biodiversity in drylands is globally important, including the source plants (wild relatives) of many of our most important food crops, such as wheat, barley, coffee, olives, and many fruit trees (Gallagher et al., 2013). The role of biodiversity in the provision of dryland ecosystem services is evident in the numerous dryland plant species of different growth forms which jointly provide services through their ground cover and structure by enhancing water regulation and soil conservation (soil crusts which consists of an assemblage of several species of cyanobacteria responsible of nitrogen fixation, fungi, lichens and mosses) as well as forage and fuelwood provision (African Acacia) and climate regulation (Shachak and Pickett, 1997).

However, this dryland biodiversity is highly threatened by not only land degradation, but also by invasive foreign species, poaching and illegal trade of biodiversity products that generate habitat loss, fragmentation and competition between local and alien species. These threats may cause losses of the dryland's specific keystone species (Paine, 1966) and ecosystem engineer species which modify the dryland environment for the benefit of other species (Jones et al., 1994).

2.2.5. Soil characteristics

Soils in drylands, are diverse in their structure and physiochemical properties but in general they are mostly Aridisols and Entisols, but other soils include Alfisols, Mollisols and Vertisols (Dregne, 1976). Whatever their type, soils are a basic resource of drylands as they provide the medium in which plants grow, and their properties, such as texture and water holding capacity, determine the proportion of rainfall available to plant growth. The specificity of these soils is illustrated in their soil ecosystems and their species that have developed specialised and resilient interactions in response to the harsh conditions. For example, termites play a vital role in savannas in recycling organic matter and maintaining soil porosity, particularly in the driest and poorest soils where vegetation grows more vigorously and is more drought resistant around termite mounds (Black and Okwakol, 1997).

Dryland soils are facing a range of important management challenges that are amplifying consequences of the dry conditions, including crusting and compaction, restricted soil drainage, wind and water erosion, low fertility levels and shallow soils that are stony, saline or sodic (Dregne, 2002).

2.2.6. Water resources and management challenges

The total renewable water supply from dryland groundwater resources is estimated to constitute around 8% of the global renewable water supply (about 3.2 trillion m^3/yr) (Vörösmarty et al., 2005). Almost one third of the global population depend on this 8% of the world's renewable water resources, per capita availability in drylands is just 3.6 litres/person/day, substantially lower than 50 litres/person/day regarded as a minimum by the FAO (FAO, 1993).

However, many of these drylands water resources are under pressure (overexploitation). According to World Bank (2018) statistics, the most water poor countries are located in the Middle East and the Mediterranean (MENA area) where 6 % of the world's population live

and this region holds only 1% of the earth total renewable freshwater resources. The water crisis in these countries is not only a hydrological management issue, it extends beyond that to be a serious challenge and critical national security situation (Cudennec et al., 2007). Besides that, socio-economic status is challenging since these regions are often characterised by poverty, poor agricultural production, weak governance, very limited or unavailable data, difficulties of changing behaviours toward the environment and in several cases, local and regional conflicts (Schwilch et al., 2014).

In many dryland regions, important reservoirs of fossil groundwater, groundwater that has remained in an aquifer for millennia (Foster and Loucks, 2006), are used by human populations. Extraction of fossil ground water is often called mining because it's a non-renewable resource. For example, in India 15% of food supply is produced by mining groundwater (Brown, 2008).

Water resources that are available to employ in many dryland regions are renewable but are frequently used at rates that exceed the recharge rate which in turn leads to salinity and mineralisation of these resources (Koohafkan, 2012).

2.2.7. Potential threats

Following the poor management practices and the overexploitation of natural resources in drylands for long decades, together with fragile conditions and the absence of ecosystem preservation measures, land degradation has become the main threat to dryland sustainability, and it is getting more serious and harder to reverse and can progress in some cases into desertification and ecological collapse (Dregne, 2002). Land degradation can disrupt water cycles and diminish water quality through the siltation of rivers and reservoirs. Degraded landscapes are also prone to flooding as rainwater runs off rather than soaking into the soil, increasing the loss of topsoil and biodiversity (Palmer and Bennett, 2013). FAO (2000) defined land degradation as the loss of production capacity and defined desertification as land degradation in drylands caused by climate variability and human interventions. Currently, several developing countries like sub-Saharan and south Mediterranean countries are expressing their concerns about the closely related challenges of desertification, land degradation and drought and their impact on migration, conflict and overall human security (UNCCD, 2012). Reynolds et al. (2007) have estimated that there was severe degradation on approximately 10-20% of drylands and another recent study of 25 year trends, using remote sensing to measure inter-annual vegetation index NDVI, found that land degradation hotspots

covering about 29% of global land area with dryland dominated biomes affected to an above average extent (Le et al., 2016).

2.2.8. Drylands inhabitants

Communities that have thrived in drylands for centuries can be grouped into nomadic people (pastoral groups that depend on livestock and farming whenever possible), semi-nomadic people (pastoral groups depending largely on livestock and agricultural cultivation at a base camp), transhumant populations (combine farming and livestock during wet seasons and might migrate for grazing land during drought seasons) and sedentary small-holder farmers (practice rainfed or irrigated agriculture often combined with livestock) (Ffolliott et al., 2002). These rural people are usually highly adapted to the challenges of water scarcity and climatic uncertainty (UNCCD, 2011b). The Bedouin inhabitants of the Jordan's Badia (desert landscape with diverse and fragile ecosystems) are mainly considered as a transhumant (see Chapter 3).

Traditional knowledge is a fundamental part of the cultural identity of dryland people employed in their environment and natural resources management including water harvesting, cultivation practices, weather forecasting and the use of dryland medicinal plants. The degradation of this knowledge and pursuit of large profits has led to the adoption of unsustainable practices and technologies. The committee of science and technology of the UNCCD reported that the exploration, conservation and integration of dryland traditional knowledge with adapted technologies are priority actions in the future (ICCD, 2022).

2.3. Dryland agricultural systems

The dryland characteristics described above combine in dryland agricultural systems, the focus of this thesis.

Rainfed dryland agricultural systems are inherently fragile and are defined as agriculture in areas with annual precipitation less than 500mm (Stewart & Thapa, 2016). Dryland farming is practiced when annual potential water evaporation exceeds annual precipitation (Peterson, 2018) due to environmental abiotic factors. This varies in terms of the deficit rate and the time of the year it occurs. Dryland farming systems emphasise water conservation, sustainable crop yields, limited use of fertilisers and pesticides, also wind and erosion constraints (Stewart and Thapa, 2016). Statistics indicate that 44% of croplands and 50% of livestock of the whole world are found in drylands (UNCCD, 2012). Dryland farming systems are very diverse, including a

variety of shifting agriculture systems, annual croplands, home gardens and mixed agriculture–livestock systems. They also include fallow systems and other indigenous intensification systems (FAO, 2004) for soil moisture and soil fertility restoration. The major farming systems of drylands vary according to the agroecological conditions of these regions. Thus, depending on the agroecological zone of the drylands, crops are grown either as a monoculture or as an intercrop with a legume at low planting density. A study was conducted within the Land Degradation Assessment in Dryland project based on socioeconomic information, agroecology and possibility of irrigation, showing that the majority of the drylands are used for cereal cultivation (LADA, 2008). Over time dryland farmers have applied several main agricultural management practices that turn around three main goals which are: enhance the accumulation and the retention of water from natural resources in the soil; reduce water loss risks like evaporation and runoff and use species and cultivars that fit with water availability (Stewart, 2016).

Tillage operations and the form of tools used are not randomly selected by farmers. The main objectives of tillage for dryland farmers are to prepare a seed bed, to promote infiltration, to conserve water within the soil profile, to prevent erosion, to improve the depth to which the roots grow and to aerate the soil for microorganisms' development. The agronomist's recommendation to cultivate the soil after harvesting or before the next rains to assist infiltration are often inapplicable in drylands because farmers profit from grazing residue after harvesting as well as because of the high costs and power required for dry soil tillage before the first rains.

The choice of appropriate crops and cultivars with optimum physiology, morphology and phenology must be carried out considering environmental conditions in the area which include climate factors and soil characteristics and especially moisture availability in the soil. Sowing timing and rate must be considered in this equation between crop and environmental conditions. Mainly, it is crucial to cultivate crops that are drought tolerant and that fit the precipitation patterns (Stewart and Thapa, 2016). Repeated sowing in dry cropland is common due to delays in rainfall. Weeding is usually done by hand and external outputs such as fertilisers and pesticides are improperly applied or limited to particular dryland areas.

During the last decades, attention has been paid to the creation of more sustainable productive and stable systems through improved cropping system management. The suggested practices

packages should fit with the agroecological conditions and farmers perspectives. According to that, successful dryland farming requires the integrated management of soil, water, crops and nutrients. Small holders, farmers with small-scale and poor resources, usually subsistence-based, operate and survive in these varied, changeable, and hazardous environments by being able to manage the multiple risks through diversification, flexibility and adaptability (Mortimore and Adams, 1999). With suitable cropping patterns and wise resource exploitation, dryland farming systems can be considered at best a risky enterprise. However, the risk of low productivity in years when precipitation is greater than average but occurs at times when crop water requirements are low, needs to be considered. In such cases, short-duration varieties that mitigate the impact of drought period or the delay of rainfall (often occurring at the beginning and the end of the growing season and getting longer due to climate change) are urgently needed and being developed. These short life cycle cultivars, that should have higher harvest indices for the farmers profit, are considered as a key component of management strategies to adapt to climate patterns in the future. Many of the currently available varieties are however susceptible to pests, diseases, bird damage and requiring additional costly management practices. Currently, in the west Asia and north Africa regions (WANA), the cultivars should be tolerant to frost, drought and heat stresses, also resistant to pests and diseases, with a high yield capacity and vigorous early growth.

Using manure, compost, and mulches, nutrient conservation, fertilizer micro dosing, integrated livestock management strategies, crop rotation and selecting a sustainable mixed cropping as well as effective soil conservation techniques, are the main pathways for sustainable and efficient production in drylands and for long-term local food security (Pretty and Bharucha, 2014). Dryland farming practices include agroforestry and fallow lands that conserve both soil moisture and fertility, practices that are for example increasingly being adopted in India.

No- or low-till farming minimizes soil disturbance and maintains crop residues and other organic matter in the soil surface where it helps to reduce evaporative losses and increase infiltration. Experiments have shown that no-till agriculture can lead to a greater concentration of soil organic carbon near the surface which often translates into improved productivity (Powlson et al., 2014). The impact of no-till on the overall soil carbon balance is still not fully understood, but there is clear positive benefit for climate change adaptation. No-till agriculture requires substantial changes in farming practices; nevertheless, it can be more profitable than conventional farming by reducing the cost of labour, fuel, irrigation, and machinery. No-till

agriculture is practiced to the greatest extent in the drylands of the world's leading grain-exporting nations, such as Australia and Argentina, and in the US where it accounts for 22.6 % of all cropland areas (Shaxson et al., 2008).

2.4. Cereal production in drylands and yield gaps

2.4.1. Overview

Cereals continue as the fundamental source of total food consumption in developing countries where direct consumption of grains provides 54% of total calories and 50% for the world as a whole (FAO, 2006). The dominant cereals are wheat, barley, oat, rye, rice, maize, sorghum and millet. These eight cereal grains provide 56% of the food energy and 50% of the protein consumed on Earth. Wheat, rice and maize constitute approximately 85% of global cereal production. Adapted cereal crop species and cultivars within each species are found in all latitudes from 60ºN to 50º S, on soils ranging from slightly acid to alkaline in both dry and wet regions (Kent-Jones, 2023). Among these cereal species, wheat is the most widely grown cereal crop and is extensively grown in dryland regions under both non-irrigated and irrigated conditions. About one half of global wheat is produced in semi-arid climates with a precipitation between 250 and 450mm (Fischer et al., 2012). In terms of food security, a positive fact is that cereal production has increased at a faster rate in the developing countries than in the developed ones. From 1961 to 2006, cereal production in developing countries increased 2.7 times compared to 2.3 times for the developed countries (FAOSTAT, 2012). Although the absolute rate of cereal yield increase has been nearly linear over the past 50 years, the high relative rates of yield increase during the green revolution years of the mid-20th century that started in Mexico and Indian sub-continent (the period of farming progress that saved the world from serious food shortages in early 20th Century) have since been steadily falling as yield rises (FAOSTAT, 2012). In addition, the main reason behind the increase in cereal production in the developing countries is the expansion of the cultivated area and not only the increase of yield per land unit. Between 1961 and 2020, the harvested area in developing countries was doubled (especially in Africa) with 70% increase in yield rate per land unit. However, the harvested area in Europe has decreased by 25% and the yield has dramatically increased 2.7 times per land unit since 1961 (Figure 2.2).

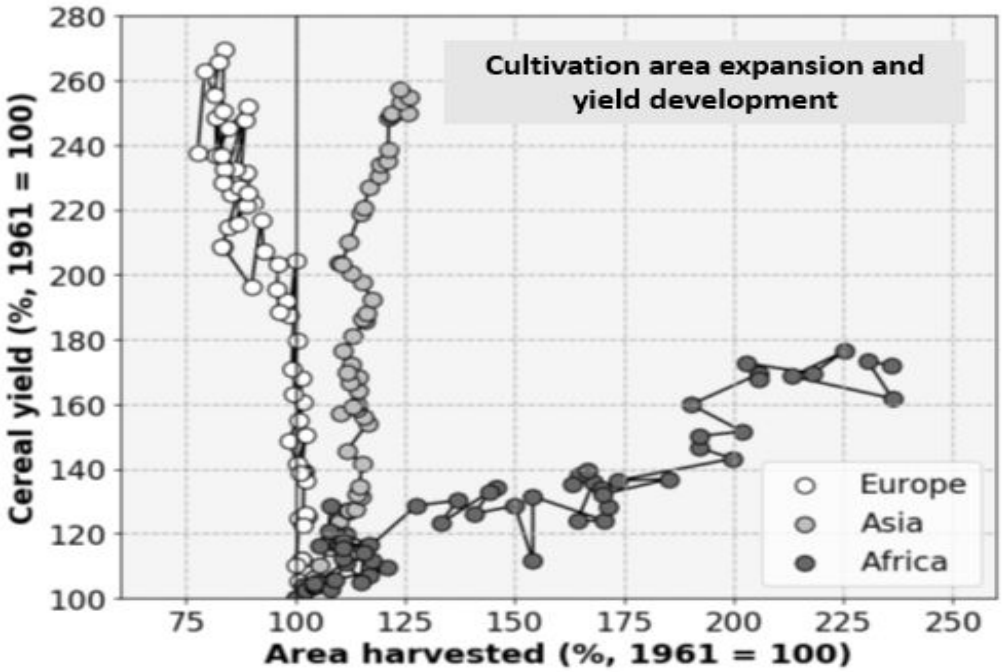

Figure 2.2: Yield intensification and cultivation area expansion trajectories in Europe, Asia and Africa (1961-2020). *Source*: Global Yield Gap Atlas (http://www.yieldgap.org).

2.4.2. Management variation across dryland farming systems

Cereal production systems in drylands are limited primarily by available water, and threatened by current and projected climate change in many regions where these systems occur (Fraser et al., 2013; Hijmans et al., 2005). This is why agricultural practices in dryland cereal systems are different from those cereal systems in wetter areas, to meet the specificity of these regions in terms of climate, natural resources availability (water and organic matter) and geomorphological and biodiversity characteristics.

Seeding rates for wheat in drylands are lower than in humid lands rates. In wetter areas, deep tillage after harvesting and surface tillage before sowing are common practices to aerate the soil and to control weeds. This cannot be done in drylands because deep tillage will invert the surface soil layer (which is the richest part of the dryland soils with organic matter and nutrient decomposed from crops residues and livestock manure) and such practice will prevent early-stage plant growth to take advantage of it.

Cultivars used in drylands have particular characteristics that adapt to the harsh conditions in these environments. Generally, these cultivars have a short life cycle which make the sowing dates different from cultivars used in wetter lands. The dryland cultivars have acquired resistance to drought, diseases, low soil fertility and hazardous situations like frost. Most dryland cultivars have been developed and selected from landrace and wild antecedents that

have already acquired, through the time, the ability to survive in such conditions (Nazco et al., 2012). Often, grain yield of these cultivars is much lower than wetter land varieties.

Chemical control of diseases, pests and weeds in drylands is rare and depends on the season and crop growth. These treatments are risky in drylands because they need to be done in specific weather conditions like optimum temperature and very low wind. Following is a well-known farming management technique in dryland cereal cropping systems. It has been the primary yield stabilising tool used by farmers in the majority of the dryland areas worldwide. Simply, fallowing means leaving the land out of use as every other year to accumulate moisture and nutrients in the soil. The stored water and nutrients increase the probability of producing an adequate crop yield in the season after fallow. Generally, fallows are practiced free of weeds if water conservation is a concern, but in some areas, farmers allow weeds to grow for their livestock herds to graze and for the weed residue that returns to the soil (Peterson et al., 2006). No or low-till crop production is a technique that has been strongly recommended by researchers and agronomists especially in drylands for cereal production. This technique minimises soil disturbance and maintains crop residues and other organic matter on the soil surface. It reduces water loss by evaporation and carbon release. The latter will lead to a greater concentration of soil carbon near the surface which often translates into improved productivity.

No till farming is considered more profitable than conventional farming by reducing the cost of tillage and fuel. Despite its benefits, most farmers in developing countries do not use this technique because they cannot consider it because they don't have the machinery needed for no till crop production. Farmers in these areas are obliged to apply tillage so they can cover the seeds after sowing. Currently, no-till agriculture is practiced in the greatest extent in the drylands of the world's leading grain producing countries such as Australia and Argentina and the USA where it accounts for 22.6% of all cropland areas (Friedrich et al., 2008).

Crop rotation based on legumes is an important technique adopted by farmers in drylands to improve soil quality by enhancing physical, chemical and biological properties and increasing nitrogen content (nitrogen fixation) in the soil. According to Harris (1995), farmers of several millennia ago were aware of the value of legume cultivation for cereal yields and how it was a common cropping system in drylands. Usually, in wetter regions (rainfall > 350mm per season), wheat (durum and soft) is alternated with faba bean, lentil and chickpea as winter sown species, or melon, sunflower, cotton, maize, sorghum and vegetable sown in spring or summer.

In drier areas (< 300mm) a wheat-barley rotational cropping system is adopted. In recent decades cereal monoculture has become more common in dryland areas applying high land use pressure on available resources (water and organic matter). Giving up these traditional rotations is a consequence of several factors including higher profit from cereal, unstable prices of legumes, harvesting costs (machinery high prices), marketing issues and low demand of legumes (Peterson et al., 2006).

2.4.3. Yield gaps

According to Van Ittersum et al. (2013), a yield gap could be defined as the difference between potential (Yp-irrigated crops) or water-limited potential yield (Yw-rainfed conditions) and actual farmers' yield (Ya). Yp is the maximum yield that could be achieved by a current and suitable cultivar when cultivated free of water and nutrient stress and with effective weed, pest and disease control. Yw is defined the same as Yp but considering the impacts of water limitations on crop growth due to rainfed conditions (suboptimal distribution of rainfall during the growing season). Ya is the yield actually achieved by farmers which is usually less than Yw due to nutrient limitations and biotic stresses such as weeds, pests and diseases. Ya could reach 80% of Yp or Yw when suitable management is applied during the growing season. Yield gaps differ widely across the world regions. For example, the yield gaps of wheat and barley in drylands such as sub-Saharan Africa, India, Portugal and Jordan are around 70 to 80% of the potential yield and could reach the 90% in Tunisia. In contrast in northwest Europe, which is a wetter, the yield gap is around 20 to 40% (http://www.yieldgap.org). It is believed that yield gaps are a consequence of water shortage due to harsh climate conditions like drought in addition crop management aspects that contribute to yield gaps (Giller et al., 2021). In this context, yield gaps can be classified under three main types:

1) Efficiency yield gaps are related to suboptimal time, space and type of inputs applied by farmers. For example, planting cultivars that are not suitable for a particular microclimate, doing chemical disease control during the flowering stage (damage flowers) or during hot or windy days, also adopting inappropriate rotational cropping system,

2) Resource yield gaps are due to the suboptimal amounts of inputs used by farmers, for example over-irrigation that could induce plants asphyxia or using massive quantity of nitrogen fertilisers that could block other nutrient absorption like calcium and cause flower fall is several species,

3) Technology yield gap which can be explained by the current technologies used by farmers not being able to reach Yp or Yw. For example, harvesting machinery could be a reason for yield loss during the harvesting if it's not well prepared (Van Dijk et al., 2020).

2.5. Climate change impacts on dryland cropping systems: a threat or an opportunity?

2.5.1. Overview

Climate change is affecting food production at local, regional and continental levels, therefore influencing the lives of all human beings, plants and animals (Ahmed, 2020; Williams et al., 2020). Worldwide, the impact of high temperatures, drought, and/or elevated CO_2 are the greatest challenges in the current century. In consequence, several cropping systems are being negatively affected by climate change and global warming, but cropping systems in drylands are particularly vulnerable due to the low and discontinuous availability of resources needed for crop growth (Ahmed et al., 2022). During the last few decades, global drylands have experienced anthropogenically induced climate changes that are predicted to continue and even to accelerate during the present century (Webb et al., 2017). The increasing frequency of extreme climate events and their severity have made drylands more vulnerable to ecosystem changes and land degradation (Spinoni et al., 2014).

2.5.2. Impact of climate change on crop growth and biotic factors

In a rainfed cropping system, the influence of climate variables like air temperature, drought and elevated CO_2 is complicated and significant. On average, an increasing drought frequency of 100% will appear under high emission scenario for dry regions especially in sub-tropical region, while drought frequency in northern hemisphere there is a probability of drought occurrence probability under the warmest future scenario (Balting et al., 2021). Unlike other extreme events, droughts can expand slowly over a large area (Luo et al., 2008) causing instability in the hydrological cycle which affects soil moisture, reservoirs, river flows and ground water. Drought in drylands significantly impacts physiological mechanisms during crop growth especially photosynthesis with a reduction between 60 to 92% as compared with free stress conditions. Serious water shortage during heading for wheat results is a shorter grain filling period and lower green flag leaf area index (Asseng et al., 2019). Higher air temperature stress during growth decreases crop productivity by restricting crop growth and shortening the crop cycle. For example, it hastens flowering and induces floral aberrations, as well as reducing the grain filling period and negatively influencing grain quality (Hatfield and Dold, 2018; He

et al., 2018). Zhao et al. (2017) assessed the impact of global temperature increase on the production of three major cereal crops (wheat, rice and maize) and found that each 1°C increase in global mean temperature would on average reduce global yields of wheat by 6%, rice by 3.2% and maize around 7.5%. However, in this evaluation they ignored the impact of CO_2, adaptation management and cultivar genetic improvements. The combination of high temperature and drought in time and space have shown a negative effect on crops like barley and wheat and have been found to be more severe than a single stress (Shah and Paulsen, 2003). In addition, a recent meta-analysis conducted by Cotter et al. (2020) to illustrate the impact of high temperature and drought on crop yield and yield components has shown large negative perturbations of crop life cycle, seed number, seed size and seed composition followed by a low harvesting index. Regarding CO_2 elevation, it showed a positive effect on growth and development which was greater during the early growth stages. Thompson et al. (2017) evaluated the effect of elevated CO_2 on photosynthesis and concluded a greater production of carbohydrates and biomass. Other studies have also revealed that under elevated CO_2 the crops productivity and yield are higher due to increased photosynthesis metabolism (Bocianowski et al., 2019). To be more specific, CO_2 rise currently benefits yields of C3 crops (convert CO_2 to phosphoglycerate during carbon fixation) like wheat by around 0.2% per annum production but has a negligeable effect on the yield of C4 crops (fixes CO_2 into a molecule containing four carbon atoms) such as maize. Overall, is case of no adaptations, it is estimated that by 2050 combined yield effects from +2°C warming and 26% increase in CO_2 for C3 crops will be close to zero, but about -8% for C4 crops which are mostly found in dry areas (Fischer et al., 2014).

Climate change is likely to lead to more water scarcity and reduced crop yields in most drylands and due to these present circumstances, it is obvious that dryland farming is a risky enterprise. For this purpose, understanding of climate change is important to design adaptation options for dryland agricultural systems. However, studying the impact of climate change on dryland farming systems must be done individually by assessing the specificity and the complexity of each system according to the surrounding factors. Generally, careful management of the available resources is a current need as it will play a crucial role in the coming decades to ensure food security. Technology such as precision agriculture (software and IT services), remote sensing, modelling, and artificial intelligence will also play a great role in adaptation approaches and decision making.

2.5.3. A threat or an opportunity

The impact of climate change on the agricultural sector in drylands varies according to different factors, hence it is difficult to generalise. Although most studies emphasise the negative impact of climate change on agriculture and food production, there are other studies that show some positive climate change impacts in such regions. Besides the fact of the positive impact of elevated CO_2 on crop fertilisation and productivity, we can define other positive impacts like the expansion of areas available for production of crops that need higher temperatures, expansion of two crop farming due to the increased cultivation period, reduction of damage to winter crops by frost and reduction of heating costs for crops grown in green houses or under indoor farming system (Kim et al., 2009). Other projection studies have also shown that precipitation will decrease in some dryland areas, falling more as heavy rainfall storms in short periods (Tabari, 2020). As a result, such precipitation might cause floods and erosion that could damage crops, but in areas where they practice water-harvesting techniques, potential damage could be avoided.

2.6. Small-holder farmers

Smallholder farmers produce 30 to 34% of global food supply on 24% of global cropland area. There are more than 570 million farms in the world and 84% of them are smallholders (<2ha) (Lowder et al., 2016). They provide around 70% of food calories to people especially in Asia and sub-Saharan Africa (Samberg et al., 2016). Herrero et al. (2017) conducted a transdisciplinary analysis and concluded that by using different farm size thresholds, globally, small medium-sized farms (under 50ha) produce 51 to 77% of nearly all commodities and nutrients. They also concluded that small farms (<2ha) are important and have a local significance in south and south-east Asia and sub-Saharan Africa. Smallholder farmers production is a crucial contribution to global food security. However, this important contribution is uncertain because many smallholders' households are food-insecure themselves due to several factors like low income, unstable productivity, climate change and low capital. In lower income countries, smallholders are often looking for off farm opportunities to earn more income in addition to the farm's uncertain incomes. Smallholders are the key to both their own food security and economic development of their poor countries. To answer the question "who are the farmers of the future", Giller et al. (2021) suggested that farming systems based on alternative production systems, such as agroecological and organic farming, may be more environmentally friendly and earn a premium producer price (higher income), however their

yield is lower than conventional agriculture. Such systems could serve as a model for global future agricultural development, but they would require much more agricultural land.

2.7. Resilience in agricultural systems

Over thousands of years, agriculture has developed marking the transition of humans from hunter-gatherers to settled agriculturalists and from foraging for what land provided, to managing land to provide what humans need (Mazoyer and Roudart, 2006). Although the technological development of the agricultural system since the beginning of plant domestication, and its spread all over the globe, the reliance on ecosystem services is a fact until today. However, it is not clear whether current agricultural systems, which humans have designed, are sufficiently sensitive to ensure continuing persistence and renewal of these ecosystem services. This anxiety is related to the current and future uncertainties due to the increasing population and the accelerated climate change impacts on agriculture. This is where we need to mention the role of resilience in agriculture to face these external threats. Generally, resilience focuses on a system's ability to absorb or adapt to change and persist before losing its functioning capacity (Holling, 1973).

Current agricultural production systems are adapted to a range of local climate regimes, characterised by seasonal and inter-annual variations, however, this adaptation could not persist under climate change projections. Extreme conditions like heat waves and droughts are getting move severe by the time and become more frequent and intense during growing season (Furtak and Wolińska, 2023). Therefore, agricultural systems that are considered resilient under current conditions are likely to become less resilient. At this point, the role of farmers management decisions is crucial to build a resilient cropping system and consistent productivity. Farmers tend to manage environmental variation by reducing and controlling it by adopting tools such as fertilisers, pesticides and deep tillage, rather than working with and building on it using crop rotation, cover crop, low tillage and manuring techniques. In poor country drylands, smallholder farmers are obliged to build a resilient agricultural system because they have no alternative income source and because the shortage and the rarity of tools used for intensive production. However, they are, and they will be the group mostly affected by climate change now and in the future. For this purpose, those vulnerable farming systems in drylands required well-studied management strategies based on scientific research to reduce the damage.

2.8. Conclusion

Despite their variability and vulnerability in terms of environmental factors that would impact cropping systems and its management approach, dryland farming systems are able to provide an important part of the world's food. However, recent studies have predicted that climate change impact on these systems will be negatively significant on most of these lands and need to be studied and evaluated using different tools. The distinctive features of these agricultural systems due to their particular environments need to be considered while conducting analysis. That's why exploring these systems characteristics, defining their components and limiting factors independently is an important task. The next chapters therefore take a case study approach to investigating the broad issues outlined in this chapter, using Q'a Shubayqa.

Chapter 3: Agriculture, water, and climate in Jordan and Q'a Shubayqa

3.1. Introduction

Agriculture in Jordan is a particularly constrained sector, accounting for 51% of the national water consumption under a dry climate and a limited quantity of water resources (IFPO, 2023). Jordan is among the four driest countries in the world, with only 61 m^3 of water available for consumption per person annually, far below the international water poverty line of 500 m^3 per year (MWI, 2023).

Most of Jordan is arid or semi-arid with low annual precipitation levels, only 8% receives more than 200 mm annually (World Bank, 2022), making it almost impossible to cultivate and produce cereals like wheat and barley under a rainfed system (Chapter 2). Climate change and its impact on agriculture has become an everyday reality that farmers must face, and need to adapt their practices to (Cammarano et al., 2012).

Q'a Shubayqa is one cultivated dryland catchment in Jordan where farmers can usually produce wheat and barley yields with an acceptable quality, which therefore distinguishes it from many other catchments in the region. To help understand the agricultural system at Q'a Shubayqa. and define the main factors that have contributed to maintaining productivity levels and resilience over the long term, three approaches are adopted in this chapter. First an exploration of the agricultural specificities of the study area, including the wider Jordanian agricultural situation and that of the wider Azraq basin in which Q'a Shubayqa is located, was undertaken. Second, soils from within the basin were analysed, and third a survey of local farmers was conducted. Combined these approaches provide a concise overview of the farming system in Q'a Shubayqa.

3.2. Environmental and agricultural background of the study area

In this section, the environmental and agricultural background investigation is split into discussion at three scales; country scale (Jordan, section 3.2.1), Basin scale (Azraq basin, section 3.2.2) and local scale (Q'a Shubayqa, section 3.2.3).

3.2.1. Jordanian background

3.2.1.1. Environmental situation in Jordan

Jordan is located 80 km inland from the eastern coast of the Mediterranean Sea between 31° 14′ 24″ N and 36° 30′ 36″ E, covering 89,000 km^2, in southwest Asia. Jordan comprises three

main areas distinguished by topography and climate. These areas are: the highlands, the Jordan valley, and the desert (Badia) (Figure 3.1).

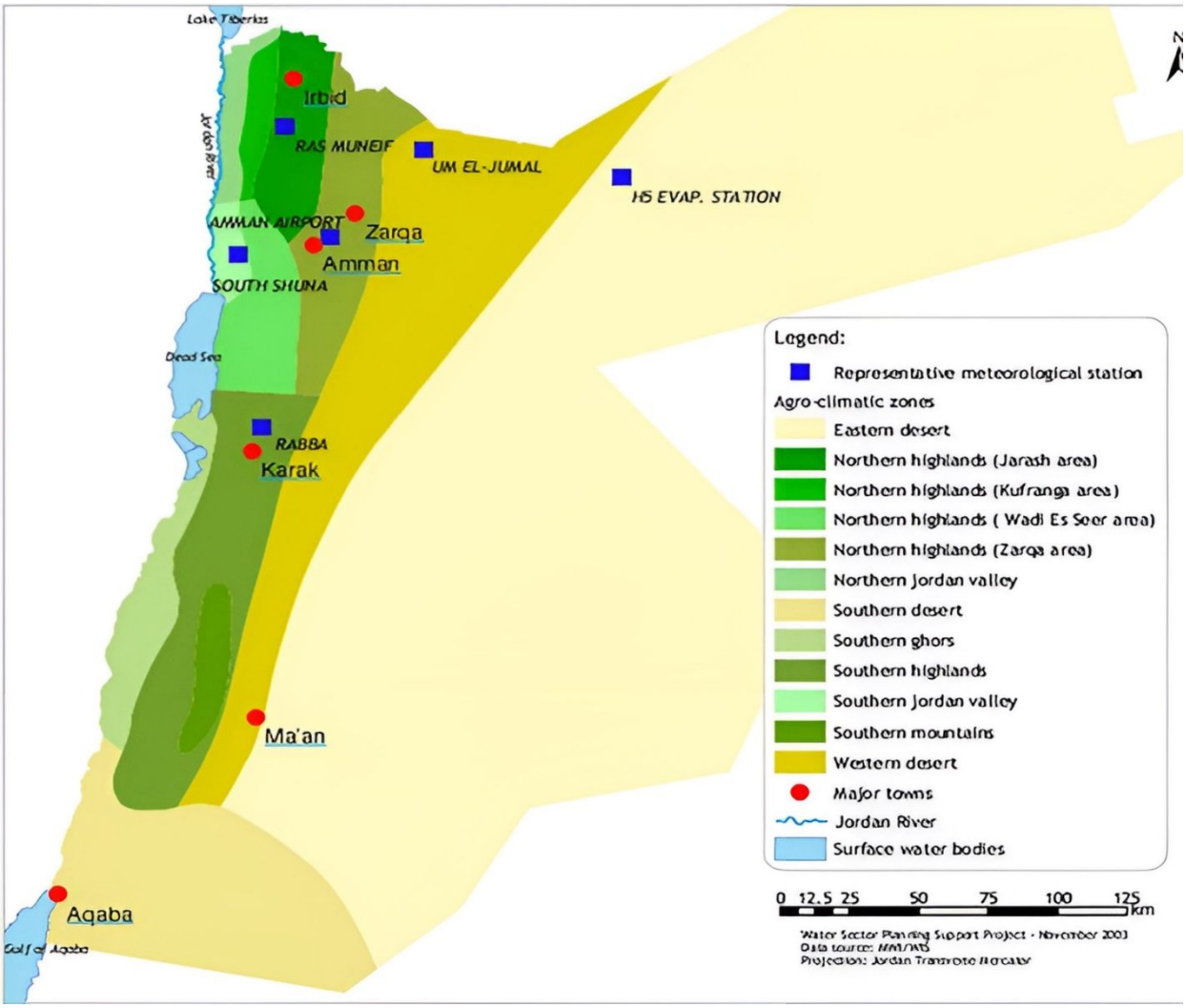

Figure 3.1: Jordanian area classification based on climate and topography (*Source:* GTZ and MWI *(2004) National Water Master Plan 2004. Amman, Jordan).*

The climatic conditions are characterized by cold winters and hot summers with short transitional periods of spring and autumn. Average minimum annual temperatures are recorded in January (5°C), while the average highest temperature is recorded in August (35°C). Temperature in Jordan varies from one region to another. This spatial distribution is controlled largely by the topography (Freiwan & Kadioglu, 2008; Q. Tarawneh & Kadıoğlu, 2003).

Physiography and latitude are also the major factors controlling the spatial distribution of rainfall (Abandah, 1978). Precipitation in Jordan varies from less than 50 mm/yr in the south-eastern desert area of the country, to more than 650 mm/yr in the highlands and northern

mountains, with high variability between and within the regions. Precipitation usually falls between October and April. Ecological characteristics also vary from one zone to another depending on climate type (Al-Ansari et al., 2014).

Jordan can be subdivided into five geological regions (see Figure 3.9): Limestone with flint in the interior west desert and the highlands; Sandstone hills in the Jordan rift margins and Wadi Rum area in the south east; Primeval basement rocks north of Aqaba; Basalt desert in the north-east and the Jordan rift valley located at the country's western border (Andrews, 1995).

The soil distribution in Jordan closely follows the climate, topography, and geology. Most of Jordan's soils formed on limestones or basalt and are red in colour (Terra Rossa or red Mediterranean soil in the old classification system (Vingiani et al., 2018); Vertisols and Incepitsols orders due to their high clay and oxide contents in the USDA soil taxonomy).

3.2.1.2. Agriculture and food production

Jordan's population is around 11.3 million. About 80% of the population live in urban centres like Amman, Al-Azraq, Irbid and Zarqa (DSJ, 2022). The rest of the population are rural residents, including Bedouins who mainly practice farming and livestock breeding.

The total agricultural area in Jordan is about 970,000 ha, representing only 3.3 % of Jordan's total land area and mostly located in the north-east (Jordan valley). According to the latest statistics in 2010, 49% of the agriculture area is cultivated with crops (cereals, forage), while fruit trees represent about 37%, and vegetables 14% (FAO, 2018). The most profitable crops are citrus, stone fruit trees (apricots, flat apricots, peach and nectarines) and vegetables (tomatoes, aubergines, cucumbers, cauliflowers, cabbage). Agricultural products represent 17.6% and 16% of the total national exports and imports respectively (MoA, 2010). Jordan is self-sufficient in potatoes, olives, olive oil and lemon production, and has a surplus in tomato production (MoA, 2010). The country is almost completely dependent on cereal imports. 80% of the cultivated area in Jordan depends on rainfall, and consequently the agricultural sector is characterised by unstable production (FRD, 2006).

3.2.1.3. Cereal production in Jordan

Jordan used to achieve self-sufficiency in wheat and barley production where the average wheat production between 1960 and 1970 was around 148,000 tonnes (Figure 3.2) with an average

production of 600 kg/ha. The self-sufficiency was due to a larger cultivated area and a smaller population. During the last decades, the government of Jordan has encouraged technology adoption among farmers through several means including use of improved seed cultivars, water harvesting techniques, integrated pest management and reasonable prices. Since 1970 several national and international institutions like the Ministry of Agriculture (MoA), the Arab Centre for Agricultural Research in Dry Lands (ACSAD), the International Centre for Agricultural Research in the Dry Areas (ICARDA), have conducted a national breeding programme using adapted foreign wheat varieties (Momany, 2001). The consequences of these interventions were an increase of the average productivity per land unit to reach 1068 kg/ha. However, Jordan is currently producing less than 10% of its wheat needs (1.3 million tonnes) and this 10% depends on predicatable precipitation amounts during the winter season.

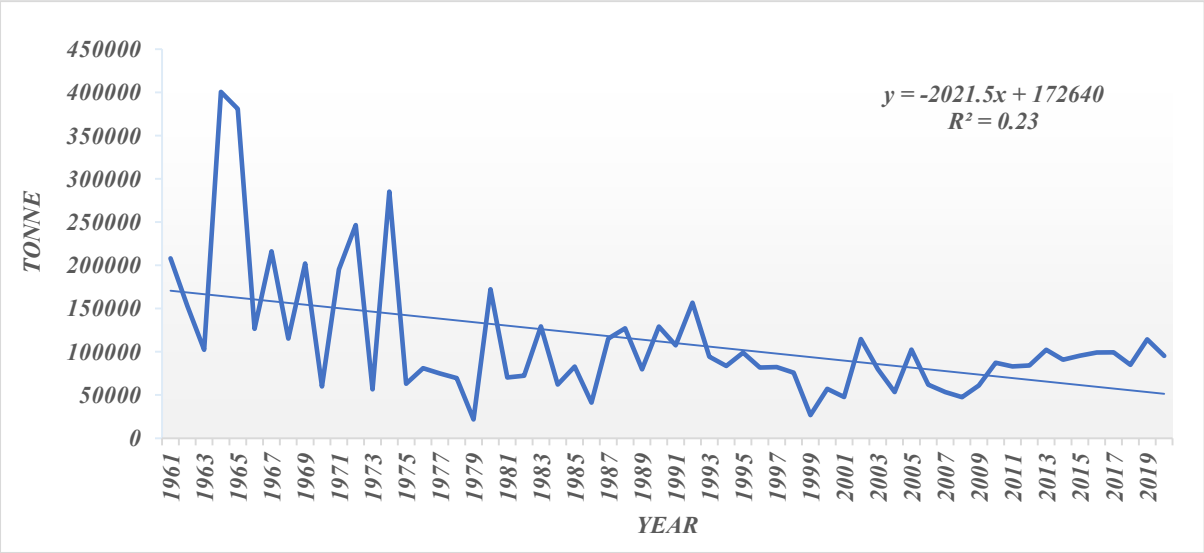

Figure 3.2: Harvested wheat yield in Jordan from 1961 to 2020 (Source: Jordan Department of Statistics. Plant Production Report. http://www.dos.gov.jo)

The decrease in wheat production from self-sufficiency to only 10% indicated by the trend line of Figure 3.2 is mainly due to the decline in cereal cultivated area, where in 1960 land under cereal production was about 238,000 ha and in 2020 it declined to 55,000 ha. According to the Ministry of Agriculture (MoA, 2010), the factors which contributed to the decline was due to the absence of legislation to protect this type of land from fragmentation, construction, population growth and forced migrations, in addition to the expansion of profitable fruit tree planting on these lands rather than cereals.

3.2.1.4. Hydrology and water management

Jordan is one of the countries with the scarcest water resources worldwide (see above), with its groundwater resources abstracted beyond the aquifers' safe yield, surface water resources almost fully diverted, and unpredictable precipitation fluctuations (Courcier et al., 2005).

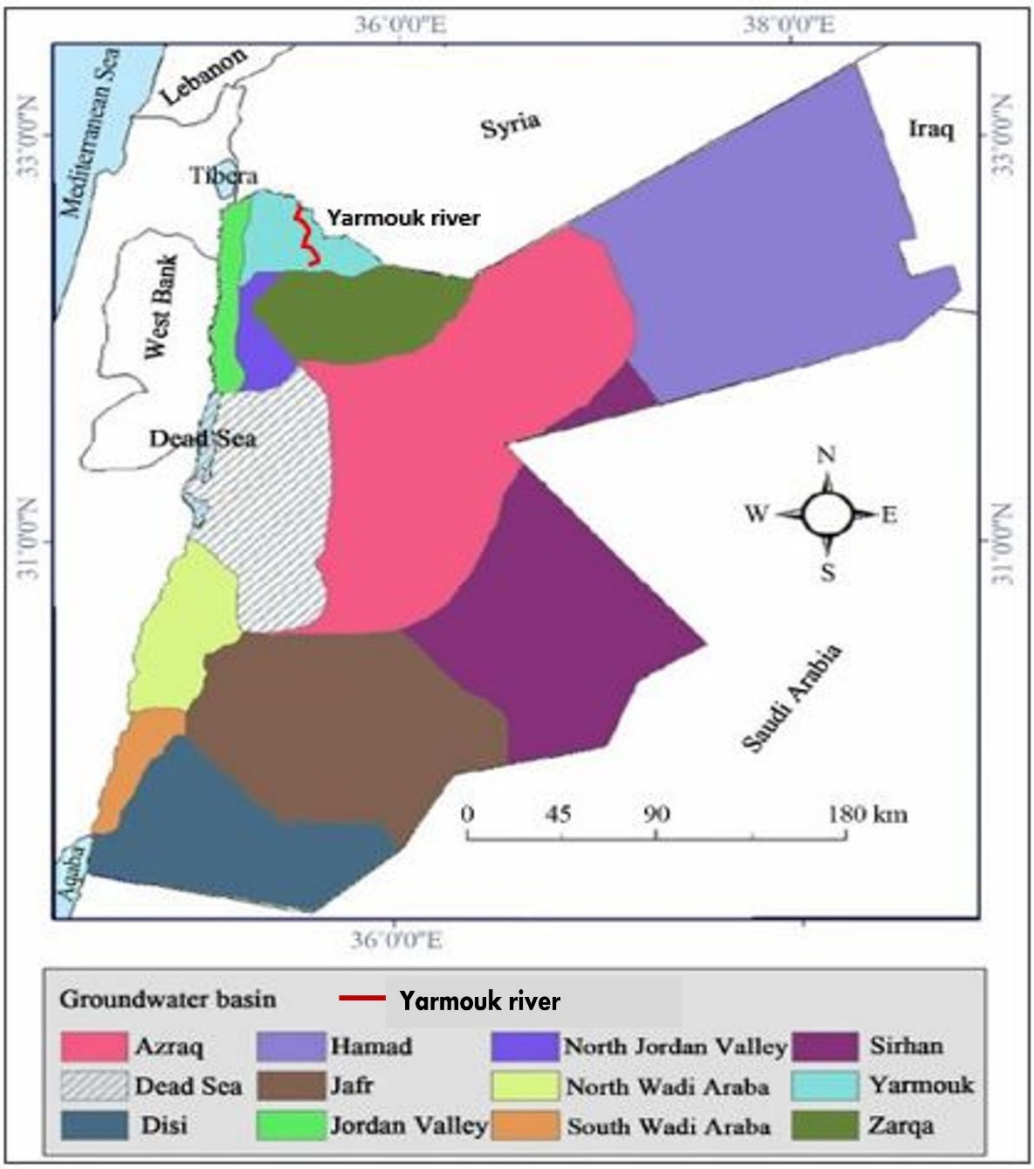

Figure 3.3: Groundwater basins distribution in Jordan (Al-Ansari et al., 2014).

Surface water resources (575 Mm^3/yr) are mainly the Yarmouk River (Figure 3.3) (40% of the overall surface water) and the other eastern tributaries of the Jordan River. Jordan shares the exploitation of the Yarmouk River with Israel and Syria.

Groundwater resources (275 Mm^3/yr) in Jordan are distributed among twelve major basins (Figure 3.3), ten of which are renewable groundwater basins and two (in the southeast of the

country) fossil groundwater aquifers (Al-Ansari et al., 2014). Renewable groundwater resources are concentrated mainly in the Yarmouk, Amman–Zarqa and Dead Sea basins and the main non-renewable aquifer presently exploited is the Disi aquifer (sandstone fossil) in southern Jordan and the Jafr Basin.

In 2019, the cumulative water volume derived from conventional sources (ground water and surface water) reached approximately 906.7 Mm^3 (Al-Addous et al., 2023), while total demand could reach 1000 Mm^3/year (JMD, 2011). The gap between water demand and water supply is now covered by over pumping in both renewable and fossil aquifers. The agricultural sector which uses around 70% of the total water resources in Jordan, in addition to the growing population inflated by the large numbers of refugees (due to conflicts in the Middle-East), are the principal causes of water demand, and the main environmental challenge that Jordan faces is water scarcity (Abuhalaweh, 2017).

The Jordanian Badia (desert) area is considered an important source of water for the country. The water sources are underground and on the surface. The underground water of Jordan is estimated at 93,000 Mm^3 (Al Naber & Molle, 2017) and mostly exist under Azraq, Hamad, Sirhan, Jafr and Disi basins which they lie in Jordanian Badia. The quantity of surface water depends mainly on annual rainfall and evaporation. The Badia receives low rainfall and has high temperatures (around 40° C in summer) which cause rapid evaporation, thus the opportunities to use surface water are restricted. Nevertheless, surface water is estimated in the Jordan's Badia at 126 Mm^3. There are some dams built to harvest the surface water for agricultural and range purposes. These dams can hold a total of 12 Mm^3 (Al Naber and Molle, 2017).

3.2.1.5. Climate change impact

Climate change is expected to have significant impacts on water supplies and agricultural production in Jordan.

The country's second national communication (MoEnv (Ministry of Environment), 2009) report presented climate change scenarios that were conducted using three ocean-atmosphere general circulation models (OAGCMs) for monthly temperature and precipitation. The GCMs (CSIROMK3, ECHAM5OM, HADGEM1) forecast a reduction of the annual precipitation by 0%, 10% and 18% by 2050 and a maximum increase of air temperature by 1.7 °C by 2050. Due

these climate changes scenarios, most surface water basins will suffer from decreased rainfall amounts in the range of 10–20%. However, the basins of the eastern desert (where the Azraq basin is located) and the basins of the Jordan River north side wadis could have a percentage increase in rainfall (Table 3.1). This increase of rainfall would, however, have insignificant impact on water resources at the country level as the rainfall amounts in these basins are already low (<100mm/year) (Al-Bakri et al., 2013).

Table 3.1 Climate change scenarios with expected change in air temperature and rainfall in the years 2030 and 2050 for the different surface water basins in Jordan (MoEnv, 2009). The study area Q'a Shubayqa belong the Azraq basin (highlighted).

Basin	Temperature change (°C)		Precipitation change (%)	
	2030	2050	2030	2050
Yarmouk river	+1	+2	-10	-20
Jordan river north side wadis	+1	+2	+5	+10
Jordan river south side wadis	+1	+2	-10	-20
Zarqa river	+1	+2	-10	-20
Dead Sea wadis	+1	+2	-5	-10
Wadi Mujib	+1	+2	-10	-20
Wadi Hasa	+1	+2	-10	-20
North Wadi Araba area	+1	+2	-10	-20
South Wadi Araba area	+1	+2	-10	-20
Wadi Yutum	+1	+2	-10	-20
Azraq	+1	+2	+5	+10
Jafir	+1	+2	+5	+10
Hammad	+1	+2	+10	+20
Sirhan	+1	+2	+5	+10
Southern Desert (Disi)	+1	+2	-10	-20

The impact of climate change on crop production is strongly related to the base temperature (minimum and maximum) for normal vegetative development starting from germination until

the harvesting stage, as well as an optimum temperature range during which the plant develops rapidly (Backlund et al, 2008).

An increase in temperature often accelerates crop phenological phases that may lead to shorter lifecycles associated with small plants and low yields. Higher temperatures at the reproductive stage may also affect pollen viability, fertilization, grain filling and fruit development, thereby reducing crop yield potential. The impacts may become severe for rainfed crops, such as barley and wheat. A summary of climate change impacts on the rainfed cultivated wheat and barley in Jordan is shown in the below Table 3.2.

Table 3.2 Expected changes in crop productivity under the different climate change scenarios in Jordan (Al-Bakri et al., 2011).

Crop	Climate change scenario		Change in Yield (%)
	Temperature (°C)	Rainfall (%)	
Rainfed barley	+1	-10	-18
	+2	-20	-35
Rainfed wheat	+1	-10	-7
	+2	-20	-21

3.2.1.6. Livestock in Jordan

Livestock contributes about 55% of the volume of business transactions related to the national agricultural production in Jordan. Sheep and goats are the predominant livestock species. The animals are generally raised on a crop-residue, planted fodder and barley grain-based system, with the rangeland contributing about one month of livestock feeding in normal years. This contribution is severely reduced in overgrazed areas and during extended drought periods. The maximum potential contribution of improved rangeland is not expected to exceed 30% of the daily feed requirements of one adult sheep or goat (Sidahmed 2011). Supplementary feed has been encouraged by government barley subsidies (price reductions) and reducing forage availability and has as a result led to decreasing profit margins of producers and low competitiveness of their products in national and international markets. Twenty years of subsidies and ease of transportation around the desert starting from the early 1990s have

encouraged the livestock industry to become dependent on subsidized barley grain, which accounted for 63% of feed costs for producers (Khader et al., 2019). The government policy for subsidizing prices of imported inputs, especially during the dry seasons has also encouraged livestock herders to keep large number of animals exceeding the carrying capacity of the rangeland (Al-Tabini et al., 2012). Livestock raising in Jordan is considered as important and traditional farming attitude for most of the Jordanian farmers especially in Badia because it provides economical balance for farmers during the low-income season for mixed farming systems.

3.2.2. Azraq basin

The Azraq Basin is located within the north-eastern desert of Jordan with an area of 12,710 km^2 (Figure 3.4). It is a mostly flat to slightly hilly area east of the Jordanian Highlands; the largest part of the catchment (94%) is within the Jordanian borders while the rest lies in Syria (5%) and Saudi Arabia (1%). The basin covers three Jordanian governorates: Zarqa represented by Azraq district; Mafraq, represented mainly by a part of North Badia (location of the study area: Q'a Shubayqa) district; and Amman Capital represented mainly by a part of Al Jiza district (Al-Naber, 2016; Alraggad and Jasem, 2010; Halah, 2007; Shahbaz and Sunna, 1998).The basin's ecological importance is represented through the Azraq wetland, also called Azraq Q'a located in Al-Azraq (Figure 3.4), which was an oasis and a prosperous provider of ecosystem services in the area which has deteriorated over the time due to the excessive water abstraction from ground water resources (Al-Eisawi, 2005; Riebe, 2018).

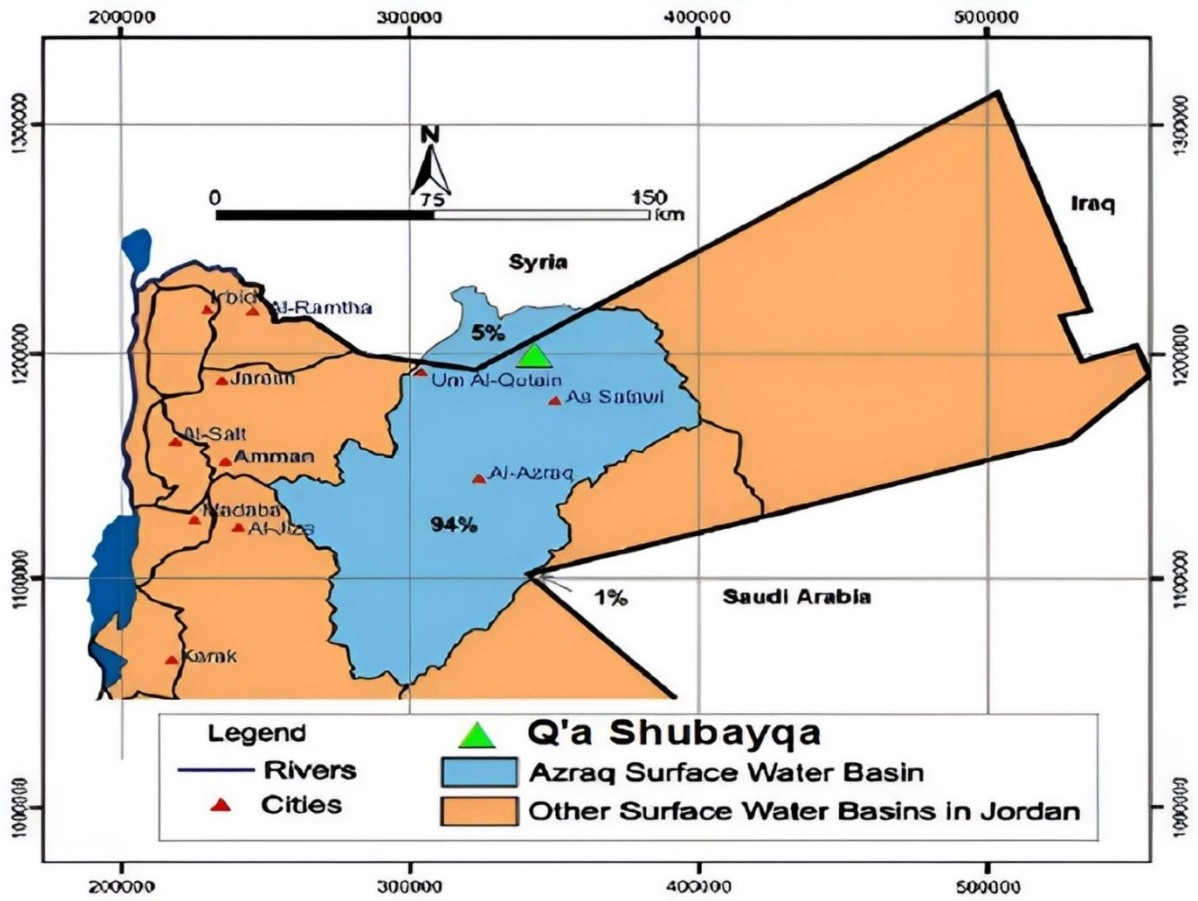

Figure 3.4: Azraq basin location within Jordan area (Ibrahim and El-Naqa, 2018).

3.2.2.1. Azraq recharge and groundwater flow pattern

The mean annual rainfall across the basin ranges from c. 50mm/year in the central Azraq Oasis area (Al-Azraq, Figure 3.4) to 500mm/year in the Jabal Druze area in southern Syria (Figure 3.5). The average precipitation for the entire basin is 87 mm/year, mostly occurring between January and March. The mean daily temperature in winter is less than 10ºC and the maximum temperature in summer is 45ºC. The average evaporation rate in the area is 2,400 mm/year (El-Naqa et al., 2007).

The Azraq basin consists of three aquifer systems (Figure 3.3), upper, middle and deeper, hydraulically connected in certain parts. The depth to the groundwater table is from a few meters in the centre of the oasis, to 400 m in the northern catchment area. Groundwater flows from south Syria towards Jordan from high to lower elevations (1,200 m above sea level (ASL) to 500 m (ASL) towards the Azraq depression (Figure 3.5).

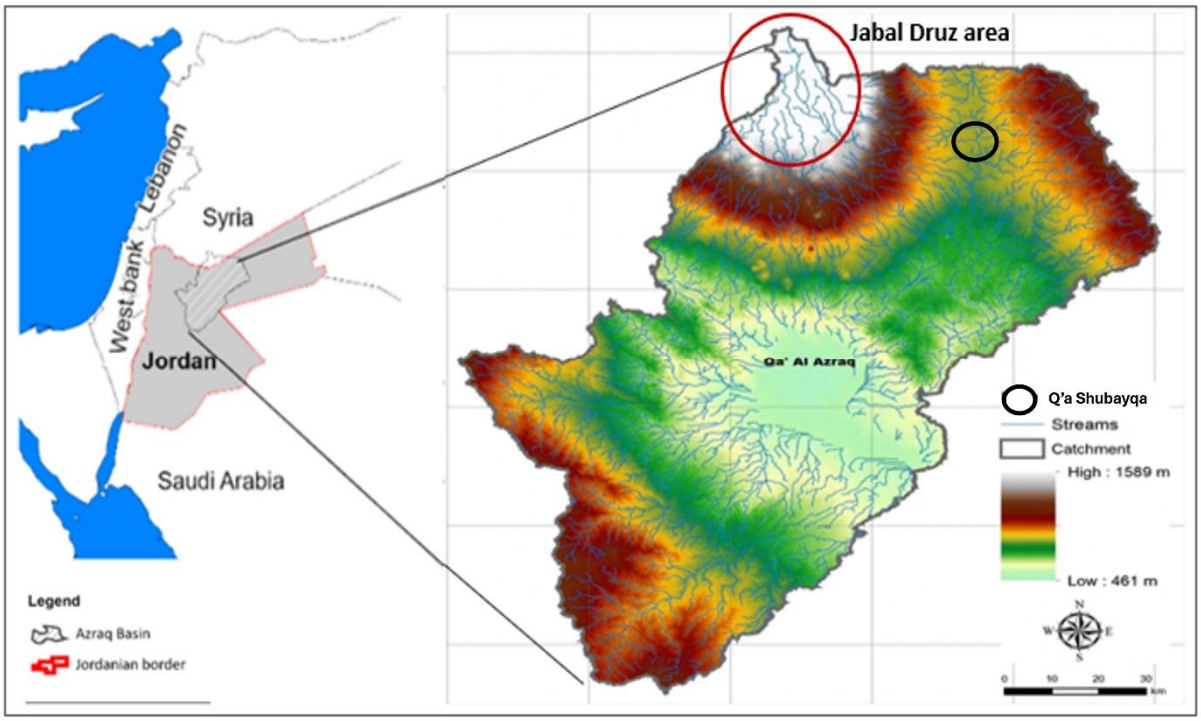

Figure 3.5: Azraq basin elevation and main drainage patterns (Alqadi et al., 2021; Ibrahim and El-Naqa, 2018)

The main recharge of the upper aquifer originates from infiltration through from the high rainfall areas around Jabal Druz (Figure 3.5). Intensive thunderstorms and flash floods in the Azraq Basin also contribute to minor groundwater recharge. The estimated total recharge is about 34 Mm^3/yr (Bajjali, 2006). Most of the water in the Azraq Basin is concentrated in the upper aquifer, and that is the main source of water in the region (Figure 3.6). Water resources are scarce, fluctuating and uneven both spatially and temporally, with high inter- and intra-annual variations of precipitation.

During the 1980s, numerous wells were drilled in the basin, and water that was pumped to meet the water needs of the farmers in the area and those of greater Amman (the capital), where 40% of Jordan's population live (MWI, 2010). Increasing demands on this aquifer, however, have caused the water table to decline by 25 meters during the period between 1985-2013 (MWI, 2013), even in the Azraq Q'a (Oasis), where it used to be at the surface. As a result, some of the Azraq springs became saline, some dried up, and the oasis areas, such as that which is now the Azraq Nature Reserve was severely damaged (Al-Naber, 2016).

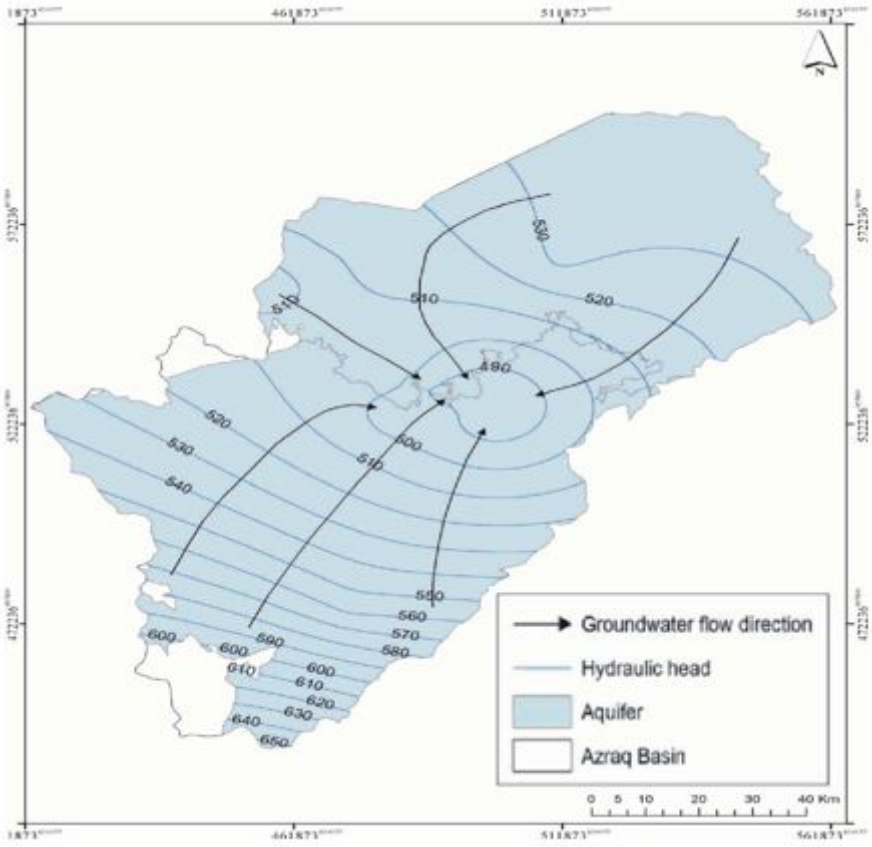

Figure 3.6: Groundwater flow system in Azraq basin upper aquifer (Alraggad and Jasem, 2010)

3.2.2.2. Soil type and characteristics

Most of the soil in the Azraq basin is characterised as arid soil, with a high soluble salt content in the subsurface horizons. The predominant soil type is Silty Clay Loam (Drury et al., 1993). In the Azraq region (East Jordan Limestone Plateau), soil is mostly poor and either clay, Hammada (conventional term of gravelly desert plains), saline or calcareous. Soils are primarily composed of limestone with flint scattered all over or covered by basalt pebbles and boulders that resulted from volcanic activities centred on Jabal Druze. In the middle of the Badia and to the south of Azraq, soils become saline and contain gypsum (Ababsa, 2013).

In the North Jordan basalt Plateau (Figure 3.9), formed from basaltic lava from Jabal Druze, soil is developed on parent lava rock and aeolian silt is likely to have contributed to soil formation (Khresat and Qudah, 2006). Soils are deep with 4.5 m (northern Azraq basin) and slightly gravely, with a fine silty loam texture in the surface, and subsoil horizons rich in $CaCO_3$. The high silt content of the surface soil, and the very low organic content (<1%) makes

soils highly susceptible to gully and wind erosion, particularly when disturbed by ploughing or subjected to over-grazing (Khresat et al., 2004).

According to Rawajfih et al. (2005), and after a several studies and soil analysis in different areas of the basin, there was a recommendation to manage some areas so that a sustainable irrigated-agricultural system, based on harvested water, could be employed. Some of the areas studied represent potential new lands provided adequate water supplies of good quality are available. These recommendations were based on livestock manure which is an essential component of intensive rehabilitation of arid lands and deserts, and therefore its application is a must, if a sustainable use of arid soils is to be accomplished.

The future use of the Azraq basin for crop production would depend on appropriate management, especially using drip irrigation system instead of surface irrigation for crops, which will reduce the amount of water used and decrease the stress on ground water. In addition, employing magnetic water treatment devices as part of the solution to reduce groundwater and soil salinity. Farmers are also encouraged to use saline tolerant species and convert to organic agriculture (MIRRA, 2019).

3.2.2.3. Farming system and typology

Farming systems in the Azraq basin vary from small scale farms with simple cropping patterns and cultivation techniques, to highly sophisticated and modern farms run as enterprises with hired labour. It is surprising however to find the former type in the Azraq basin given its climatic conditions, dryland, not very favourable for cultivation and with water scarcity and quality problems. During the last decades and due to the absence of water management policy and regulations that prevent farmers from overuse of groundwater by digging illegal wells in Azraq and Mafraq governorates (located in Badia where rainfall is insufficient to grow rainfed crops), agricultural land areas have been extending on a yearly basis. The total cultivated area in the Azraq area in 2005 was 6100 ha and increased in 2011 to reach 11400 ha (MWI, 2013). According to official data from the agriculture and extension department, an important variation of cropping systems was recorded in Azraq lands such as arboriculture (olives, grapes and date palms), fodder crops (alfalfa) and cereals (wheat and barley) (Figure 3.7). An important increase in olive plantation was recorded with 4200 ha in 2005 to 8100 ha in 2011 (Al-Naber, 2016) which was due to high incomes, easy maintenance and low labour demand,

in addition to the olive tree characteristics like low water requirement and moderate tolerance of saline water (Chartzoulakis, 2005).

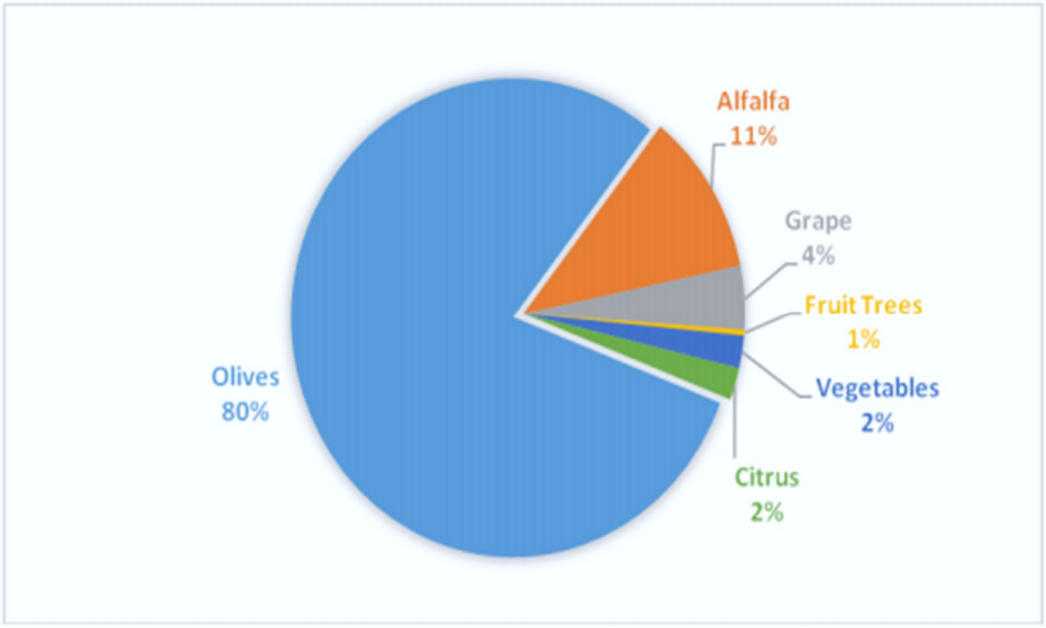

Figure 3.7: Cultivated area in Azraq basin in percentage (Al-Naber, 2016)

In the International Water Management Institute (IWMI) Project report (2016), the farms typologies used were defined based on the cultivated area, cropping pattern, irrigation techniques, management practices and farm revenue but without taking into consideration the initial investment cost (difficult to assess accurately). Profits were calculated based on farm production as most farmers started their cultivation on state land or inherited land, and water bills were not paid until 2004 (for the most part). It can be said that agriculture was productive and profitable until the early 2000s. The yield and profit decreases after that date can be related in part to water quality (salinity increase) directly affecting crop production. Towards the mid-2000s production costs had increased, with labour wages rising from U.S $99 /month (1990s) to U.S $395 /month. Energy costs also increased following the war in Iraq in 2003 (the price of one oil barrel rose from U.S $8.5 to U.S $147). As a result of the increase in costs, several farms have been abandoned, and locals have left the area. On the other hand, some farms in Azraq, particularly in the south, are still being cultivated and some in the eastern area were found to be profitable. Olive is the dominant cropping system adopted in Azraq among 6 types of farms (Arranz-Otaegui et al. 2018, see also Figure 3.7). Alfalfa is the second cultivated crop after olives because of its important profits, but the issue is about the high-water requirement during growth. In spite of the sensitive situation of water resources in Azraq, during my field

work, most of vegetable farmers confirmed to me that they are intending to cultivate Alfalfa in the future, likely needing the excavation of more wells for more water supply.

The farming systems adopted in the Mafraq governorate part of the Azraq (see section 3.2.2) basin is totally different from the Azraq governorate part, despite both areas being located inside the same basin. Mafraq's aquifer is deeper and underlies the aquifer system exploited in Azraq; groundwater is found at around 350 m below the surface, making groundwater abstraction very expensive (pumping costs). The dominant farming system in the Mafraq (North Badia) area is based on stone fruit trees, where dry weather conditions are suitable for this type of tree by reducing the occurrence of fungal diseases. Stone fruit farms cover around 44% of the Mafraq planted area that belong to the Azraq basin, and farmers agricultural practices are based on high technology and having good marketing know-how. Farms in the Mafraq area produce 300,000 tonnes/year of stone fruit during the harvesting period between May and the mid-August. Only 5% of this production is needed to satisfy the country's needs for this product, while the rest is exported to the Gulf countries and Syria (Demilecamps and Sartawi, 2010). Vegetable farms cover 32% of the planted lands in the Azraq basin, mainly tomato, melon and watermelon, and cabbage in open fields. Some vegetable farms are associated with an olive orchard or stone fruit orchard. Vegetable farms are using the land only for a year, then rotating for five years interval, as there is no pressure on land (MoA, 2008). The rest of farmlands in this area are mainly used for fodder crops or cereal-based rainfed cropping system such as in Q'a Shubayqa (study area).

3.2.3. Q'a Shubayqa

The Q'a Shubayqa (Figure 3.8) is a playa, or dry lake, used as agricultural land, situated 130 km northeast of the Jordanian capital Amman and 22 km north from the modern town of Safawi. Q'a Shubayqa geographically belongs to the arid basalt plateau desert (Harrat Al_Sham) of northeastern Jordan (altitude: 750m) and hydrologically it is considered as a subbasin of the Azraq watershed. The Q'a covers an area of approximately 12 km^2. Several wadis flow into the basin and the most substantial are the Wadi Rajil, that flows from the east, and Wadi Selma, that flows from the north-west (Figure 3.9). The Wadi Rajil is also the major outlet of Shubayqa watershed draining to the southeast whence it continues southwards towards Safawi and all the way to the Azraq Oasis.

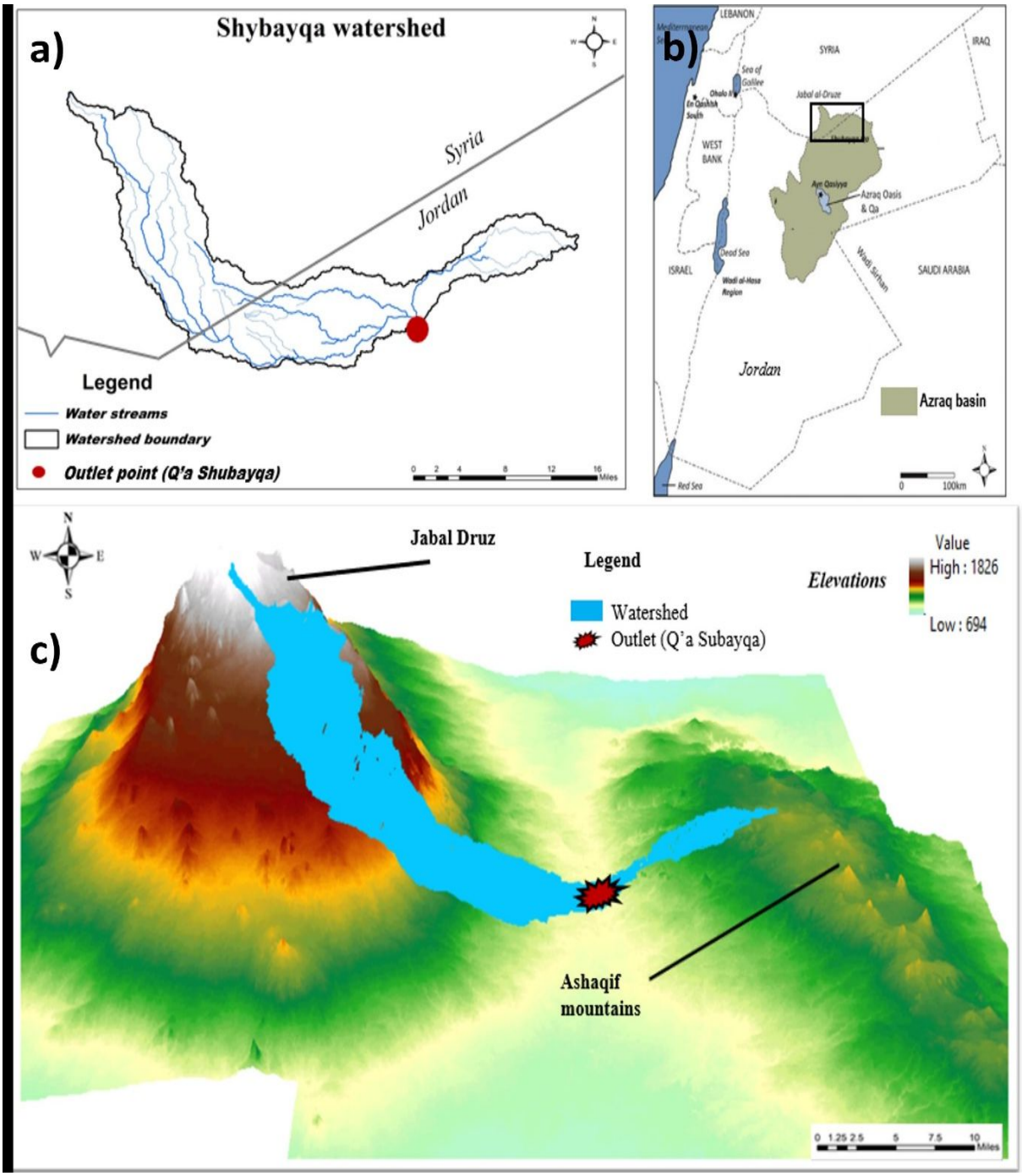

Figure 3.8: Maps representing the location and components of Shubayqa watershed: a) map of the extent of Shubayqa watershed between Jordan and Syria, b) map of watershed location within Azraq basin (Maher et al., 2015), c) map showing watershed between Jordanian hights and Syrian hights.

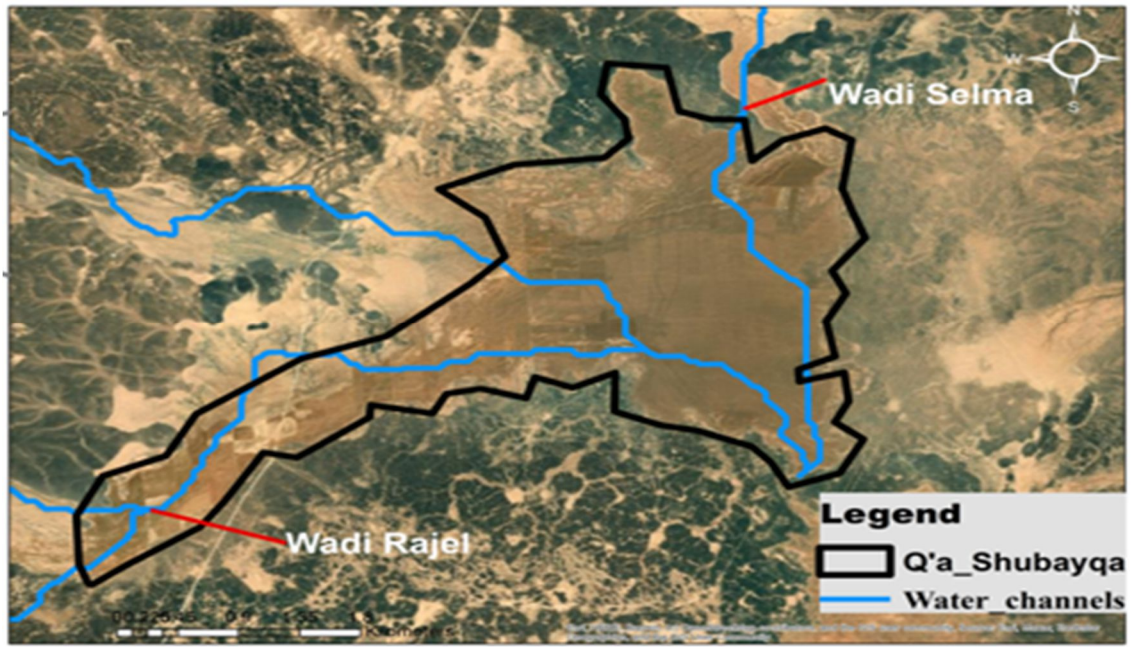

Figure 3.9: Maps of Q'a Shubayqa agricultural land location in Jordan and main wadis (Bany,2016).

The physiography of the area is presented as a depositional basin, with wadis and associated alluvial fans, cutting through the largely rocky, basalt, desert. The Shubayqa watershed covers an area of 709 km^2 and is geographically bordered by latitude 32°38'54.361" and 32°28'49.713"N and longitude 36°43'25.059" and 37°29'42.107"E. The climate in this watershed varies from arid in Q'a Shubayqa, where annual precipitation is 100-150mm and daily average maximum temperature reaches 38°C during the summer, while the average winter temperature is 10°C (JMD, 2011), to Mediterranean subtropical climate in Jabal Druz mountain (altitude = 1803m) where annual precipitation ranges from 200mm to 600mm with seasonal snow storms, and average summer temperature reaches 20°C, while the mean winter temperature is 5°C.

3.2.4. Why Q'a Shubayqa matters: Archaeological evidence

Around the Qa Shubayqa basin, an archaeological survey and preliminary excavations made by Alison Bets and her team in the 1980s, documented two late Epipalaeolithic (14,500–11,500 BP) sites: Shubayqa 1 and 3 (Betts, 1999). A small excavation at Shubayqa 1 confirmed the presence of architecture and dense concentrations of finds at this site north of the Qa Shubayqa.

More recently excavations lead by Tobias Richter (e.g. Richter et al., 2018) at Shubayqa 1 produced many finds, such as various chipped- and ground-stone tools, as well as faunal remains, marine shell pendants and stone beads, bone tools, and a small number of incised stone objects. One of the most startling discoveries was the large amount of charred plant remains recovered from the site.

Botanical remains are rarely preserved at Natufian (Late Epipaleolithic archaeological culture 15,000 to 11,500 BP) sites in the southern Levant (geographical term referring to a large area in the eastern Mediterranean region of West Asia) (Asouti and Fuller, 2012). By contrast Shubayqa 1 has tens of thousands of charred pieces of plants, including seeds, tubers, fruits, and wood. This material provides an unprecedented insight into the past environment in the area and how humans used plants at the site. The discovery of wetland plant species (shrub fruits) in what is today a largely hot and dry environment was surprising, since it suggested that a substantial wetland must have existed in the Qa' Shubayqa during the late Pleistocene.

The palaeoenvironmental evidence found in the archaeological site of the bakery (Figure 3.10) in Qa Shubayqa shows that these settlements were possible because extensive wetland settings existed in the Badia (Richter et al., 2017). The large amounts of evidence recovered from the archaeological sites in Q'a Shubayqa, as well as other sites in the area, suggest that plant foods probably played an important role in the inhabitants' diets, but it is not clear whether they ever went further to manage these resources (Richter et al., 2017).

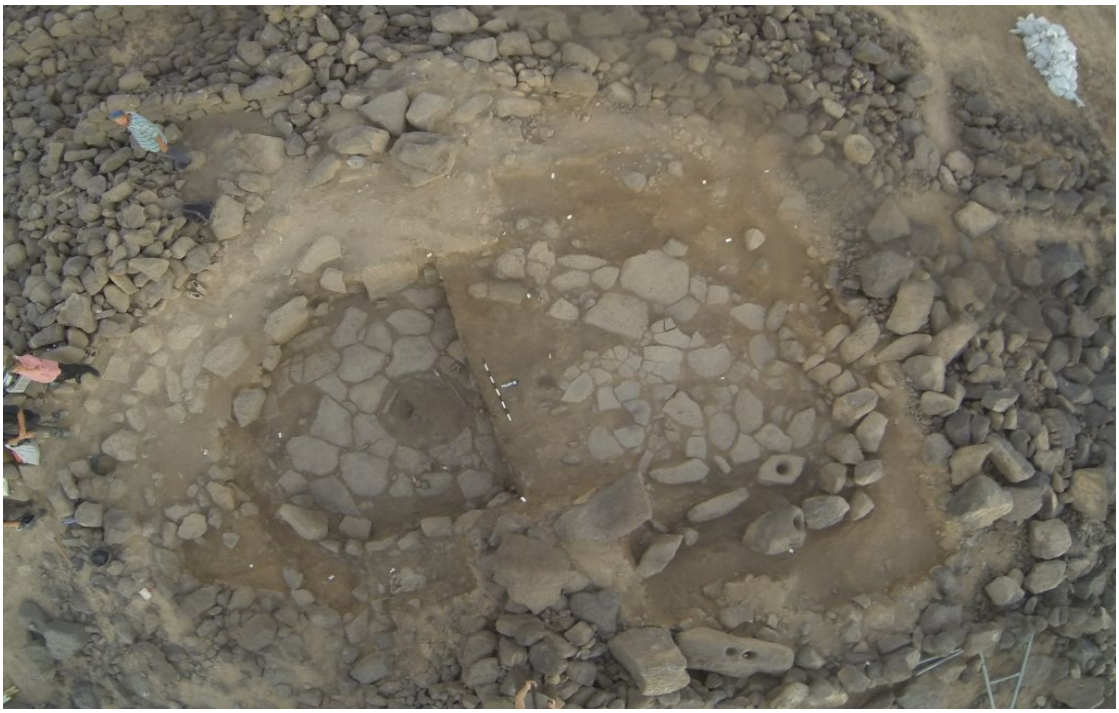

Figure 3.10: Oldest bakery in the world, 4000 years before the dawn of agriculture (14,400year-old); from Qa' Shubayqa, Jordan (Arranz-Otaegui et al., 2018)

3.3. Soils in Q'a Shubayqa

3.3.1. General description

Soil descriptions of the Q'a Shubayqa and surrounding lands from previous soil surveys reports have shown that the area is characterised by three main soil types (West, 1970). The first type is fine, mixed, thermic and typic camborthids dominating the area (35% of basin). The soils are strong brown, deep silty clay loam to clay lacking $CaCO_3$ concentration but with moderate structure. In the wadis and Q'a respectively, soils are very highly calcareous and moderately to very saline. The second dominant type is fine to fine loamy, mixed, thermic and deep families of typic calciorthids. Occupying 15% of the total area, this type is strongly brown, deep clay loam to silty clay loam with calcic horizon, usually between 15 to 50cm. May also be, very highly calcareous and very saline. It occurs on fans, terrace remnants and in Q'a. The third soil type is fine, mixed, thermic and deep family of Xerochreptic Camborthids covering 14% of the area. The soil is brown to strong brown, structured silty clay loam lacking $CaCO_3$ concentrations. The soil may also be very highly calcareous and moderately saline in wadi alluvium (Lucke et al., 2013).

However, To evaluate an agricultural system, soil analysis is considered a valuable tool to determine caracteristics such as physicochemical properties (Akça et al., 2023). A full soil analysis will allow soil issues to be diagnosed and, therefore, soil quality improved (Demattê et al., 2019). The soil sampling in the study area was due to be done after the harvesting period (late May to early June 2020) during a field work trip, but this was cancelled due to Covid. In June 2022, I was able to travel to Jordan for field work where I met Bedouin farmers, researchers and decision makers in the agricultural sector and collected soil samples from the cultivated area of Q'a Shubayqa. Multiple soil analyses were undertaken in the University of Nottingham laboratory to evaluate the situation of the cultivated soil and to meet the data requirements of the crop simulation model DSSAT that will be employed later in this research (Chapter 8). Methods of soil sampling and analyses are described in Appendix A.

3.3.2. Soil analyses

3.3.2.1. Soil sampling

Soil sampling was undertaken at nine different sites selected randomly to cover all the cultivated area in Q'a Shubayqa (Figure 3.11). Due to the planned modelling, we tried to make selected soil sample sites match with farm locations of the surveyed farmers. Another, 10th , sampling site was also selected outside the cultivated area (at the edges) for soil analysis comparaison purposes.

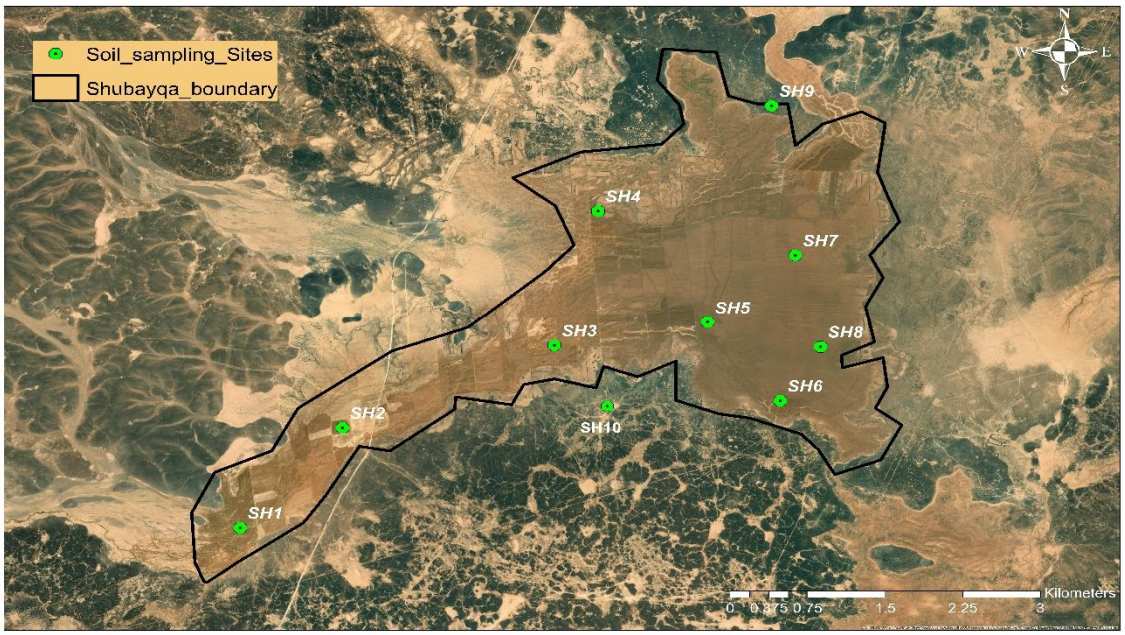

Figure 3.11: Soil sampling sites in Q'a Shubayqa

From each site, five subsamples were collected at different depths (0 to 10cm, 10 to 30cm, 30 to 50cm, 50 to 75cm and 75 to 100cm). Soil subsamples were packed and labelled in plastic bags. A handheld GPS (GRAMIN-Etrex 10) was used to record the selected sampling sites location. Sampling was performed with a hand auger following removal of plant residue from the surface. A total of 50 soil subsamples were sent to the laboratory of soil analysis in the School of Geography (University of Nottingham). A DEFRA licence for the import and movement of prohibited soil for chemical and physical analysis, was used.

3.3.2.2. Soil analyses and mapping

Loss on ignition was carried out by following a standard method based on sample combustion under different heat levels using an oven (105°C) and a furnaces (550 and 950°C) to determine the bulk density, organic matter content and carbonate content (Dean 1974; Heiri et al. 2001). Organic matter is of great importance in agricultural soils because of its impact on soil caracteristics like physical, chemical and biological properties. Soil organic matter is an essential factor to promote soil aggregate stability and therefore water infiltration, percolation and retention capacity. It also enhances chemical properties of the soil by increasing cation exchange capacity and nutrient supply for cultivated crops. Biologically, it stimulates the activity and the diversity of existing micro-organisms (Allison, 1973).

Soil texture was analysed by using laser particle size analyser (Beckman Coulter LS 13,320) after preparing the samples. Soil samples of 0.5g were added into centrifuge tubes and filled with hydrogen peroxide (10%) to chemically remove organic material from the soil samples by dipping the tubes in an 80°C water bath for five hours.Tubes were then centrifuged at 3000rpm for 4 minutes to separate peroxide from the soil. Repeat washing using distilled water was carried out to ensure that peroxided had been removed and leaving a plug of soil at the bottom of the tubes. Seiving samples at 2mm was undertaken and 10% Calgon (sodium hexametaphosphate and sodium bicarbonate) was added to soil samples to ensure soil was well dispersed for analysis. Laser particle size analysis will then provide data for grain size range between 0.041 to 2000 μm.

Nitrogen (N) is the most important plant macro-nutrient which promotes foliar growth and increases yield (Prakasa Rao & Kavi, 2000). In soil, it accurs in organic and inorganic forms. To quantify the Total Nitrogen levels in the collected soil samples, elemental analysis was conducted using CHN elemental analyser (detects small element quantities by complete

conbustion of the sample) at the University of Nottingham's Sutton Bonington campus. This type of analysis in an analytical technique applied to determine which elements are present and how many percent by mass of each chemical element is contained in the tested substance. CHN elemental analysis determines the amount of carbon (C), hydrogen (H) and Nitrogen (N) and is based on controlled and dynamic combustion of samples in a reactor and mesurement of the amount of the corresponding oxides. Soil sample preparation for such CHN elemental analysis starts by drying soil samples at 105°C, weighing 0.5g of each, and grinding these samples using a pestle and mortar to reduce agglomeration and ensure homogenety. Prepared soil samples are then placed into crucibles and entered into the elemental analyser. Another six crucibles, each filled with 0.5g of EDTA calibration samples (9.57% nitrogen) were also prepared and put in the analyser. This calibration substance that contains C, H and N are used to calibrate the analyser for accurate results.

A Palintest photometer was used to analyse the content of the other major available macro-nutrients (phosphorus and potassium). These analyses have been carried out for each soil sample and for different layers. The tests are carried out by first extracting the nutrients or trace elements from the soil (see below) and then testing the extracts by simple colorimetric test procedures. The palintest soil test system accurately assesses the colour formed after extraction and displays the reading as a digital readout which should gives an accurate measure (mg/l) with two decimal numbers of the tested soil parameter.

The phosphate in the soil sample was extracted using 0.5M sodium bicarbonate at a soil:water ratio of 1:25. The extracted phosphate is then reacted with ammonium molybdate under reducing conditions in an acidic solution to form a blue coloured complex. The intensity of the blue coloration is proportional to the phosphate level in the sample.

The potassium content in soil samples was also analysed by using Palintest. Magnesium acetate (0.1M) was used for soil potassium extraction at a soil:water ratio 1:25. The extracted potassium was then reacted with sodium tetraphenylboron to form an insoluble white complex which produces a turbidity in the test sample. The potassium level (mg/l) could be measured based on the sample turbidity.

Likewise, soil pH was measured to define the type of the soil (acid or alkaline). pH is actually a measure of hydrogen ion concentration in the soil where a very acid soil has a low pH and high hydrogen ions concentration and at high pH (alkaline) values, the hydrogen ions

concentration is low. Soil pH is an indicator for nutrient uptake availability for cultivated crops where pH around 7 is the optimal level for overall nutrients availability (Khaidem et al., 2018). The pH test was measured using a Palintest pH sensor after calibrating using ionised water (pH=7).

Soil analysis results like texture, soil organic matter and total nitrogen were then mapped using ArcMap tools. Kriging was used in this process of mapping (see above). The output maps showthe distribution of these results over the cultivated area and can be related to landuse and cropping practices.

3.3.2.3. Soil texture and spatial distribution

Particle size analysis results of Q'a Shubayqa soil samples are presented in Table 3.3. Soil texture is considered as one of the most important properties of soil, and it greatly affects water holding capacity, aeration, susceptibility to erosion, organic matter content, cation exchange capacity and soil tilth (Berry et al. 2007). Soil texture type directly affects nutrient retention and drainage capabilities. Based on the USDA particle size classification, these results divide Q'a Shubayqa soil texture into 5 types distributed over the Q'a (Figure 3.12) with silt dominating in all the areas except SH1. The five soil types of Q'a Shybayqa are: Loam (7.2% of the total cultivated area), Clay loam (10.9%), Silty clay (7.4%), Silt loam (12.6%) and the dominant texture, Silty clay loam (61.8%).

Table 3.3: Laser particle size analysis results of Q'a Shubayqa soil presented as percentage by size fraction

Site Name	Depth (cm)	%Clay	Clay% Weighted average	%Silt	Silt% Weighted average	%Sand	Sand% Weighted average	Weighted average Bulk density (g/cm3)
	0-10	18.27		42.37		39.35		
	10-30	21.93		45.14		32.93		
SH1	30-50	25.40	22.01	33.55	38.86	41.10	39.15	1.01
	50-75	23.10		38.35		38.59		
	75-100	19.75		37.20		43.05		
	0-10	31.60		45.53		22.87		
	10-30	34.90		42.11		23.02		
SH2	30-50	30.93	32.81	41.16	43.82	27.91	23.38	1.01
	50-75	32.67		41.55		25.78		
	75-100	33.27		48.90		17.84		
	0-10	21.42		40.27		38.31		
	10-30	34.40		48.85		16.75		
SH3	30-50	33.70	34.64	43.69	48.36	22.63	17.01	1.06
	50-75	38.64		51.62		9.74		
	75-100	36.86		51.67		11.47		
	0-10	20.97		50.16		28.87		
	10-30	30.41		45.77		23.82		
SH4	30-50	24.86	28.58	52.58	53.50	22.56	17.93	1.11
	50-75	28.02		58.80		13.18		
	75-100	33.69		56.44		9.87		
	0-10	25.34		66.82		7.84		
	10-30	33.32		57.32		9.36		
SH5	30-50	36.39	37.88	56.07	55.52	7.54	6.60	1.09
	50-75	46.75		53.25		0.00		
	75-100	38.86		51.40		9.74		
	0-10	35.88		59.53		4.58		
	10-30	36.97		58.00		5.03		
SH6	30-50	42.93	41.62	49.18	53.32	7.90	5.06	1.23
	50-75	50.81		48.28		0.91		
	75-100	37.41		55.43		7.16		
	0-10	27.42		59.70		12.88		
	10-30	31.79		51.63		16.58		
SH7	30-50	32.34	34.71	60.20	56.78	7.47	8.51	1.21
	50-75	31.21		59.79		9.00		
	75-100	45.37		53.98		0.65		
	0-10	25.94		63.47		10.58		
	10-30	39.99		59.99		0.02		
SH8	30-50	35.00	39.54	49.64	52.49	15.35	7.97	0.97
	50-75	42.99		49.38		7.63		
	75-100	44.82		47.47		7.71		
	0-10	23.60		59.04		17.36		
	10-30	21.10		54.46		24.44		
SH9	30-50	19.42	22.83	49.80	55.39	30.78	21.78	1.27
	50-75	28.59		58.98		12.43		
	75-100	20.89		55.56		23.55		
	0-10	35.53		46.82		17.65		
	10-30	22.30		46.23		31.47		
*OSH1**	30-50	10.00	15.50	25.96	40.41	64.05	44.09	1.44
	50-75	11.21		43.15		45.64		
	75-100	10.74		42.02		47.24		

*: Soil sample from outside the cultivated area of Q'a Shubayqa

Soils with dominant silt percentage usually retain water more than sandy soils and have a floury appearance when dry and a smooth feel when wet (Jaja, 2016). Silty soils would be suitable for large variety of crops including cereals like wheat (Barton, 2013).

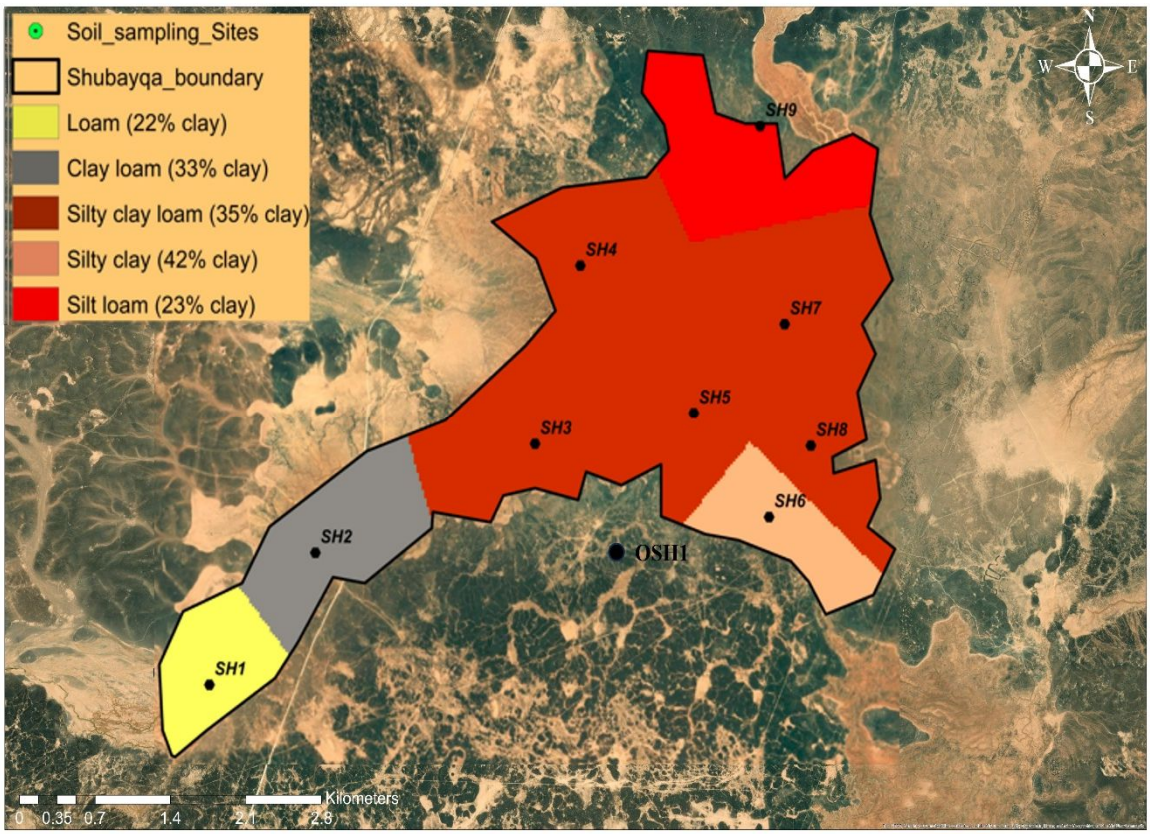

Figure 3.12: Soil texture map of Q'a Shubayqa

If we compare clay content in all Q'a Shubayqa sites (between 22% and 42%) and the clay content of OSH1, which is a soil sample from outside the basin of Q'a Shubayqa (surrounding area), we can notice that clay % in OSH1 is very low compared with soil samples from the basin. This is due to the nature of Q'a Shubayqa soil which is an alluvial soil developed from transported parent materials by floods from Jabal Druz, in contrast to OSH1 soil, which is thought to be a residual soil, developed from local plant material. Bulk density measures (Table 3.3) are moderate and suitable for root growth, penetration and water diffusivity in soil (Stirzaker et al. 1996).

3.3.2.4 Organic matter and major nutrients

Loss on ignition of soil samples shows that organic matter (SOM) in Q'a Shubayqa varies from approximately 4% to 7% depending on the sampling site (Table 3.4). According to the

classification of SOM (Table 3.5) described by Tan (1994) and Theng (1987), the SOM in Q'a Shubayqa lies between medium and very high. These levels are considered higher than usual in terms of soil organic matter observed in similar dryland soils. Bashour et al. (2016) have reported that the soil organic matter levels in most cultivated arid soils in the region of the Middle East and north Africa (MENA), for example in Syria and Lebanon, are less than 1% and could reach 2% in uncultivated virgin lands. These low levels in such cultivated areas in MENA are due to the wide spread of tillage which stimulates high rates of soil organic matter decomposition, also due to the summer bare (tilled) fallow and overgrazing of crop residues (Haddaway et al., 2017).

Table 3.4: Loss on Ignition and soil nutrient analysis results

Sampling Site	Depth (cm)	SOM (%)	Weighted average SOM (%)	Total Nitrogen (%)	Weighted average total Nitrogen(%)	Phosphate (mg/l)	Weighted average Phosphate (mg/l)	pH	Weighted average pH
	0-10	4.51		0.06		15		7.3	
	10-30	4.20		0.03		10		7.3	
SH1	30-50	4.09	4.31	0.02	0.03	20	10	7.3	7.3
	50-75	4.36		0.02		4		7.3	
	75-100	4.44		0.02		6		7.3	
	0-10	5.27		0.06		13		7.5	
	10-30	4.92		0.04		1		7.5	
SH2	30-50	5.88	5.98	0.03	0.03	14	12.3	7.6	7.57
	50-75	6.66		0.03		6		7.6	
	75-100	6.51		0.02		26		7.6	
	0-10	7.31		0.06		16		7.2	
	10-30	7.20		0.04		12		7.2	
SH3	30-50	6.53	6.92	0.03	0.03	17	17.9	7.5	7.51
	50-75	6.72		0.02		9		7.7	
	75-100	7.04		0.02		33		7.7	
	0-10	6.20		0.02		8		7.6	
	10-30	6.52		0.02		13		7.6	
SH4	30-50	6.41	6.74	0.01	0.01	13	10.75	7.8	7.79
	50-75	6.99		0.01		4		7.9	
	75-100	7.12		0.01		15		7.9	
	0-10	7.09		0.02		6		7.5	
	10-30	6.69		0.02		21		7.5	
SH5	30-50	6.72	6.88	0.01	0.01	16	11.25	8.1	7.895
	50-75	6.65		0.01		13		8.1	
	75-100	7.28		0.01		0		8	
	0-10	6.10		0.01		17		7.9	
	10-30	6.56		0.01		5		7.9	
SH6	30-50	6.55	6.52	0.01	0.01	2	4.6	8	7.87
	50-75	6.69		0.01		3		7.8	
	75-100	6.48		0.01		3		7.8	
	0-10	6.73		0.01		1		7.8	
	10-30	7.00		0.01		20		7.8	
SH7	30-50	6.68	6.69	0.01	0.01	23	11.2	8	8.14
	50-75	6.63		0.01		10		8.4	
	75-100	6.51		0.01		0		8.4	
	0-10	6.46		0.01		10		7.9	
	10-30	6.57		0.01		9		7.9	
SH8	30-50	6.91	6.99	0.01	0.01	46	32.75	8.1	8.19
	50-75	7.20		0.00		40		8.4	
	75-100	7.41		0.01		43		8.4	
	0-10	6.27		0.01		19		8.1	
	10-30	6.18		0.01		24		8.1	
SH9	30-50	6.30	6.33	0.01	0.01	31	23.15	8.1	8.025
	50-75	6.46		0.01		17		8	
	75-100	6.39		0.01		24		7.9	
	0-10	5.45		0.02		25		7.9	
	10-30	6.91		0.12		8		7.9	
*OSH1**	30-50	5.65	6.56	0.15	0.14	8	6.45	6.5	6.92
	50-75	6.67		0.22		0		6.5	
	75-100	7.33		0.12		3		6.5	

*: Soil sample from outside the cultivated area of Q'a Shubayqa

Table 3.5: Soil classification based on organic matter content.

Soil organic matter	Rating
>6.0	Very high
4.3-6.0	High
2.1-4.2	Medium
1.0-2.0	Low
<1.0	Very low

Source: Tan (1994)

Several natural factors influence the amount of soil organic matter in Q'a Shubayqa which include topography, soil texture and human interventions. In terms of topography, organic matter accumulation is often favoured at the lowest elevations and usually organic matter is transported to the lowest points in the landscape through runoff and erosion (Quideau, 2002). This phenomenon occurs in Q'a Shubayqa when seasonal floods pour into the Q'a through Wadi Rajel and cover most of the cultivated area **(see section 3.2.3)**.

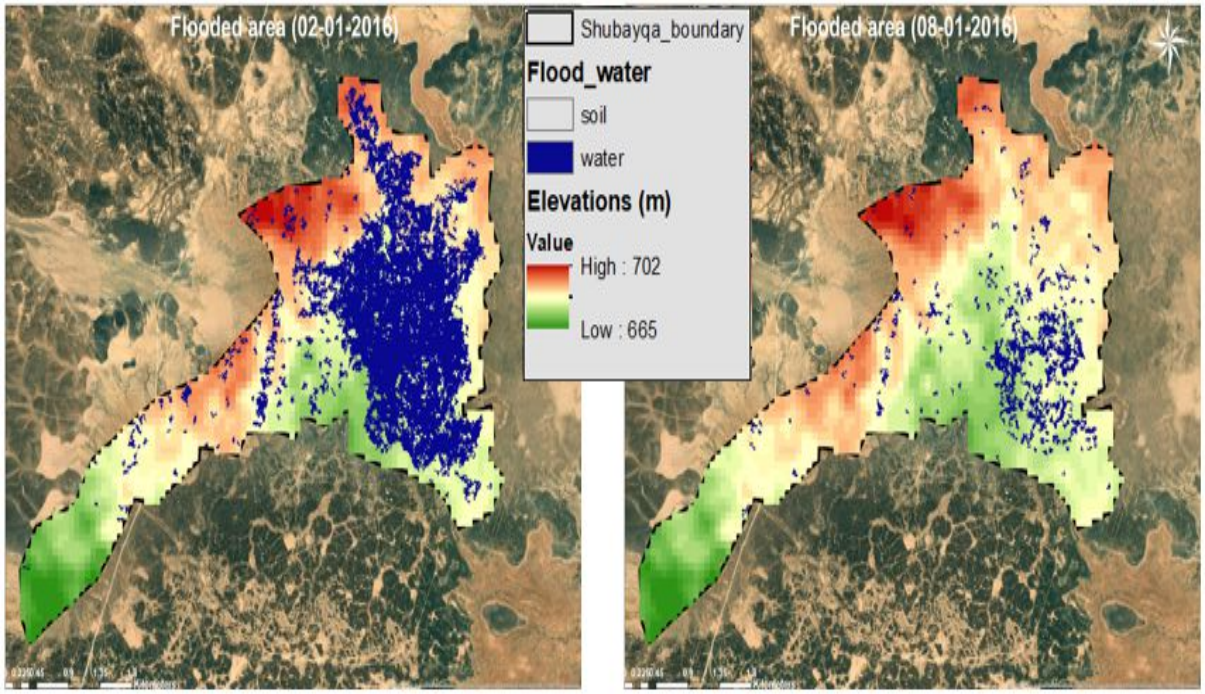

Figure 3.13: Maps showing spatial distribution, accumulation and drainage process of flood water over Q'a Shubayqa land between 02/01/2016 and 08/01/2016 (Landsat 8)

The floods originate in either the Jabal Druz Mountain located in south Syria, or the AShaqif highlands located east of Q'a Shubayqa (Fig. 3.8). The flood water takes from 4 to 6 days to drain and to evaporate (low evaporation rate during winter period) from the Q'a Shubayqa basin (depending on elevation) which gives enough time for the transported particles carried out by floods to settle and sediment on the Q'a surface. Figure 3.13 shows evidence of this phenomenon with two satellite pictures showing flood water accumulation and drainage in Q'a Shubayqa in early January 2016.

Soil texture is an important factor that could affect SOM content in the soil as well. Soils predominated by silt particles and containing high clay content like Q'a Shubayqa (clay between 22% and 41%) tend to have higher amounts of SOM. This mainly depends on two mechanisms: first bonds between the surface of clay particles and organic matter delay the decomposition process and the second mechanism is that when clay content is high, the potential for aggregate formation increases and macroaggregates physically protect organic matter molecules from further mineralisation (Rice, 2002). Otherwise, under similar weather conditions, SOM content in sandy soils is 2 to 4 times lower than clayey soils (Power and Prasad, 1997). Figure 3.14 presents the spatial distribution map of SOM in Q'a Shubayqa created using Kriging interpolation method (a spatial interpolation technique used to estimate values at unmeasured locations based on known values at nearby locations). Using this map, we can see that the highest SOM contents were found in the soil samples where clay content is higher than 34% (SH3, SH5, SH6, SH7 and SH8) with average SOM values more than 6.5%. SH1 where clay content was low (22%), has the lowest SOM among all the sampling sites with only 4.3%. The alluvial soil of Q'a Shubayqa is mainly developed from basalt parent material transported by flooding to the Q'a from the Syrian Heights. These basalt parent materials also influence organic matter accumulation through its effect on soil texture.

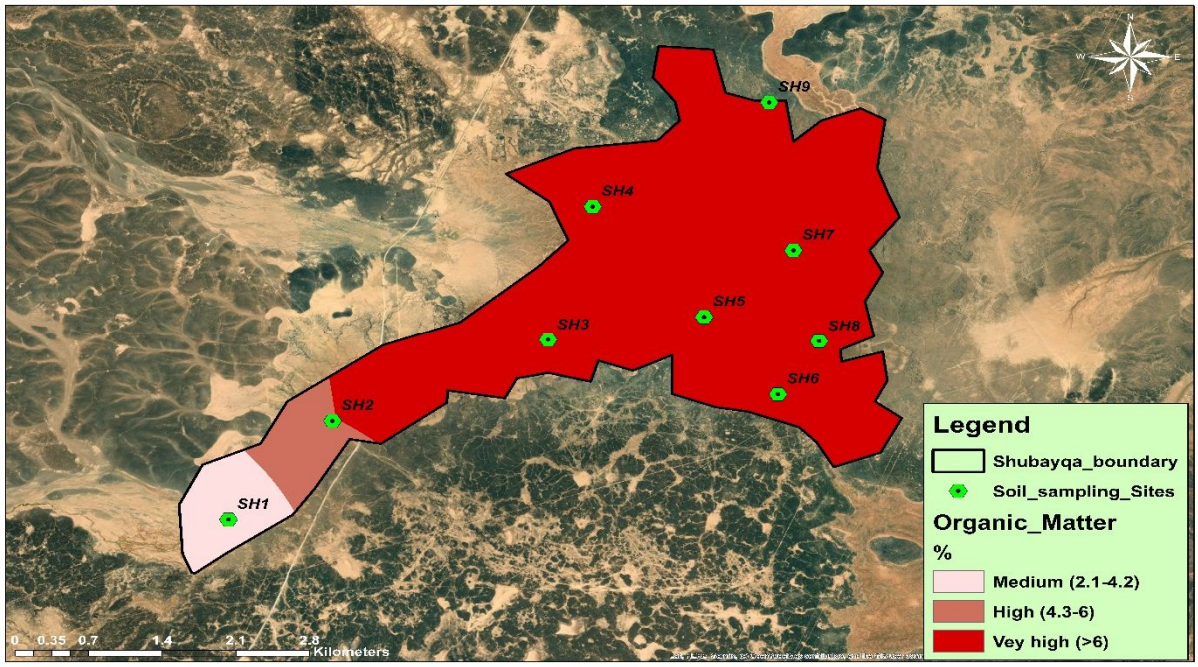

Figure 3.14: Map showing spatial distribution of the % soil organic matter rates over Q'a Shubayqa

Farmers practices in Q'a Shubayqa have also contributed to the increased level of SOM through grazing on the harvested land where manure is returned to the soil **(**see sections 3.4.2.4 and 3.4.2.5). In addition, tillage practices in Q'a Shubayqa are low with just two per season, which contribute to minimising aeration and decreasing SOM decomposition processes by keeping soil microbes in an anaerobic environment. Farmers also use bare fallow after harvesting which helps soil to regenerate its original state of productivity. The cereal-based monoculture system in Q'a Shubayqa could reduce microbes in soil leading to lower SOM decomposition rates. The latter practice contributes to maintaining the SOM levels in the soil by reducing the decomposition process but does not contribute to restoring the SOM in Q'a Shubayqa where the main source of organic matter is particles transported by seasonal floods. Since these floods are rare and less frequent over the last decade **(see section 3.4.2.6)**, farmers need to think about farming practices that could restore the SOM in Q'a Shubayqa sustainably.

Figure 3.15 presents the spatial distribution of the total nitrogen content in Q'a Shubayqa soil. Nitrogen is the most essential element for the normal growth of plants, especially cereals (Sinclair and Rufty, 2012). All vital biological processes of a plant are related to the existence of nitrogen which is a basic constituent of functional plasma. In addition, nitrogen is a basic element in plant metabolism (Defoer et al., 2000). Total Nitrogen amounts in Q'a Shubayqa, which is the sum of nitrate (NO_3), nitrite (NO_2), organic nitrogen and ammonia, range between

very low to medium according to Tan's (1994) classification . The map shows that the soils of the eastern area of Q'a Shubayqa have the highest amounts of Total Nitrogen up to 0.06% (land around SH1, SH2 and SH3). According to Cattaneo et al. (2014), Lal et al. (2011) and, Woźniak and Soroka (2015), cereal-based cropping systems affect soil quality by intensively decreasing organic matter, organic carbon and total Nitrogen contents. This was obvious in Q'a Shubayqa soil, in particular total nitrogen, where total nitrogen % in OSH1(uncultivated lands) is 5 to 10 times higher than total nitrogen amounts in the cultivated ones (Table 3.4). Organic matter contents are still higher and can reach 7.3% in cultivated lands due to seasonal floods.

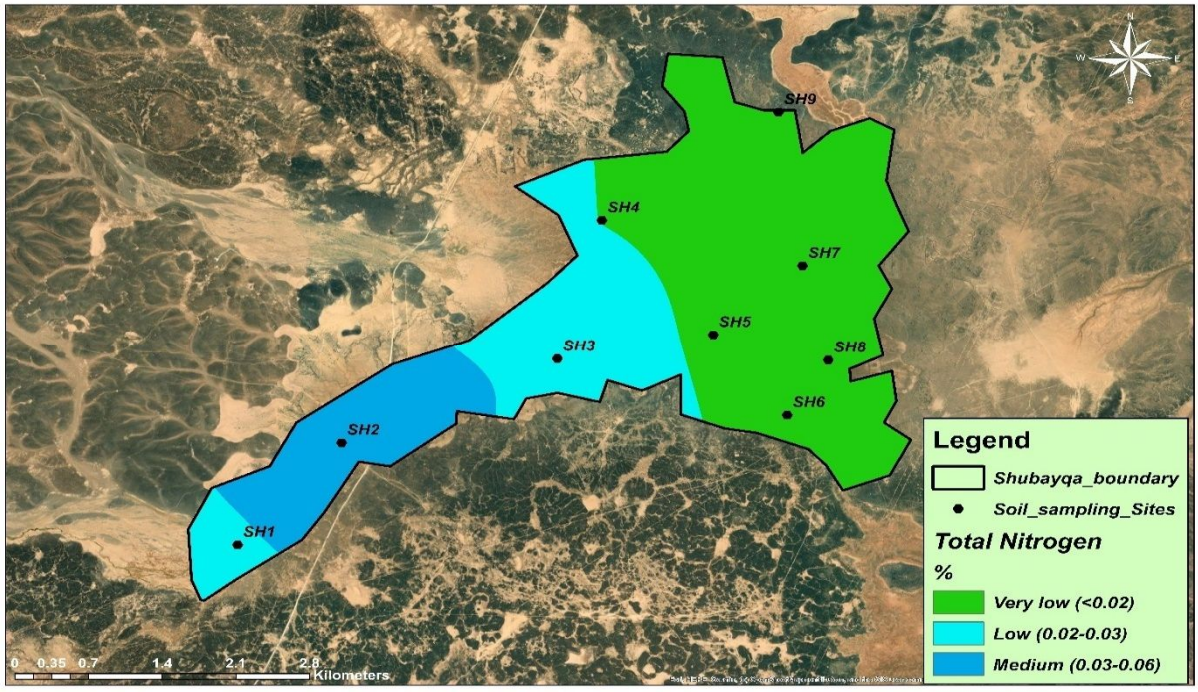

Figure 3.15: Map of spatial distribution of Total Nitrogen rates over Q'a Shubayqa

Phosphate is commonly a limiting nutrient required for plant growth and development (Razaq et al., 2017). In Q'a Shubayqa soil, Phosphate contents are low (between 4 and 32mg/l) and its availability depend on soil type. The organic form of phosphorus is released by a mineralisation process involving soil micro-organisms. This process is accelerated in warm well drained soils (not the case for Q'a Shubayqa). The solubility of the inorganic phosphorus compounds affects the availability of phosphorus for plant uptake. Solubility is highly affected by soil pH. In alkaline soil, like Q'a Shubayqa, inorganic phosphate rarely becomes available for plant uptake because in such conditions, phosphate tends to precipitate with calcium.

Soil pH is a key factor that intervenes in controlling availability of nutrients, microbial activity and crop productivity and yield quality. According to the pH tests on Q'a Shubayqa soil

samples (Table 3.4), soils vary from slightly to moderately alkaline with pH ranging between 7.5 and 8.4. Generally, drylands are known for their high pH level because of the dry climate which contributes to the retention of many alkaline base cations in soil. However, increased precipitation enhances the leaching rate of these base cations (Chytrý et al., 2007). Such pH levels are favourable for microbial activities that contribute to the decomposition of the organic matter and enhance the availability of nitrogen, sulphur and phosphorus in soils (Arnold et al., 1998).

3.4. Farming system

3.4.1. General overview

Bedouin today use the lands of Qa Shubayqa (Figure 3.16) to cultivate, mostly, barley and wheat and sometimes sorghum (when precipitation exceeds 100mm/year) under rainfed conditions i.e. without using irrigation systems.

Figure 3.16: Photos from the cultivated area in Q'a Shubayqa from field work in December 2019

This farming system depends totally on the floodwaters and soil materials from the runoff that flows from the surrounding highlands (Jabal Druz and Al-Shaquif). Floodwater that reaches Q'a Shubayqa through the main wadis (Rajel and Selma) is diverted onto cropped land using a network of natural water channels distributed all over the Q'a (see Figure 3.9, Figure 3.13).

These water channels are then filled with water powered by the floods causing temporary submergence of the surrounding land by floodwater and giving crops what they need. In Q'a Shubayqa, no irrigation system is adopted, not even a water harvesting system.

Furthermore, the agriculture system in Q'a Shubayqa is an integrated system; farmers are primarily livestock breeders as they have extensive and rich rangelands for grazing over the year. They also profit from livestock manure left on the soil surface during grazing which should improve the soil quality by providing nutrients and increasing soil capacity for water retention. According to their statements during the field work, farmers believe that the livestock contribution to the cropping system is significant.

The harvesting season starts normally in late spring and early summer, the yield depends on the precipitation of the cold season and the seasonal floods timing and frequency, but generally the yield is much lower that yields of wetter lands. However, no fertilizers or pesticides are used on crops in this area.

3.4.2. Survey outcomes

A survey was undertaken with a sample of 25 farmers from Q'a Shubayqa. The questionnaire (Appendix A) contained several sections investigating different relevant subjects targeting information about natural resources, agricultural practices (cultivated species and varieties, planting dates, harvesting date, livestock, etc.) and to identify the main limiting factors and current challenges, including climate change impacts, on crop production from the perspective of Q'a Shubayqa farmers.

3.4.2.1 General information about farmers

In this section, questions were designed to understand the personal situations of the 25 participant (male) farmers. The questions were about the farmers' age, living location (to understand the accessibility of this land) and visit frequency per season. Other questions were about if the farmer had a second job besides farming, the location of his land on Q'a Shubayqa's map and situation of land tenure (owner or renter). Results are shown in Figure 3.17.

The answers show that 52% of farmers are between 41 and 60 years old and 64% have a second job besides farming and the rest depend on farming only. 70% of farmers with no second job are herd owners. All farmers live outside Q'a Shubayqa with 52% of them in Safawi village

24km away (nearest urban area to the Q'a). The rest live in the surrounding villages located in the north Badia at the edges of the Amman-Safawi Road (150km away) due to second job commitments, which prevent most of them who lives away from doing a periodical visit during the season to check the plant growth, flood state and to protect it from intruders such as other herd owners. All the farmers own their lands and belong to the same clan (Al-Shuroufat) and according to them, there is a very restricted rule agreed inside the clan that prevents selling land to people who don't belong to that clan. 80% of the farmers are considered as a small holders, owning less than 10ha of cultivated land (FAO, 2013).

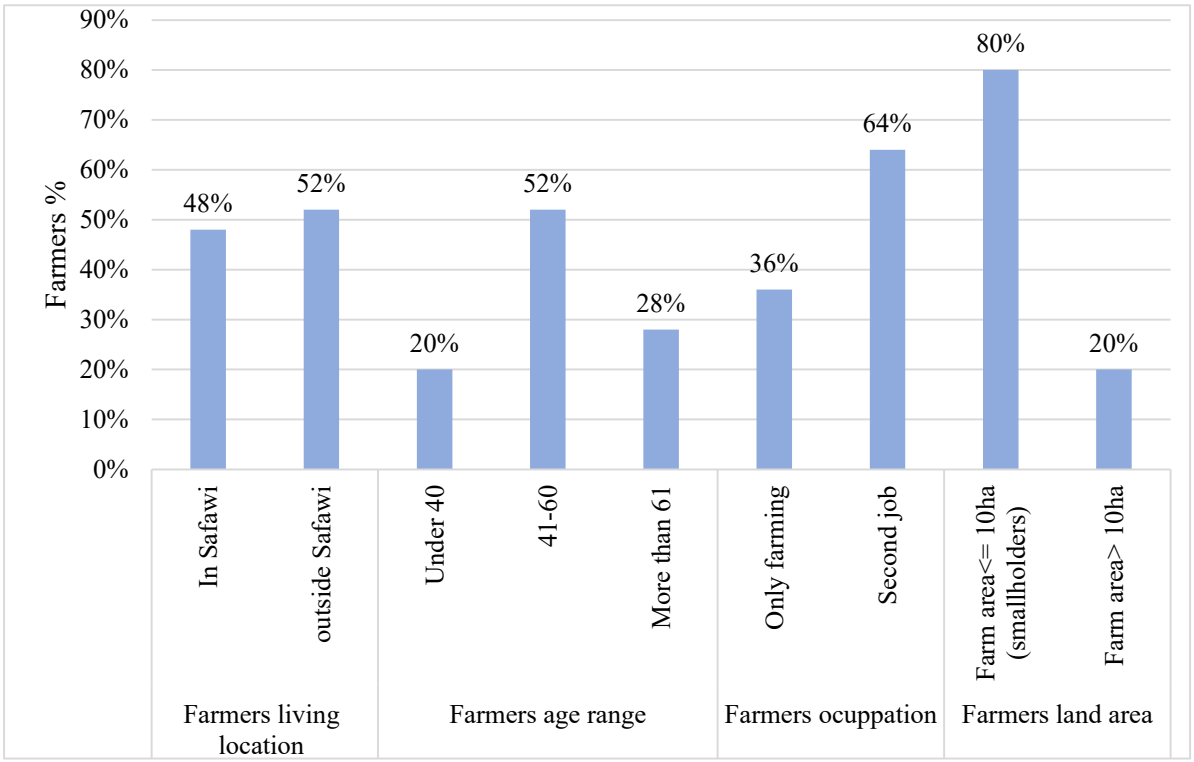

Figure 3.17: Interviewed farmers answers on basic demographic question and land question

These small-scale farms are a result of the inheritance system where land is usually divided between successors and not just passed to the eldest. Farmers were able to approximately locate their own lands on the Q'a Shubayqa map (Figure 3.18). We found out that farmers split Q'a Shubayqa into 3 regions with different local names as presented in Figure 3.18. According to farmers, these local names were inspired by different factors like yield quality, ground elevation and names of wild weeds that grow in the area. For example, the Maftas area is called this due to its low elevation where flood water can persist for several days and cause plant death. Maftas is a local Arabic word meaning 'the drowning area'.

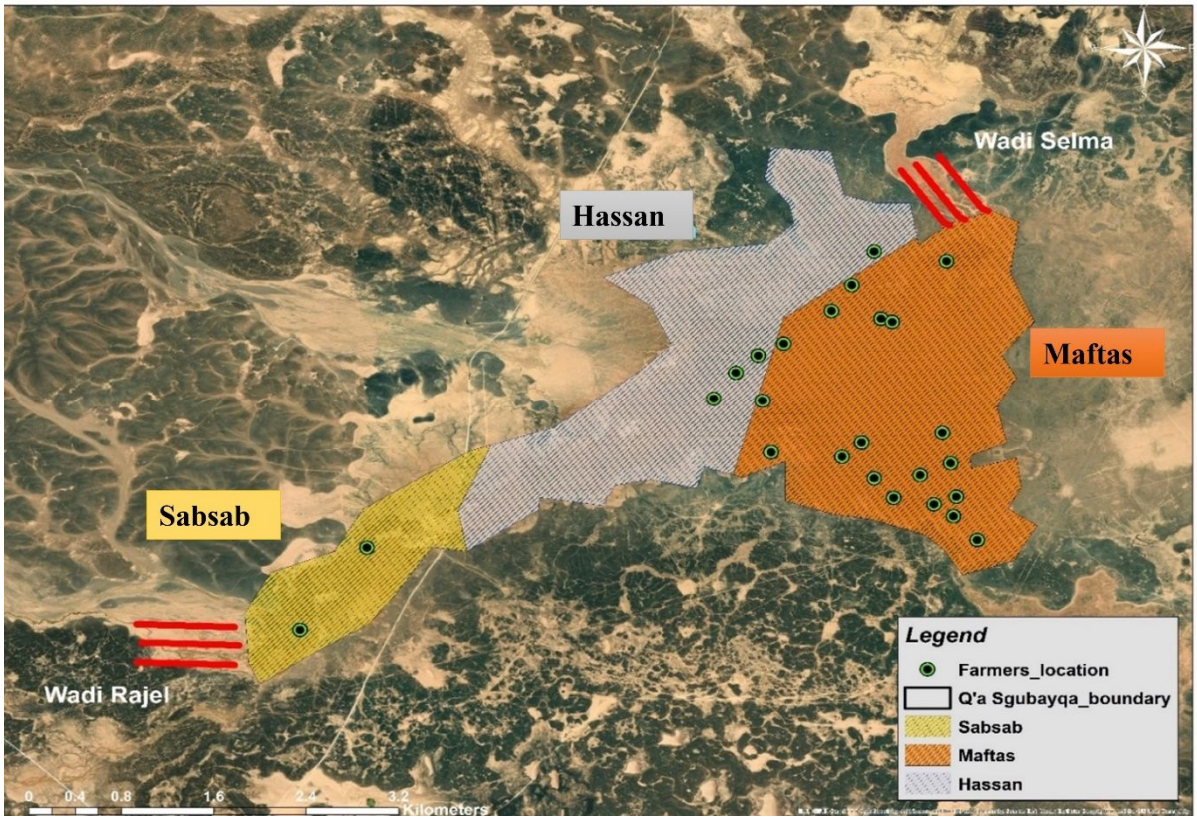

Figure 3.18: Map representing spatial distribution of participant farmers lands and locally named areas (Sabsab, Hassan and Maftas) of Q'a Shubayqa.

3.4.2.2. Farming background and agricultural practices

The questions in the second section were about farming background and agricultural practices. According to the farmers answers, Q'a Shubayqa is a rainfed agricultural system depending mainly on seasonal floods that come to the Q'a through two main wadis (wadi Rajel and wadi Selma) (Figure 3.18) and direct precipitation. There are two types of farming system adopted in this area: arable crop production (68% of farmers) and mixed systems (32%) (Figure 3.19). The latter is a mixture between crop production and livestock rearing (mainly sheep and goats). According to farmers, the main cultivated crops in Q'a Shubayqa are wheat and barley. Sorghum is also cultivated but under specific circumstances such as delayed floods or after wheat and barley crop death due to high magnitude or long period floods. Most farmers (54%) grow only wheat as a monoculture, 25% of them cultivate wheat and barley but they declared that the choice between these two species depend on the timing of the floods. If floods reach the Q'a early in the growing season (October or November) the farmers cultivate wheat, otherwise, they grow barley if floods are late (December or January). Floods make the large

cracks in the soil (Figure 3.20) caused by summer dryness disappear which makes tillage easier, and seeds will not get lost into them. Farmers believe that early rainstorms alone would not make the soil cultivable. Under such conditions, the sowing date of wheat and barley could vary from late September to end of November. Depending on their experience from previous seasons, farmers confirmed that planting wheat in late season usually results in lower grain yield. Only 25% of farmers cultivate sorghum as an alternative to wheat and barley (see above). Farmers say that sorghum cultivation depends on flood timing because in particular drought seasons, the floods arrive late in March or April and to save the season, farmers cultivate sorghum to profit from these late floods. Otherwise, they cultivate sorghum after the failure of wheat and barley crops due to waterlogging caused by continuous wet conditions, especially in lower elevation lands (Maftas). After maturity and canopy growth, farmers don't harvest the sorghum, they usually feed it to their herds by direct grazing. Farmers who don't own livestock sell the sorghum to herd owners of the area. The previous information has confirmed that farmers there is no crop rotation system adopted by any farmers in Q'a Shubayqa.

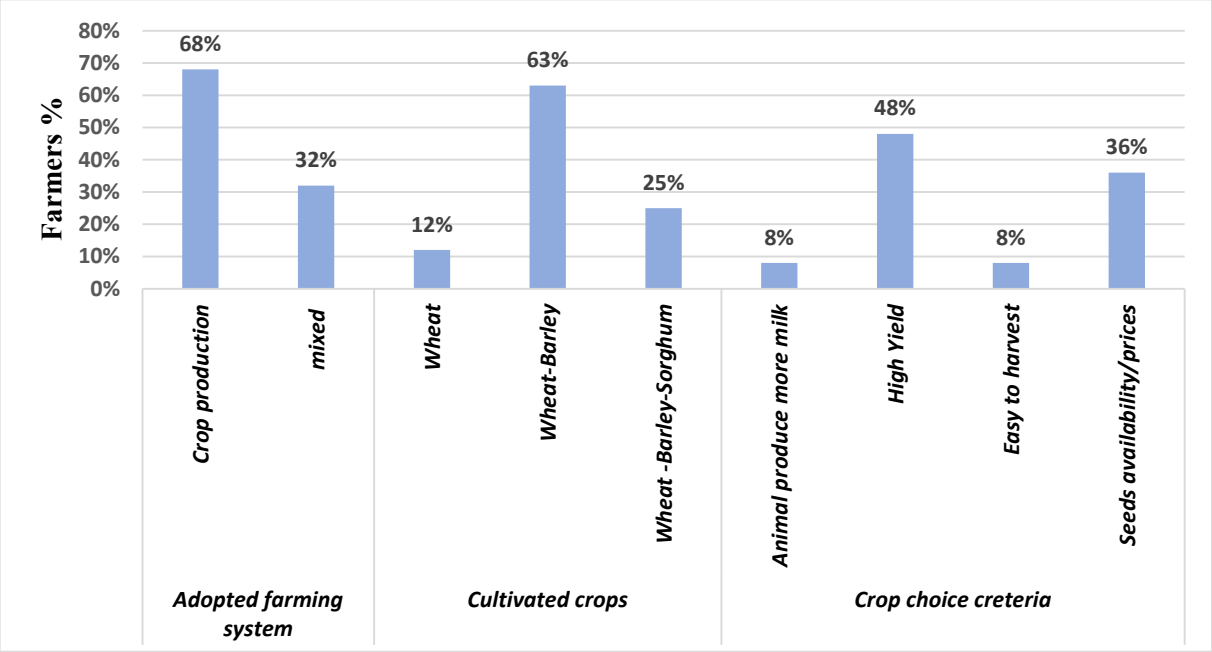

Figure 3.19: Statistics of interviewed farmers presenting information about farming system and cultivated crops in Q'a Shubayqa

We also asked the farmers about their criteria for choosing cultivated crops (wheat, barley and sorghum) and specific species of these. 48% said that the reason is high yield productivity and for the financial profit of these crops, while 36% identified seed availability in the area and low

seed price as the main reasons. Only 8% said the reason of doing wheat, barley or sorghum is to feed their livestock and the other 8% believe sorghum is easier to harvest than other crops. Farmers said that during drought seasons and when the grain yield and the canopy heights are low, they usually don't harvest barley and wheat crops, but they make their animals graze it or they sell it to herds owners as a grazeland. All farmers buy their seeds from a known seed trader located in Mafraq. They don't conserve seeds anymore because it became available from grain traders.

Figure 3.20: Pre-floods Q'a Shubayqa soil showing large cracks (by Khalid Al-Masaeed)

The sowing rate of wheat and barley in Q'a Shubayqa ranges from 50kg/ha to 120kg/ha depending on the farmers decision. 44% of farmers use sowing rates that range between 60 to 90kg/ha and 36% use sowing rate more than 90kg/ha. The rest use low sowing rate of less that 60kg/ha. Most of farmers (68%) use a seed spreader as a sowing tool and the rest do it manually (Figure 3.21).

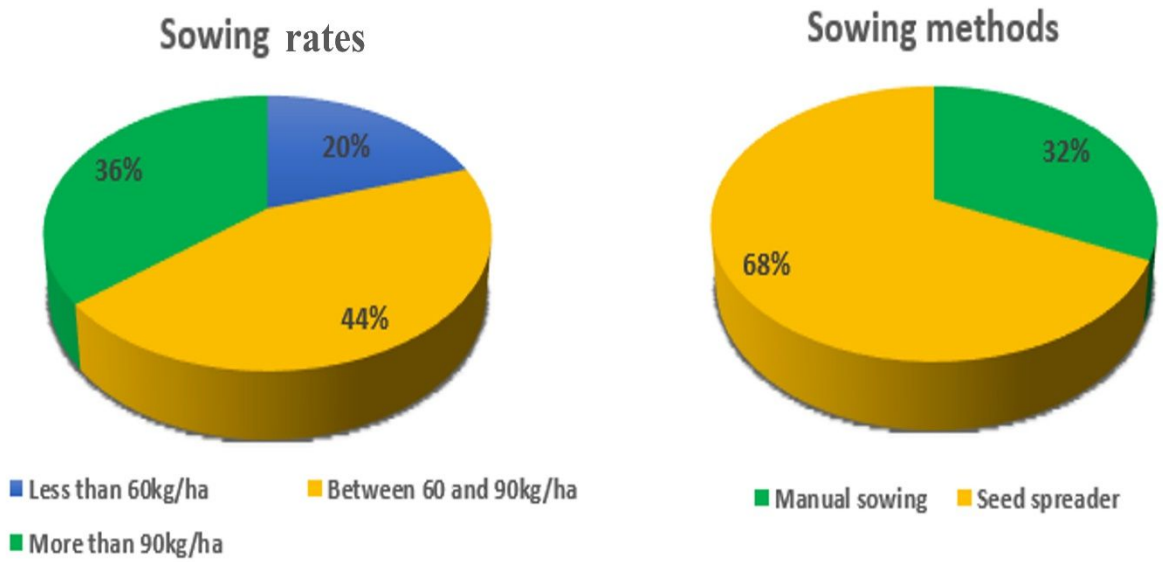

Figure 3.21: Statistics on sowing rates and methods used by farmers

To prepare the seedbed, farmers use a chisel plough (straight point) for soil tillage (Figure 3.22). Besides its main role to plough the soil, this tool creates trenches in the soil to facilitate the runoff of flood water and avoid soil waterlogging. According to farmers, they only need two surface tillage operations, before sowing to remove cracks and prepare the seedbed and after sowing to cover the seeds. The sowing and the tillage processes can be done in one day, just a few days after the floods to profit from the soft moist soil and the disappearance of the cracks. Wheat and barley harvesting is usually done by a harvester (Figure 3.22) between mid-May and mid-June (according to the sowing date). According to old farmers, mechanical tools like seed spreaders, tractors and harvesters were not available in the past, all the practices were carried out by hand or by using cattle.

Figure 3.22: Tillage and harvesting tools used in Q'a Shubayqa (Khalid Al-Masaeed)

According to the farmers statements, the quantity and the quality of harvested grain yield by the end of the season depends on several factors. First, the flood frequency where farmers think that three flood events during the season with time interval of at least one month are enough to produce a good yield. A second factor is the location of the land in the Q'a and a third factor is the occurrence of sudden harsh climate events like frost and heat waves that can threaten yield quantity and quality.

3.4.2.3. Crop production

According to the farmers responses, wheat and barley average grain yield in normal (free stress) seasons varies from 700kg/ha to 2500kg/ha. A spatial distribution map of grain yield for wheat and barley was created using the Kriging interpolation method of ArcMap tools box (Figure 3.23). The map shows that there is a spatial variation of grain yield where the better drained Sabsab and Hassan areas have higher harvested yields of wheat and barley than Maftas (section 3.4.2.1, Figure 3.18).

All farmers in Q'a Shubayqa denied using any fertilizers or any pesticides. They believe that Q'a Shubayqa soil is very fertile and there is no need for expensive fertilisers. Pesticides are not used because no diseases appear during the season. Added to that, weed management by chemicals is absent because farmers think that the weeds that grow in Q'a Shubayqa do not affect crop growth or grain yield.

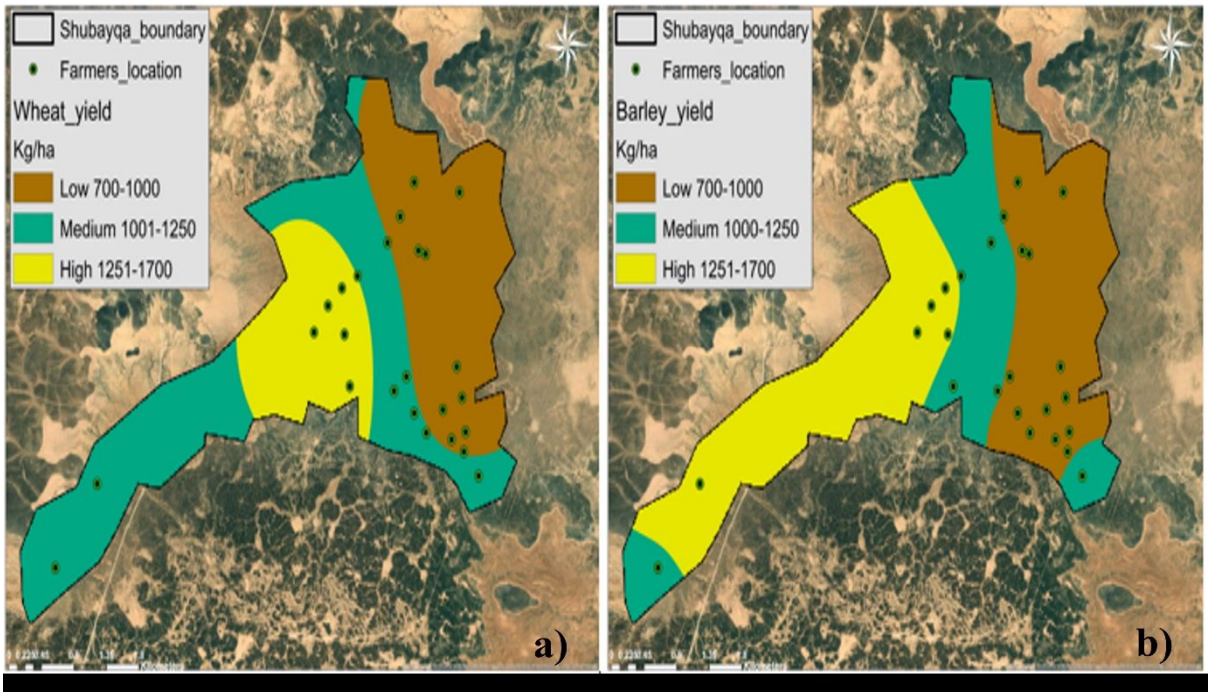

Figure 3.23: Map a) represent spatial variation of wheat yield and map b) represent spatial variation of barley yield across Q'a Shubayqa

The name of wheat and barley cultivars planted in Q'a Shubayqa are unknown by the farmers. They use local names to identify these cultivars. During my field work in June 2022, I visited local authority offices in the Jordanian north Badia like the Directorate of Agriculture in Mafraq and talked to crop production engineers regarding the farming system in Q'a Shubayqa. I found out that they didn't have any knowledge about the existing farming system in this area and they confirmed that they have no official records or information about it such as information about farmers, yields, cultivated varieties, farming practices. However, I went to the National Agricultural Research Centre- (NARC) located in Amman where I met the director Dr. Nizar Haddad and two senior researchers in field crops (Dr. Faddel Ismail and Dr. Khaled Aboulaila). They also confirmed that they didn't have any previous research conducted in Q'a Shubayqa or any recorded data. The only way for me to identify the varieties was to collect samples of cultivated wheat and barley plants from the Q'a. The samples that I collected in June 2022 (Maturity stage) were sent to the senior researchers of NARC and they were able to identify the scientific names of these cultivars (Table 3.5).

Table 3.5: Wheat and barley cultivars cultivated in Q'a Shubayqa

Crop	Type	Local cultivar name	Conventional cultivar name
Wheat	Durum wheat	Baladi	Ascad 65
		Gatmah	Hourani
Barley		Bethar	Rum
		Baladi	Muta'a

3.4.2.4. Soil and water resources

In the third and the fourth section of the questionnaire, the questions were designed to investigate the natural resources (soil and water) situation in Q'a Shubayqa. Farmers believe that Q'a Shubayqa soil is very fertile and has a strong water holding capacity because it is mainly alluvial, transported by seasonal floods usually with high levels of organic matter. In addition, farmers think that livestock manure added to the soil during grazing is a second important factor that contributes to improving soil fertility.

However, farmers have confirmed that soil types in Q'a Shubayqa vary from one region to another. According to the farmers water drainage in area such as The Maftas (Figure 3.18) takes more time than the other parts of the Q'a. Usually, farmers need to plant the soil for a second time if major floods occur. The Hassan area located in the centre of the Q'a is the best cultivable land of Q'a Shubayqa according to farmers because of its soil quality and higher elevations. Sabsab is the western part of the Q'a and is known for moderate productivity (Figure 3.18).

As described earlier, the only water resources in Q'a Shubayqa are floods and rainfall. There is no irrigation system, water harvesting system, or wells. Farmers affirmed that they are facing a great challenge with reduced flood frequency and magnitude because of the Abu-Zeriq dam located on the Jabal Druz mountain in Syria. They think that, since this dam was built in the 1970's flood event frequency has decreased and become insufficient to irrigate the cultivated soils, especially lands located at the edges of the Q'a.

3.4.2.5. Livestock and rangeland

The survey indicates that the approximate number of livestock in Shubayqa is between 8000 and 10000 head. Sheep are the majority of livestock and according to farmers, the impact on the cropping system is advantageous because of their manure. Farmers-herd owners in Shubayqa stated that the grazing period starts from April until July during productive seasons where they profit from crop residues after harvesting. Further, they buy crop residues of harvested lands from neighbours for grazing. In the last decade, livestock owners have noticed a decrease in vegetation cover in the Shubayqa rangelands, the extinction of several plants including medicinal plants and the appearance of poisonous plants (come with cereal seeds). This has probably been associated with an increase in the number of livestock, although the farmers did not state this directly.

3.4.2.6. Climate change impact on Q'a Shubayqa farming system

The final section of the questionnaire was about climate changes during recent decades noticed by the farmers and the impact of these changes on farming system productivity and natural resources sustainability. Figure 3.24 shows information about farmers' answers regarding observed long-term changes in seasonal weather variables. Most of the farmers (24) stated that increased temperature is the most noticeable weather change observed in Q'a Shubayqa, the second change was in the number of rainfall storms which have decreased together with the rainfall intensity. They also noticed a delay in the first seasonal floods.

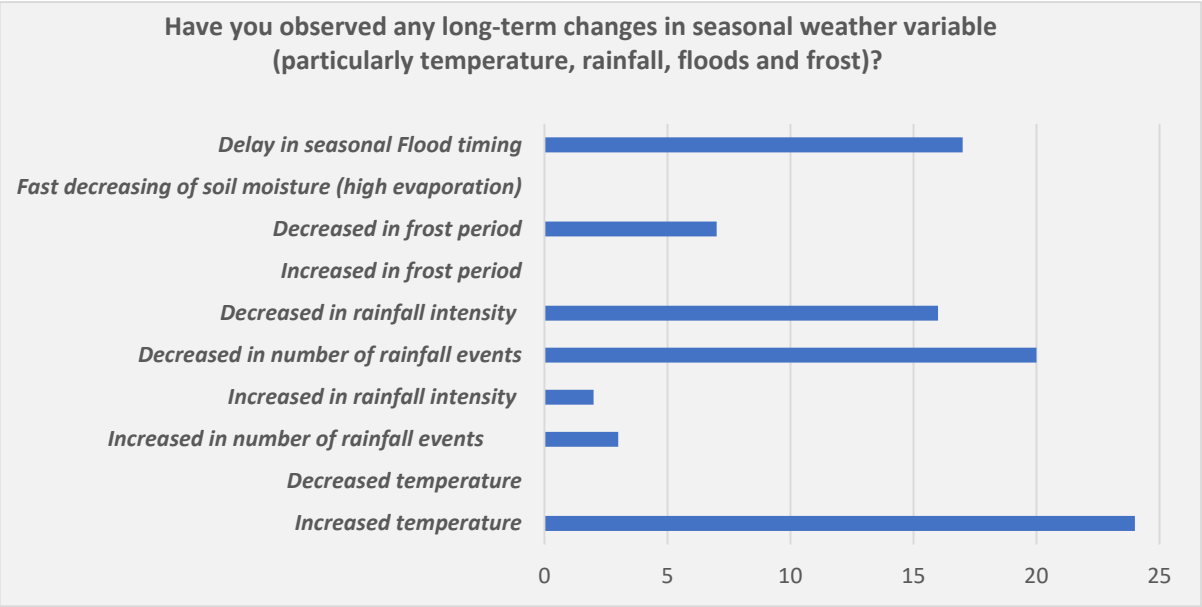

Figure 3.24: Farmers (25) perspectives regarding long-term changes in weather variables

Another question was asked about the vulnerability of the agricultural practices in relation to several factors. Figure 3.24 shows that farmers think that factors like flood shortage, decreased rainfall and drought have had major impacts on farming practices in recent seasons. Furthermore, they think that farming practices are also vulnerable to increased temperature and changes in rainfall timing.

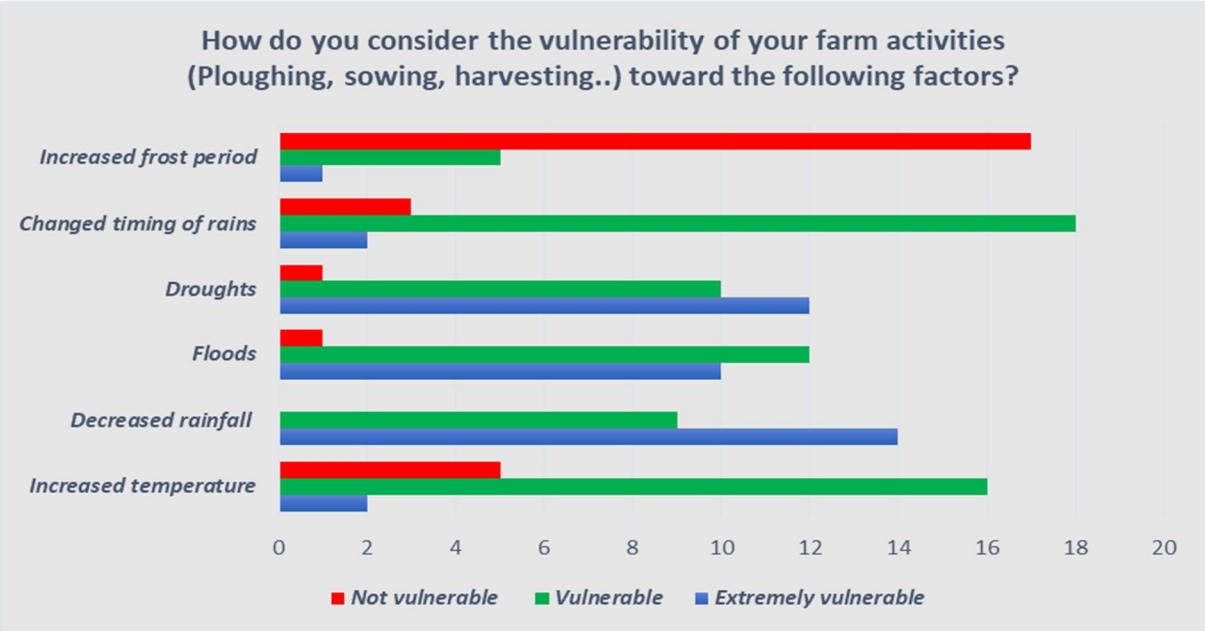

Figure 3.24: Farmers (25) perspective regarding farming practices vulnerability to weather

Figure 3.25 illustrates farmers perspectives regarding the severity of climate change impacts on crop production in Q'a Shubayqa. Farmers noticed that increased frequency of drought and crop failure, heat waves during the spring (anthesis period) and rainfall timing are the most observed changes that have been affecting grain yield and crop growth.

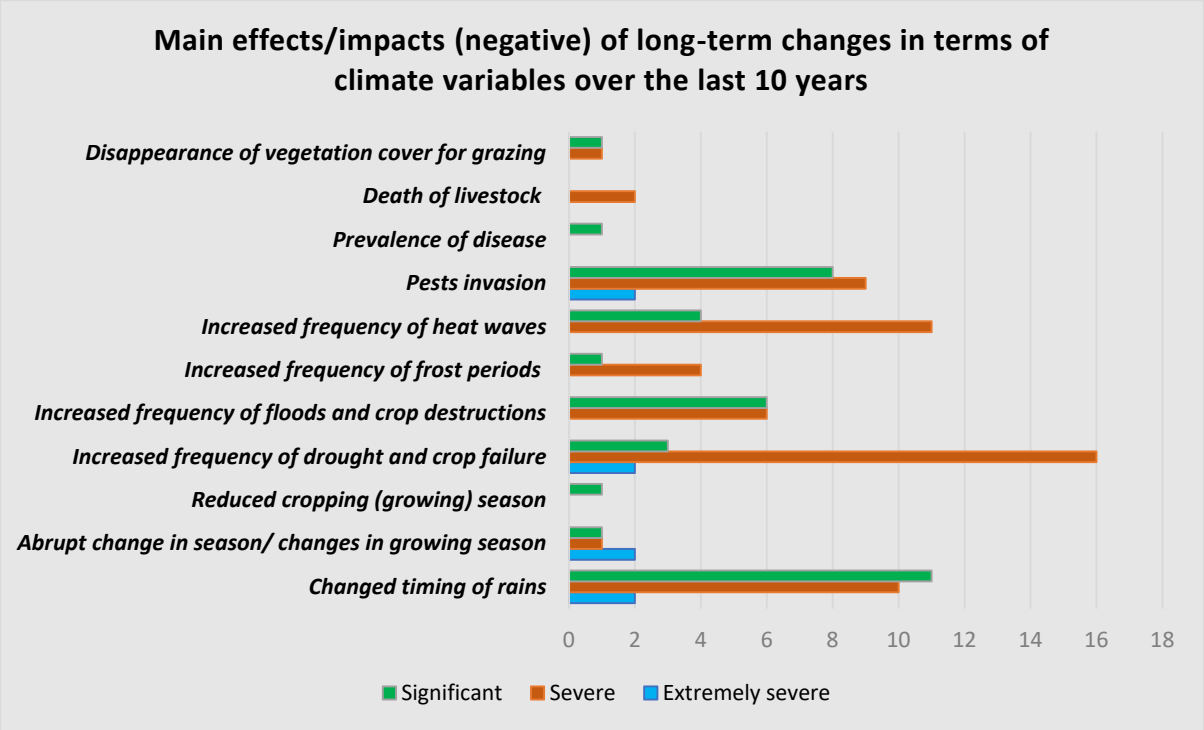

Figure 3.25: Consequences of changing climate patterns observed by Q'a Shubayqa farmers

3.5. Interpretations and conclusion

This chapter provided a description of the different environments and agricultural systems by geographical hierarchy of the study area from the largest scale (Jordan), through ecological scale (Azraq basin) to the local scale (Q'a Shubayqa).

Q'a Shubayqa is rare, in that crop production here depends on surface water and has shown some resilience in its farming system. According to the information provided in the survey, we can conclude that the agricultural system in Q'a Shubayqa is complicated, where several factors interact to shape its specificities. These vary from environmental factors like climate type, seasonal floods and the topography of the area, to human intervention factors like farmers agricultural practices. The environmental factors have contributed together to produce advantageous conditions for the existence of a resilient sustainable agricultural system, for millennia. Seasonal floods take place 2 to 3 times a year, from sowing dates in October to the harvesting date in early June. In addition to being the most important sources of water, floods

also transport soil particles and organic matter to the Q'a from upstream. According to the soil analysis, the repetitive flooding contributes to transforming Q'a Shubayqa soil from residual soil (see above) to sedimentary alluvial soil. The topography of the area has an important effect on the soil types and the farming system, where Q'a Shubayqa is considered as a flat playa (small basin) where flood water remains for several days and covers almost all the cultivated area before being drained to the wadis that lead to the Azraq Basin.

Although these factors that have contributed to create a regenerative and sustainable farming system, the dryland cropping system is still fragile and risky, as pointed out by the modern-day farmers themselves, due to climate hazards like drought, flood delay, heat waves and unsustainable agricultural practices. The Q'a Shubayqa farming system is an opportunistic system based on intensively exploiting natural resources, which is however 'environmentally friendly' (e.g. no chemical fertiliser use). The result is a system that remains sustainable under particular conditions.

Farmers believe that producing cereals is less effort and more productive than other crops like legumes, which could help with soil fertility (see Chapter 8 for further discussion), and that the flood derived muds, rich with organic matter and nutrients, are a sufficient source to regenerate the soil, improving its quality and enhancing nutrient cycling.

There is evidence however that the farming practices are impacting the potential fertility of the soil. Total nitrogen in Q'a Shubayqa soils is much lower than uncultivated soils outside the Q'a (Table 3.4) which could be due to the adopted cereal-based monocropping system. Jones et al. (2021) have made a comparison in terms of organic content between Q'a Shubayqa and two other basins located in western south Badia of Jordan and near to the Azraq Q'a. These two basins (Q'a Qattafi and Q'a Wisad) have the same topographic characteristics as Q'a Shubayqa and are considered as a flat playa (small basins), but no crop cultivation or agricultural practices in these lands in contrast to Q'a Shubayqa. The comparisons have shown that the organic content in the uncultivated Qattafi basin is higher (10%) than Q'a Shubayqa. Based on farmers statements about grain yields (Figure 3.23) during the survey, we can notice that there is a match between land with the highest grain yields and land with highest total nitrogen content (Figure 3.15).

Farmers have noticed changes in weather during the last decades. These changes like heat waves, flood delays, drought and rainfall shortages have an important impact on crop

development and harvested yields according to the farmers. The next chapters of the thesis will further investigate these changes, using quantitative methods to evaluate the climate change impact in the previous decades, and to quantify water resource change using hydrological modelling. These analyses can then be used to predict future potential climate change impacts and assess potential management strategies to face such challenges in the near future.

Chapter 4: An overview of historical climate trends in the Shubayqa region

4.1. Introduction:

Climate change impacts on agriculture, the hydrological cycle, ecosystems and humanity have become more remarkable and evident during recent years (Hausfather, 2023). The frequency and intensity of extreme weather events, such as extremely high temperatures and heavy rainfall, have increased over terrestrial regions giving rise to more compound extreme events (simultaneous or successive climatic events) and hydroclimatic hazards (flash floods, wildfire and drought) (Contractor et al., 2021; Lloyd & Shepherd, 2020; Wartenburger et al., 2017; X. Wu et al., 2021). However, the spatial and temporal patterns of these changes are not identical across the globe and vary considerably with the atmospheric circulation and the underlying surfaces at a regional or local scale (Ji et al., 2014; Portmann et al., 2009). Hence, it is important for this study to understand climate change and its consequences in Q'a Shubayqa during the recent past and to better understand its potential impact on the existing agricultural system.

Q'a Shubayqa belongs to the driest lands of Jordan which make it sensitive to climate change and an ecologically vulnerable area. Based on the undertaken survey (Chapter 3), farmers reported that during the last three decades, the area has experienced increasing climate stress, affecting crop growth and productivity. In addition, farmers confirmed a notable shortage of water resources and temporal variations in the waters arriving at the Q'a from upstream (i.e. Jabal Druz) (see Chapter 3, section 3.4.2.4). This chapter aims to investigate the climate patterns during this period, between 1985 and 2021, in Q'a Shubayqa and the surrounding region and the associated climate extreme events.

4.2. Material and methods

4.2.1. Precipitation and temperature data

Daily weather data from two stations were obtained for use in this analysis. Precipitation, minimum and maximum temperature were recorded at the Safawi/H5 meteorological station located in the north-east of Jordan at Safawi village (Longitude: 37.18, Latitude: 32.31, elevation=738m; 26km from Shubayqa) and obtained from the Water Authority of Jordan. Precipitation data recorded at the Ein AlArab meteorological station located on Jabal Druz (Longitude: 36.67, Latitude: 32.62, elevation=1557m) in south-west Syria were obtained from the Directorate of Agriculture and Agricultural Reform in Sweida, Syria. Daily data are available for the period between 1985 and 2021.

Although Safawi is outside the Q'a Shubayqa basin and precipitation in such areas (drylands) can be very localised, this site was chosen because it is the nearest station to Q'a Shubayqa. Precipitation data from Jabal Druz is used in relevant extreme indices analyses in addition to precipitation data from Safawi, because according to farmers statements, the flash floods originating in Jabal Druz flow into Q'a Shubayqa and are the main source of water for crop growth and development. Using gridded meteorological data products can provide longer time series, but they are based on model estimations, averaged across grid cells, and so the original local data were preferred for use here.

4.2.2. Extreme indices analysis

Studies have shown that some climate extremes will become more frequent, more widespread and more intense during the 21st century (IPCC, 2023). To measure potential changes there is now a need for descriptive indices, based on climate variables, to be used for temporal evaluation of the extremes behaviour including frequency, amplitude and persistence (Chen et al., 2014). For this purpose, the joint World Meteorological Organisation Commission on Climatology (CCI) and the Climate Variability and Prediction (CLIVAR) Expert Team on Climate Change Detection and Indices (ETCCDI) has worked to produce climate indices and software to aid collaborative international research (Karl et al., 1999; Peterson et al., 2001). A core set of 27 indices has been developed by the ETCCDI to standardize the definitions and analysis of extremes (Klein Tank et al., 2009). Improvements have been made to the indices over recent years (Peterson et al., 2008), and these have been incorporated into the RClimDex software used to calculate the indices.

Here, such climate indicators are used to demonstrate how the climate and the frequency and intensity of extreme weather in Q'a Shubayqa and the surrounding area has been changing. Among the 27 ETCCDI indices, those related to temperature and precipitation are employed here as they are considered the most important in causing variation in the hydrological cycle (Dinpashoh et al., 2014) and, in turn, crop development and productivity.

Two temperature extreme indices and three precipitation extreme indices were selected (Table 4.1) in this research and calculated using RCLimDex (X. Zhang & Yang, 2004).

The temperature extreme indicator TXx is selected for investigating farmers claims about the increased frequency and intensity of heat waves that have damaged yield especially during the

anthesis period (usually between February and March) of wheat and barley crops. Fluctuation in daytime and night time temperatures due to climate change could be detected in the diurnal temperature (DTR) indicator trend assessment as large variation in its amplitude, especially for C4 crops like cereals, could negatively affect physiological process and the morphology of the cultivated crops (Sunoj et al., 2020).

Precipitation extreme indices (Rx1day, Rx5day and R99p) were selected based on the role of these events in causing flash floods. Analysing these extreme indices trends allows testing of whether the frequency and the magnitude of the floods is likely to have increased or decreased under a changing climate because there are other variables that control flooding.

Table 4.1: Definition of extreme temperature and precipitation indices chosen for this study and calculated using RCLimDex

Code	Name	Definition	Unit
TXx	Max Tmax	Monthly maximum value of daily maximum temperature	°C
DTR	Diurnal temperature range	Monthly mean difference between *maximum daily temperature* and *minimum daily temperature*	°C
Rx1day	Max 1-day precipitation amount	Monthly maximum 1-day precipitation	mm
Rx5day	Max 5-days precipitation amount	Monthly maximum consecutive 5-days precipitation amount	mm
R99p	Extremely wet days	Annual total precipitation when RR>99th percentile	mm

4.2.3. Trend analysis

The Mann–Kendall nonparametric trend tests are employed to the temperature and precipitation indices time series to identify trends. The Mann–Kendall nonparametric trend test has been widely-used in long-term trend analysis of meteorological and hydrological time series. There are two advantages of using this test. First, it is a non-parametric test and does

not require the data to be normally distributed. Second, the test has low sensitivity to abrupt breaks due to inhomogeneous time series (Tabari et al., 2011). According to this test, the null hypothesis H0 assumes that there is no trend (the data is independent and randomly ordered) and this is tested against the alternative hypothesis H1, which assumes that there is a trend.

The software used for performing the statistical Mann-Kendall test is XLSTAT. The null hypothesis is tested at 95% confidence level for temperature, precipitation and climate extremes index time series.

4.3. Results:

4.3.1. Climate variables analyses

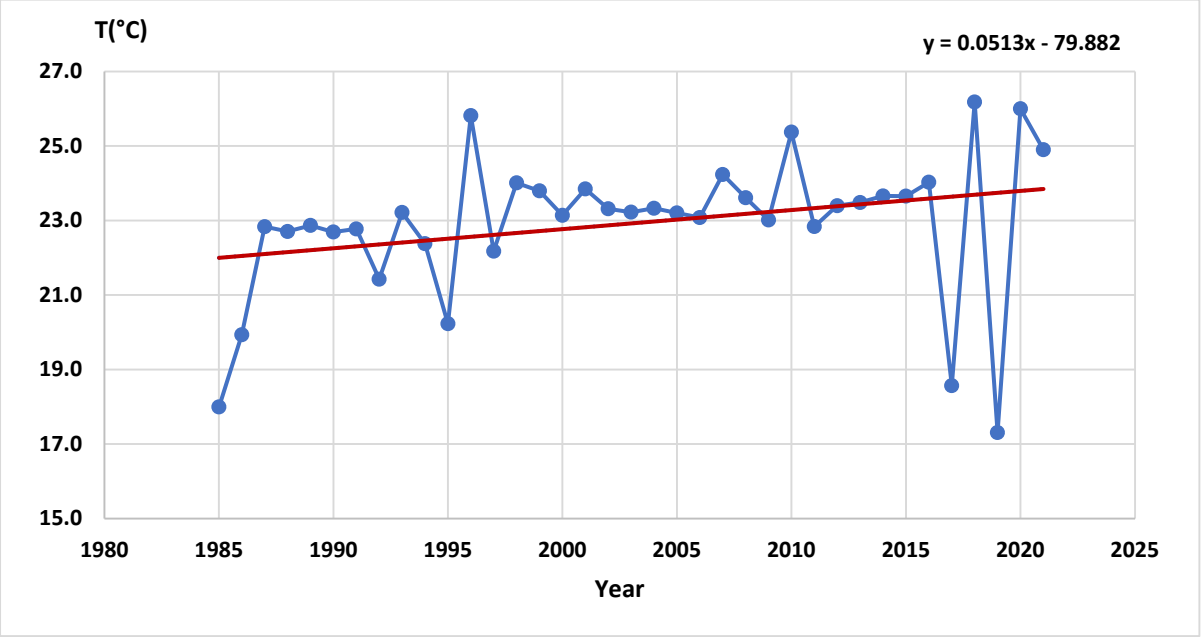

Figure 4.1: Annual average temperature data from Safawi meteorological station and calculated linear trend

Figure (4.1) shows the annual average temperature observations for the cultivated area of Q'a Shubayqa (1985-2021). Mann-Kendall test result shows that the time series has a monotonic upward trend with S = 221 >0 and p-value =0.001, such that the increasing trend of temperature is statistically significant. During particular years (1985, 1995, 2017 and 2019), it is notable that average annual temperature was dramatically under the usual range of temperature for the rest of the season. These cold years are due to lower temperatures recorded during particular winter months; January, February and sometimes March.

This change in temperature can affect crop growth stages (wheat and barley) in this area by minimising the grain filling period and in consequence decreasing individual grain weight and grain yields (Djanaguiraman et al., 2020). The increasing temperature trend may also affect the hydrological cycle of the area by increasing the evapotranspiration rates and minimising the duration of soil water holding capacity (Lal et al., 2011; Lin et al., 2023).

Figure 4.2 presents annual precipitation time series from Jabal Druz (1985-2021) where Mann-Kendall tests indicate the existence of an upward trend with S= 4.2. However, the p-value (0.59) shows this trend is not statistically significant.

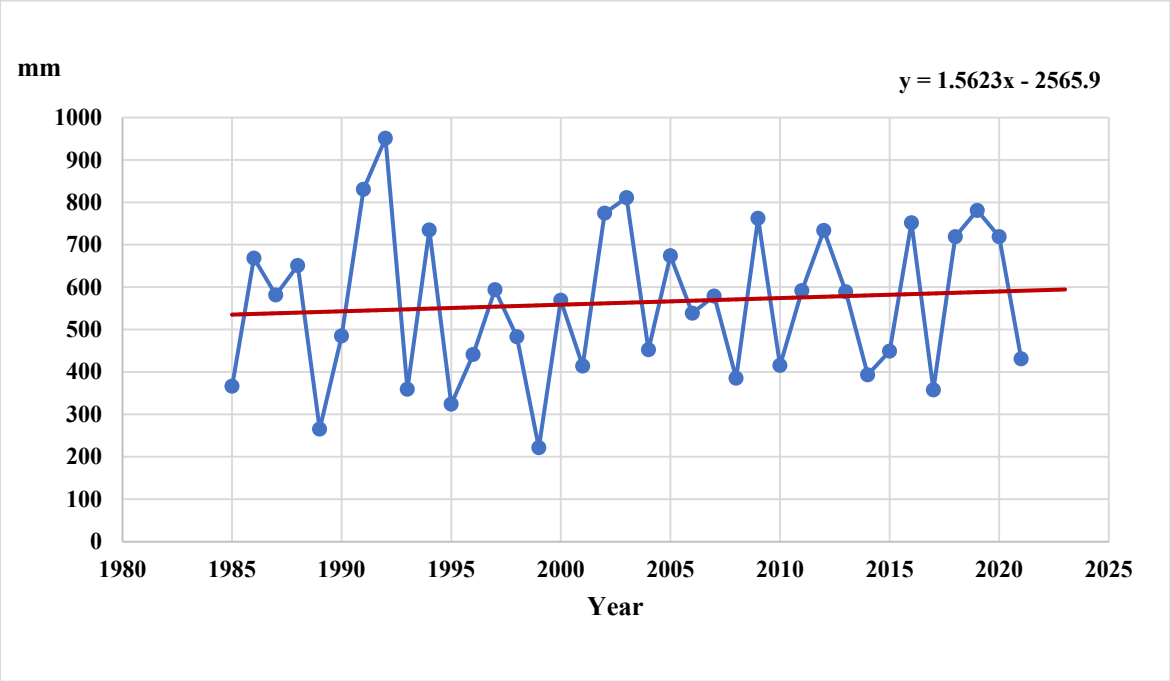

Figure 4.2: Annual precipitation of Ein Al-Arab meteorological station and calculated linear trend

Although there is no significant trend in precipitation in Jabal Druz over the studied period, annual precipitation values have shown an acute variation, varying between 951mm in 1992 to 221mm in 1999. The unstable rhythm of annual precipitation was expected due to the characteristics of the Mediterranean climate (Médail, 2008). These annual variations of the Mediterranean region rainfall are found to be mostly associated with year-to-year differences in winter synoptic and mesoscale cyclonic disturbances in combination with largre scale circulation features and land-sea temperature contrasts (Homar et al., 2007; Lionello et al., 2005; Trigo, 2006).

The results of this analysis of climate variables intersects with surveyed farmers declarations (Chapter 3, section 3.4.2.6) about climate change in the last decades, especially warming temperatures.

4.3.2 Climate extremes analysis

Temperature extreme indices for the Q'a Shubayqa region illustrate statistically significant increasing trends for the period between 1985 to 2021 (Figure 4.3).

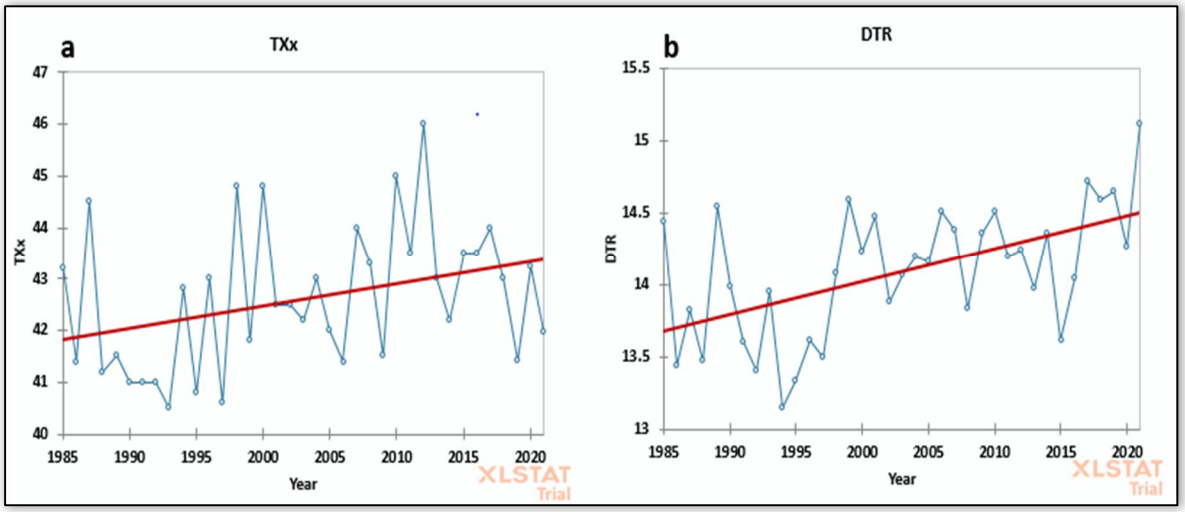

Figure 4.3: Evolution of annual temperature extreme indices (TXx and DTR) in Q'a Shubayqa from 1985 to 2021

The MK trend test was applied to the maximum value of daily maximum temperature index (TXx) (Figure 4.3.a) and shows a significant increasing trend where S= 162>0 and p-values=0.035 < α=0.05 (H1 is accepted). The second temperature extreme index used for this study is the mean difference between Tmax and Tmin index (DTR). This index (Figure 4.3.b) has also shown a significant increasing trend where MK test results shows that S= 256 and p-values=0.001< α=0.05 (H1 is accepted).

The increase in maximum value of TX and diurnal temperature range, provide evidence of climate change in Q'a Shubayqa and support local farmers complaints (chapter 3) regarding frequent heat wave events during the spring period (grain filling stage) which cause serious harm to the crops and decrease yield.

Figure 4.4.a shows the annual evolution of annual maximum 1-day precipitation (RX1day) precipitation extreme index in Jabal Druz, where the MK test illustrated a significant increasing

trend of RX1day with S= 200 and p-value= 0.009< α=0.05 (H1 is accepted). Similarly, the extremely wet days index, annual total precipitation when RR>99th percentile (R99p), witnessed a significant increasing of the trend line (Fig 4.4.b) during the studied period with S=145 and p-value=0.033< α=0.05. In contrast, the trend line of the RX5day index shows an insignificant trend (Fig 4.4.c) where the MK test gave a p-value=0.219 which is greater than the significance level α=0.05 (H0 is accepted).

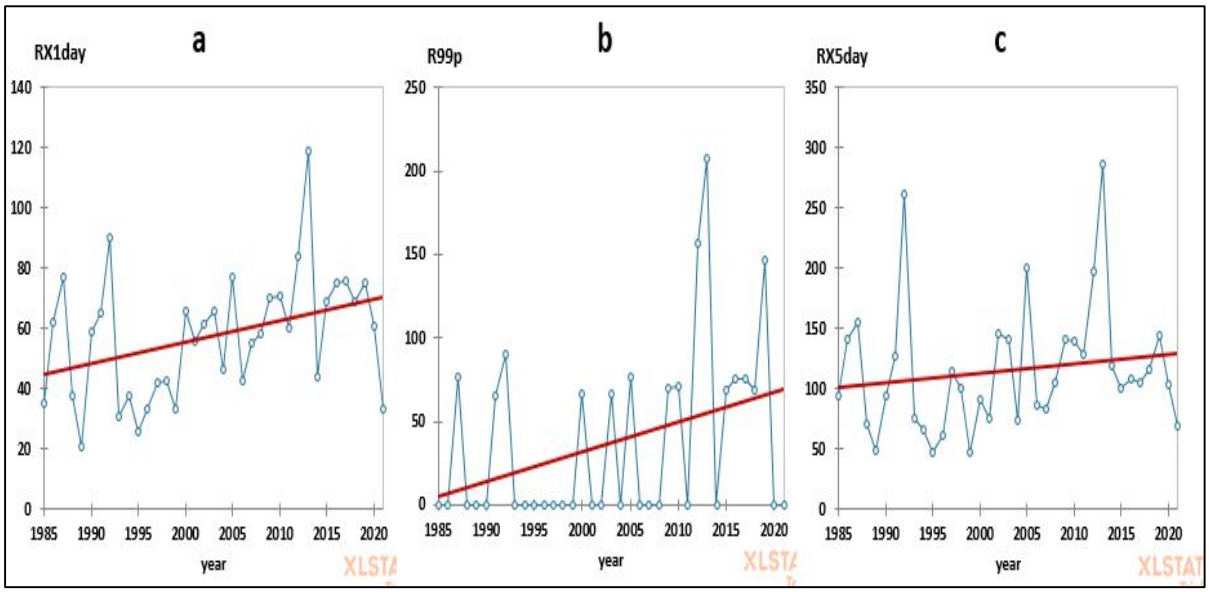

Figure 4.4: Fluctuations of precipitation extreme indices (RX1day, R99p and RX5day) in Jabal Druz from 1985 to 2021.

Regarding Jabal Druz precipitation, MK tests on precipitation extreme indices R99p (extreme wet days) and RX1day (annual maximum one day precipitation) time series have shown significant increasing trends, while time series trend of RX5day index (annual maximum consecutive 5 days precipitation) was insignificant.

These results could reflect the impact of climate change on precipitation patterns in such dryland area as explained in Chapter 2 (Section 5) where rainstorms may have become more frequent within a reduced time interval. This type of storms would cause major flash floods that cause soil erosion that can destroy cultivated crops and the ecosystem of the area. This will be investigated in next chapter.

4.3.3. Seasonal trend analysis

The analyses presented in this section addresses the historical precipitations and extreme indices patterns (trends) during specific critical time period of the crop life cycle.

In Figure 4.5, Patterns of seasonal precipitation in Q'a Shubayqa that usually starts in November until April from each season were assessed. The analyses of the trends are based on two time periods. The first period is whole period of study between 1985-1986 and 2020-2021 seasons (blue line values) and second period is between 1985-1986 and 2012-2013 seasons (red line values). The reason of selecting different period for trend analyses is related to the noticed apparent downward trend (blue line value) that would be affected by the recovery of seasonal rainfall after the 2012-2013 season.

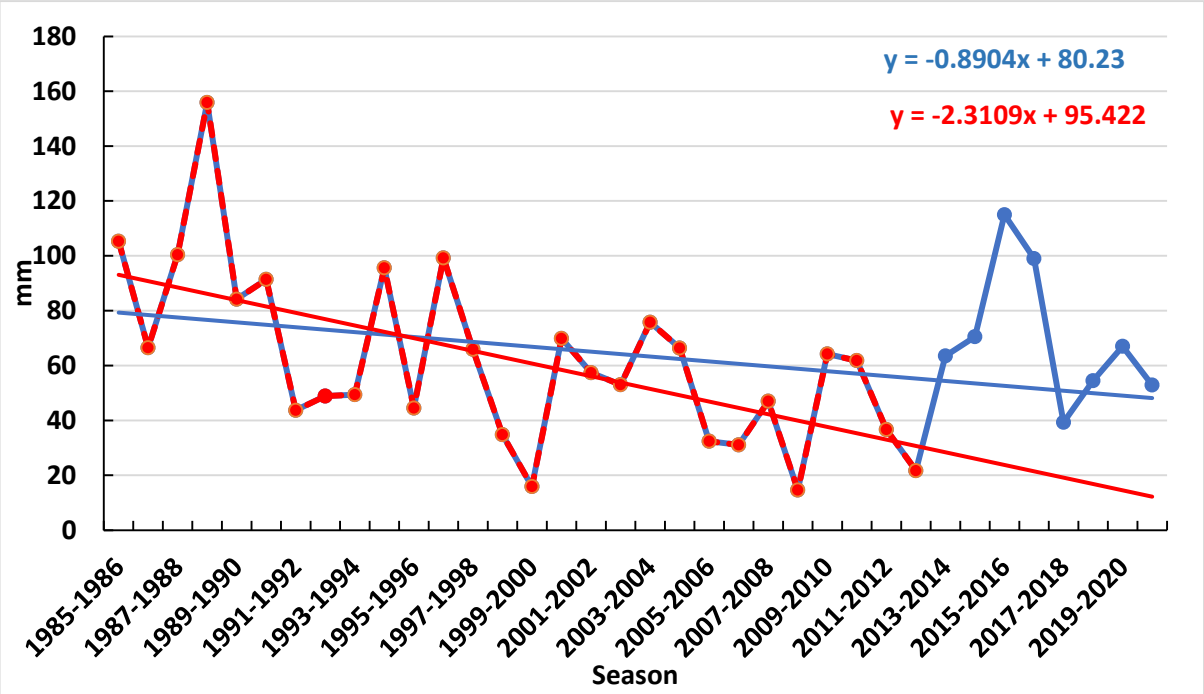

Figure 4.5: Time series and trend lines of November to April precipitation in Q'a Shubayqa

The Mann-kendall trend test applied on Q'a Shubayqa seasonal precipitation (November to April) (Figure 4.5) has shown an insignificant decreasing trend with p-value = 0.076> α=0.05 (H1 is rejected). However, the partial analysis of the seasonal precipitation trend until the season of 2012-2013 using Mann-kendall test have shown a significant negative trend with S= -167 and p-value = 0.001< α=0.05 (H1 is accepted).

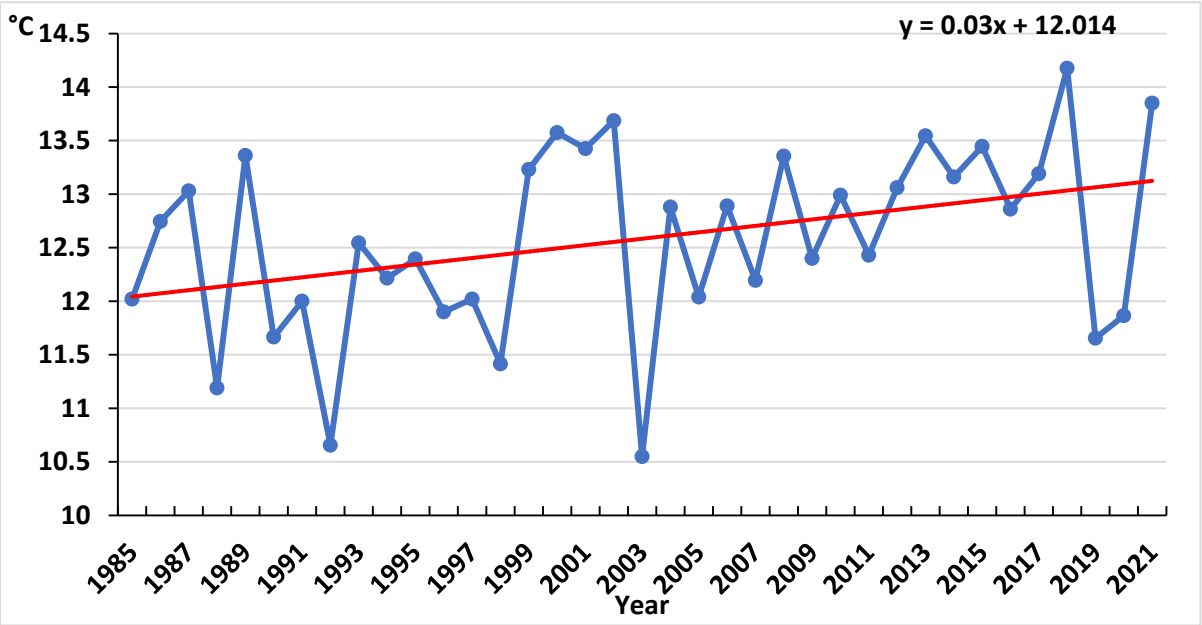

Figure 4.6: Time series of seasonal diurnal temperature range (DTR) for February and March and trend line patterns of Q'a Shubayqa

Figure 4.6 represents time series of the average seasonal extreme index DTR (diurnal temperature range) of February and March (anthesis period) of each year. The Mann-kendall test applied to the time series shows a positive (S=179) and significant trend with p-value =0.019 < α=0.05 (H1 is accepted). This means that the difference between day temperature and night temperature during the critical period of February and March has been increasing through the years affecting crop development and production in Q'a Shubayqa (Chapter 3, section 3.4.2.6).

The analyses presented in Figure 4.7 mainly focus on seasonal daily maximum temperature indicator (TXx) in Q'a Shubayqa. However, the analyses of the trends are split on two time periods. The first period is whole period of study between 1985 and 2021 (blue line values) and second period is between 1985 and 2013 (red line values). The reason of choosing different period for trend analyses is related to the noticed apparent upward trend (blue line value) that would be affected by the decrease of TXx after 2013.

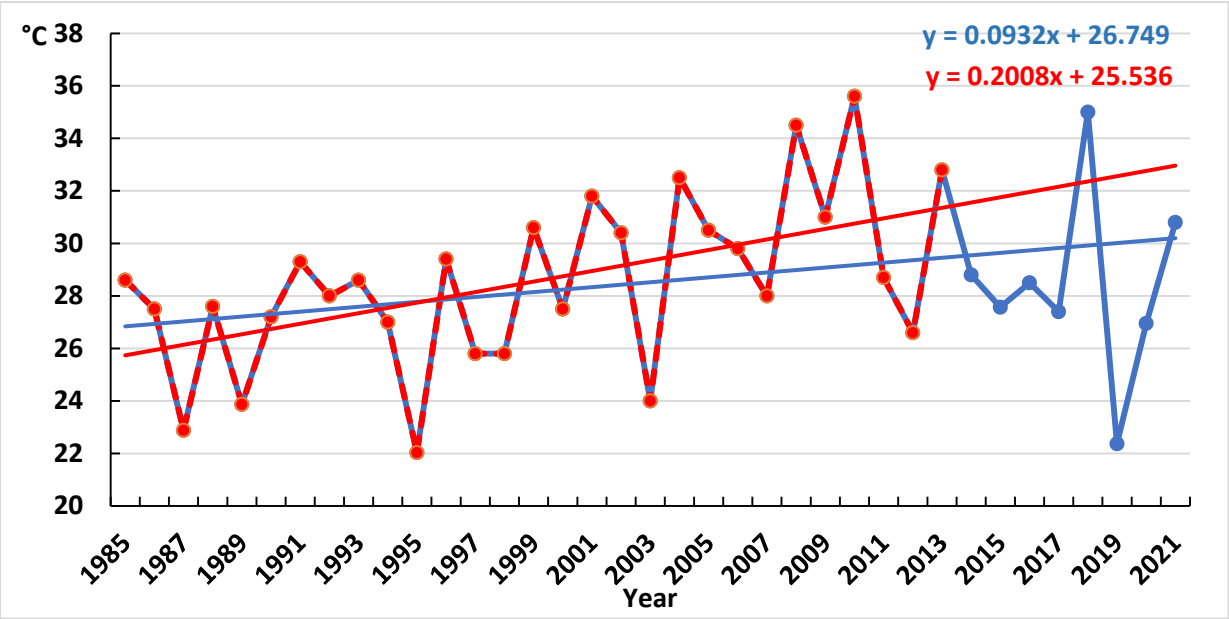

Figure 4.7: Time series of seasonal daily maximum temperature (TXx) for February and March and trend line patterns of Q'a Shubayqa

Figure 4.7 represents time series of the maximum value of daily maximum temperature (TXx index) recorded during February and March of each year in Q'a Shubayqa. The Mann-kendall test applied on the TXx time series shows an increasing but insignificant trend with p-value = 0.086> α=0.05 (H1 is rejected). However, when Mann-kendall test was applied partially on TXx time series between 1985 and 2013, the results have shown an increasing trend with S=148 and p-value= 0.005< α=0.05 (H1 is accepted).

4.4. Discussion

In this chapter, the main focus was shedding light on climate change that occurred over the last 37 years in Q'a Shubayqa and Jabal Druz. Daily observed meteorological data were tested to investigate weather climate patterns has been changing (according to farmers) or not using trend analyses of daily temperature and precipitation data and derived extreme climate indices.

The findings presented in this study demonstrate that, during the past four decades, the agricultural system in Q'a Shubayqa has been experiencing a significant increase in annual air temperature with a rising maximum daily temperature and diurnal temperature range. Seasonal trend analysis of the two indices (TXx and DTR) during the most critical period of the crop development and growth (February and March) have also shown a significant increase that would directly affect crops physiological process including anthesis and grain filling stages. Non-significant increases in annual precipitation were detected in Jabal Druz, although a

significant decrease in Q'a Shubayqa seasonal precipitation has occurred during the majority of the studied period. Trend analysis of relevant extreme events in Jabal Druz has shown that heavy rainstorms in limited time (one day) have become more frequent and more severe. Based on these results, flash floods that occur in Jabal Druz and flow in to the Q'a are likely to have become more frequent, however the increasing heating through the years caused by global warming, will directly affect the hydrological system of the area leading to higher evapotranspiration rates and thus surface drying, thereby increasing duration and intensity of drought which reduce water availability for cultivated crops

In the same context of these findings, significant changes have been shown in increasing mean annual temperature and increasing or decreasing mean annual rainfall (Parry et al., 2007), as well as in extreme events in the Middle East region and Mediterranean area (Alpert et al., 2002; X. Zhang et al., 2005). Extreme climate events such as heavy rainfall storms and long dry periods can have significant and devastating impact at the local level specifically on agriculture and water resources. A recent study undertaken by Tarawneh (2022) have shown findings that consist with this chapter results where he investigated the climate change in Jordan using observed data between 1990-2020 (almost the same study period in this chapter) and they found that several temperature extreme indices (including annual maximum of daily maximum temperature (TXx)) have been increasing while trends of precipitation extreme indices decreased through the study period.

These consequences of changing climate and extreme climate events of agricultural system in Q'a Shubayqa will be investigated in the next chapter based on farmers declarations (see Chapter 3) regarding very long period of hot days and severe heat waves during the last decades in addition to flooding perturbation in terms of quantity and timings that directly affect very important for several agricultural practices (planting date) and water stress of the cultivated crops. In the next chapter, further comparisons between time series of climate variables and extremes with spectral indices time series that represent the patterns of cultivated crops and water availability are undertaken, as a crucial step to investigating the impact of climate change on crop growth and health in Q'a Shubayqa.

Chapter 5: Spectral indices of water and vegetation in Shubayqa, and their responses to climate extremes

5.1 Introduction

Changes in climate such as precipitation, temperature, and increases in atmospheric CO_2 affect crop production (Xue et al., 2014). The scarcity of freshwater is one of the major constraints caused by climate change that could affect food production, especially in dryland areas, due to inter-annual variability that occurs with climate anomalies (extreme weather events) (Dinar et al., 2019). Assessing and understanding the impact of climate variability on crop growth, particularly water resource availability and other climate extreme events in such areas, is crucial for any prospective effective management strategies, to help with planning to reduce profit shortfalls and to avoid any social and economic crises that can appear in semi-arid or arid regions.

Time series data acquired through remote sensing instruments can provide information about ecosystem dynamics at medium temporal resolution and at a frequency that makes it possible to study abrupt and gradual change in response to climate alterations (Palacios-Orueta et al., 2005). In addition, remote sensing has significant benefits for related research owing to its time/cost saving, provision of abundant information, multi-platform operation, and multi-temporal resolutions (Guangming et al., 2007). Spectral indices are the most common tools employed for remote sensing data analyses (Huete et al., 1997a; 1997b). These indices are based on combinations of a small number of spectral bands that enhance specific spectral properties. NDVI (Normalized Difference Vegetation index) is a universal index that has been extensively used to evaluate spatio-temporal variation of vegetation and is considered as a suitable indicator for biomass condition by estimating its greenness intensity (DeFries et al., 1999). The NDWI (Normalized Difference Water index) is also one of the widely used spectral indices dedicated to detecting water content in soil and vegetation. Both indices (NDVI and NDWI) are very useful to evaluate cultivated crops and relevant hydrological systems over time and space.

According to Q'a Shubayqa farmers (Chapter 3), climate change has been affecting crop growth and productivity in the last few decades. Farmers have also talked about inter-annual climate extreme events that occur in Q'a Shubayqa and the surrounding area such as spring

heat waves, that can damage vegetation and reduce yield. The previous chapter (sections 4.3.1 and 4.3.2) shows a significant increase of temperature and related extreme indices during the last few decades. This chapter aims to test if there is a correlation between crop condition, represented by NDVI values, and temperature variation represented by extreme event indices. In addition, NDWI time series that represent water availability in Q'a Shubayqa will be correlated with upstream precipitation (source of floods) and relevant extreme indices, with the aim of confirming the main sources of water, and hydroclimate processes responsible for crop growth and productivity.

5.2. Literature review: Spectral indices

NDVI has been used extensively to monitor and assess ecosystems in both spatial and temporal domains (DeFries et al., 1999). NDVI is widely used by researchers to estimate green biomass, leaf area index and plant phenology as it is the best indicator of vegetation's ability to absorb photo-synthetically active radiation (Asrar et al., 1984; Goward and Dye, 1987; Prince, 1991). Variations in climatic factors, in particular rainfall, have a strong influence on variations in NDVI for a given site. Ichii et al. (2002) have investigated the relationship between NDVI and climatic variables on a global scale using the Pathfinder AVHRR land NDVI dataset and observed weather data. They have identified a significant correlation between NDVI, temperature and precipitation in northern and southern semi-arid regions. They reported that, in southern semi-arid regions, NDVI decrease is strongly related to a decrease in precipitation amounts. Wang et al. (2010) have studied the temporal and spatial patterns of NDVI and their relationship to precipitation in the Loess Plateau of China, they used 250 m MODIS NDVI 16-day composite data and observed precipitation data to evaluate the interaction between vegetation cover and precipitation by employing principal component analyses. The results of this study revealed that precipitation is a major factor for vegetation dynamics, but farming practices during the growing season could also perturbate the NDVI-precipitation relationship.

NDWI is the most useful index to identify waterbodies and surface water spread over time and to illustrate water content in vegetation leaves (Acharya et al., 2018; McFeeters, 1996). These datasets provide the physical features and spatio-temporal variation of surface waterbodies at various spatial scales at regular time intervals (Schimel et al., 2013; Wallace et al., 2006). Spatio-temporal surface water assessment is also applied for the monitoring and management of natural water resources, prediction of ecosystem health and prevention of water related disasters using Google Earth Engine (GEE). Soltanian et al. (2019) have evaluated flood areas

in the agricultural regions of Golestan in Iran by using standard NDWI and a modified NDWI (can enhance open water features while efficiently suppressing and even removing built-up land noise as well as vegetation and soil). They confirmed that standard NDWI seem more suitable to sites with vegetation.

These spectral indices (NDVI and NDWI) have also been considered as appropriate methods to examine the impact of climate change on vegetation and water availability. This can be done by comparing temporal fluctuations in NDVI and NDWI with climatic factors e.g. Chen et al. (2015) and Yao et al. (2018).

5.3. Material and methods

5.3.1. Spectral indices (NDVI and NDWI)

- ***NDVI:*** provides the user with an approximation about the vitality and density of vegetation at a pixel scale based on different intensities of reflected sunlight from the visible (VIS) and near-infrared (NIR) spectrum that are picked up by the satellite sensors (Weier and Herring, 2019). While healthy plant leaves mostly absorb light from the red spectrum using chlorophyll to produce glucose from carbon dioxide and water in the process of photosynthesis, their cell walls strongly reflect light from NIR spectrum. If there is more light reflected in the NIR that in VIS wavelengths, the pixel is likely to be vegetated with healthy leaves because light from the red spectrum (VIS) has already been absorbed by the plants. The NDVI can also serve as an indicator of photosynthetic activity, used to detect changes in land cover and land usage, and identify anomalies in growing seasons.
  The index ranges from -1 to 1 and is calculated by:

$$NDVI=\frac{(NIR-VIS)}{(NIR+VIS)}$$ from the satellite frequency bands.

where NDVI equal to 0.1 indicates stone, sand or snow, 0.3 indicates sparse vegetation, 0.6 indicates temperate forest and 1.0 indicates the highest density of vegetation or leaves. NDVI values below zero indicate the presence of water (Weier and Herring, 2019).

- ***NDWI:*** is derived from the Near-infrared (NIR) and Short-Wave Infrared (SWIR) channels. The SWIR reflectance reflects changes in both the vegetation water content and the spongy mesophyll structure in vegetation canopies, while the NIR reflectance is affected by leaf internal structure and leaf dry matter content, but not by water content. The

combination of the NIR with the SWIR removes variations induced by leaf internal structure and leaf dry matter content, improving the accuracy in retrieving the vegetation water content (Ceccato et al., 2001). The amount of water available in the internal leaf structure largely controls the spectral reflectance in the SWIR interval of the electromagnetic spectrum. SWIR reflectance is therefore negatively related to leaf water content (Tucker, 1980). The NDWI product is dimensionless and varies between -1 to 1, depending on the leaf water content but also on the vegetation type and cover, it is computed as shown below: $\text{NDWI}=\frac{(NIR-SWIR)}{(NIR+SWIR)}$

where High values of NDWI (>0.6) correspond to high vegetation water content and to high vegetation fraction cover, otherwise low NDWI values correspond to low vegetation water content and low vegetation fraction cover. In period of water stress, NDWI will decrease.

5.3.2. Methodology

To create long-term time series of NDVI and NDWI for Q'a Shubayqa, two remote sensing data sets products were employed; temporally fused Landsat 5 and Landsat 8, and MODIS terra. Supporting data was obtained from a third remote sensing product, ERA5-Land.

USGS Landsat 5 (L5) and Landsat 8 (L8) Surface Reflectance Tier 1 datasets are the atmospherically corrected surface reflectance from the L5 ETM sensor and L8 OLI/TIRS sensors (https://developers.google.com/earth-engine/datasets/tags/landsat). L5 data cover the period between 1985 to 2012 and L8 data cover the period between 2013 to 2021. L5 observed images with a repeat cycle of 16 days, contain 4 visible and near-infrared (VNIR) bands and 2 short-wave infrared (SWIR) bands processed to orthorectified surface reflectance, and one thermal infrared (TIR) band processed to orthorectified brightness temperature. The VNIR and SWIR bands have a resolution of 30m / pixel. The TIR band, while originally collected with a resolution of 120m / pixel (60m / pixel for Landsat 7) has been resampled using cubic convolution to 30m (Schmidt et al., 2013). These data have been atmospherically corrected using LEDAPS, and include a cloud, shadow, water and snow mask, produced using CFMASK, as well as a per-pixel saturation mask. L8 images contain 5 visible and near-infrared (VNIR) bands and 2 short-wave infrared (SWIR) bands processed to orthorectified surface reflectance, and two thermal infrared (TIR) bands processed to orthorectified brightness

temperature. Landsat 8 orbits allow 8-day repeat cycle that cover any Landsat scene area on the globe. These data have been atmospherically correct using LaSRC and include a cloud, shadow, water and snow mask produced using CFMASK, as well as a per-pixel saturation mask.

Moderate Resolution Imaging Spectroradiometer (MODIS) datasets, provide land data products to support global change research and natural resource management by providing valuable information about vegetation health and moisture availability. In this study, the NDVI and NDWI products generated from MODIS high radiometric sensitivity images were selected and obtained from the cloud-based GEE platform. NDVI and NDWI datasets products generated from MOD09GA version 6 (Vermote et al., 2015), available from January 2000, which provides bands 1-7 in a daily gridded L2G product in the sinusoidal projection, including 500m reflectance values and 1km observation and geolocation statistics. MODIS products has become one of the most important and widely used sensors for a broad range of application like monitoring vegetation condition in near real-time with very high temporal (daily) and low spatial (463m) resolution (Meroni et al., 2019). In addition, MODIS product datasets have been used in drylands for multiple analysis and have shown successful detection of changes in photosynthetically active vegetation and served as an indicator of moisture availability in plants (Borana and Yadav, 2018; Santra and Chkraborty, 2011; Wardlow et al., 2007).

The global volumetric soil water (soil moisture) dataset ERA5-Land (Muñoz Sabater, 2019) expressed in m3 water per m3 of soil (m3/m3) is a monthly scale dataset providing a consistent view of the evolution of land variables over several decades at an enhanced resolution (~9km grid spacing) compared to ERA5. ERA5-Land has been produced by replaying the land component of the ECMWF ERA5 climate reanalysis. Reanalysis combines model data with observations from across the world into a globally complete and consistent dataset using the laws of physics. Reanalysis produces data that goes several decades back in time (from 1950 to near real-time), providing a description of the climate of the past. The native spatial resolution of the ERA5-Land reanalysis dataset is 9km. Among its land variables, the only variable extracted from this dataset for the study area is the monthly maximum volume of water in soil layer 1 (0 - 7 cm) of the ECMWF Integrated Forecasting System. The surface is at 0 cm. The estimation of the volumetric soil water is associated with the soil texture (or classification), soil depth, and the underlying groundwater level.

The reason for using both Landsat and MODIS for NDVI and NDWI calculations is due to the difference in spatio-temporal resolution of the two data sets. Despite its low spatial resolution (250-1000 m), MODIS high temporal resolution (daily basis) can help to track changes in the landscape by providing near-daily global coverage (Justice et al., 2002). In addition, remote sensing images obtained from MODIS data are mostly rain and cloud free on the polar orbiting platform due to the use of cloud removal algorithms (Jönsson & Eklundh, 2004). Landsat 5 and 8 data, have high spatial resolution compared to MODIS data, making it more appropriate for local-scale remote sensing analyses (Jacob et al., 2023). However, Landsat 5 and 8 return period (16 and 8 days respectively) with cloudy and rainy weather could markedly reduce the availability and the utility of extracted images (Jia et al., 2014).

In this study, by using remote sensing data derived from two satellite sensors with different spatial and temporal characteristics, we aim to understand the potential use and application of these differing satellite images in analysing vegetation development and water availability in the specific study area.

Monthly NDVI and NDWI time series were extracted from Landsat 5 and 8 and MODIS data by considering the maximum monthly values of the two spectral indices. This method of selecting the maximum value rather than the average monthly value is to avoid the very low values of NDVI and NDWI caused by clouds and rainfall occurrence, even given the cloud removal algorithms used in MODIS. These time series will allow to the detection of crop vegetation and water availability (floods and local rainfall). Correlations between monthly NDVI/NDWI time series and monthly precipitation in Jabal Druz (Syria) will help confirm farmers statements around the importance of Jabal Druz floods as a source of water for crop growth and development in Q'a Shubayqa. To support these analyses, another comparison will be undertaken between time series of monthly precipitation and maximum monthly values of soil moisture of Q'a Shubayqa measured from ERA5-Land.

In terms of climate change impact on crop production, this will be investigated by correlating annual extreme temperature indices from Safawi (TXx and DTR; see Chapter 4, section 4.3.2) with annual NDVI time series to evaluate the impact of the increasing frequency and intensity of heat waves on the physiological processes of Q'a Shubayqa crops. Annual precipitation extreme indices from Jabal Druz (Rx1day, Rx5day and R99p) will be correlated with annual NDVI time series to explore to what extent precipitation extreme events contribute in the

occurrence of floods from upstream that flow in Q'a Shubayqa and submerge crops to provide its water needs. Annual NDVI values used for this comparison are the maximum value recorded in March of every year because in March the biomass greenness intensity of the cultivated crops is at the highest level of the whole season and is normally the peak growing timing (Saba et al., 2010). In this comparison, only Landsat_5 NDVI data (1985 to 2011) will be employed rather than MODIS data because Landsat 5 spatial resolution is higher than MODIS and would be more accurate at a very local scale like in Q'a Shubayqa. In addition, Landsat_5 NDVI data cover the longest part of the study period (27 years).

5.3.3. Extracting time series using Google Earth Engine (GEE)

GEE is well suited to allow extraction of detailed time series for long-term temporal analysis (Valerio et al., 2024). In this study, the time series of NDVI and NDWI were extracted from both MODIS and Landsat 5/8. The times series extracted from MODIS cover the period between 2000 and 2021 (see above section 5.3.2), while the Landsat data combination (L5 and L8) can provide data that cover the period between 1985 and 2021. This study period was selected based on the available meteorological data that we have collected from stations in Safawi (Q'a Shubayqa) and Ein Al-Arab (Jabal Druz in Syria).

GEE code editor is a web based integrated development environment for the Earth Engine JavaScript Application Programming Interface. GEE enables users to call a wide set of functions that have been developed specifically for computing in Earth Engine and apply them over many images simultaneously using Google computational infrastructure. It contains a data catalogue that hosts multiple petabytes of satellite imagery in the cloud including Landsat datasets, sentinel (1&2), MODIS and others. Over 6000 scenes are added daily from active satellite missions. Using the GEE code editor, users are able to write commands that are sent to GEE for processing, also users can filter large collections of images to dates and areas of interest, map algorithms over collection of images, apply algorithms to individual images or image collections and compute aggregate statistics through time and space without any need to download any data (Velastegui-Montoya et al., 2023).

To create time series by using this interface, first I defined the study area boundaries by creating a polygon in the displayed GEE map (Appendix B). Second, I imported the dataset type (image collection) used for each time series from the GEE catalogue. Then I wrote functions of require indices according to the dataset type and spatial and temporal scale.

The NDVI and NDWI time series based on the daily MODIS dataset are extracted using one band extraction function for the period between 2000-2021 because they are already calculated in GEE. However, for Landsat 5&8, the NormalizedDifference() function was needed to compute NDVI by selecting NIR and VIS bands as function parameters, and similarly for NDWI by selecting NIR and SWIR bands as the NormalizedDifference() parameters. The code editor scripts used to extract time series from MODIS and Landsat 5&8 using GEE can be found in Appendix B.

The soil moisture time series was clipped from global volumetric soil water (soil moisture) dataset ERA5-Land using GEE code editor script.

5.4. Results

5.4.1. Interaction between precipitation and NDVI, NDWI, Soil moisture and flood area

To reveal the relationship between precipitation in Jabal Druz (Syria) and vegetation growth in Q'a Shubayqa (Jordan), Table 5.1 shows the correlation values between NDVI extracted from both MODIS and L5&L8, and precipitation in Jabal Druz. NDVI_MODIS shows a significant correlation coefficient of around 0.46 with Jabal Druze precipitation. However, NDVI_L5&L8 corelation with Jabal Druz precipitation is not significant, with a low coefficient value (r^2 = 0.22). This could be due to technical recording issues like clouds or flood water that may cover the cultivated area, knowing that L5 and L8 only produce two images per month unlike MODIS data which are daily. However, NDWI_L5&L8 has a significant correlation with precipitation (r^2 = 0.49, p-value<0.05) unlike NDWI_MODIS where the correlation coefficient value was very low (r^2 =0.06).

These correlations between NDVI/NDWI and precipitation at Jabal Druz were conducted to investigate the relationship between Jabal Druz precipitation (source of floods) and crop production in Q'a Shubayqa. The significance of these correlations illustrates the flood impact on vegetation health and density presented by NDVI index and water content of plant leaves presented by NDWI index, in Q'a Shubayqa as described by the local farmers (Chapter 3).

Table 5.1: Correlations between monthly Jabal Druz precipitation and monthly NDVI/NDWI at Qa Shubayqa.

Indices (monthly scale)	Correlations with precipitation in Jabal Druz
NDVI_L5&L8 (1985-2021)	0.223
NDWI_L5&L8 (1985-2021)	0.487*
NDVI_MODIS (2000-2021)	0.460*
NDWI_MODIS (2000-2022)	0.066

*: Significant at p-values<0.05

To find out more about the relationship between precipitation amounts in Jabal Druz and crop growth in Q'a Shubayqa, Figure 5.1 was created to clarify the interaction between precipitation, NDVI and NDWI. The correlations between spectral indices and precipitation time series were significant. But when looking at the chart we can notice that during particular crop growing seasons precipitation is low, but NDVI and NDWI show high values, and vice-versa during other seasons.

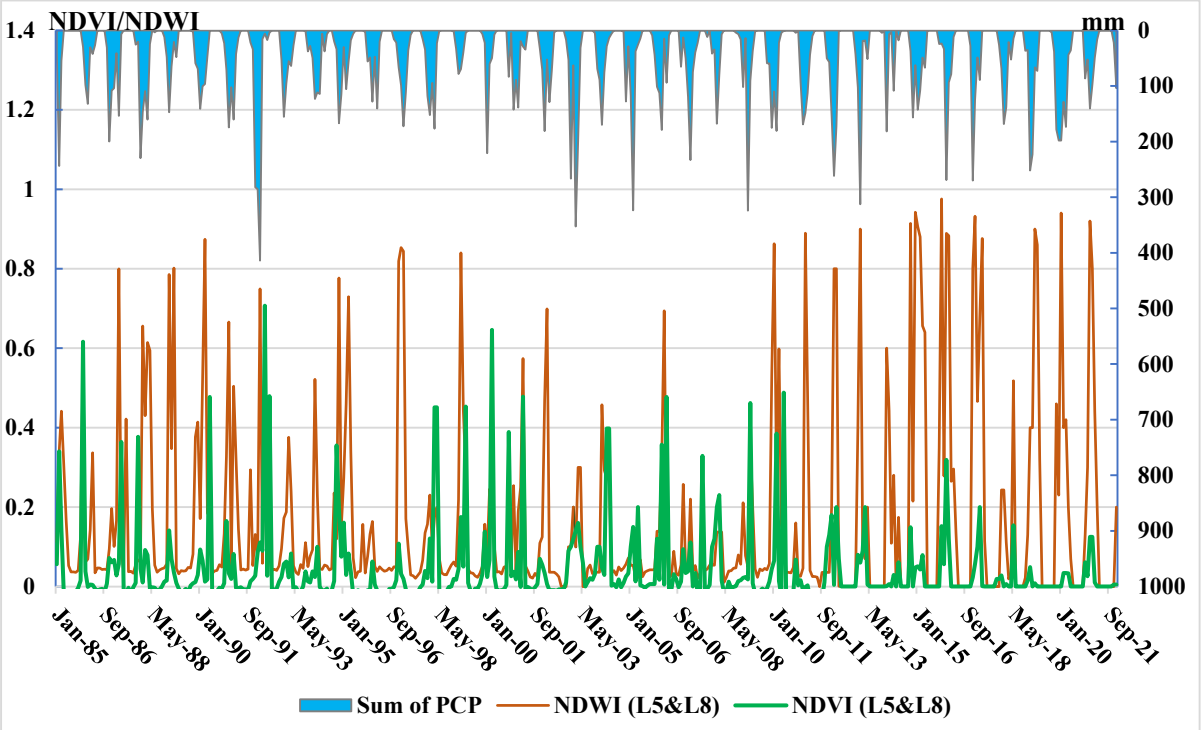

Figure 5.1: Interaction between monthly precipitation at Jabal Druz and maximum monthly NDVI and NDWI for the period 1985-2011

For example, in the wet seasons of 1989-1990 and 2000-2001 monthly precipitation peaks were very limited which means that the probability of floods occurrence is low, but the NDVI and NDWI show high values. This could be due to the local, direct, precipitation in Q'a Shubayqa which are not very abundant (80 to 100mm/year at nearby Safawi) but its timing can make the difference in seasons when precipitation in Jabal Druz is limited. During other wet seasons, like 2002-2003 and 2004-2005, monthly precipitation peaks were high (e.g. around 330mm of cumulative rainfall in February 2003), but NDVI and NDWI were very low. According to the data set of daily precipitation in Jabal Druz, severe and frequent rainfall storms of 266mm and 334mm occurred respectively December 2002 and in February 2005 during a short period (12 to 17 days of successive rain). The consequences of intense rainfall can be the destruction of crops caused by flash floods, and the surveyed farmers have witnessed similar phenomena during some seasons (see Chapter 3, Figure 3.25). The impact of these immense floods could not have the same destructive action on all Q'a Shubayqa crops. It could vary from one region to another within Q'a Shubayqa, for example in Maftas area (Chapter 3, Figure 3.18) where elevations are low and water drainage capacity is limited (according to farmers), crops in this area are less likely to survive these large floods.

To back up the previous findings showing the relationship between NDVI, NDWI in Q'a Shubayqa, from Landsat and MODIS, and precipitation of Jabal Druz, we have also compared monthly remote sensing soil moisture time series acquired by GEE from ERA-5 Land data for the area of Q'a Shubayqa, with the same monthly precipitation time series for the period 1985-2021. The correlation (Fig. 5.2) between precipitation and soil moisture was significant, with an acceptable coefficient (Schober et al., 2018) of R^2=0.65 (p-value<0.05), which again supports farmers statements about the crucial role of precipitation in Jabal Druz and its resulting floods in providing cultivated crops in Q'a Shubayqa with water needs for growth and productivity.

The chapter's objective of investigating the relationship between seasonal floods and Q'a Shubayqa crop growth and productivity, as described by farmers statements, has been achieved and illustrated by the significant correlations between long-term monthly cumulative precipitation recorded in Jabal Druz and different spectral indices related to vegetation greenness and water availability in Q'a Shubayqa. Findings and interpretations have also shown that seasonal floods are usually beneficial for crop growth in Q'a Shubayqa, but under certain circumstances they could be ruinous.

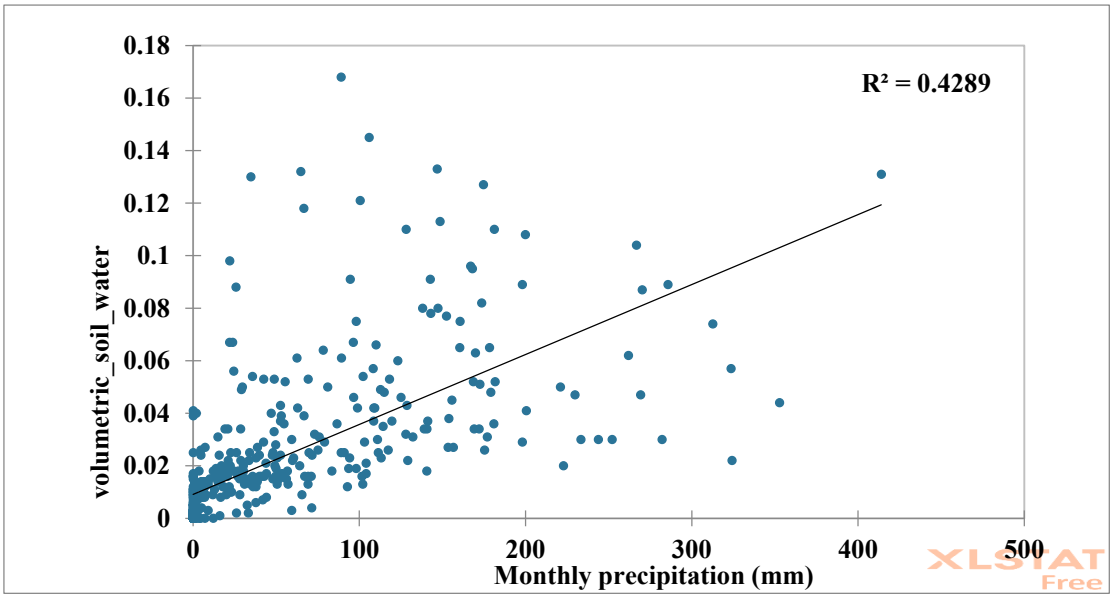

Figure 6.4: Correlation between monthly precipitation in Jabal Druz and monthly Q'a Shubayqa soil moisture

5.4.2. Response of NDVI to temperature and precipitation extreme indices

Table 5.2 shows the correlation between temperature and precipitation extremes (TXx, DTR, Rx1day, Rx5day and R99p) and March NDVI_L5 from 1985 to 2021. Annual maximum Tmax (TXx) and diurnal temperature range (DTR) had a negative correlation with March_NDVI which means that the increasing values of these indices negatively affects vegetation health and growth in Q'a Shubayqa. In addition, increases of annual TXx will enhance the evaporation and reduce the amount of available soil moisture. Otherwise, the increasing levels of diurnal temperature range may affect several physiological processes in plants, for example central carbon metabolism, stomatal opening, and the timing component of photoperiodism, which regulate seasonal reproduction such as flowering and the transition from vegetative to reproductive growth (Michael et al., 2003). Furthermore, higher diurnal temperature variation would promote net assimilation with increased photosynthesis during the light period and decrease respiration during the dark period causing life cycle acceleration and short grain filling period for crops like wheat and barley (yield reduction) (Yang et al., 2016) .

Table 5.2: Correlation coefficient between March NDVI _L5 and Climate extreme indices

Indices		**Correlations with NDVI_L5 (1985-2011)**
Temperature	TXx	-0.258*
	DTR	-0.252*
Precipitation	Rx1day	0.26*
	Rx5day	0.044
	R99p	0.586*

*: Significant at p-values<0.05

Precipitation indices, Rx1day and R99p, show a positive significant correlation with NDVI. This positive interaction between annual maximum one day precipitation index and NDVI could confirm that floods that occur due to a one-day heavy rainfall storm have a crucial role in vegetation growth and back up what farmers said about how these floods are the main source of water for cultivated crops in Shubaqya (Chapter 3). We can also notice that the positive significant correlation between the annual extremely wet day index (R99p) and NDVI is important (0.586) which supports the fact that particularly high amounts of precipitation are more likely to reach the Q'a and confirm that Jabal Druz floods are a key source of water for the crops cultivated in the Qa.

5.5. Discussion

The research conducted in this chapter was dedicated to exploring the role of floods, that initiate upstream in Jabal Druz and flow in Q'a Shubayqa, in providing water needs of the cultivated crops during the growing season. This was done based on three types of remote sensing data (MODIS, Landsat_5&8, and ERA5-Land) with different temporal and spatial resolutions. Results have shown that there is generally a strong relationship between canopy greenness (NDVI/NDWI), soil water content (ERA5-Land soil moisture) and precipitation in Jabal Druz.

Monthly NDVI_MODIS data was positively and significantly correlated with precipitation time series, however the comparison with NDVI_Landsat was not significant. This is probably due to the higher temporal resolution of MODIS data as we have more available imagery for

the rainy period, considering that the impact of flood water on crop canopy greenness is not instantaneous and can take a few days to be captured, which means that Landsat data (low temporal resolution) was not effective in detecting the floods' impact on crops. Saba et al. (2010) have undertaken analysis of Jordanian vegetation dynamics using NDVI_MODIS data and the results of a Pearson correlation comparison showed a significant response of monthly NDVI to monthly rainfall, again pointing to the usefulness of the MODIS images in recording this relationship.

Regarding the water content indicator represented by NDWI, the analyses have shown that Landsat data used to acquire NDWI time series have shown a significant positive correlation with Jabal Druz precipitation in contrast to NDWI acquired from MODIS data, which means that data with higher spatial resolution like Landsat is better at detecting water content variation at small, basin, scale levels. The response of March NDVI_Landsat5 to the annual temperature extreme indices, TXx and DTR was evaluated to investigate their impact on crop growth and yield. The correlations between NDVI and both temperature indices were negative and significant confirming that increasing maximum daily temperatures, in addition to the large ranges between day and night temperatures, are negatively affecting crop health and growth presented by NDVI. Annual precipitation extreme indices were also correlated with March NDVI time series and results have shown that annual extremely wet day index (R99p) had the greatest impact on Landsat_5 NDVI values and Rx1day had a moderate correlation with Landsat_5 NDVI. This confirms the important role of these precipitation extreme indices in the occurrence of floods that provide water needs for Q'a Shubayqa crops. These findings were boosted by the significant positive correlation between Jabal Druz precipitation and soil moisture of ERA5_Land R.S dataset.

These analyses provide an overview about climate variation control on vegetation growth in these drylands but still does not explain all the variation in terms of spectral indices, especially NDVI. Findings also confirm the farmers claims about the main source of water to the q'a. i.e. floods from Jabal Druz. These results open the way for further assessment relevant to the studied agricultural system such as modelling the hydrological system of Q'a Shubayqa to better quantify and confirm the water cycle patterns suggested in this chapter (Chapter 6), including the amount of water that reaches the cultivated crops every season. This is turn will provide inputs to an agricultural system model.

Chapter 6: Modelling the Q'a Shubayqa hydrological system

6.1. Introduction

The scarcity of freshwater is a major constraint on food production in dryland areas, with variable seasonal rainfall patterns and often non-existent or poor water storage infrastructure (Chapter 2, section 2.2.6). Assessing and understanding hydrological systems is crucial for any prospective modelling of these, and in turn, helps with planning and monitoring of these water resources, to reduce food shortages and to avoid any related social and economic crises that can appear in these regions.

According to Q'a Shubayqa farmers (Chapter 3, sections 3.2.3 and 3.4.1), the study area of this research is characterised by a complex hydrological system where seasonal floods that occur in the Jabal Druz area flow into Q'a Shubayqa and are a limiting factor for growth and crop management. Comparisons between derived spectral indices from the cultivated lands and seasonal precipitation of Jabal Druz have also shown a strong relationship between precipitation amounts and timing and greenness and water content (Chapter 5, section 5.4.1).

The aims of this chapter are to study the existing hydrological system in Q'a Shubayqa and quantify flood waters that reach the Q'a by using a water balance rainfall-runoff model. These models have been shown to be a useful tool for understanding the relationship between rainfall and runoff especially for ungauged dryland catchments (Abdulla and Al-Badranih, 2000). The Soil and Water Assessment Tool (SWAT) model (Arnold et al., 1998; Neitsch et al., 2004), which is one of the most widely used worldwide, will be employed for this research. In this chapter, the performance of SWAT models in estimating ungauged watershed discharge based on calibration and validation using remote sensing (R.S) actual evapotranspiration (AET) data will be evaluated. This step of the PhD research is very important to estimate the quantity of flood water that submerges the cropped lands in Q'a Shubayqa during each flood event, and to be used as input data for crop-simulation models as water availability is considered as a particularly limiting factor for dryland crop productivity, and in Q'a Shubayqa specifically.

6.2. Literature review

6.2.1. Watershed hydrological systems

6.2.1.1. General Concepts

A watershed (or catchment). a closed hydrological unit entirely drained by a particular stream, is often used as a physical and socio-economic-political unit for the planning and management of natural resources (Brooks et al., 2012; Hrachowitz et al., 2016; Sheng, 1990). Studying hydrological systems was historically simplified by relying on a key assumption of temporal stationarity in conditions such as topography, land use, climate and flow patterns. Due to the increasing recognition of hydrological system complexity, the applicability of this assumption has diminished, and temporal-spatial combinations are now required in catchment hydrological modelling (Ehret et al., 2014). This is a challenge in some regions where the stationarity assumption may be enforced on the model system as a best solution because of limited and scarce data.

6.2.1.2. Hydrological modelling of ungauged watershed in drylands

Most hydrological models were designed for use in humid and sub-humid areas and in arid/semi-arid areas their performance varies considerably (Li et al., 2015). Although SWAT has received international recognition as a robust interdisciplinary catchment-scale modelling tool (Bärlund et al., 2007), its application in arid and semi-arid regions is still challenging due to the unavailability of recorded runoff data for model calibration and validation (Mengistu et al., 2019). Model parameters used in calibration and the values found to produce optimal calibration for each parameter vary substantially among studies and watersheds (Sinnathamby et al., 2017).

Hydrological models simulate all components of the hydrological cycle, but streamflow is the component of the model output most often used for comparison during the calibration process, which is not possible for ungauged watersheds or those with large data gaps. Using another hydrological component in the parameter calibration process is, therefore, an alternative method to represent all processes in the watershed hydrological cycle. These methods include first the regionalization approach where the modeller needs to find a similar gauged catchment to be parametrised and calibrated; the gauged catchment parameters will be transferred to the ungauged similar watershed (e.g. Rafiei Emam et al., 2016; Reichl et al., 2009; Swain and Patra, 2017). A second method is the calibration of SWAT based on crop yield but this method

is field-scale approach that was recommended to reduce the plant growth related systematic error component of larger-scale hydrological processes such as runoff (Nair et al. 2011; Sinnathamby et al., 2017). The third method is calibration based on using satellite remote sensing data such as actual evapotranspiration (AET) data and soil moisture data (Jajarmizadeh et al., 2012; Odusanya et al., 2018; Rajib et al., 2016; Tobin and Bennett 2017; Zhang et al. 2017).

6.2.2. Why SWAT?

The Soil and Water Assessment Tool (SWAT) (Arnold et al., 1998) was developed at the United States Department of Agriculture (USDA). It is a process-based and spatially semi-distributed hydrological and water quality model created to calculate and route water, for continuous simulation, streamflow, sediments and contaminants from individual drainage units (sub-basins) throughout a river basin towards its outlet. The decision to use SWAT in this work was taken based on several factors and characteristics. SWAT is capable of simulating all water flows and water balance components including evapotranspiration of different land units at various temporal scales. Second, SWAT allows easy representation and use of spatially variable data, processes and results through a GIS interface (ArcSWAT). Finally, SWAT's various applications have been documented by a large number of publications outlining the model's high performance and efficiency for predicting the effect of climate and management decision on water, sediments, nutrients and yields with reasonable accuracy in large, ungauged catchments (e.g. Dile & Srinivasan, 2014; Ndomba et al., 2005; Xue et al., 2014). Besides that, SWAT has a wide development and user community with open access to the model documentation and source code. Many official institutes have adopted SWAT as the main model to assess and study any climate or management impact on a watershed, such as NRCS, Universities, NOAA and environmental consulting firms (Arnold et al., 2012).

In Jordan, Abdulla and Al-Shurafat, (2020) have applied SWAT to investigate its capability to simulate streamflow for the Yarmouk river basin (7004 Km^2) which is a trans-boundary watershed crossing Jordan and Syria. The watershed modelling was operated under two conditions (pre-development without any man-made change and post-development after watershed modification). They reported that, although there were challenges in modelling the Yarmouk River basin hydrological water cycle due to the poor quality of data in Syrian part, the modelling performance metrics were satisfactory at the monthly scale under both conditions for both calibration and validation processes. They also recommended using the model outputs

to enhance the water resources management in the Yarmouk River basin and that it could be used to investigate the impact of climate change on the surface water resources of this catchment.

In China, Qi et al. (2017) have applied SWAT and GWLF (Generalized Watershed Loading Functions) models to study streamflow and sediment yields in two catchments, one located in a humid area and the other in a semi-arid area, both characterised by data scarcity. The models of both catchments show that SWAT performs better for detailed representations than GWLF. However, the latter is easier for users in terms of data requirements. They recommended SWAT for projects where higher accuracy and resolution are required. Likewise, Zhang et al. (2016) have applied SWAT and DLBRM (The Distributed Large Basin Runoff Model) models to a watershed located in the arid northwest of China to study and estimate runoff. They have reported that both models were capable of producing reasonable outputs with some differences in performance due to data availability, landscape variations and interpolation schemes. They recommended using SWAT because it is a conceptual model with a wide capability and performance in simulating complex hydrological system successfully.

In Michigan (USA), Herman et al., (2018) have adopted SWAT to evaluate the role of AET remote sensing (R.S) data in improving hydrological modelling predictability. Two different techniques were used to calibrate the SWAT model (multi-variable and genetic algorithms) based on two types of AET datasets. The performance of the hydrological model using both calibration techniques and R.S actual evapotranspiration datasets was improved, achieving satisfactory performance metrics. Results from this assessment show that incorporation of remotely sensed and spatially distributed data can improve the hydrological model performance. This type of research has had a radical effect on the adopted hydrological modelling method (calibration and validation) applied in this study which is dealing with an ungauged watershed.

Calibration of spatially distributed hydrological models is frequently limited by the availability of ground observations, whilst remotely sensed hydrological variables provide an alternative source of observations to inform models and extend modelling capability beyond the limits of ground observations. In this context, Kunnath-Poovakka et al. (2016) selected the SWAT model to examine the efficacity of calibrating a hydrological model using different types and sources of remotely sensed actual evapotranspiration (AET) and soil moisture datasets for

streamflow prediction. This method was applied to 11 catchments in eastern Australia with different flow rates (low, medium and high) depending on the climate type of each catchment. This study showed that the quality of AET data for calibration is critical to produce reliable streamflow predictions as AET and streamflow comprise the major output fluxes in steady-state rainfall-runoff processes. Furthermore, the accuracy of the satellite products can vary greatly across large regions due to climate variability and heterogeneity in land surface conditions such as land cover and topography. The conclusion of this study revealed that accurate AET product can improve streamflow predictions in catchments with low or high runoff rates.

Odusanya et al. (2018) calibrated and validated the SWAT model with satellite-based AET from two sources, for a large ungauged basin (20,292 Km^2) located in southwestern Nigeria. But before that, they applied three potential evapotranspiration (PET) equations (Hargreaves, Priestley–Taylor and Penman–Monteith) in SWAT simulation of AET, to obtain a high performing model for the studied basin. They found that using freely available satellite-based AET for SWAT calibration of ungauged catchments is useful and produced satisfactory performance metrics result which means estimating an accurate streamflow output. They also recommended testing the three PET equations in SWAT to simulate AET whenever SWAT calibration is carried out with any satellite-based AET products.

SWAT presented a good performance (0.9 correlation and less than 4% relative error) in simulating the effects of ecological engineering on monthly water yield and soil water content in the arid Qilian Mountain of northern China (Tian et al., 2016). The applicability of SWAT in the arid Hetao oasis in China was assessed by Wu et al. (2016), where simulated discharge has shown an acceptable NSE (Nash-Sutcliffe efficiency) around 0.62. Jajarmizadeh et al. (2017) used SWAT to estimate runoff volume in the arid Roodan watershed in Iran. They obtained satisfactory performance metrics (NSE and PBIAS are equal to 0.75 and 1.5%, respectively), suggesting that SWAT can successfully estimate hydrological patterns of arid regions and provide a supporting hydrological tool for water management projects to estimate water discharge. In the semi-arid Onkaparinga catchment in Australia, the performance of SWAT was evaluated by Shrestha et al. (2016) who found that SWAT can reasonably capture the low flow conditions in semi-arid areas.

All previous mentioned studies and published research have testified that the SWAT model was capable, in comparison with other similar models, of estimating streamflow of ungauged watersheds located in arid or semi-arid regions accurately by relying on satellite remote sensing satellite data such as AET and soil moisture to calibrate and validate the watershed.

6.2.3. Evapotranspiration estimation in SWAT

Evapotranspiration is considered as a key process in the hydrological cycle and the most difficult component to determine. Several equations have been developed to estimate PET (Lu et al., 2005) and SWAT adopted three PET estimation methods from which the user can choose depending on the data availability. These methods are: the Penman-Monteith method, the Priestley-Taylor method and the Hargreaves method. Before running any simulation, SWAT offers the user the chance to choose one of these equations according to the input amount required for each one.

Actual evapotranspiration (AET) is estimated in SWAT after PET is determined, where SWAT first evaporates any rainfall intercepted by the canopy. Second, it calculates the maximum amount of transpiration, sublimation and soil evaporation. Finally, the actual amount of sublimation and evaporation from the soil surface is calculated. If snowfall exists in the HRU (Hydrological Response Units), sublimation can occur. If not, only evaporation from soil surface is calculated. A detailed description of SWAT evapotranspiration equations can be found in Neitsch et al. (2011). This variation of PET estimation equations makes SWAT models more flexible for the user and capable to adapt with input data availability.

6.3. Hydrological modelling of Q'a Shubayqa watershed: material and methods

6.3.1. Data acquisition

The main data (Table 6.1) required to run SWAT model simulations (Figure 6.5) are topographic data (DEM), Land Use Land Cover (LULC) data and soil property data. SWAT also requires spatially explicit datasets of daily weather data (precipitation, maximum and minimum air temperature, relative humidity, wind speed and solar radiation). These data were collected and processed from various locally and globally available sources for the Shubayqa watershed. Due to the unavailability of discharge measurement in the study watershed and to calibrate and validate SWAT model, three satellite-based AET datasets were retrieved for the period of 1987 to 2014 for the study area to fit the simulation output period because in SWAT, the first two years of simulated period are used as a warm-up period, and no output will be

presented. This process will help to evaluate the role of AET remote sensing data in improving SWAT model predictability.

Table 6.1 Data used for SWAT modelling, calibration and validation of Q'a Shubayqa watershed.

Data Type	Source and description
DEM	The ALOS DEM with 12.5 m resolution, downloaded from the Alaska Satellite Facility (ASF) https://asf.alaska.edu/data-sets/derived-data-sets/alos-palsar-rtc/alos-palsar-radiometric-terrain-correction/
Soil data	-Syrian Part: RS and GIS Laboratory (ACSAD-1998). -Jordanian Part: Jordan Ministry of Agriculture.
LULC data	Global map of land use/land cover areas at 10 km for year 2000 from the International Water Management Institute: http://waterdata.iwmi.org/Applications/GIAM2000/
Precipitation and Temperature	-Water Authority of Jordan: Station of PRINCE HASAN Safawi/H5 (LAT=32.316, LONG=37.188, ELEVATION=738m) -Directorate of Agriculture and Agricultural Reform in Sweida-Syria: Station of Ein Arab (LAT=32.628, LONG=36.67, ELEVATION=1557m)
Relative humidity, Solar radiation and Wind	The National Center for Environmental Prediction (NCEP) https://globalweather.tamu.edu/#pubs CFSR weather could be a valuable option for hydrological predictions where conventional gauges are not available (Dile & Srinivasan, 2014).
GLEAM *(R.S AET dataset)*	**GLEAM** (Global Land Evaporation Amsterdam Model- v3.0a) is available on a spatial resolution of 28-Km2 latitude-longitude regular grid (Miralles, Holmes, et al., 2011), (Miralles, De Jeu, et al., 2011).

MOD16 *(R.S AET dataset)*	**MOD16** global actual evapotranspiration (AET) dataset is regular 1-km^2 land surface ET datasets for the 109.03 Million km2 global vegetated land areas at monthly interval. (Mu et al. 2007; Mu et al. 2011).
TerraClimate *(R.S AET dataset)*	**TerraClimate** is a dataset of high-spatial resolution (4-km^2) monthly climate and climatic water balance for global terrestrial surfaces from 1958–2015 (Abatzoglou et al., 2018).
USGS Landsat 5 Surface Reflectance Tier 1 (1985-2015)	Landsat 5 data is the atmospherically corrected surface reflectance from the Landsat 5 ETM sensor. https://gee.stac.cloud/BJmBzK1uPSS1r6Qod58emr3zT5PPn4BKPZRsT
ERA5-Land volumetric soil water (1985-2015)	ERA5-Land is the volumetric soil water (soil moisture) dataset expressed in m^3 water per m^3 of soil (m^3/m^3), extracted using GEE for Q'a Shubayqa area (Muñoz Sabater, 2019).

6. 3.2. SWAT (The Soil and Water Assessment Tool) model parametrization

6.3.2.1. Overview

The whole theoretical and practical description of SWAT can be found in Neitsch et al. (2002), but below we focus on the most relevant aspects related to the hydrological components, as this was the main objective of the present study.

The representation of the hydrology of a watershed within SWAT's conceptual framework is divided into two major parts. The first one is the land phase of the hydrological cycle where the river basin is divided to several sub-basins, each one composed of one or several Hydrological Response Units (HRUs), which are the areas of relatively homogeneous land use/land cover and soil types. Generally, the characteristics of the HRUs define the hydrological response of a sub-basin. The HRU water balance calculation (land phase) defines the contribution of each sub-basin output to the discharge. The second phase is the river network which connects the different sub-basins outlets and the routing phase determines movement of water through this network towards the whole watershed outlet point (Neitsch et al., 2002).

The hydrological cycle in SWAT is based on the following water balance equation, where SW_f is the final soil water content, SW_o is the initial soil water content, t is the simulation period (days), R_i is the precipitation, Q_{surf} is surface runoff, E_a is evapotranspiration, W_{deep} is the aquifer recharge and Q_{gw} is the return flow where all these hydrologic processes are calculated on each day i and have the unit of mmH_2O (Githui et al., 2009).

$$SW_f = SW_o + \sum_{i=1}^{t} R_i - Q_{surf} - E_a - W_{deep} - Q_{gw}$$

6.3.2.2. Runoff simulation methods in SWAT (SCS-CN and G&A)

The first option is the ***Soil Conservation Service Curve Number*** procedure that includes the soil water content dependence and the evapotranspiration dependence retention parameters methods. The second option is the ***Green & Ampt infiltration method*** which is considered as one of the most complicated methods for better estimating the impact of land use on runoff. However, unlike the SCS-CN method, employing the Green & Ampt method requires several additional parameters which are mainly related to the watershed characteristics that have a considerable influence on the infiltration process (Dahdouh & Lahbassi, 2018).

During the hydrological modelling process of this study, the SCS curve number method was applied on Shubayqa watershed modelling process rather than Green and Ampt equation because the limited weather data available on a daily basis. In addition, the aim of the hydrological process is estimating daily discharge of the studied watershed (SCS-CN method) and not hourly discharge (Green& Ampt method).

The SCS curve number method is a rainfall-runoff model that was designed for computing excess rainfall (direct runoff). This method estimates the “before” and “after” hydrological response from events, is basically empirical, and provides a consistent basis for estimating the amount of runoff under varying land use and soil types. SCS curve numbers in SWAT were developed by the U.S Department of Agriculture (USDA) (National Engineering Handbook) in 1954 (Jha et al., 2004; Xu, 2002).The SCS-Curve Number mass balance equation is (Arnold at al., 2005):

$$Q_{surf} = \frac{(R - I_a)^2}{R - I_a + S} = \frac{(R - 0.2S)^2}{R + 0.8S}$$

where **Qsurf** is the accumulated overland flow (mm/d), R is the daily rainfall (mm/d), **S** is the retention parameter (mm) and Ia is the initial abstraction that is commonly approximated as 0.2S. The retention parameter is defined as:

$$S = 25.4\left(\frac{1000}{CN} - 10\right)$$

where CN is the curve number for the day, which is a function of the soil type, land cover and antecedent moisture condition.

In SWAT G&A infiltration rate is defined as:

$$f(t) = K\left[\frac{\psi \Delta\theta}{F(t)} + 1\right]$$

Where f(t) represents the infiltration rate (mm·h–1), K is the hydraulic conductivity (mm·h–1), ψ is the wetting front soil suction head (mm), Δθ is the change in moisture content, F(t) is the cumulative infiltration (mm), and t is time (h).

6.3.2.3. Runoff channel rooting methods

There are two main categories of routing methods, hydraulic methods that depend on solving partial differential equations of unsteady open channel flow, and hydrologic methods, based on the continuity equation within lumped systems and the relationship between storage of the reach and discharge at its outlet. The latter is applied within SWAT for Shubayqa watershed by introducing the variable storage rooting method (Williams and Rust, 1969). SWAT follows a sequence of steps to perform channel rooting. These steps start with calculating water volume in reach segment and cross-sectional area of flow from channel dimensions, estimating the flow rate in the reach, calculating the variable storage coefficients, and finally estimating discharge out of the reach and water storage in the reach at the end of the time step.

6.3.3. Land Use Land Cover LULC

In hydrological modelling, details of the catchment landuse/landcover are one of the most important input datasets. The LULC map of Shubayqa watershed was extracted from the Global map of land use/land cover areas at 10 km for year 2000 (Table 6.1). Figure 6.1 and Table 6.2 show the distribution of the different landcover classes over the study area, the percentage of each class and the corresponding SWAT landcover codes that were used in this simulation, where 72% of the catchment area is barren land and only 26.5% is agricultural land which includes the cultivated area of Q'a Shubayqa (12 km^2) and the rest is distributed over the Jabal Druz Heights.

Table 6.2: Distribution of landcover/landuse classes for the Shubayqa catchment

Landcover class	SWAT code	Area (km2)	% of the watershed
Winter Pasture	WPAS	3.25	0.46
Agricultural Land-Close-grown	AGRC	187.98	26.52
Residential-Low Density	URLD	4.02	0.57
Barren	BARR	513.05	72.37
Water	WATR	0.70	0.09

International Water Management Institute (IWMI) (http://waterdata.iwmi.org/Applications/GIAM2000/)

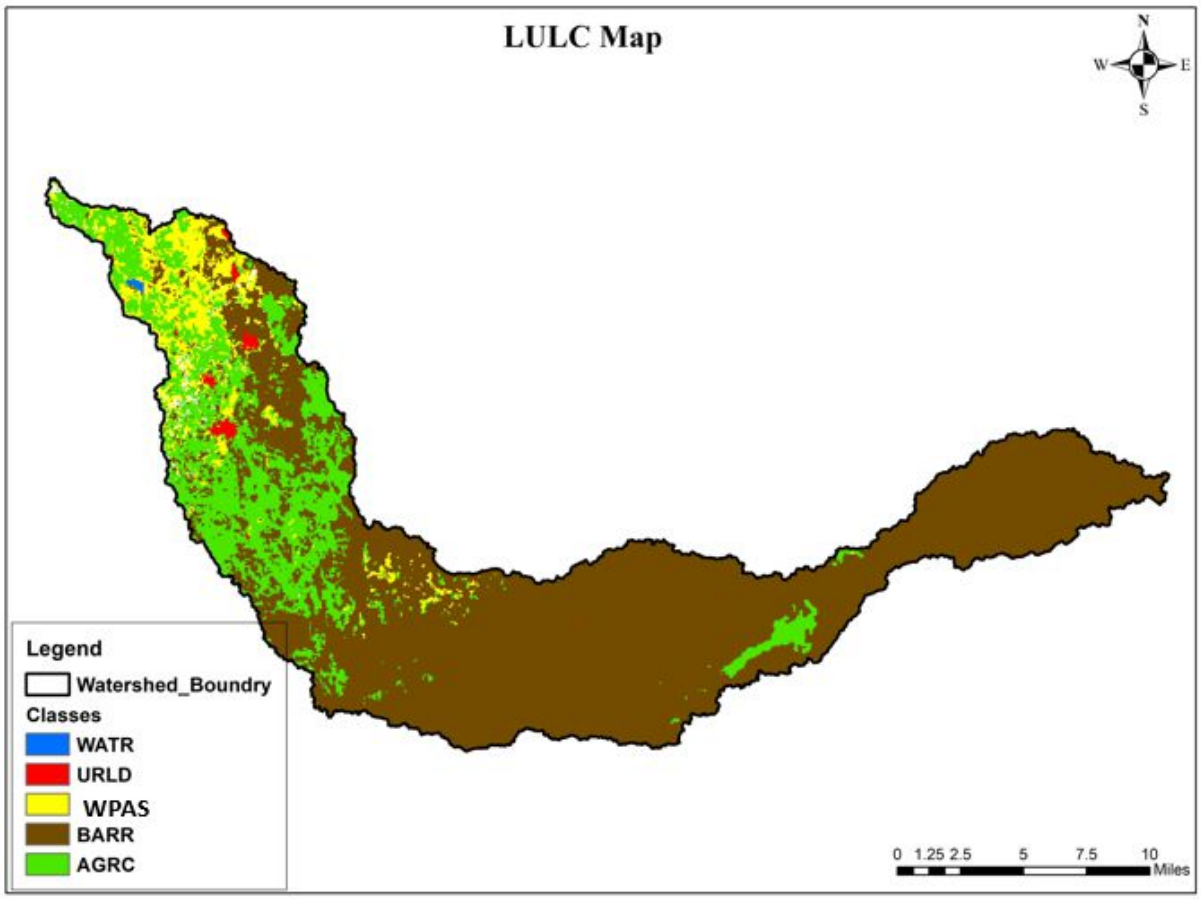

Figure 6.1: Landuse /landcover map of Shubayqa watershed (*WATR: water, URLD: residential-low density, WPAS: winter pasture, BARR: barren land, AGRC: agricultural land-close grown)*

6.3.4. Soil type and characteristics

Soil type has a major influence on catchment hydrology. Physical soil characteristics are required by hydrological models such as SWAT and include soil hydrologic group (SHG), depth of soil layers, available water capacity, moist bulk density, saturated hydraulic conductivity and percentage of silt, sand and clay (Neitsch et al., 2011). Shubayqa catchment soil data were obtained from two different sources for Jordan and Syria (Table 6.1). The soil data (based on soil subgroups) from the Jordanian part was clipped from a reconnaissance soil map with a scale of 1:250,000 for the whole country, produced by the Jordanian Ministry of Agriculture (National soil map and land-use project, 1994), this map is based on analysis of Landsat TM imagery and aerial photography and a soil sampling density of one observation per 7.6 Km^2. The area where the Shubayqa watershed lies is known as the north Jordan basalt plateau and it consists of a basaltic lava plateau with aeolian silt deposits. A transitional xeric-aridic moisture regime is dominant, while a xeric regime exists in a few wadis and depressions.

The thermic temperature regime dominant all over the region where annual soil temperature at 50cm depth is between 15 and 22 °C, except the southern margin at the Azraq basin where a hyperthermic temperature regime (annual soil temperature >22 °C) prevails.

The major soil subgroups are: xerochreptic calciorthids, soils with basalt or limestone parent rocks type and soil textures varying between silt loam to silty clay loam. This soil subgroup is mostly located on the middle and upper slopes of the interfluves. Xerochreptic paleorthids are the second most common subgroup with limestone parent rocks and mainly loam soil texture. This soil subgroup could be found on the very gently sloping interfluves. Lithic subgroup soils are also common in this area on the crests and hollows while camborthids occur in the valleys, basins and lower foot slopes (MoA, 1995). The only soil characteristics provided in these maps were the soil subgroup, the percentage of sand silt and clay, and SHGs.

Concerning the Syrian part, the only source available was a soil map for the whole country at a scale of 1:1000.000 prepared by M. Ilaiwi and processed in the RS and GIS Laboratory of the Araba Centre for the studies of Arid zones and Dry lands (ACSAD-1998). This soil map only provides information about soil group and subgroup and its spatial resolution is considered low, however it still the only available option for this study. The Syrian part of the watershed contains two major soil subgroups: Lithic Torriorthents with a loam texture and basalt parent rocks and Chromic Haploxererts with silty clay loam texture.

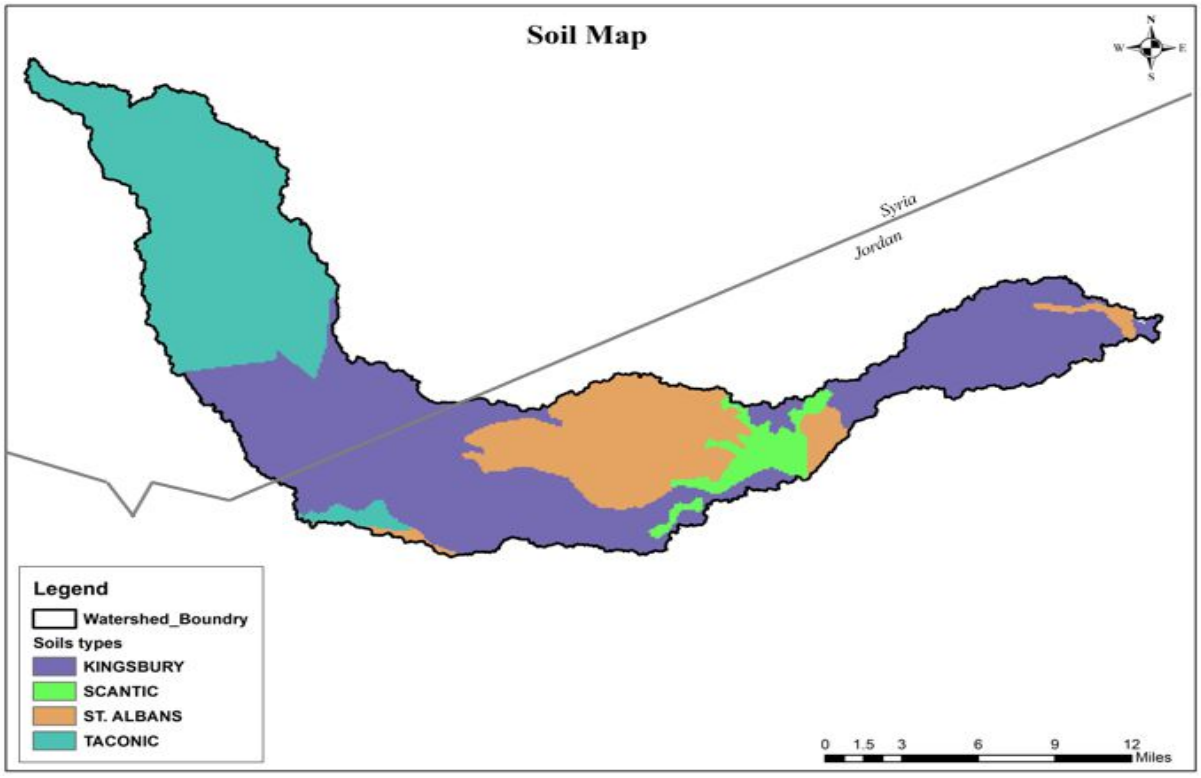

Figure 6.2: Shubayqa watershed soil classification using soil series selected based on Jordan and Syria soil characteristics

It was obvious that the collected data were missing a several soil parameters that are required for the SWAT model. To avoid adding random parameter values, my approach was to use the list of soil series (more details at: https://soilseries.sc.egov.usda.gov/) provided by SWAT which allows users to select the soil series name. Since we already have some of these parameters (subgroups, SHG and texture), the selection of the soil series from the SWAT interface was based on the approximative similarity with the soil parameter values already collected from the soil maps of the Jordanian and the Syrian parts of the studied watershed. Figure 6.2 illustrates four main soil categories identified in Shubayqa watershed.

6.3.5. Weather datasets

Meteorological data (Table 6.1) used for SWAT modelling parametrization contain limited missing data. SWAT provides a weather generator tool that assists in completing missing climate records for certain periods of time in the simulation periods (Neitsch, S.L et al., 2011). Here, the weather generator was not needed, and the catchment meteorological data was taken from two nearest weather stations to the q'a (Figure 6.3). The altitudes of these stations vary from 738m in Safawi to 1557m in Jabal Druz which allows the micro-climate regions of the

study catchment to be represented. However, these stations are not located inside the watershed boundary (Figure 6.3). In such situations, SWAT allocates the closest weather station for each sub-basin centroid.

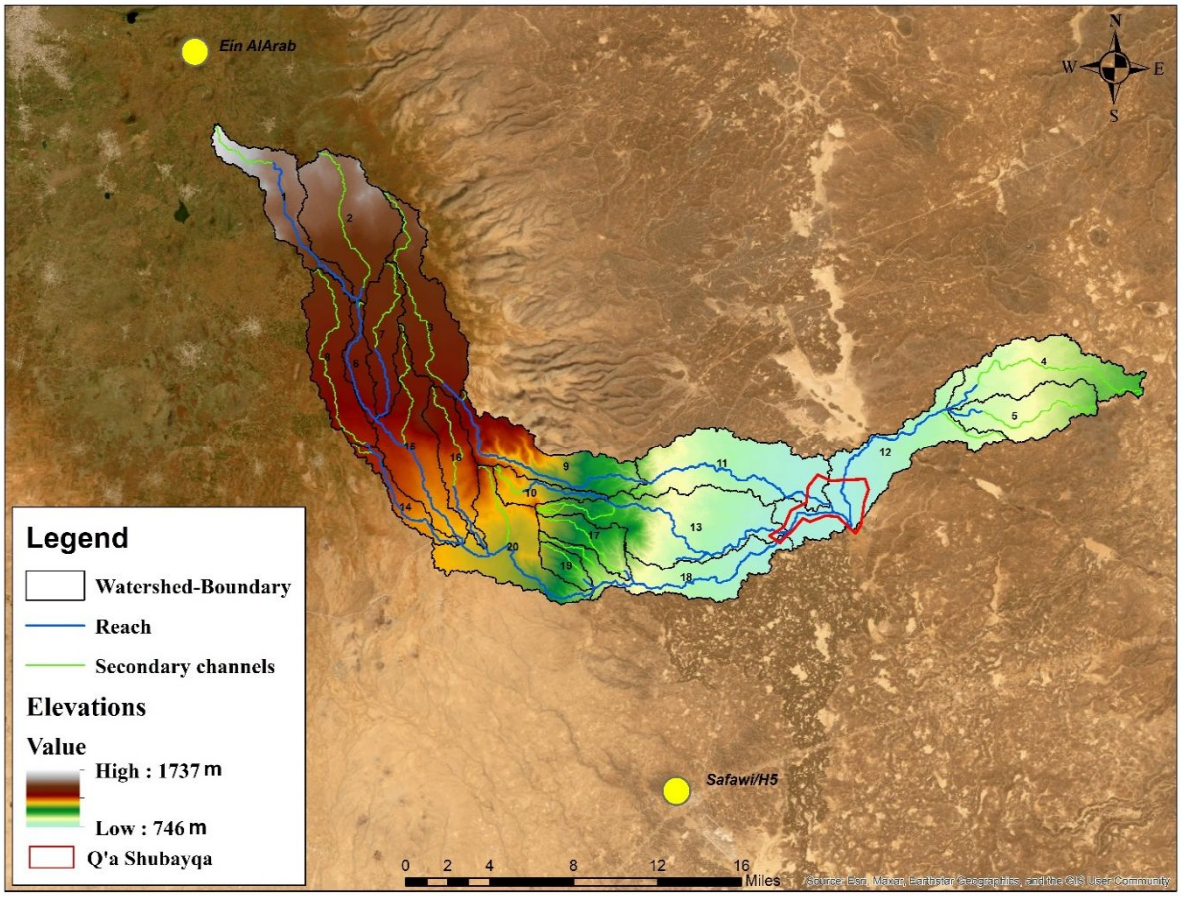

Figure 6.3: Hydrological features of the study catchment as defined by SWAT using ArcMap

The SWAT model also requires other climatic variables data as an input like relative humidity, solar energy and wind speed, not available from the two meteorological stations. In such cases, when meteorological data are scarce, using secondary data as an alternative is the only alternative way to run a model. The SWAT developers suggest using the Climate Forecast System Reanalysis (CFSR) secondary climate data produced by the National Centers for Environmental Prediction (NCEP). These data were designed and executed as a global, high resolution (0.5 deg x 0.5 deg latitude and longitude resolution), coupled atmosphere-ocean-land surface-sea ice system to provide the best estimate of the state of these coupled domains over this period. CFSR weather could be a valuable option for hydrological predictions where conventional gauges are not available (Dile & Srinivasan, 2014).

6.3.6. Data used for model calibration and validation

- **Evapotranspiration datasets**

Evapotranspiration (ET) is one of the main components of the watershed soil-water balance and a key agrometeorological element in dry environments. Due to the unavailability of discharge measurements in the study watershed and in order to evaluate the role of ET remote sensing data in improving SWAT model predictability, three satellite-based AET datasets were employed (Table 6.1). **GLEAM** (Global Land Evaporation Amsterdam Model- v3.0a) is a set of algorithms that separately estimate the different components of land evaporation (often referred to as 'evapotranspiration'): transpiration, bare-soil evaporation, interception loss, open-water evaporation and sublimation. It is available on a spatial resolution of 28-Km^2 latitude-longitude regular grid. More detailed information about GLEAM can be found in Miralles et al., (2011). **MOD16** global evapotranspiration (ET) dataset which is regular 1-km^2 land surface ET datasets for the 109.03 million km^2 global vegetated land areas at monthly intervals. The dataset covers the time period 2000 – 2010. More information about MOD16 can be found in Mu et al. (2007 and 2011)). **TerraClimate**, which is a dataset of high-spatial resolution (4km) monthly climate and climatic water balance for global terrestrial surfaces from 1958–2015. TerraClimate combines spatial climatology from WorldClim with time-varying datasets from the coarser resolution information from other sources to produce a monthly dataset of precipitation, maximum and minimum temperature, wind speed, vapor pressure, and solar radiation. 'Spatiotemporal aspects of TerraClimate were validated by developers using annual temperature, precipitation, and calculated reference evapotranspiration from station data, as well as annual runoff from streamflow gauges. TerraClimate datasets (climatic water balance) showed noted improvement in overall mean absolute error and increased spatial realism relative to coarser resolution gridded datasets (Abatzoglou et al. 2018).

6.3.7. Model setup and configuration

In this study, the ArcMap GIS interface for SWAT 2012 (Winchell et al., 2013) was used to configure and parametrize the SWAT model. After creating a new project, the first step in the simulation procedure was the watershed delineation by using the DEM ALOS PALSAR RTC with 12.5-m spatial resolution. During this procedure, the watershed was delineated into 20 sub-basins with the main outlet at Q'a Shubayqa (cultivated area). Flow directions, flow

accumulation points, stream networks and outlets for each sub-basin were established (Figure 6.3) in addition to parameter calculation (sub-basins area, reaches distances and outlets localization). The delineated area of study was found to be 709 Km^2.

After the watershed delineation process was completed, the definition of HRUs was continued by using commands from the HRU analysis of the ArcSWAT toolbar. Three spatial datasets (LULC, soil map and slope) are important for the definition of HRUs. The threshold percentage LULC, soil and slope factors for the creation of HRUs was given as 1%, 4% and 1% respectively. First the landuse/landcover (LULC) map (Figure 6.1) was fed into the model together with a lookup table which contained the classification of the watershed LULC and its percentages. Similarly, the soil map (Figure 6.2) and relative lookup table were provided to the model. After characterization of LULC map and soil map, multiple slope classes were selected. The number and the range of the slope classes can be defined by the user convenience. In this study five slope classes were used (0-0.01 %, 0.01-3.5%, 3.5-8.7%, 8.7-26.8%, 26.8-9999%) respectively (Figure 6.4). The slope classes are selected according to Demek (1972).

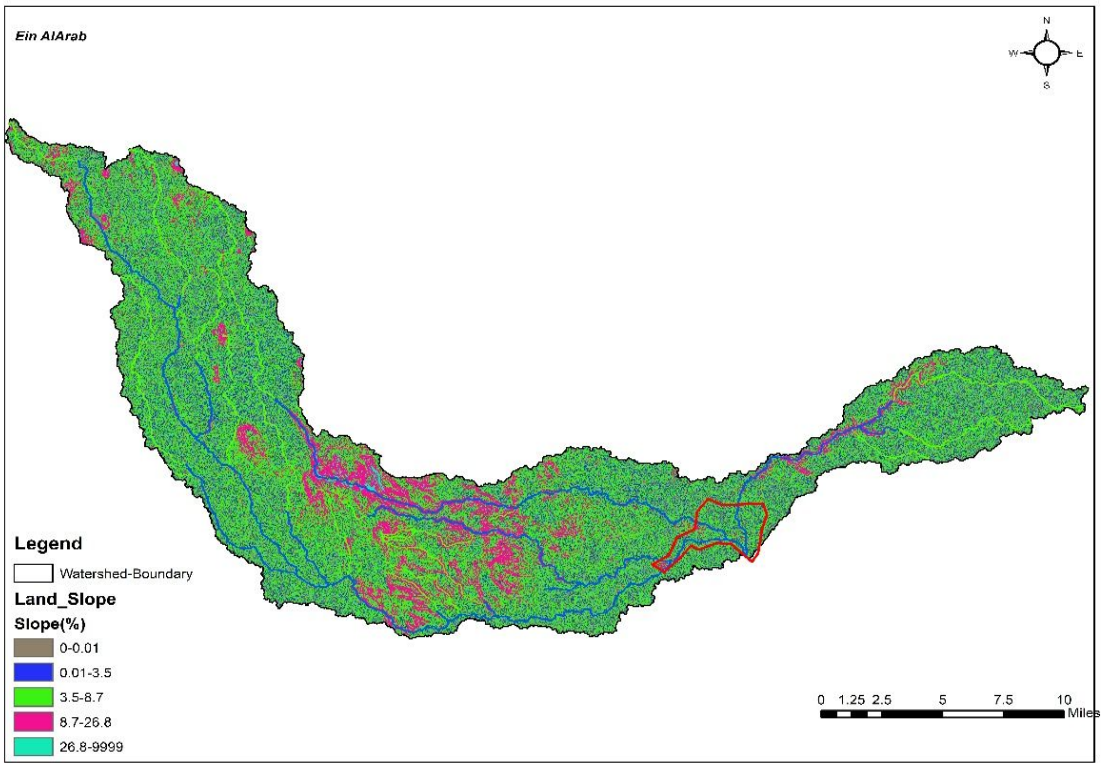

Figure 6.4: Slope classes map of Q'a Shubayqa watershed from ArcMap using ALOS DEM

After this process, each sub-basin was subdivided into hydrologic response units (HRUs) (see section 6.3.2.1) which generate a total number of HRUs in Shubayqa watershed of 255 units over 20 sub-basins (Figure 6.3).

All required climatic variable datasets need to be converted to the required SWAT format before being entered into the model. The weather generator tool in ArcSWAT interface was assigned to fill in the gaps in case of missing weather data. Before running any simulation, the estimation method SCS-Curve Number of rainfall-runoff process was selected. Likewise, among three evapotranspiration estimation methods, SWAT enables the user to choose the appropriate equation according to data availability. In this study, among the three methods of PET estimation provided in SWAT (see section 6.2.3), the Penman-Monteith equation was selected for estimating evapotranspiration as meteorological datasets needed for this equation are already available.

SWAT uses Manning's equation to define the rate and velocity of flow. Water is routed through the channel network using the Variable storage rooting method or Muskingum River routing method. Both methods are variations of Kinematic wave flood rooting model (Chow, 2010). In this model simulation, channel water rooting was set to be estimated by the Variable Storage Routing method (see section 6.3.2.3). After all the above processes were completed, the SWAT simulation run was conducted. During simulation, a two-year period (1985-1986) was specified as a warming-up period for the model. The total simulation period (including the warm-up period) was set to run from 1985 to 2021 (37 years).

6.3.8. Sensitivity analyses and model calibration and Validation

The successful application of hydrological models is highly dependent on the calibration and sensitivity analysis of the parameters (Abbaspour, 2015). The calibration and validation processes are usually employed with observed data. Discharge data has a critical role in this procedure. However, the study area (Shubayqa watershed) has no gauging station for stream flow measurement. Model calibration and validation was therefore carried out for actual evapotranspiration on a monthly time step based on satellite derived AET from TerraClimate by using Sequential Uncertainty Fitting Algorithm (SUFI-2), which is a calibration and uncertainty analysis tool within SWAT-CUP (SWAT-Calibration and Uncertainty Program) package (Abbaspour, 2015). SUFI-2 (Abbaspour, 2004) is one of the programs available in SWAT_CUP that is a multi-site, semi-automated, inverse modelling procedure used for calibrating model parameters. It is based on a stochastic procedure for drawing independent parameter sets using Latin Hypercube Sampling (LHS).

The first step in the calibration and validation preprocess in SWAT is the determination of the most sensitive parameters for a given watershed (Figure 6.5). Sensitivity analysis is the process of determining the rate of change in model output with respect to change in model inputs (parameters). It is necessary to identify the key parameters and parameter precisions required for calibration depending on the calibrated component of the water balance and the environmental characteristics of the study area (Ma et al., 2000). The sensitivity of the parameters is computed by multiple regression systems represented in next the below equation which returns the parameters generated by LHS versus the objective function values (Abbaspour, 2007).

$$g = \alpha + \sum_{i=1}^{m} \beta_i b_i$$

Where g is the objective function value, b is the parameter, α is the regression constant, β corresponds to the technical coefficient attached to the variable b, and m is equal to the number of parameters. The mean of the variation in the objective function estimates the sensitivity. It is computed by altering each parameter, one by one, while all other parameters remain the same. The sensitivity estimation is evaluated by the values of **t-stat** and **p-value.** The t-stat provides the measure of parameter sensitivity where a larger absolute value is more sensitive, and p-value determines the significance of the sensitivity where a value close to zero has more significance. When the p-value is <0.05, it means that we can reject the null hypothesis, and this means that the parameter affects the relevant variable, thus it is sensitive. The value of 0.05 indicates that there is a 95% probability that a parameter change will affects the relevant variable (Karim C Abbaspour et al., 2009).

In this research, an initial pre-selection of 26 parameters **(Appendix C)** based on literature research (Ha et al. 2017; López López et al. 2017; Odusanya et al. 2018; Rafiei Emam et al. 2016; Wang et al. 2006) was undertaken to identify the most sensitive parameters to AET, streamflow and snow melt, as the Shubayqa watershed upstream (Jabal Druz) may witness several snow storms during the cold season.

The initial parameters ranges were set at default values based on Neitsch et al. (2011) and two rounds of LHS comprising of 300 and 1000 simulations respectively, was carried out. Based on the sensitivity analysis, among the selected parameters, 9 were selected for further

calibration using SUFI-2 as they are the most sensitive parameters influencing evapotranspiration.

6.3.9. Calibration and validation approach

Calibration is an effort to better parametrize a model to a given set of local conditions, thereby reducing the prediction uncertainty (Arnold et al., 2012). After defining the most sensitive parameters (9 parameters) from the pre-calibration process, these parameters will be re-entered into SWAT-CUP with their new uncertainty ranges estimated during the pre-calibration, together with the selected remote-sensing AET data during pre-calibration. Each sub-basin among the 20 watershed sub-basins (HRUs) has its own AET data which will be considered as observed data and compared with the simulated AET from the model. The SWAT model was calibrated and validated on a monthly basis for evapotranspiration using SUFI-2. It is recommended that calibration and validation are typically performed by splitting the available observed data into two datasets: one for calibration, and another for validation. Data are most frequently split by time periods, carefully ensuring that the climate data used for both calibration and validation are not substantially different where wet, moderate, and dry years must occur in both periods (Gan et al., 1997). For the Shubayqa watershed, the data period (1987-2014) was split into a calibration period (1987-2003) and a validation period (2004-2014) making sure that this period contained wet, average and dry years to ensure calibration efficiency. This auto-calibration (SWAT-CUP) with AET from TerraClimate, had a sample size of 500 for the first iteration, and 1000 for the second iteration, resulting in 1500 simulations. To go from one iteration to the next, SUFI-2 suggests new ranges for parameter values based on their performance in the current iteration. The calibration scheme used for this study is the single variable calibration, where the model was only calibrated for actual evapotranspiration.

SWAT module validation is the procedure where the calibrated model is executed and evaluated for a different time interval and/or sub-basins by running the model using parameters that were determined during the calibration process and comparing SWAT AET predictions with satellite-based AET data (observed data) not used in the calibration. The objective is to compare the model estimates with observed data that were not used on the calibration process and demonstrate that the model is able to make sufficiently accurate estimates (Arnold et al., 2012), although ‘sufficiently accurate’ can vary based on project goals (Refsgaard, 1997).

The model validation of the study area was conducted for a period of 11 years (2004-2014) for 20 sub-basins. The new values of the most sensitive parameters that were estimated by SWAT_CUP during the auto-calibration process were added to ArcSWAT interface by using Manual Calibration Helper toolbar option and old model parameters were updated with new ones from the calibration outputs. A simulation run was then conducted for the validation period at monthly scale.

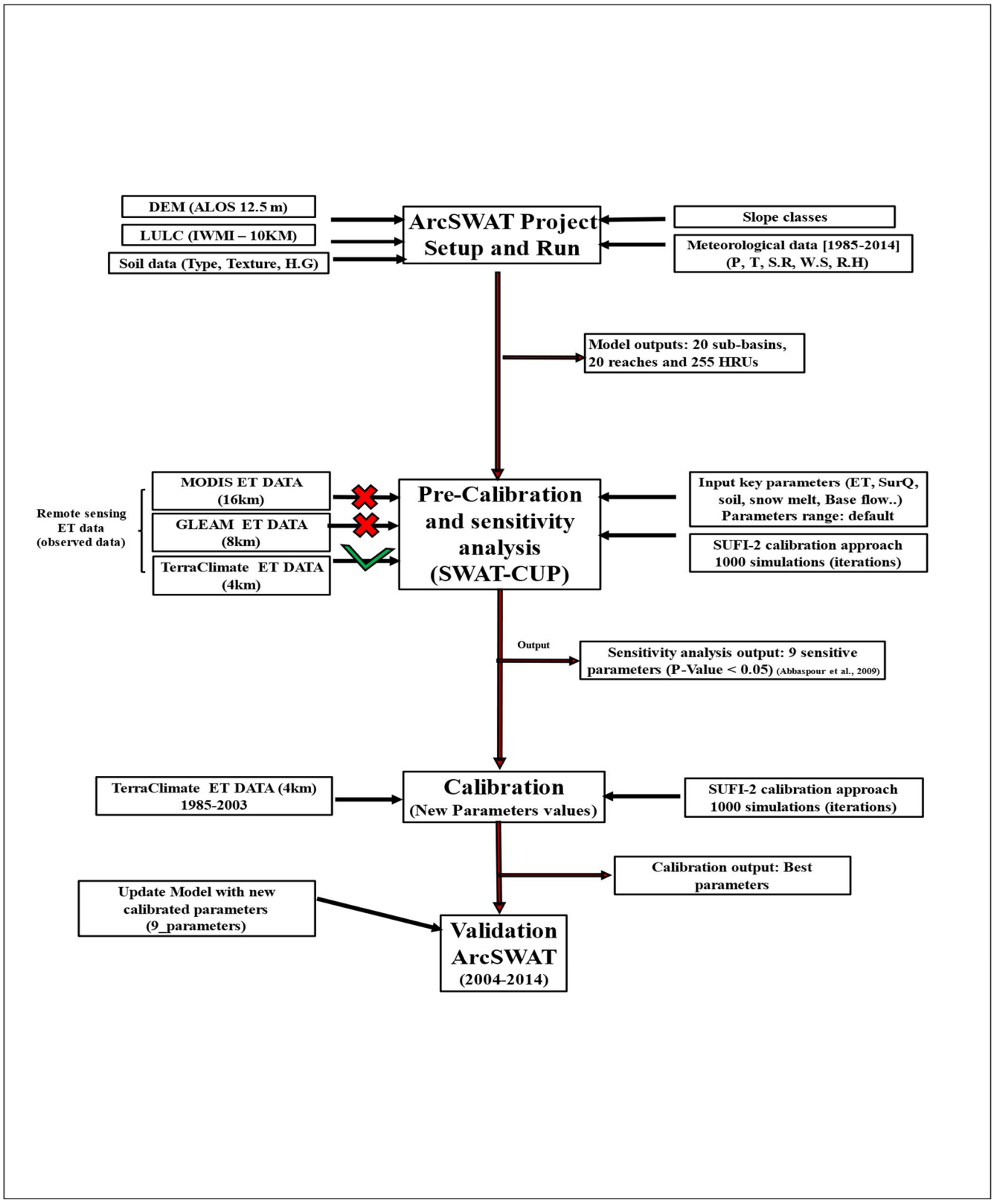

Figure 6.5: Framework showing major procedures in the hydrological modelling process

6.3.10. Model performance metrics

The performance of the SWAT model for calibration and validation processes is analyzed based on graphical representation of remote sensing AET (observed) from TerraClimate and model AET predictions, as well as various statistical methods. SUFI-2 has many options of model performance statistical parameters. For this study, Nash-Sutcliffe Efficiency (NSE) (Nash and Sutcliffe, 1970) was used as a major objective function in the calibration and validation processes. The coefficient of determination (R^2), percent bias (PBIAS), and ratio of the root mean squared error to the standard deviation of measured data (RSR) were additional criteria used for the evaluation of the model performance. By far the most widely used statistics reported for calibration and validation of SWAT model are R^2 and NSE (Arnold et al. 2012). These performance metrics were computed by SWAT-CUP (SUFI-2) as an output of the calibration process, while for validation process, the metrics were calculated on MS Excel by using its relevant equations.

The NSE quantifies the relative magnitudes of the residual variance compared to the measured data variance.

$$NSE = 1 - \frac{\sum_{i=1}^{n}(O_i - P_i)^2}{\sum_{i=1}^{n}(O_i - \bar{O})^2}$$

Where Pi and Oi are the simulated and observed ET, $\bar{O}$ is the mean value of observed AET, and n is the total number of observations.

Generally, NSE ranges from $-\infty$ to 1, with NSE=1 being the optimum value. Values between 0.5 and 1 are viewed as acceptable levels of performance whereas negative values or zero indicate that the mean observed values is better predictor that simulated values indicating unacceptable performance **(**Table 6.3**).**

The R^2 is the percent of variance explained by the model. It is a statistical measure of how close the data are to the fitted regression line. R^2 ranges from 0 to 1 with higher values indicating less error variance.

$$R^2 = \left(\frac{\sum_{i=1}^{n} (O_i - \bar{O})(P_i - \bar{P})}{\sqrt{\sum_{i=1}^{n} (O_i - \bar{O})^2} \sqrt{\sum_{i=1}^{n} (P_i - \bar{P})^2}} \right)^2$$

Where Pi and Oi are the simulated and observed AET, Ṗ and Ō are the mean value of simulated and observed AET, respectively and n is the total number of observations.

Percent bias (PBIAS) is the deviation of data being evaluated and expressed as a percentage. It measures the average tendency of the simulation data to be larger or smaller than the observation (Gupta et al., 1999). Negative values indicate model overestimation and positive values indicate model underestimation. It ranges from - ∞ to ∞, where low magnitude values indicate better simulations. The optimum value of PBIAS is 0 in percentage terms.

$$PBIAS = 1 - \frac{\sum_{i=1}^{n} (O_i - P_i)}{\sum_{i=1}^{n} O_i} \; x \; 100$$

Where Pi and Oi are the simulated and observed AET, and n is the total number of observations.

RMSE-observations Standard deviation ration (RSR) standardizes the root mean square error using observation standard deviation.

$$RSR = \frac{\sqrt{\sum_{i=1}^{n} (Oi - Pi)}}{\sqrt{\sum_{i=1}^{n} (Oi - \dot{P})}}$$

Where Pi and Oi are the simulated and observed AET, Ṗ and Ō is the mean value of simulated AET, and n is the total number of observations.

In this study, the model performance ratings criteria for recommended performance metrics for monthly time step are presented in Table 6.3.

Table 6.3: Performance metrics rating criteria for hydrological modelling (Kouchi et al., 2017; Moriasi et al., 2007)

Objective Function	Value range	Performance Classification
R^2	0.7 < R 2 < 1	Very good
	0.6 < R 2 < 0.7	Good
	0.5 < R 2 < 0.6	Satisfactory
	R 2 < 0.5	Unsatisfactory
NSE	0.75 < ENS ≤ 1.00	Very good
	0.65 < ENS ≤ 0.75	Good
	0.50 < ENS ≤ 0.65	Satisfactory
	0.4 < ENS ≤ 0.50	Acceptable
	ENS ≤ 0.4	Unsatisfactory
PBIAS	PBIAS < ±10	Very good
	±10 ≤ PBIAS < ±15	Good
	±15 ≤ PBIAS < ±25	Satisfactory
	PBIAS ≥ ±25	Unsatisfactory
RSR	0.00 ≤ RSR ≤ 0.50	Very good
	0.50 < RSR ≤ 0.60	Good
	0.60 < RSR ≤ 0.70	Satisfactory
	RSR > 0.70	Unsatisfactory

6.3.11. Model uncertainty analysis

SUFI-2 was also used for the uncertainty analysis of the AET modelling process. In this step, the procedure depicts the 95% prediction uncertainty (95PPU) of the model compared with satellite-based AET. The 95PPU was estimated at the 2.5% and 97.5% levels of the cumulative distribution of the ET simulated output variable derived through LHS. SWAT-CUP calculates two statistical indices to quantify all the sources of uncertainty, P-factor and R-factor (Abbaspour et al., 2004). The P-factor represents the percentage of observed data plus its error bracketed by the 95% predictive uncertainty (95PPU) band and varies from 0 to 1. Where 1 indicates a 100% bracketing of the observed data within model prediction uncertainty. While

the R- factor is the ratio of the average width of the 95PPU and the standard deviation of the observed variable, this value ranges between 0 and infinity. These two indices were also used to judge the strength of the calibration and validation in which the ideal situation would be a P-factor of 1 and R-factor of 0 to indicate that the simulation exactly corresponds to the measured data.

6.4. Results and discussion

6.4.1. Pre-calibration using different ET datasets

To evaluate the quality of these ET datasets and their performance to calibrate the model, a pre-calibration process was conducted. The performance metrics of the model pre-calibration show that among these datasets, TerraClimate ET data were the most reliable compared with the other ET data. Pre-calibration performance metrics from GLEAM were unsatisfactory because of its low resolution, but MOD16 was rejected because its dataset duration does not cover all the period of the model simulations. Therefore, in this study TerraClimate ET dataset was adopted for model calibration and validation. Figure 6.6 shows the spatial distribution of TerraClimate ET data at monthly temporal resolution over the watershed and each sub-basin may contain one or several points of TerraClimate data. Our approach for this study is to adopt the ET average values of the different TerraClimate data points for each sub-basin.

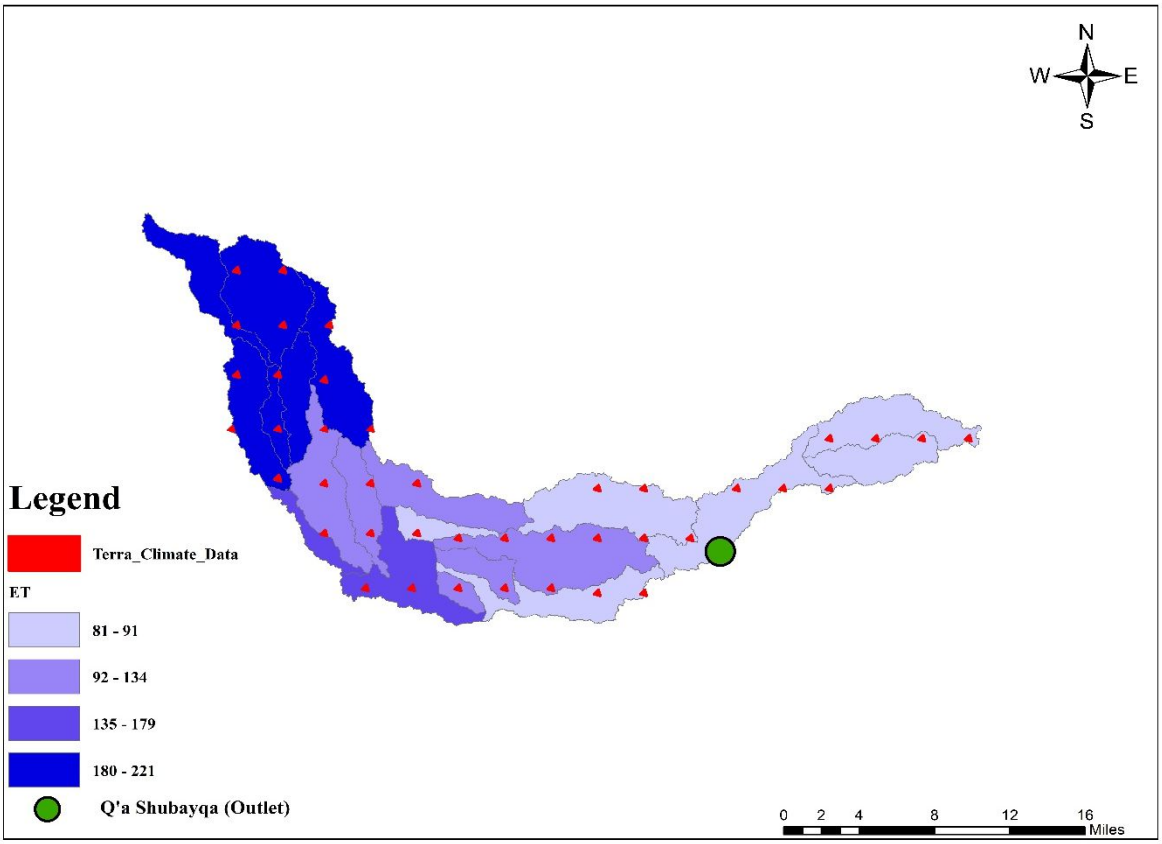

Figure 6.6: Mean annual evapotranspiration (mm) of TerraClimate for each watershed sub-basin from 1987-2014. Red triangles indicate the centres of the data grids (16km^2).

6.4.2. Comparison between local precipitation and R.S actual evapotranspiration data (Terraclimate AET)

Before starting any modelling process for the Shubayqa watershed and before using AET data for calibration and validation process, it is insightful to explore the relationship between used TerraClimate AET R.S data and observed seasonal rainfall (cumulative rainfall between October and April of each season) from both meteorological stations Safawi and Ein al-Arab (see sections 6.3.1 and 6.3.5). Figure 6.7 represent the interaction between seasonal precipitation from both met stations and cumulative seasonal AET for each sub-basin of Shubayqa watershed. We can notice an inter-seasonal variation of AET values and an important disparity between sub-basins AET values among the same seasons. For example, during the season 2001-2002, cumulative AET vary from 77.2mm in sub-basin number 10, reaching 221mm in sub-basin number 1.

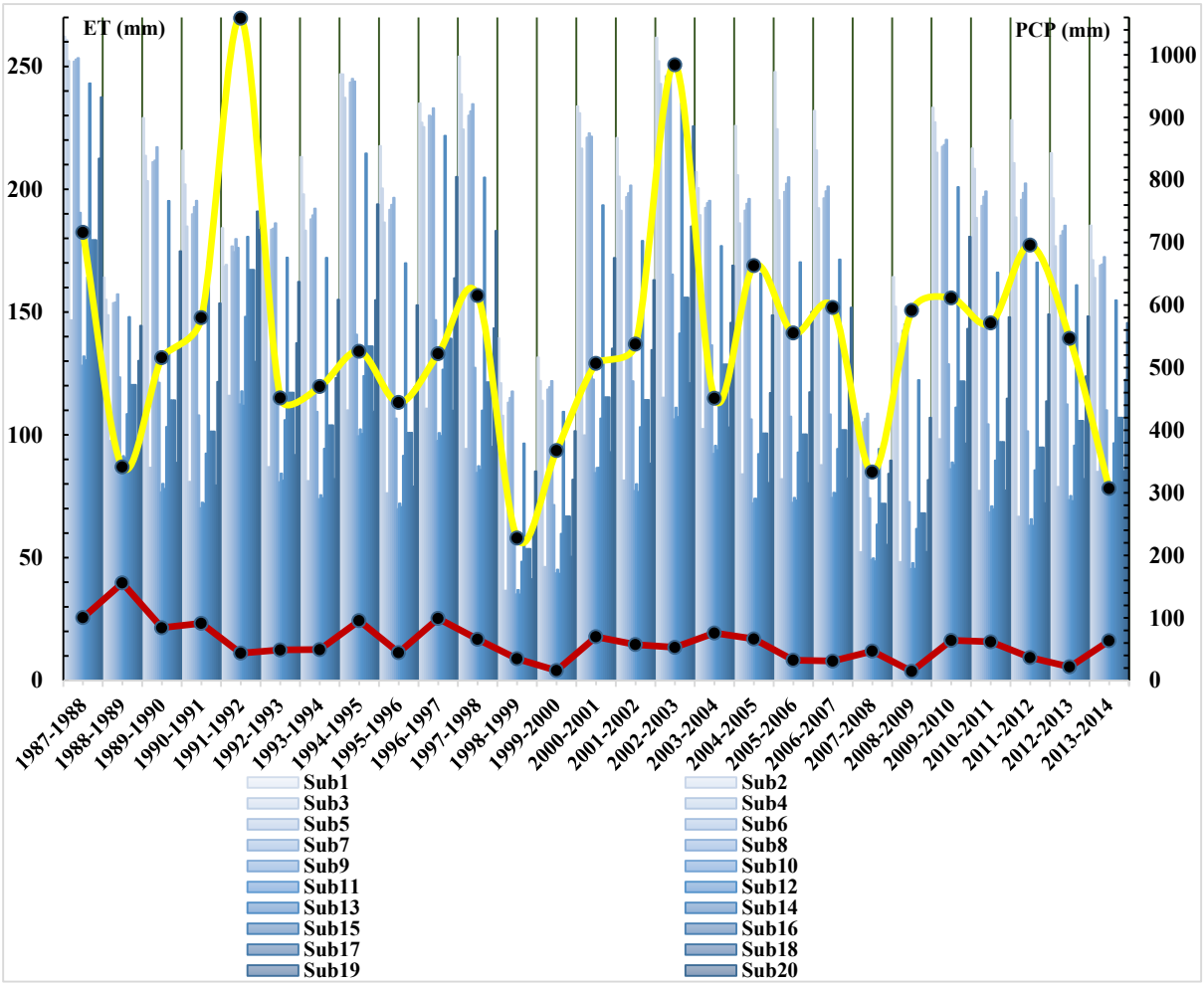

Figure 6.7: Interaction between seasonal rainfall (PCP) of the Safawi and Ein al-Arab meteorological stations with seasonal remote sensing AET of Shubayqa watershed sub-basins for the period between 1987-2014.

Table 6.4 represent the correlations between seasonal precipitation recorded in both met stations and AET for each sub-basin. The comparison between Ein al-Arab precipitation and AET has shown that there is a moderate positive correlation (varying from 0.5 to 0.7) for all the 20 sub-basins. These results could be reasonable for most of the sub-basins because flood water will usually reach all the watershed surface. However, flood water caused by Jabal Druz precipitation usually flows into Q'a Shubayqa sub-basin (N°12) and cannot reach the farthest sub-basins 4 and 5 located at Al-Shaquif heights (see Figure 6.4). Under these circumstances, it is expected that there is no relationship between AET in sub-basins 4 and 5 and seasonal rainfall recorded in Ein al-Arab station and correlation values should be negligible, which is not the case for the relevant calculated correlations. Other remarkable correlation values from Table 6.4 that were not expected are related to sub-basins N° 1, 2 and 3, because correlation of these sub-basins AET with seasonal precipitation are moderate, however, these sub-basins are the closest sub-basins to Ein al-Arab station and they receive the highest rainfall quantities,

which means they should have high positive correlation between seasonal precipitation and AET.

Such inapprehensible correlations between AET and seasonal precipitations of some watershed sub-basins could be one of the limitations affecting the model spatial performance when using such R.S AET data for the hydrological system model calibration and validation.

Table 6.4: Relationship (correlation) between local watershed seasonal precipitation and actual ET of each sub-basin of Shubayqa watershed

	Correlation between	
Sub-basin Nº	**Ein al-Arab PCP and actual ET**	**Safawi PCP and actual ET**
1	0.532	0.243
2	0.516	0.307
3	0.531	0.38
4	0.542	0.583
5	0.542	0.583
6	0.537	0.379
7	0.53	0.37
8	0.542	0.369
9	0.652	0.483
10	0.581	0.552
11	0.593	0.543
12	0.569	0.567
13	0.508	0.629
14	0.584	0.435
15	0.634	0.503
16	0.634	0.503
17	0.634	0.503
18	0.607	0.532
19	0.659	0.464
20	0.616	0.464

Regarding the correlation between AET and Safawi seasonal precipitation, the values with the watershed sub-basins vary from negligible (0.243 for sub-basin 1) to moderate positive (0.629 for sub-basin 13) correlation. These correlation values seem to be realistic when we note that the closest sub-basins to the Safawi meteorological station have shown a higher positive correlation such as sub-basins Nº 4, 5, 11, 12, 13 and 18 (see Figure 6.8).

6.4.3. Hydrological modelling results from SWAT

6.4.3.1. Parameterization and sensitivity analysis

After the delineation of the Shubayqa watershed and its subbasins, and the calculation of the relevant parameters using SWAT, the most sensitive parameters (9 of 26 parameters, see section 6.3.8) are now defined. The result of this global sensitivity analysis revealed that SCS runoff curve number (CN2.mgt), which indicates the flow portioning into runoff and base flow, is the most sensitive to SWAT's simulations of AET according to p-values measurement.

The new parameter intervals adjusted by SWAT-CUP during the global sensitivity analysis were considered during the calibration process of the simulated AET with an extracted TerraClimate remote sensing-based ET dataset.

6.4.3.2 Calibration and validation results

The calibration process output for the period between 1987-2003 has given a list of the best calibrated parameter values (Table 6.5). If the performance measures of the calibration process are classified between acceptable and very good, these obtained best parameters values suggested using SUFI-2 will be re-entered to SWAT model for the validation process during the period between 2004 to 2014. This time-period was chosen because TerraClimate AET data are only available until 2015.

Table 6.6 presents the model performance evaluation during calibration and validation processes (see section 6.3.9). The four calculated performance measures (NS, R^2, PBIAS and RSR) have shown that all the performance indicators for both calibration and validation of the model, vary between satisfactory to good ranges (Kouchi et al., 2017; Moriasi et al., 2007). To summarise, the statistical analyses using performance measures indicate that there is a good agreement between the remote sensing measurements and simulated evapotranspiration from SWAT.

Table 6.5: Sensitive parameters new calibrated values suggested by SWAT_CUP used for the model validation.

Parameters	Description of abbreviation	Fitted Values
r__CN2.mgt	Initial SCS runoff curve number for moisture condition II	-0.023
v__EPCO.bsn	Plant uptake compensation factor	0.76
r__SOL_K().sol	Saturated hydraulic conductivity	0.08
v__CANMX.hru	Maximum canopy storage	5.44
v__FFCB.bsn	Initial soil water storage	0.48
v__SFTMP.bsn	Snowfall temperature	-4.82
v__SMFMN.bsn	Melt factor on snow on December	5.84
v__ESCO.hru	Soil evaporation compensation factor	0.19
v__SOL_BD().sol	Moisture Bulk density	0.08

Table 6.6: Performance metrics of calibrated and validated model.

	Objective Function	Value (Whole watershed)	Performance
Calibration (1987-2003)	***NSE***	0.51	Satisfactory
	R^2	0.61	Good
	PBIAS	30.30	Unsatisfactory
	RSR	0.69	Satisfactory
Validation (2004-2014)	***NSE***	0.43	Acceptable
	R^2	0.53	Satisfactory
	PBIAS	21.02	Satisfactory
	RSR	0.70	Satisfactory

The spatial distribution of the model performance metrics values from the calibration and validation processes over the 20 sub-basins of the watershed, are presented in Figures 6.8 and Figure 6.9. The attached pie charts show the proportion of sub-basins in the different range categories. We can notice that for the calibration, performance values of R^2, NSE and RSR for

most of the watershed sub-basins range between satisfactory to good. The values of R^2 are significant in 95% of sub-basins, whereas NSE and RSR are significant in 70% and 60% of the sub-basins respectively. Only PBIAS showed unsatisfactory model performance during the calibration, in contrast to the PBIAS value during validation process which was satisfactory.

Regarding the validation process, the spatial distribution of performance metric values over the watershed sub-basins is presented in Figure 6.9. The significant values of R2, NSE and RSR cover 65%, 60% and 50% respectively of the watershed sub-basins. Regarding PBIAS, it is clear that the model performs well during the validation process, where PBIAS significant values cover 65% of the sub-basins. According to the difference between the calibration PBIAS values and validation PBIAS values, and although using the same parameter values during both processes, we can conclude that the TerraClimate algorithm has overestimated AET values during the calibration period.

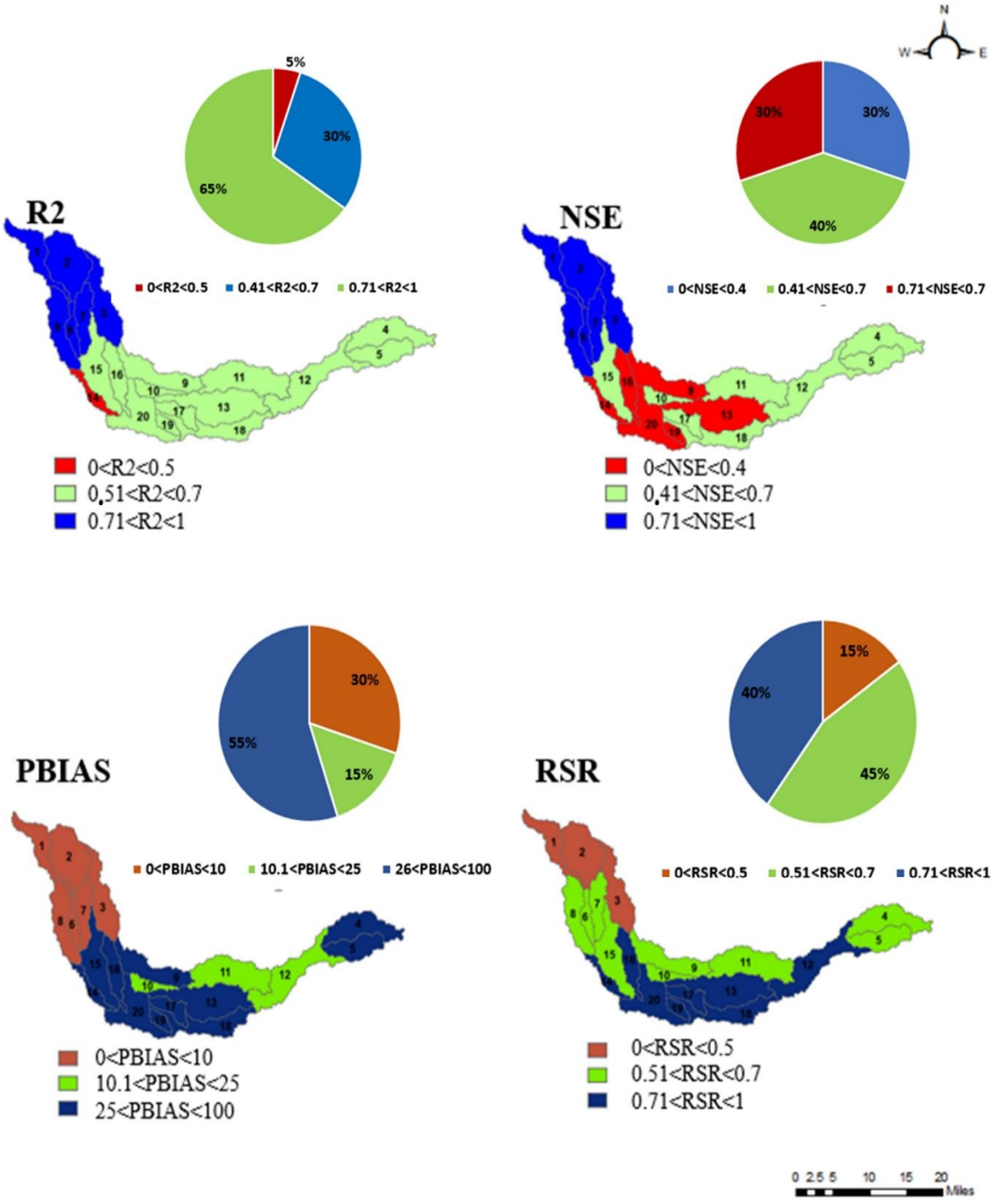

Figure 6.8: Classification and **s**patial distribution of calibration performance metrics values (R^2, NSE, PBIAS and RSR, very good to satisfactory, see Table 6.3) for AET over the watershed sub-basins.

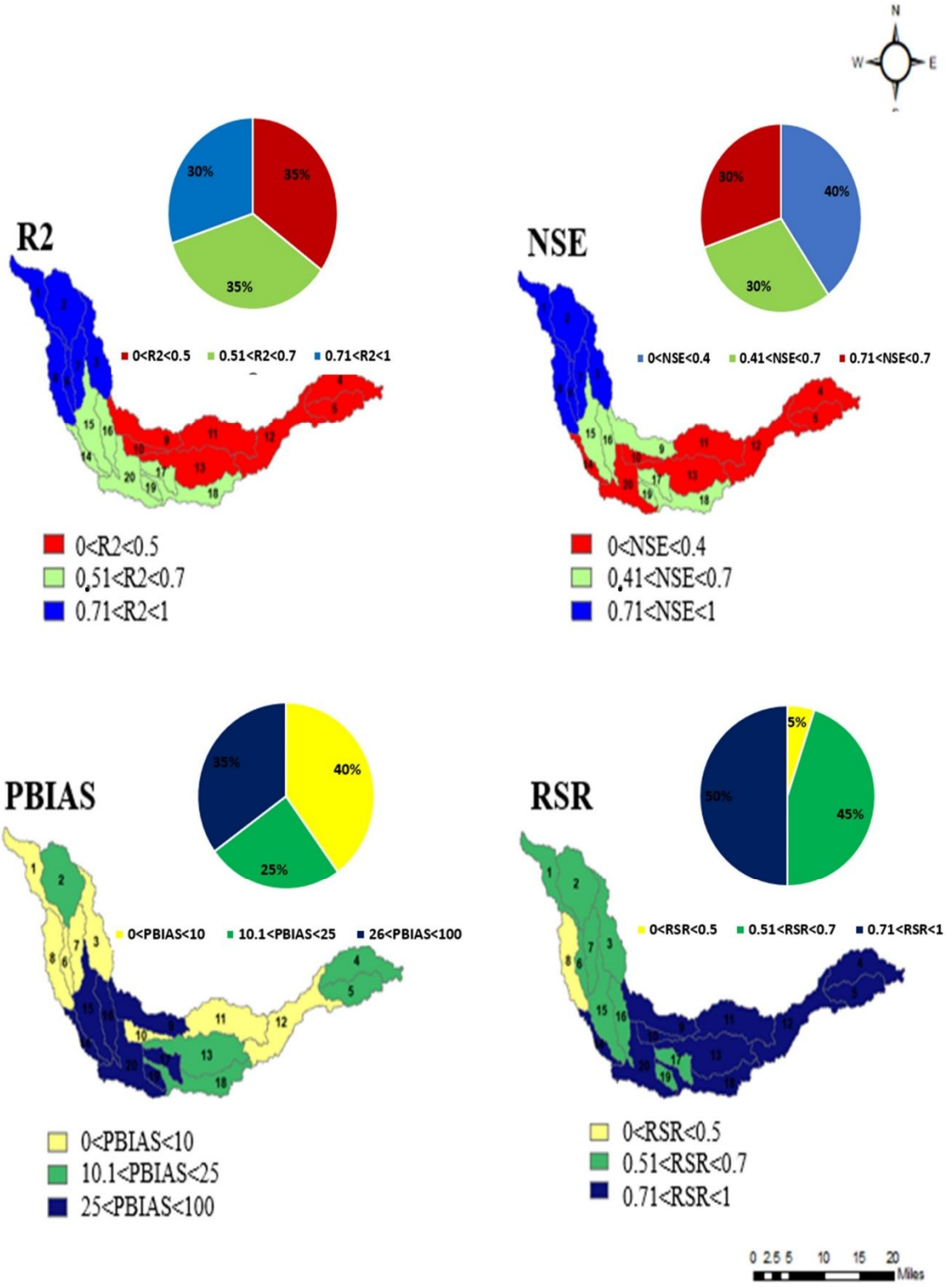

Figure 6.9: Classification and spatial distribution of validation performance metrics values (R^2, NSE, PBIAS and RSR) for AET over the watershed sub-basins.

Figure 6.10 shows an example of the comparison between TerraClimate AET and simulated AET during the whole period of modelling (28 years). The performance metrics for this sub-basin are classified as good. The importance of this sub-basin is its location in the upstream heights of Jabal Druz where most rainfall and highest evapotranspiration occur (see Figure 6.3).

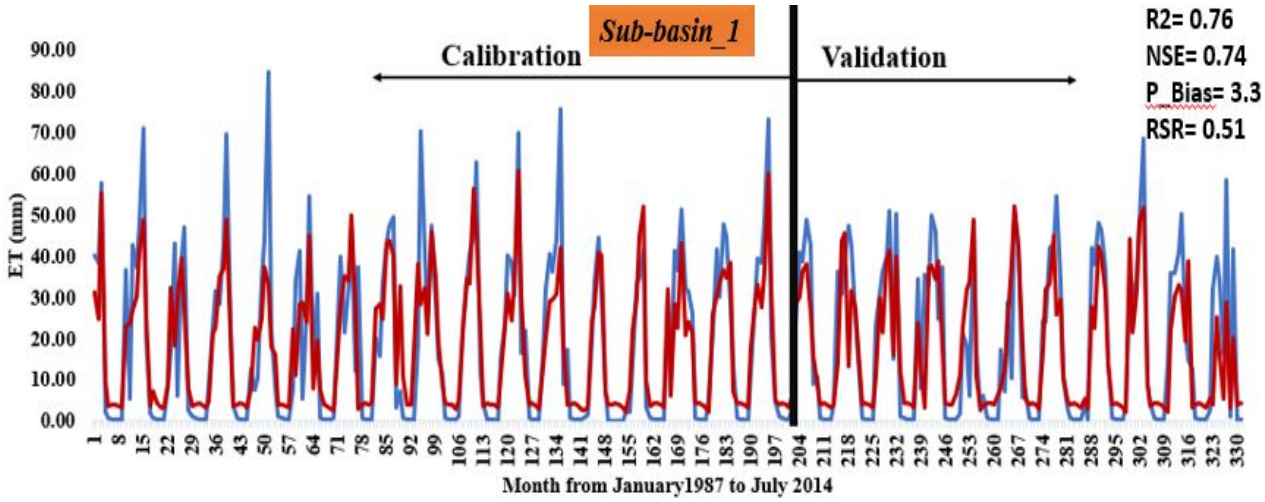

Figure 6.10: Comparison between remote sensing (Blue line) and simulated (red line) actual evapotranspiration for Sub-basin No.1

Figure 6.11 represents the most important output of the hydrological modelling of the Shubayqa watershed estimated by SWAT and shows the inter-seasonal variation of the quantity and the timing of flood waters that flow into Q'a Shubayqa sub-basin and submerge cultivated lands for the studied period between 1987 and 2021. The quantity of cumulative monthly flood water varies from one season to another where the lowest peak of water quantity recorded during the studied period was in the 1998-1999 season (January 1999) with 45.6 m^3/s (yellow arrow on Fig 6.11). The highest peak was recorded during the 1991-1992 season (February 1992) with 952 m^3/s (green arrow on Fig 6.11). Regarding the flood timing, it varies from season to season, for example first seasonal floods can occur between October and December, however the majority of first floods events appear in November and December. The timing of first flood is considered a limiting factor by Q'a Shubayqa farmers as it determines the starting date of the sowing season and allows cultivating the soil (See Chapter 3, section 3.4.2.2).

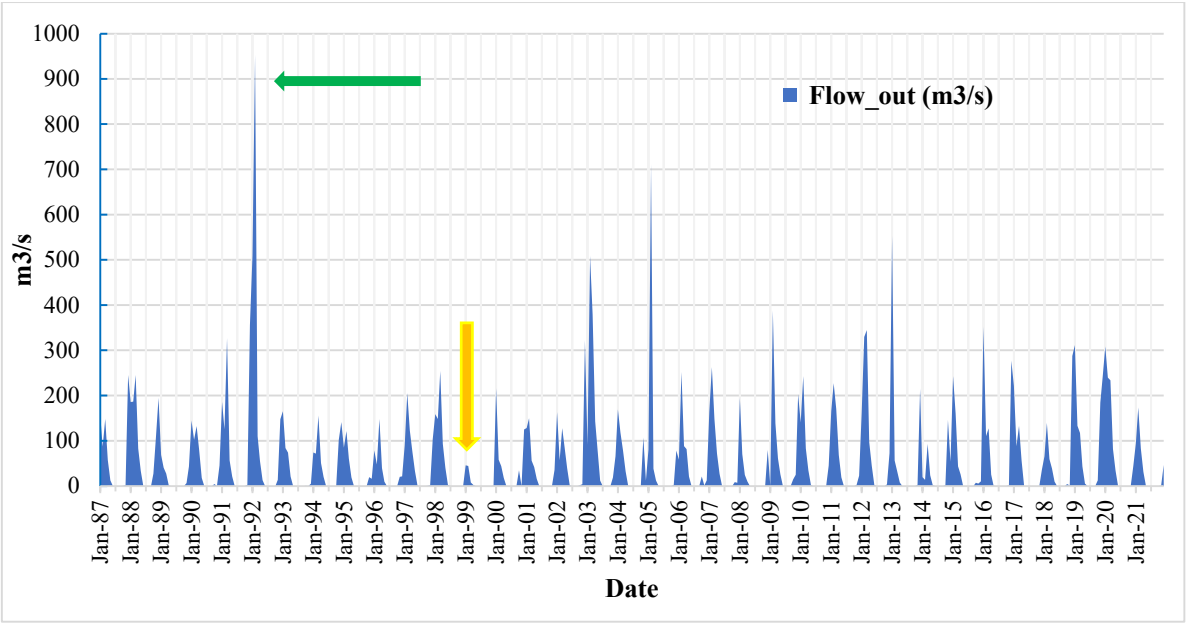

Figure 6.11: SWAT simulated monthly floods discharge (m^3/s) of Q'a Shubayqa watershed for the period between 1987-2021 (green arrow: highest discharge peak, Yellow arrow: lowest discharge peak)

The daily flood water quantity obtained from SWAT hydrological modelling process will be employed in the next chapter within the CERES crop simulation model as irrigation water input.

6.4.3.3. Verification of the model performance

In addition to the calibration and validation processes, a verification process of the model performance was conducted by correlating the simulated streamflow with two different remote sensing data sets (ERA5-Land and Landsat) extracted from within the Q'a Shubayqa boundary. Figure 6.12 represents a comparison between monthly streamflow estimated by the SWAT model after calibration and validation processes, and the soil moisture remote sensing dataset extracted from the ERA5-Land dataset (Table 6.1). The extraction of the soil moisture time series was limited to the cultivated area of Q'a Shubayqa which is also considered as the discharge point of the whole watershed (see above). The Pearson correlation between these variables was significant and positive with $\mathbf{R^2}$**=0.34**. Likewise, the comparison between NDWI extracted from Landsat 5 and Landsat 8 and simulated streamflow (Figure 6.13) shows a significant and positive Pearson correlation with $\mathbf{R^2}$**=0.22**. These results of a long-term comparison (35 years) for a large watershed (709 km^2), could be another suitable evaluation

and verification tool for such an ungauged watershed in drylands. In addition, using R.S data would be a good approach to improve the confidence in model outputs.

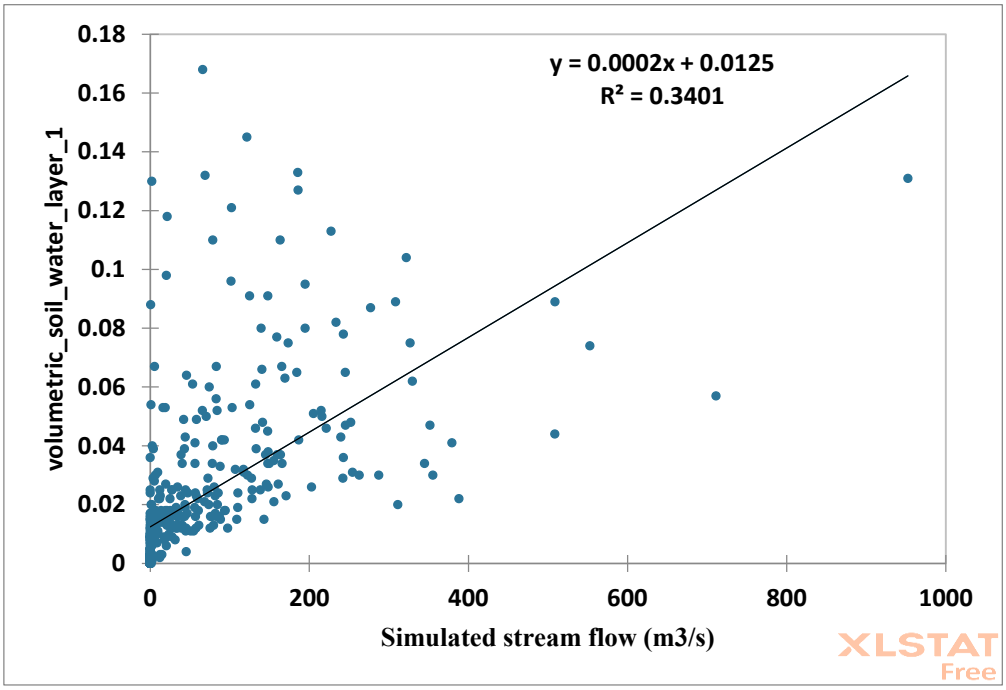

Figure 6.12: Comparison between monthly simulated streamflow and monthly R.S soil moisture (**ERA5-Land)** for the period from 1987 to 2021

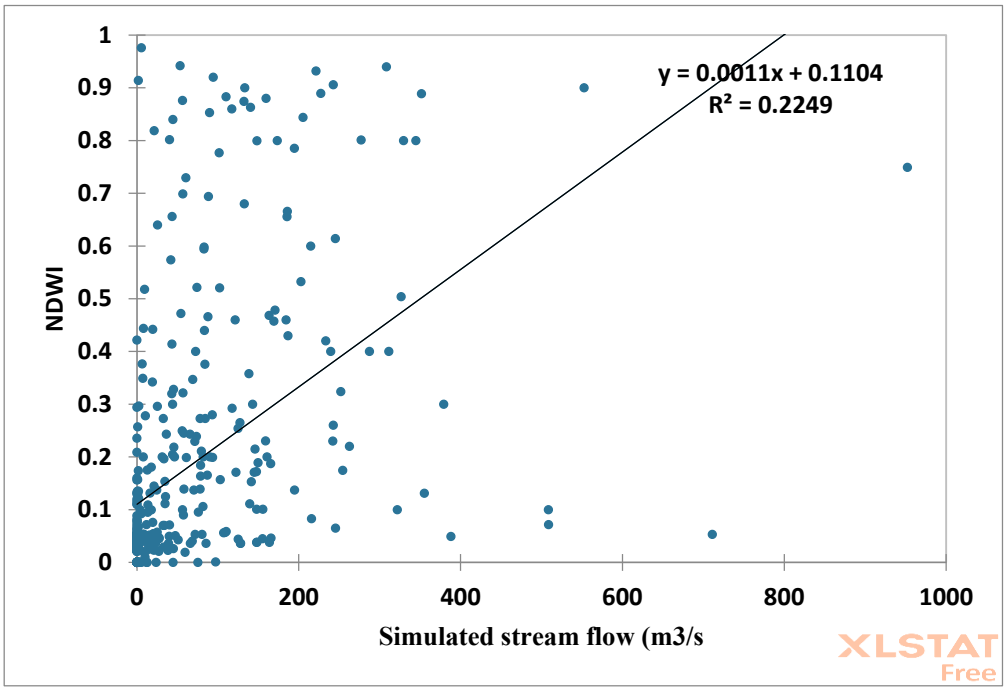

Figure 6.13: Comparison between monthly simulated streamflow and monthly NDWI (L5 and L8) for the period from 1987 to 2021

4.5.5. Uncertainty analysis

The prediction uncertainty in SUFI 2 (95 percent prediction uncertainty) (see section 6.3.11) was applied to evaluate the performance of the best parameter set (Table 6.5) selected in the sensitivity analysis and model uncertainty. Two main statistical indices were calculated to evaluate the model uncertainty, the P-factor and the R-factor. P-factor is the percentage of observed data covered by our modelling results (95PPU) and the R-factor is the thickness of the 95PPU envelop. Abbaspour (2015) has recommended that the P-factor should be at least 0.7 and R-factor around 1 for streamflow simulation using observed data. Regarding Shubayqa watershed model, P-factor and R-factor vary from one sub-basin to another where values are from 0.3 to 0.6 and 0.5 to 0.8 respectively for both factors. The difference in P-factors and R-factors values within sub-basins is probably due to over or under estimation of evapotranspiration data of TerraClimate used for the model calibration and validation.

6.5. Discussion and Conclusion

The hydrological modelling of the Shubayqa watershed had several limitations in terms of input data such as needing to use remote sensing actual ET data for model calibration and validation (see section 6.3.6) to avoid the lack of this type of data in an ungauged watershed. These R.S actual ET data have shown inappropriate values for some sub-basins when compared with local precipitation (see section 6.4.2). Having to use very limited and low-resolution soil data like that available for the Syrian part of Shubayqa watershed (see section 6.3.4) was another problem. These limitations related to SWAT input data were manifested in the modelling process output and affected the performance of the model spatially, where the disparities of these performance metrics value spatially between sub-basins were obvious. However, as an overall result the average performance metrics of the calibration and validation processes for the whole watershed were mostly balancing between acceptable, satisfactory and good. Furthermore, the verification process of the model performance has shown a moderate positive correlation between time series of monthly discharge obtained from SWAT modelling and monthly Landsat NDWI and monthly R.S soil moisture of ERA5-Land. The 95% uncertainty analyses of the SWAT simulated variable bracketed most of the satellite based actual ET data in each sub-basin. Odusanya et al.'s (2018) results obtained from SWAT modelling using satellite based actual ET datasets have contributed to better understanding of the ease and suitability of using such R.S data in a tropical sparsely gauged catchment for calibration and validation by sub-basin thereby reducing the uncertainty related to the long-established

calibration on a limited number of observed streamflow datasets. Dangol et al.'s (2023) study have shown the potential of using remote sensing-based hydrologic variables like Actual ET to improve the calibration of SWAT for robust representation of hydrologic processes, however they recommended careful assessment of the quality of the R.S datasets used and assessing the performance of SWAT under different type of R.S datasets as it is a critical step for ensuring reliable model performance in a defined study area.

Overall, the SWAT model proved efficient in simulating watershed discharge and capturing the seasonal variability of the water balance components at the outlet of the watershed. Therefore, output from the hydrological modelling using the R.S based actual ET dataset are considered reliable and can be used to run crop simulation models like CERES within DSSAT, to estimate variation in crop productivity in Q'a Shubayqa during the last decades (see Chapter 7). In addition, the created model of the study watershed will be used to predict future daily discharge using future climate estimates under different scenarios obtained from a GCM (see Chapter 8) for future crop simulations.

Chapter 7: Modelling the agricultural system of Q'a Shubayqa

7.1. Introduction

Due to increasing pressures on cultivated land to feed the fast-growing global population (UNDESA, 2017) there is an increased need for detailed knowledge of these agricultural systems. This is particularly true in dryland areas. Data from traditional agronomic research methods are not sufficient to meet this need because they are typically conducted at particular points in time and space, producing very specific results and can be considered as a time consuming and financially wasteful process (Kephe et al., 2021).

Crop models were designed and developed to assist in the synthesis of research analysis about the interactions and the contribution of genetics, physiology, and environmental factors, to yield productivity (Boote et al., 1996). Such models can assist in pre-season and in-season management decisions on farming practices, particularly fertilization, irrigation, and pesticide use (Leroy et al., 2013; Malik & Dechmi, 2019; Si et al., 2021). Crop models can assist decision makers in policy design by simulating a range of processes, such as soil water extraction, nitrogen plant uptake, crop components growth and mass, phenological alteration over the growing season and forecasting yield under climate change scenarios (Jame & Cutforth, 1996). However, appropriate use for a particular purpose depends on whether the chosen model complexity is appropriate to the question being asked and how the model has been tested under diverse and appropriate environmental conditions (Boote et al., 1996).

There is a need for a range of complexities in models available. In some cases, simple models are not appropriate because they are not programmed to address a particular phenomenon (Boote et al., 1996). In other cases, it is challenging when employing complex models in particular agricultural systems, because they may require inputs that are not practical to obtain in a field situation. Generally, this type of complex model incorporates information about cultivar specific traits to estimate daily growth and development as the crop responds to weather variations, soil characteristics and management practices (Boote et al., 2018).

The Decision Support System for Agrotechnology Transfer (DSSAT) is one of these complex software application programs that comprises dynamic crop growth models (Jones et al., 2003). In addition to the environmental (soil and weather) and management data required for DSSAT, cultivar specific trait information is also crucial for the successful implementation of the model (Hunt & Boote, 1998; Hoogenboom et al., 2012). These cultivar-specific traits are referred to

in DSSAT, and other concept models (e.g. the Agricultural Production System sIMulator (APSIM)), as Genetic Coefficients, which describe the phenotypic expression of the of cultivar's genes under different environments and can vary based on the phenological stages within a crop's life cycle, and relate crop physiology and productivity to specific-site environmental factors and agricultural practices (Boote et al., 2001). The information about new cultivars needed for the calculation of genetic coefficients is mainly extracted from the observed data from crop performance field tests. The genetic coefficients are then derived during the calibration process of the crop simulation model.

In this study, we simulate crop growth and yield of two wheat and two barley local genotypes usually cultivated by farmers in Q'a Shubayqa (see Chapter 3). The CERES-Wheat/Barley (Ritchie & Otter, 1985) growth and development model is one of the DSSAT model packages used, together with two DSSAT built-in tools (with different estimation methods); the Genetic Coefficient Calculator (GENCALC) (Hunt et al., 1993) and the Generalized Likelihood Uncertainty Estimation (GLUE) (He et al., 2009), specified for model calibration and genetic coefficients estimation by ensuring the best adjustment between simulated and observed data.

After an extensive literature search and investigation by meeting researchers from relevant research institutes in Jordan (see Chapter 3, section 3.4), we discovered that no field experiments on crop performance were conducted on the wheat and barley cultivars in Q'a Shubayqa itself. The alternative approach adopted in this research is to calibrate DSSAT by estimating the genetic coefficient of the main wheat and barley cultivars grown in Shubayqa based on observed data of field trials that were previously conducted in different regions of Jordan under different environments and over different seasons.

The objectives of this chapter are, therefore, to explore the ability of the DSSAT crop simulation model (CERES-wheat/barley) to predict phenology and yield components using genetic coefficients that were developed using DSSAT tools (GENCALC and GLUE), and to test the stability of the estimated unique genetic coefficients across these different regions and in the study area Q'a Shubayqa. The overall objective of this chapter is to develop stable genetic coefficients for the identified wheat and barley genotypes that could be reliably used for further long-term evaluation of these crops' patterns in Q'a Shubayqa either in the past, e.g. to help with ongoing archaeological research (Arranz-Otaegui et al., 2018), or in future decades e.g. for understanding the resilience of the system to projected climate change.

7.2. The Decision Support System for Agrotechnology transfer (DSSAT)

7.2.1. DSSAT overview

The Decision Support System for Agrotechnology Transfer (DSSAT) was originally developed by an international network of scientists, cooperating in the International Benchmark Sites Network for Agrotechnology Transfer project (IBSNAT, 1993, Tsuji, 1998, Uehara, 1998, Jones et al., 1998), which integrates the effect of crop phenotype, soil, weather and crop management through a database system and allows users to simulate different crop life cycle analysis by the application of crop models in a systems approach (Figure 7.1). Its initial development was motivated by a need to integrate knowledge about soil, climate, crops, and management for making better decisions about transferring production technology from one location to others where soils and climate differed (IBSNAT, 1993, Uehara and Tsuji, 1998). This should enable users to apply the ‘‘What if?’’ scenarios of different factors that could interfere with crop growth and productivity through its different independent programs that operate simultaneously (Jones et al., 2003).

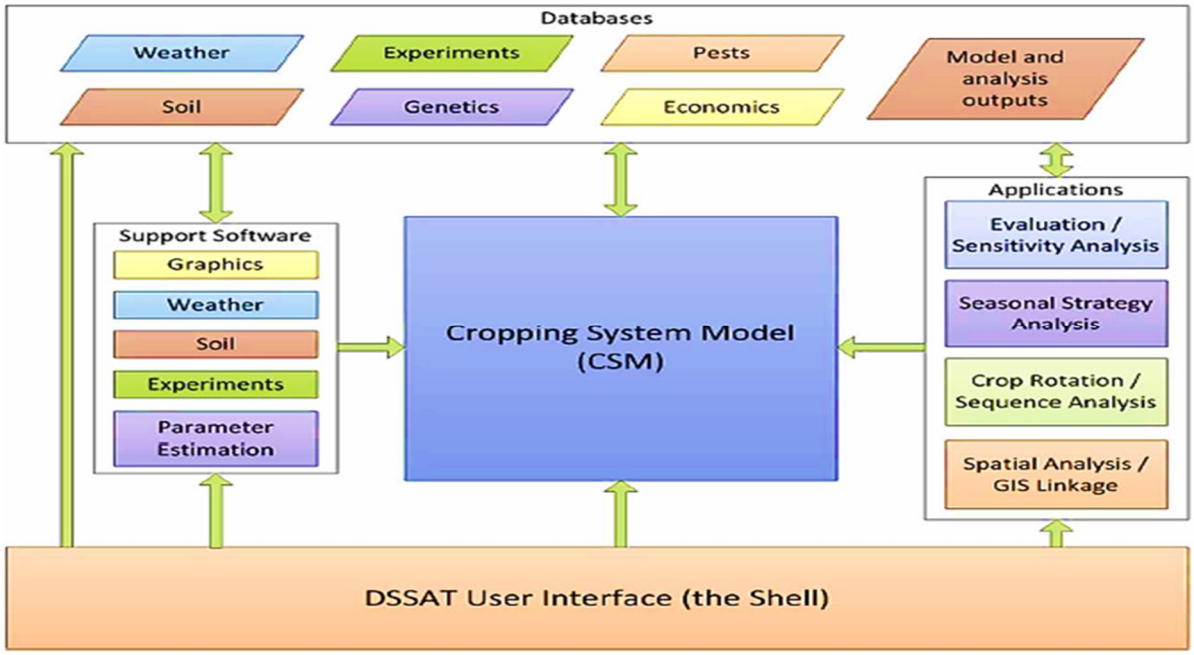

Figure 7.1: The DSSAT crop modelling ecosystem (Hoogenboom et al., 2019)

DSSAT helps decision-makers by reducing the time and human resources required for analysing complex alternative decisions (Tsuji et al., 1998). It also provides a framework for scientific cooperation through research to integrate new knowledge and apply it to research

questions. Since the development of DSSAT, large improvement and editing operations have been introduced to this software application program and currently it consists of crop simulation models for 42 crops type (Version 4.8.2), as well as data management tools to facilitate effective use of the models (Hoogenboom et al., 2023).

7.2.2. Minimum Data Set (MDS) for crop modelling

In order to run a crop simulation model successfully, a minimum set of input data is required. This is known as The Minimum Data Set (MDS) which is a concept that was first introduced during a workshop held at the International Crops Research Institute for the Semi-Arid Tropics (ICRISAT) in Patancheru (India) in 1981. In addition to the minimum data required to run a crop simulation model, this data set should include minimum data required for the evaluation of model outputs (Tsuji & Balas, 1993). MDS incorporates different types of data such as:

- Weather data from the experiment weather station and should include latitude, longitude and elevation of the station, daily maximum and minimum temperature (ºC), daily total rainfall (mm) and daily values of incoming solar radiation (MJ/m²-day) (Hoogenboom, et al., 2012). Although solar radiation is not commonly measured at many meteorological stations, especially in poor countries drylands, it is a required input for the accurate simulation of photosynthesis and potential transpiration using the Priestley-Taylor equation (Priestley & Taylor, 1972). Relative humidity and wind speed data may also be useful to enhance the model ability to simulate evapotranspiration, but they are not compulsory data. The weather data length should cover the duration of the experiment or a few weeks before and after the simulation period to allow for conducting "what-if" scenario analysis.
- Soil data to include soil classification according to the USDA-NRCS, soil surface colour, slope, drainage class, soil permeability. The soil profile data by horizon should include soil texture, bulk density, soil organic carbon, upper and lower horizon depths, pH in water and root growth factor (Boote et al., 2016).
- Crop management data including the crop species and selected cultivar, planting date, plant density, row spacing, sowing depth, irrigation, and fertilizer inputs (if applicable). For irrigated treatments, the dates, amounts, and the type of irrigation system must be defined; for fertilisation treatments, the dates, amounts, and types of inorganic fertilizer must be defined, as well as depth of incorporation. For organic fertilizers using plant or animal material, the type and composition of the organic fertilizers need to be defined (Hoogenboom, et al., 2012).

- The observed experimental data needed for the evaluation of the crop simulation model are related the crop growth (phenology), biomass yield and soil water measurements (Hoogenboom et al., 2019).

Boundary, or initial conditions, at the start of the simulation are also very important, especially for the soil environment, requiring initial soil moisture, nitrate, and ammonia for each horizon or soil layer, as well as the aboveground biomass residue and roots of the previous crop and their composition (Hoogenboom et al., 2021). Although these conditions can be challenging to measure unless equipment and personnel are available, they can be estimated using the tools and utilities that are provided within DSSAT.

7.2.3. CSM-CERES-Wheat/Barley model

The basis for the CSM design is modular, structured to allow replacement or addition of modules. These modules are a soil module, a crop template module that can simulate different crops, a weather module, and a module for dealing with competition for light and water among the soil, plants and atmosphere. It is also designed to be employed for different types of application that allow users to evaluate the DSSAT-CSM during the simulation of crop production over time and space for different purposes (J. W. Jones et al., 2003). As a soil-plant-atmosphere dynamics model, CERES-Wheat/Barley can simulate the main processes of crop growth and development such as timing of phenological stages, total above-ground biomass development, reproductive plant parts, extension growth of leaves and stems, senescence of leaves and root system dynamics. The model is also capable of simulating the soil and crop water balance and nitrogen balance and their deficiency effects on photosynthesis and carbohydrate pathways inside the plant tissues. CERES-Wheat/Barley considers the specificity of the simulated cultivar by the inclusion of the cultivar-specific traits to allow the model to predict the cultivar's patterns in terms of plant ontogeny and yield components in addition to its response to weather (Ritchie and Otter, 1985; Godwin, 1990; Palosuo et al. 2011). It has become one of the most widely used wheat/barley models in the world (Li et al., 2019).

7.3. Why DSSAT

DSSAT, and its associated crop simulation models, is the most widely used tool for investigating agricultural systems at different spatial and temporal scales for a wide range of applications (Khan, 2015). DSSAT has been used by more than 25,000 researchers, educators, consultants, extension agents, growers, and policy and decision makers in over 187 countries worldwide (Hoogenboom et al., 2023). DSSAT has been employed to simulate different factors

related to crop patterns under different weathers and across the majority of Earth's continents (Easterling, 2011; Reilly & Schimmelpfennig, 1999).

In dry climates, several studies on wheat and barley have used DSSAT-CSM for different purposes. For example, Maldonado et al. (2015) applied DSSAT on three spring wheat varieties under a Mediterranean environment to estimate genetic coefficients and to evaluate the ability of the model in predicting yields. Soldevilla et al. (2013) conducted a study to analyse various agricultural practices (tillage-rotation combinations) on barley yield and biomass under rainfed semi-arid environment in Central Spain using DSSAT. DSSAT was also used to assess the impact of climate change on cereal production in dryland regions like western India (Gunawat et al., 2022), and in the arid regions of the north Nile Delta of Egypt where Ali et al. (2020) used the DSSAT crop simulation model to determine the optimum sowing date of wheat by evaluating different management scenarios (planting date) to explore its contribution in reducing the impact of climate change on crop productivity. The CSM of DSSAT was also incorporated to simulate water balance and nitrogen balance under an irrigated wheat cropping system with different N-application in a semi-arid sub-tropical environment in north-west India (Arora et al., 2007). DSSAT crop models have been cited by the United Nations Framework Convention on Climate Change (UNFCCC) as a tool which can be combined or integrated with other tools or methods to evaluate impacts of climate change, vulnerability, and adaptation of particular agricultural systems to climate change (Salvacion, 2011).

7.4. Wheat/Barley Genetic Coefficients

Cultivar specificity is primarily a matter of genetic variability. Crop models account for this genotypic variation in different ways, and have different numbers of cultivar coefficients, i.e. sets of parameters based on mathematical constructs that illustrate quantitively the responses of a particular cultivar to environmental factors (Hunt and Boote, 1998). These coefficients summarise various aspects of the genotype's performance and describes how a cultivar divides up its life cycle into phase durations that mainly depend on critical daylength, daylength sensitivity and vernalization requirements. They also describe the vegetative attributes and reproductive attributes of the specific cultivar (Getachew et al., 2023).

DSSAT-CSM-CERES Wheat/Barley makes use of seven genetic coefficients that describe various aspects of the cultivar's performance.

Values of the genetic coefficients are determined through model calibration using DSSAT relevant tools like the GENCALC and/or GLUE that conduct genetic coefficients estimations for particular cultivar based on input observed data from field experiments.

GENCALC needs a standard value for each genetic coefficient, and it uses a deterministic stepwise procedure to automatically adjust the coefficients with values within the plant's realistic physiological ranges. When GENCALC finds a good fit to each observation, it averages the coefficients and calculates the coefficient of variation (CV). The process is repeated by the user until the lowest CV is reached (Buddhaboon et al., 2018; Hunt et al., 1993). GENCALC has been widely and successfully used to estimate wheat and barley genetic coefficients for both spring and winter varieties (Abera, 2019; Gardi et al., 2022; Gunawat et al., 2022; O. M. Ibrahim et al., 2016).

GLUE is a genetic coefficient estimator that uses model output to select maximum likelihood value, based on comparison between simulated and observed variables (He et al., 2009; He et al., 2010) GLUE has also been extensively and successfully used to estimate winter and spring wheat/barley cultivars (Maldonado et al., 2015; Mereu et al., 2019; Nikou & Mavromatis, 2023).

7.5. Material and methods: Deriving stable genetic coefficients for Q'a Shubayqa wheat and barley genotypes

7.5.1. Wheat and barley cultivars description

The farming system in Q'a Shubayqa is a cereal-based cropping system where farmers mainly grow wheat and barley for several environmental, economic and management reasons (see Chapter 3, section 3.4). Two essential durum wheat (*Triticum turgidum* subsp. *durum*) cultivars are cultivated in Q'a Shubayqa (Hourani and Acsad 65) according to NARC researchers (see Chapter 3, section 3.4). Hourani (locally called Gatma) released in 1976, is a Jordanian improved selection from local landrace and well adapted to local environmental conditions. Acsad 65 (locally called Baladi) is an improved variety developed by the International Maize and Wheat Improvement centre (CIMMYT) and released in 1988. These two wheat cultivars are winter-sown spring wheat crops suitable for rainfed agriculture and drought resistant (Allouzi et al., 2010). Barley (*Hordeum vulgare* L.) is also considered as the second most common cereal grown in Q'a Shubayqa, where most local farmers use it as a rotational crop with wheat. Two main barley cultivars are sown in Q'a Shubayqa: Rum, locally called Bethar,

is 6 row cultivars which was developed from two genotypes (Harbinger-Arivat and Attiki) by CIMMYT and released in 1986 in Jordan. Mutah, or Balady as the farmers call it, is an improved 2 row cultivar developed from three barley genotypes (Roho, Arabi Abiadh and 6250) by ICARDA (International Centre for Agricultural Research in the Dry Areas) and released in 2004. These two cultivars are also winter-sown spring barley crops and known for their stable productivity under arid conditions and considered as drought tolerant varieties (Al-Ajlouni et al., 2016).

7.5.2. Approach to estimating stable genetic coefficients

To enhance credibility of a created model and to get sufficiently accurate simulated results, calibration, validation and evaluation processes of the model in the environment of interest are required (Hunt and Boote, 1998; Timsina, 2007). To simulate a crop's (cultivar's) performance in a specific soil and climate, for a particular set of management inputs, cultivar traits are required because of the genetic variations between cultivars of any crop which allow models to simulate differences in yield and phenological traits (Bertin et al., 2010; Boote, 1999). Using observed data collected from field experiments is the most common approach used to calibrate a model by estimating the cultivar's genetic coefficients that are unknown for most of crop varieties. For a crop simulation model like DSSAT, the calibration process is based on cultivar traits parameters obtained from variety trials. This information is used to generate genetic coefficients for each new cultivar tested in a particular region. Typical data collected from a field experiment during the growing season of wheat and barley crops could be divided into two sets: phenological measures such as emergence day, anthesis day, grain filling period, physiological maturity day; and grain yield observed data like harvested yield weight, biomass weight and thousand kernel weight. Weather data and soil data from the experiment site, in addition to management information, are also required to run and calibrate the model. Calibration of the crop simulation model DSSAT is by adjusting parameters and coefficients until a good agreement is achieved between simulated and observed data.

Regarding Q'a Shubayqa, there was no field experiment data that have been collected before on wheat and barley cultivars and could be used for calibrating DSSAT and estimating relevant genetic coefficients. During my field work trips to Jordan, I've been in touch with many researchers from the NARC, ICARDA and from the Faculty of Agriculture at The University of Jordan and talked to them about any potential experiments on wheat and barley growing performance in Q'a Shubayqa region, but unfortunately, they were unaware of any relevant

projects in this region. However, they confirmed that field trials to assess the performance and the behaviour of such crops and cultivars were conducted in different research stations across the country over multiple seasons. The measured and observed information from these experiments is based on phenological and biomass yield (including grain yield). Under these circumstances, the alternative approach is to estimate stable genetic coefficients of the wheat and barley cultivars planted in Q'a Shubayqa using all available experiments data from different environments across Jordan.

This approach will allow transferrable stable genetic coefficients to be developed that could be tested over diverse regions and expose the model to new and different environments to test its robustness e.g. Piper et al. (1998). At the same time, we will test the DSSAT-CERES model's ability to predict phenology and seed yield when using genetic coefficients that were developed in different regions. In other comparable research conducted by Mavromatis et al. (2002) , a stepwise procedure was applied to derive soybean genetic coefficients for several cultivars grown in different environments in Georgia and North Carolina, USA. They first used trial data from Georgia to estimate cultivar coefficients for a number of soybean varieties, then used the coefficient estimated from North Carolina field experiment data to estimate the patterns of the same varieties in Geogia. They were able to demonstrate the importance of using routinely collected data from field trials for both estimating stable genetic coefficients and for model robustness evaluation. In this research, using the DSSAT tools like GENCALC and GLUE, the estimation of stable genetic coefficients for each wheat and barley cultivar will be based on crop growth performance data in addition to environment data from five different research station across Jordan.

7.5.3. Calibration and validation process

7.5.3.1. Field experiments data

Wheat and Barley cultivars were grown during multiple seasons in different regions across Jordan (Figure 7.2) by researchers from the NARC (Dr Faddel Ismail and his team) and the University of Jordan (Dr Ayed Abdallat and his team) to evaluate cultivar behaviour under different types of environments. Observed data from these field experiments are not published yet. The research sites (Table 7.1) are characterised by a Mediterranean climate but receive different seasonal precipitation amounts and are located at different altitudes.

Among the five experimental sites, three of them were dedicated to wheat and barley trials together and for the other two sites, only experiments on one crop type were established. The number of experimental seasons for each site varied between two and three successive seasons. Usually, wheat and barley growing seasons are between November and May.

Table 7.1: Experiment sites and seasons of wheat and barley cultivars

Station Name	Altitude (m)	Soil type	Tested crop	Wheat exp seasons	Barley exp seasons	Average seasonal rainfall (mm)
Maru_station	530	Clay	Wheat	2018-2019 2019-2020 2020-2021	None	475
JUST*_station	585	Silty clay	Barley	None	2018-2019 2019-2020 2020-2021	217
Rabba_station	958	Silty clay	Wheat & Barley	2018-2019 2019-2020 2020-2021	2018-2019 2020-2021	266
Jubaiha_station	1015	Clay loam	Wheat & Barley	2016-2017 2017-2018	2018-2019 2020-2021	520
Mushager_Station	770	Clay loam	Wheat & Barley	2018-2019 2019-2020 2020-2021	2018-2019 2020-2021	397

JUST*: Jordan University of Science and Technology

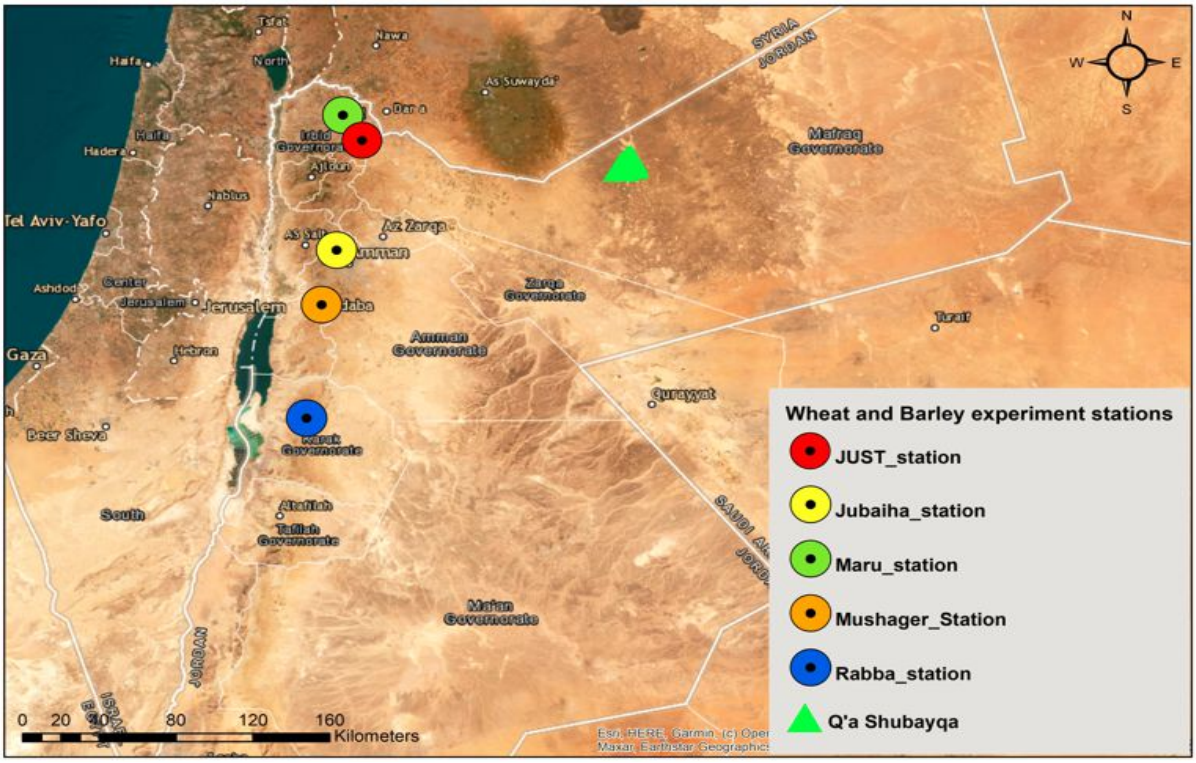

Figure 7.2: Experiment stations location across Jordan of wheat and barley cultivars

The daily weather data during the experiment seasons of these five sites were obtained from the Jordan Meteorological Department (JMD) which includes the maximum and minimum temperature, rainfall, relative humidity, and wind speed. Solar radiation data was not recorded by the JMD, so the alternative choice was to download this data from The Power Project platform (NASA Prediction Of Worldwide Energy Resources) (https://power.larc.nasa.gov/). This project provides satellite based solar and meteorological data sets from NASA research for support of agricultural needs. Soil data (Table 7.2) were also provided by the NARC. Particle size analysis has shown that these experiments on wheat and barley growth patters were managed in three different types of soil (clay, clay loam and silty clay). In addition, other measured soil parameters were provided by the NARC like pH, organic matter (OM) content, total nitrogen (N), calcium carbonate ($CaCO_3$) and available phosphorus (P), to be used as input data for DSSAT. The design varies from one experiment to another in terms of plot size, sowing rates and planting dates. Sowing rates were provided in kg/ha and were converted in to seeds/m^2 as DSSAT requires by using the thousand kernel weight observed data. Generally, the sowing rate for wheat is 250 seeds/ m^2 and 150 seeds/ m^2 for barley. Most of the sowing operations for both wheat and barley cultivars were during the last two weeks of December. All experiments were conducted under rainfed conditions without any supplementary irrigation according to the researchers responsible. All field trials followed a period of fallow as a crop rotation system

and were established using hand broadcasting. A conventional tillage process was performed using a chisel plough and disk harrow. In all experimental locations, plots were managed following standard agricultural practices including weed control and chemical treatments against pathogens and diseases.

Table 7.2: Soil chemical and physical properties of the experiment sites (NARC)

Station	pH	P (ppm)	N (%)	$CaCO_3$ (%)	Clay (%)	Silt (%)	Sand (%)	Texture
Maru	7.7	3.8	0.085	14.6	55.4	37.1	7.5	Clay
Mushager	7.9	1.45	0.046	15.2	39.2	38.8	22	Clay loam
Rabba	7.8	4.1	0.065	14.6	44.1	41.6	14.3	Silty clay
Ramtha	8.2	10.38	0.19	18.3	33.4	46.2	20.4	Silty clay
Jubaiha	7.15	28	0.154	17.2	38.4	34.8	26.8	clay loam

The data from these experiments were collected during the growing seasons and mainly included phenological observation such as anthesis day, grain filling period and maturity day, in addition to measured data related to productivity like grain yield, thousand kernel weight and total biomass yield.

7.5.3.2. DSSAT input files

In order to apply DSSAT for a particular cropping system, four input data sets are required (see section 7.2.2). To enter these data sets, DSSAT provides different program interfaces. XBuild is the program interface dedicated for management data and separated into different sections for general information where we can store data such as site and experiment name, latitude, longitude, and elevation. Another section for field environment allows specification of the soil data file and weather data file for the relevant experiment from the database. The management section contained the majority of entered data, for example cultivar name, planting date, planting design, irrigation and fertilizers (not the case for our experiments), tillage tools and date, and harvest schedule. The initial conditions section allows data to be provided about previous crop (fallow for all current experiments), water and nitrogen amounts at the planting date. For this research, the water amount in the soil for all experiments was estimated for 50%

because all planting operations were conducted just after major rainfall occurs. The last section to complete is the simulation option which serves as a model calculation control. It allows the user to specify the start simulation date and provide options to activate water and/or nitrogen modules and methods to calculate weather, soil water balance and photosynthesis (Buddhaboon et al., 2018). All these data are stored in a new file called FileX created for each experiment.

For soil physical and chemical characteristics, the SBuild program was used to insert these data. Required data included numbers of soil horizons and depth, slope, colour, pH, bulk density, soil organic matter, total Nitrogen, clay and silt percentages. Other soil parameters that describe the water holding capacity were calculated based on the previously entered data, which are soil water lower limit, drained upper limit, saturation, albedo, saturated hydraulic conductivity, runoff curve number and root growth factor. All the previous parameters were estimated based on the Saxton method (Saxton et al. 1986). Furthermore, DSSAT requires various weather variables for its operation. The minimum four main variables required on a daily scale to run DSSAT are solar radiation (MJ/m^{-2}), maximum and minimum temperatures (°C) and precipitation (mm). These weather data are required from a few days before planting to a few days after maturity to allow the simulation to start before planting, providing an estimate of soil water and nitrogen content at planting time. The Weatherman program in DSSAT is used for inserting these data. ATCreate is the program designed to store selected field experimental observations during the growing season related to phenology and productivity process. These data will be used to compare with simulated data and to estimate genetic coefficients. For each experiment, a file named FileA will be created that contain this observed information.

7.5.3.3. Stable cultivar genetic coefficient estimation

DSSAT-CSM-CERES Wheat/Barley makes use of seven genetic coefficients that describe various aspects of the cultivar's performance (Table 7.3). These genetic coefficients could be classified under different categories where three of them (P1V, P1D AND P5) are related to the crop development and three coefficients (G1, G2, G3) are related to crop growth. The seventh genetic coefficient (PHINT) present the thermal time required for leaf appearance.

Table 7.3: Genetic coefficients of the DSSAT-CERES-Wheat/Barley model.

Abbreviation	Wheat and Barley genetic coefficients definition	Unit	Range	Default values
P1V	Days at optimum vernalizing temperature required to complete vernalization	Days	0-5	5
P1D	Percentage reduction in the development rate of a photoperiod ten hours shorter relative to that at the threshold	%	0-200	75
P5	Grain filling (excluding lag) phase duration	°C d	100-999	450
G1	Kernel number per unit canopy weight at anthesis	kernels/g	10-50	30
G2	Standard kernel size under optimum conditions	mg	10-80	35
G3	Standard, non-stressed mature tiller weight	g	0.5-8	1
PHINT	Phylochron interval between successive leaf tip appearances	°C d	30-150	60

In this study, GENCALC and GLUE (see section 7.4) were employed for the estimation of the wheat and barley cultivars genetic coefficients. The aim of using both tools is to make comparison between their performance in estimating the most accurate genetic coefficients. GENCALC uses a deterministic stepwise procedure by searching the output file from the crop model and then adjusting the coefficient to produce the lowest root mean square error (RMSE) between the simulated and observed data (Wallach and Goffinet, 1989). For example, the P1V coefficient which defines the cultivar's sensitivity to vernalization, could be increased or decreased to minimise the RMSE between observed and simulated data. For all wheat and barley cultivar experiments in this research, P1V should be less than 5 because spring varieties are not sensitive to vernalization (Boote et al., 2001). Several iterations are needed for GENCALC to reach the minimum values of RMSE. The same procedure was repeated for all the genetic coefficient P1D, P5, G1, G2 and G3 respectively. The PHINT value was fixed because of the absence of observed leaves number data. After the last iteration, the new adjusted genetic coefficients obtained based on observed data, are automatically or manually inserted into the .CUL file as a new cultivar.

Regarding the GLUE program, a likelihood function based on the Monte Carlo method is used as the criterion for estimating genetic coefficients as described by He et al. (2009). After selecting the cultivar and the experiments that would be used to the estimate genetic coefficient in the GLUE interface, the maximum likelihood estimation method is conducted. This method is useful tool for many statistical modelling techniques for non-linear modelling with unusual data by making the observed data most likely based on the desire probability distribution (Myung, 2003). To obtain the best genetic coefficients estimation from GLUE, a minimum of 6,000 iterations are required (Buddhaboon et al., 2018). However, in this research the number of iterations was fixed at 10,000 during the genetic coefficients' calculation process of each cultivar.

Before setting up these programs, we first need to run the model for all experiments. During these first runs, standard genetic coefficient values provided in the .CUL file within DSSAT database are considered. The approach of the genetic coefficient estimation for both programs will be based on three experiments, leaving the fourth for the validation process. Among the four experiments, three experiments will be selected in the GENCALC or GLUE interface in turn and the estimation process will be conducted four times to get the most accurate genetic coefficient. For example, for wheat we will first select Maru, Rabba and Mushager experiments in the GENCALC/GLUE interface to be used for genetic coefficient estimation. Then we will substitute Maru with the Jubaiha experiment and run the program and so on. This process was conducted using both genetic coefficient estimators. At the end, we will get eight different sets of estimated genetic coefficients from different experiment combinations for each cultivar. These derived sets will be re-entered independently as a new cultivar to the model's .CUL file and will be tested by running CERES-wheat/barley model of DSSAT for simulating development, growth and yield. Then, the comparison between the statistical results that came from the comparisons between the newly simulated data and the observed data will allow one to select the best estimated genetic coefficient set and conclude which program (GENCALC/GLUE) was able to calculate the most accurate values. The genetic coefficient set that shows the best agreement between simulated and observed data in terms of statistics, will be used for the validation process.

The statistical analysis between simulated and observed data used the Root mean square error (RMSE), normalized Root mean square error (RMSEn), the d-index (agreement index) and r^2. These comparison equations seem to be different from the metrics used for SWAT calibration

(see Chapter 6, section 6.3.10). The crop simulation model CERES-Wheat/Barley is considered perfectly estimating growth and yield parameters when RMSE and RMSEn are close to 0, while d-index and r^2 are close to 1.

7.5.3.4. Validation of the new estimated genetic coefficients

The validation process of the CERES-Wheat/Barley model is based on testing its ability to predict the phenology and seed yield characteristics of each cultivar using the new cultivar coefficients that were developed from different regions and over different seasons using GENCALC or GLUE. The approach of validation is to run the crop simulation model using the new cultivar coefficients for the experiment site (among the four sites) that was excluded during the calibration process. Then a comparison between simulated and observed parameters will clarify if the developed genetic coefficients are reliable for use in crop models across different environments. The crop growth and development parameters adopted during validation are the anthesis day, maturity day, tops weight (biological mass) and harvested yield.

7.5.4. Evaluation of genetic coefficients stability in Q'a Shubayqa

The evaluation method of the calibrated and validated genetic coefficients of wheat and barley cultivars was then applied to farmlands of the study area Q'a Shubayqa (Chapter 1). Since we know that the developed genetic coefficients were mainly estimated based on experiments conducted in a Mediterranean climate varying from semi-arid to semi-humid, this evaluation process will show the stability of the genetic coefficients and the model robustness in estimating crop growth and development parameters. The method was based on considering the different soil types of Q'a Shubayqa (see Chapter 3, Figure 3.12) (spatial analysis) and different agricultural practices. DSSAT-CERES-Wheat/barley model was applied as an experiment for 6 farmers independently over one growing season (2019-2020). During the survey (conducted in 2021) with 25 local farmers in Q'a Shubayqa, they provided us with the harvested grain yield of wheat and barley for the season 2019-2020 and they confirmed that it was the most productive season among the last couple of seasons before the survey date. In addition, management data that was reported by those farmers, such as tillage tools, planted cultivar, harvesting date, previous cultivated crop and seeding rate were used. Required soil data and weather data for Q'a Shubayqa for DSSAT simulations are already available and are used in the following chapters (see chapter 3, section 3.3.2 and chapter 6, section 6.3.5).

Regarding floods that occur seasonally in Q'a Shubayqa, simulated discharge by SWAT model (Chapter 6, Figure 6.11) during this season was inserted in DSSAT by activating the irrigation option. For this purpose, the flood irrigation method was selected among the list of methods provided by DSSAT. The simulated harvested grain yield of each farm during the particular season will be compared with grain yields that selected farmers have reported during the survey.

7.6. Results

7.6.1. Calibration process: stable genetic coefficients estimation

7.6.1.1. Wheat cultivars

Table 7.4 represents the genetic coefficients of wheat cultivars related to phenology and growth that were determined based on two different methods using GENCALC and GLUE estimators (see section 7.4). During the calibration process, the best observed data combination from different experiment sites used to estimate the stable genetic coefficients for wheat were mainly extracted from three sites which are: Rabba (2 seasons), Mushager (3 seasons) and Jubaiha (2 seasons) (see section 7.5.3.1). The new estimated genetic coefficients for wheat cultivars (Hourani and Acsad 65) are presented in Table 7.4.

P1V coefficient values of GLUE for both cultivars (63 for Hourani and 33 for Acsad65) are much higher than the value of 5 which is the maximum vernalization days required for spring wheat cultivars when using CERES-Wheat/Barley model (Boote et al., 2001). Similar P1V coefficient values of GLUE were obtained even with different observed data combinations. The rest of the coefficients will be affected by the over-estimation of P1V especially P1D and P5 because they are phenology coefficients the same as P1V.

P1V coefficient values estimated with GENCALC for both wheat cultivars are under 5 which means that these coefficients are more reasonable and could be adopted for both wheat cultivars. The reason behind this difference in estimating genetic coefficients between GENCALC and GLUE is related to the methods used because unlike GLUE, GENCALC provides options for keeping some coefficients values fixed while other coefficients are being calibrated (O. M. Ibrahim et al., 2016).

The second step of this calibration process is to re-run the model employing the new estimated genetic coefficients for each cultivar to compare between estimated and observed phenology

and growth parameters (Table 7.5). For phenology parameters, two crucial development phases were selected (anthesis and maturity dates) for this comparison. The mean observed duration of both development phases for Hourani was 108 and 141 days after planting for anthesis and maturity, respectively. GENCALC estimations were 107 and 140 days after planting for anthesis and maturity, respectively. Statistical comparison between observed and estimated phenology parameters using R^2 and D-stat were satisfactory, with values of 0.905 and 0.784 respectively for anthesis, and values of 0.984 and 0.901 respectively for maturity. The RMSEn were acceptable for both development phases (RMSEn<15) with values of 11.89 and 6.32 for anthesis and maturity, respectively. For Acsad 65, the mean observed values for both development phases were 107 and 139 days after planting for anthesis and maturity, respectively. A good agreement was also achieved between simulated and observed variables with satisfactory R^2 and D-stat values of 0.870 and 0.825 respectively for anthesis, and values of 0.775 and 0.914 respectively for maturity. The RMSEn values for the two stages were 12.09 and 6.40 for anthesis and maturity, respectively. Both simulation results were acceptable compared with observed data with RMSEn <15.

Table 7.4: Final values of the genetic coefficient of two wheat cultivars calculated with GENCALC and GLUE estimators under different environments.

		Hourani		**Acsad65**	
Wheat cultivar genetic coefficients	**Default values**	**GENCALC values**	**GLUE values**	**GENCALC values**	**GLUE values**
P1V	5	3.37	63.19	2.503	33.11
P1D	75	120.1	94.36	113.3	102.56
P5	450	501	613.3	520.5	463.22
G1	30	17	15.02	31.52	19.32
G2	35	28.14	35.92	18.28	25.91
G3	1	1.18	1.455	1.05	1.65
PHINT	60	60	60	60	60

Growth and grain yield variables were expressed by three relevant parameters which are harvested grain yield (Mat yield kg/ha), above-ground biomass yield (Tops wt kg/ha) and weight of grain unit (Weight g/unit). The grain yield average observed values were 1192 and 1480 for Hourani and Acsad 65, respectively. The simulated grain yield values based on GENCALC genetic coefficients were 1142 and 1303 for Hourani and Acsad respectively. The high correlation and good agreement between observed and simulated data is translated by the satisfactory values of R^2 and D-stat, in addition to fair values of RMSEn for both cultivars (Table 7.5). However, CSM-CERES-Wheat model have under-estimated above-ground biomass by around 2500 and 3200 kg/ha for Hourani and Acsad 65, respectively. Regarding weight of grain unit, all statistic values were unsatisfying for both cultivars. The model failure in estimating above-ground biomass and weight of grain unit using GENCALC genetic coefficients could be the consequence of the absence of several relevant observed data types such as leaf area index, leaves number per unit and grain number per unit because such types of observed data would ameliorate the estimation probability of the genetic coefficients.

Table 7.5: A comparison between observed and simulated phenology and growth data of two spring wheat varieties using GENCALC estimated genetic coefficients for model calibration

		Hourani (Mean)		Hourani				Acsad 65 (Mean)		Acsad 65			
Variable Name	**Used Obs.**	**Observed**	**Simulated**	**r-Square**	**RMSE**	**RMSEn**	**d-Stat.**	**Observed**	**Simulated**	**r-Square**	**RMSE**	**RMSEn**	**d-Stat.**
Anthesis day	7	108	107	0.9	12.8	11.89	0.78	107	101	0.87	12.94	12.09	0.82
Tops wt kg/ha	5	5594	3034	0.89	3032.6	54.21	0.72	5830	2667	0.89	3636.3	62.37	0.59
Harvest index	5	0.19	0.29	0.34	0.11	58.08	0.48	0.18	0.29	0.33	0.125	69.44	0.37
Mat Yield kg/ha	7	1192	1142	0.88	236	19.8	0.95	1480	1303	0.86	380.82	25.73	0.95
Weight g/unit	7	0.03	0.02	0.21	0.01	32.43	0.47	0.035	0.01	0.52	0.019	54.28	0.4
Maturity day	7	141	140	0.98	8.9	6.32	0.9	139	136	0.77	8.9	6.4	0.91

7.6.1.2. Barley Cultivars

Table 7.6 represent the genetic coefficients of barley cultivars related to phenology and growth that were determined based on two different methods using GENCALC and GLUE estimators (see section 7.4).

Table 7.6: Final values of the genetic coefficient of two barley cultivars calculated with GENCALC and GLUE estimators under different environments.

		Mutah		**Rum**	
Genetic coefficient	**Default values**	**GENCALC values**	**GLUE values**	**GENCALC values**	**GLUE values**
P1V	5	6.56	54.41	8.96	46.63
P1D	75	93.69	76.02	102.1	84.26
P5	450	621.7	567	556	598.1
G1	30	23.35	43.33	27.89	43.76
G2	35	48.86	22.89	39.46	25.25
G3	1	0.5	0.53	0.56	0.51
PHINT	60	60	60	60	60

Among the four experiment sites, only observed data sets from three sites were selected for this process. These sites were Rabba (2 seasons), Mushager (2 seasons) and Jubaiha (2 seasons). This combination of the observed data sets used for the calibration was particularly selected based on the quality of comparison statistics values between simulated and observed data. The derived genetic coefficients of Mutah and Rum cultivars are shown in Table 7.6 where we can notice that the vernalization coefficient (P1V) of both cultivars, that should not exceed 5 days for spring barley varieties (Boote et al., 2001), was over-estimated using GENCALC and GLUE. However, GENCALC had slightly over-estimated P1V coefficient (6.56 and 8.96 for Mutah and Rum, respectively) in contrast to GLUE which had excessively over-estimated the vernalization coefficient for both cultivars (54.41 and 46.63 for Mutah and Rum, respectively). As a consequence, only genetic coefficients derived by GENCALC method will be considered in the next steps.

Table 7.7 represents the statistical results of the comparison between observed data and simulated parameters estimated by the model using GENCALC derived genetic coefficients. The correlation and index of agreement between observed and simulated phenological stages (anthesis day and maturity days after planting date) have shown satisfactory values for Rum (R^2 >0.7and D-stat >0.8) and Mutah (R^2 >0.8and D-stat >0.8). RMSEn was < 10 for Rum and Mutah barley cultivars when comparing both phenological stages. Regarding the comparison between observed and simulated yield components, DSSAT-CERES-barley have slightly underestimated grain yields where the average observed grain yields were 3258 and 3448 kg/ha and simulated grain yields were 2504 and 2923 kg/ha, respectively for Rum and Mutah. However, comparison statistics were satisfactory with R^2 >0.7 and D-stat >0.8 for the studied barley Cultivars. Average above-ground biomass yields was widely underestimated by the model with 4623kg/ha for Rum and 5150 kg/ha for Mutah, whilst average observed were 9517 and 9542 kg/ha for Rum and Mutah, respectively. Although the underestimate of the average, we can notice that the correlations and the index of agreement were satisfying (R^2>0.7) and acceptable (0.7>D-stat >05).

7.6.2. Validation process using estimated stable genetic coefficients

7.6.2.1. Wheat cultivars

DSSAT-CERES-Wheat was validated for both studied wheat cultivars using estimated genetic coefficient from the calibration process. The validation was based on comparing simulated data with observed data from field experiments conducted in a different region (Maru experiment site) which was not used for calibration, over three different seasons (2018-2019, 2019-2020 and 2020-2021). The comparison output for phenology parameters has shown satisfactory statistical values for Acsad 65 (Table 7.8). For anthesis days after planting date, R^2, D-stat and RMSEn were 0.9, 0,9 and 3.37, respectively. For maturity days after planting date, R^2, D-stat and RMSEn were 0.9, 0.9 and 2.44, respectively. Regarding growth and grain yield parameters (Table 7.8), the weight of grain unit parameter was not considered for the validation process due to the unsatisfactory statistical values of this parameter during the calibration process. The observed and simulated average grain yield values were 2454 and 2442 kg/ha, respectively with RMSEn around 4 which shows a very close similarity between observed and estimated grain yield. As in the calibration, the model has under-estimated above-ground biomass with

Table 7.7: A comparison between observed and simulated phenology and growth data of two spring barley varieties using GENCALC estimated genetic coefficients for model calibration

		RUM (Mean)		RUM				MUTAH (Mean)		MUTAH			
Variable Name	**Used Obs.**	**Observed**	**Simulated**	**r-Square**	**RMSE**	**RMSEn**	**d-Stat.**	**Observed**	**Simulated**	**r-Square**	**RMSE**	**RMSEn**	**d-Stat.**
Anthesis day	6	107	107	0.73	9.5	8.88	0.9	98	96	0.83	8.5	8.73	0.93
Tops wt kg/ha	6	9517	4623	0.79	5760.9	60.53	0.55	9542	5150	0.76	5793.3	60.71	0.57
Harvest index	6	0.35	0.54	0.09	0.2	57.46	0.32	0.37	0.56	0.21	0.2	54.32	0.34
Mat Yield kg/ha	6	3258	2504	0.78	958.3	29.41	0.85	3448	2923	0.89	872.1	25.29	0.9
Maturity day	6	144	144	0.77	11.8	8.21	0.85	138	138	0.87	11.2	8.17	0.88

around 1700 kg/ha, but the correlation (R^2) and the agreement (D-stat) between observed and simulated data were acceptable with values of 0.5 and 0.6, respectively (Figure 7.3).

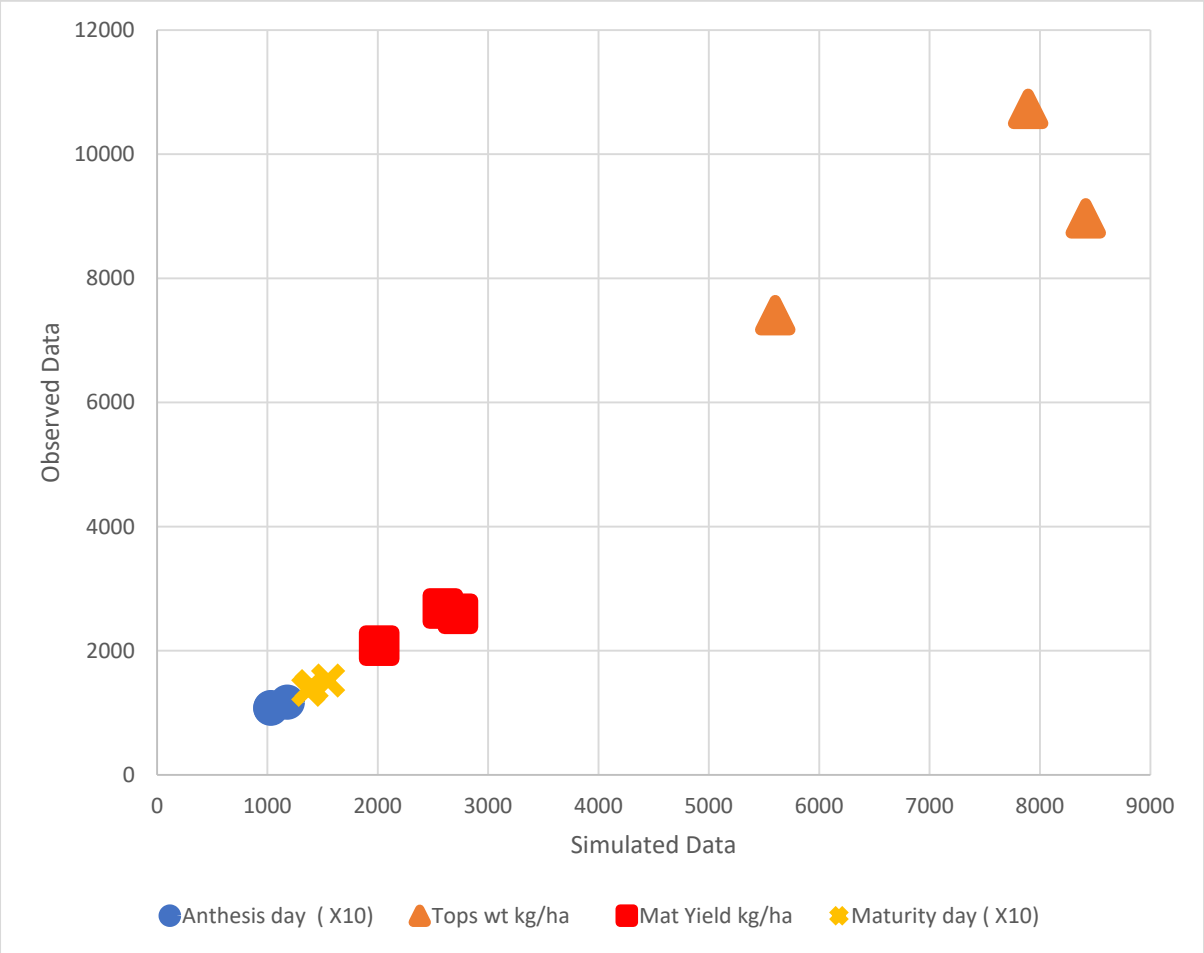

Figure 7.3: Relationship between observed and simulated phenology (day) and grain yield (kg/ha) parameters of Acsad 65 cultivar

The validation statistics for the Hourani cultivar have shown satisfactory RMSEn values for both phenology phases with 5.28 and 1.72 for anthesis and maturity duration, respectively. R^2 and D-stat were acceptable for anthesis days and satisfactory for Maturity days (Table 7.8). For grain yield, average observed and simulated were 1810 and 1799 kg/ha, respectively. In addition, R^2, D-stat and RMSEn for grain yield were 0.6, 0.8 and 13.6, respectively. Above-ground biomass was over-estimated by around 2200 kg/ha and statistic values were fair (D-stat) or unsatisfactory (R^2 and RMSEn). The comparison outputs between simulated and observed data for both wheat cultivars during the validation have shown satisfactory and acceptable values for both phenological phases (anthesis and maturity) and for grain yield. The simulated above-ground biomass was continuously under-estimated for Hourani and Acsad 65 during both the calibration and validation process.

Table 7.8: A comparison between observed and simulated phenology and growth data of two spring wheat varieties using GENCALC estimated genetic coefficients for model validation

		Hourani (Mean)		Hourani				Acsad 65 (Mean)		Acsad 65			
Variable Name	**Used Obs.**	**Observed**	**Simulated**	**r-Square**	**RMSE**	**RMSEn**	**d-Stat.**	**Observed**	**Simulated**	**r-Square**	**RMSE**	**RMSEn**	**d-Stat.**
Anthesis day	3	114	117	0.53	6	5.28	0.65	111	108	0.99	3.74	3.37	0.9
Tops wt kg/ha	3	8253	6013	0.17	2737.8	33.17	0.5	9033	7302	0.55	1967.55	21.78	0.66
Mat Yield kg/ha	3	1810	1799	0.59	246.3	13.6	0.87	2454	2442	0.9	100.36	4.09	0.96
Maturity day	3	150	150	0.99	2.5	1.72	0.98	144	144	0.93	2.44	1.7	0.96

7.6.2.2. Barley cultivars

The validation process of DSSAT-CERES-Barley model was conducted using the observed data collected from the JUST experimental station located in Ramtha during three seasons (2019-2020, 2020-2021 and 2021-2022). These observed data from JUST were not used during the model calibration process. The outputs from the comparisons between observed data and simulated parameters obtained during validation, are represented in Table 7.9. For anthesis and maturity days after planting date, the statistics were satisfying with R^2 >0.8, D-stat >0.75 and RMSEn < 10 for both studied barley cultivars. For yield components, the average simulated maturity yield was 1058 and 1077 kg/ha against 1114 and 1373 kg/ha, respectively for Rum and Mutah. Results showed a good agreement and high correlations between simulated and observed data with high RMSEn value. Despite the high correlation and the acceptable agreement values for both cultivars, above-ground biomass was under-estimated by DSSAT-CERES-Barley model with 2300 kg/ha and 2680 kg/ha for Rum and Mutah, respectively.

Table 7.9: A comparison between observed and simulated phenology and growth data of two spring barley varieties using GENCALC estimated genetic coefficients for model validation

		RUM (Mean)		RUM				MUTAH (Mean)		MUTAH			
Variable Name	**Used Obs.**	**Observed**	**Simulated**	**r-Square**	**RMSE**	**RMSEn**	**d-Stat.**	**Observed**	**Simulated**	**r-Square**	**RMSE**	**RMSEn**	**d-Stat.**
Anthesis day	3	111	111	0.94	2.1	1.94	0.98	98	95	0.9	4.5	4.6	0.92
Tops wt kg/ha	3	4157	1857	0.99	2613.8	62.87	0.68	4537	1858	0.97	3277.3	72.24	0.64
Mat Yield kg/ha	3	1114	1058	0.89	389.4	42.61	0.88	1373	1077	0.99	339.4	24.72	0.94
Maturity day	3	142	144	0.87	5.9	4.16	0.85	129	133	0.7	7.3	5.7	0.76

7.6.3. DSSAT-CERES application in Q'a Shubayqa using stable genetic coefficient

The application of the DSSAT-CERES-wheat/barley model on the agricultural system in Q'a Shubayqa using estimated stable genetic coefficients of wheat and barley cultivars was based on selecting three farmers for each wheat and barley cultivar (Chapter 3, Figure 3.18). In addition to the cultivar type, the selection was also based on choosing farmers with different land soil type and different sowing rates to illustrate the robustness of the model and the estimated genetic coefficients in predicting grain yield under different spatial conditions and different management practices.

Table 7.10: A comparison between estimated and observed grain yield of the studied wheat cultivars in Q'a Shubayqa

Farmer code	Soil type*	Wheat cultivar (sowing rate)	Obs. Yield (kg/ha)	Sim. Yield (kg/ha)	r-Square	RMSE	RMSEn	d-Stat.
1	SCL	Hourani (275gr/m2)	1590	1596	0.99	79.71	6.94	0.98
13	L	Hourani (250gr/m2)	1000	960				
10	SL	Hourani (225gr/m2)	850	718				
18	CL	Acsad 65 (125gr/m2)	1750	1701	0.97	78.41	5.53	0.97
7	SC	Acsad 65 (250gr/m2)	1050	1143				
21	SCL	Acsad 65 (250gr/m2)	1450	1536				

*: *SCL (silty clay loam), L (loam), SL (silt loam), CL (clay loam) and SC (silty clay)*

Regarding wheat cultivars, results (Table 7.10) have shown a high correlation and good agreement index between observed and simulated grain yields where R^2 values were 0.99 and 0,97, and D-stat values were 0.98 and 0.97, for Hourani and Acsad 65, respectively. In addition,

the RMSEn values were low (RMSEn<10) for both cultivars which indicate a satisfactory similarity between observed and simulated data.

Table 7.11: A comparison between estimated and observed grain yield of the studied barley cultivars in Q'a Shubayqa

Farmer code	Soil type	Barley cultivar (sowing rate)	Observed Yield (kg/ha)	Simulated Yield (kg/ha)	r-Square	RMSE	RMSEn	d-Stat.
2	SL	Mutah (240gr/m2)	1750	1311	0.98	107.67	7.67	0.93
12	CL	Mutah (240gr/m2)	1750	1642				
16	SCL	Mutah (120gr/m2)	1250	1254				
6	SC	Rum (280gr/m2)	1000	1234	0.71	208.74	20.89	0.7
9	SCL	Rum (215gr/m2)	750	1025				
24	L	Rum (240gr/m2)	850	738				

*: *SCL (silty clay loam), L (loam), SL (silt loam), CL (clay loam) and SC (silty clay)*

For barley cultivars (Table 7.11), the comparisons between observed and simulated grain yield across different soil types have shown satisfactory results for the Mutah cultivar with R^2 =0.98, D-stat =0.93 and RMSE= 7.67. The comparison results for Rum cultivars were also satisfactory, but not as strong as the other cultivars, in terms of the correlation (R^2 =0.71) and the agreement index (D-stat =0.7), however RMSEn value was slightly high and could be considered acceptable.

7.7. Discussion and conclusion

The results of this chapter confirmed that combinations of data obtained from crop performance tests representing different environments, can be used to derive stable genetic coefficients for use in crop models such as DSSAT-CSM-CERES-wheat/barley. The calibration results have also shown the model's capability to estimate phenological phases and yield components parameters when applied in-region using reliable genetic coefficients derived from the same experiments. However, the comparison between the estimated wheat and barley genetic coefficients using both tools GLUE and GENCALC has shown an important differences between the estimated genetic coefficients values, especially the ones related to phenology, where GLUE has extensively overestimated the vernalization coefficient (P1V) for both crops. Buddhaboon et al. (2018) used GLUE and GENCALC to estimate genetic coefficients of different rice cultivars based on field experiment data conducted in southeast Asia and they have found that GLUE was more accurate than GENCALC with respect to estimating the phenology genetic coefficients, while GENCALC was more accurate than GLUE for estimating growth genetic coefficients. In another study conducted by Gardi et al. (2022) to estimate genetic coefficients of barley cultivars planted in Ethiopia based on observed field experiments, they used GLUE to estimate all the genetic coefficients except PHINT which was optimised using GENCALC. Based on these different approaches used to estimate genetic coefficients, we can conclude that this step depends on several factors such as the quality and the availability of observed data, the environment type of experiments and user skills.

The use of GENCALC estimated genetic coefficients of studied wheat and barley cultivars in different environments from where they were developed during the model's validation process also resulted a high correlation, good agreement and satisfactory RMSEn between observed and simulated phenological stages (anthesis and maturity days after planting date) in addition to the grain yield. However, DSSAT-CERES failed in estimating above-ground biomass and grain unit weight for all studied wheat and barley cultivars. This failure could be due to missing information that was not recorded during the crop performance tests such as leaf number, spike number and tiller number that could enhance the description of the cultivars' traits and lead to more realistic estimation of cultivars genetic coefficients.

The transportability of the estimated genetic coefficients and the robustness of the model in estimating grain yield similarly to the calibration and validation process, were evidenced in terms of high R^2 and D-stat values when we applied DSSAT-CERES to estimate wheat and

barley grain yields for a particular season (2019-2020) and across different types of soil in Q'a Shubayqa. This will bring us to the point where we can conclude that the overall objective of this chapter is fulfilled, and reliable estimated genetic coefficients of wheat and barley cultivars were successfully used by DSSAT-CERES-wheat/barley model in Q'a Shubayqa environments to predict grain yields under different spatial and temporal condition. These results will allow us to employ the model for further research in Q'a Shubayqa such as investigating the alteration of grain yield production of wheat and barley over the last decades (1987-2022). Furthermore, the robust model and the reliable genetic coefficients will also allow to predict the impact of future climate change in Q'a Shubayqa on wheat and barley grain yield (see chapter 8).

Chapter 8: Climate change impacts on wheat and barley production: historical and future perspectives

8.1. Introduction

Climate change impacts on crop production at global and regional scales, which have been predicted by scientists over recent decades, for example through the IPCC reports (https://www.ipcc.ch/reports/), have become reality, especially through forms of extreme climate events and the consequential increased frequency of serious crop yield gaps (see Chapter 2, section 4.3).

In Jordan, national studies have shown that climate change impacts will probably decrease crop yield by the mid- 21st century as a consequence of increases in temperature and long-term seasonal drought events (MoEnv (Ministry of Environment), 2009). However, the effects of climate change factors may also cause a beneficial increase in crop yield in specific agroecological areas (see Chapter 3, section 3.5).

Studying the impact of climate change on agricultural systems needs to be conducted independently for each region to allow relevant sustainable climate change adaptation strategies to be developed and enhance the resilience of the particular dryland agricultural system (see Chapter 2, section 7). Process-based crop models are the most widely applied tools to predict future climate impact on plant development (phenology) and crop yield components by simulating responses to changing climate factors individually or as a combination of these factors (Ludwig and Asseng, 2006).

Previous studies conducted in different regions across Jordan illustrate the impact of different future climate change scenarios on rainfed based wheat and barley production systems using two different well-known agricultural system models. Al-Bakri et al. (2011, 2013) used the DSSAT model for rainfed wheat and barley crops in the Yarmouk river basin to predict the impact of multiple incremental climate change scenarios by 2050, based on temperature and rainfall combinations from three different GCMs. However, they did not consider potential future CO_2 concentration effects. The results indicated that barley would be more negatively affected. Dixit et al. (2018) have applied APSIM to conduct a decadal analysis on the future climate change impact on wheat production in Jordanian drylands using outputs from four GCMs from the Coupled Model Intercomparison Project Phase 5 (CMIP5) used in the IPCC Fifth Assessment Report (AR5) (IPCC, 2014). The future climate data from the GCMs were

extracted under two CO_2 emission scenarios, Representative Concentration Pathways (RCPs), 4.5 and 8.5. They found that the impact of climate variables alone was negative on grain yield, but this adverse effect was negated when elevated atmospheric CO_2 concentrations were also considered in the model simulations.

This chapter will primarily focus on modelling the impact of historical and current changing climate on productivity of wheat and barley varieties cultivated in Q'a Shubayqa by employing observed meteorological data along with obtained relevant data from surveys (see Chapter 3) and hydrological modelling (see Chapter 6). The second part of the chapter is dedicated to modelling future climate impact on Q'a Shubayqa farming systems using derived climate data from different GCMs under two RCP scenarios (4.5 and 8.5). These analyses will include modelling future hydrological regimes for Shubayqa watershed (see Chapter 6) using SWAT and based on future climate projections for Jabal Druz as these forecast seasonal floods are the key factor for crop development and growth in Q'a Shubayqa.

The objectives of this chapter are to: i) assess the impact of different planting dates on wheat and barley grain yields; ii) simulate historical patterns of wheat and barley grain yields using observed datasets; iii) simulate future flood water that would flow into Q'a Shubayqa under different climate scenarios; iv) evaluate the impact of future climate change scenarios on grain yield and phenology of each studied cultivar in Q'a Shubayqa and simulate the feasibility of sustainable agricultural practices in reducing climate change impact.

8.2. Materials and methods:

8.2.1. Simulating grain yield and grain filling period patterns during the last decades

In order to evaluate crop yields and grain filling period patterns of wheat and barley in Q'a Shubayqa during the past decades (1987-2021), under varying weather conditions interspersed by climate extreme events (see Chapter 4), and to understand how cultivated crops has been interacting with changing climate, the DSSAT-CERES-Wheat/barley crop simulation model was applied using the seasonal analyses option. Input weather data such as daily minimum and maximum air temperature and daily rainfall data of Q'a Shubayqa required for DSSAT simulations are already available and are used in the previous chapters (see chapter 3, section 3.3.2 and chapter 6, section 6.3.5). For soil data, according to analyses of the soil samples collected from different sites in Q'a Shubayqa (see Chapter 3), there are five different soil textures in Q'a Shubayqa where the dominant (>50%) texture is silty clay loam. Under these

circumstances, the approach is to use the dominant soil texture as input data for these seasonal simulations for both wheat and barley cultivars (see Chapter 3). Particular initial conditions details required by DSSAT (see Chapter 7, section 7.5.3.2) for these model runs were set such that antecedent cultivated crops were the same as those crops used in the simulations, assuming that initial cereal crop residues would have the same impact on soil characteristics as those through the model experiments. For the initial percentage of available water, we assumed at least 50% as farmers confirmed that they do tillage and sowing just few days after the first seasonal floods (see Chapter 3) when the soils would still be wet.

These long-term seasonal simulations are applied on the studied wheat (Hourani and Acsad65) and barley (Mutah and Rum) cultivars independently. The stable genetic coefficient of wheat and barley cultivars that were successfully calibrated, validated and evaluated under different environments and over different seasons (see Chapter 7) are employed in this study.

Regarding planting date, DSSAT allows only one date to be entered for all the simulated seasons, which is not true for Q'a Shubayqa because farmers have confirmed that the planting date depends on the first seasonal floods that usually occur between October and December (see Chapter 3). According to hydrological modelling outputs using SWAT (see Chapter 6, section 4.5), if we consider that planting dates happen around seven days from the first seasonal floods, the likely planting dates percentage for October, November and December for the simulation period 1987-2021 can be calculated (Figure 8.1). Seasonal flood water estimated using hydrological modelling is considered as the irrigation process in DSSAT. So, flood events and quantities (watershed out-flow) that occur after the selected planting date for all simulated seasons will be inserted into DSSAT using the flood irrigation method. For this purpose, the water discharge from SWAT output presented in m^3/s needed to be converted to mm/day to fit with the input type of DSSAT-CERES model using the next equation:

Flood water (mm/day) = Q(m^3/s) *1000*24*3600/ Area (m^2)

Where Q is the daily discharge obtained from SWAT (m^3/s) and Area is the whole area of the Shubayqa watershed (708,900,000 m^2).

If we intend to get more realistic results about crop development and growth patterns from the long-term seasonal simulations, we need to find an approach to avoid the model limitation related to the fixed planting date. Our approach is to create three different model runs with

different planting dates for each wheat and barley cultivar, using planting dates in mid-October, mid-November and mid-December (Table 8.1). This will allow the creation of a more realistic time series of wheat and barley cultivar yields over the period between 1987 and 2021 by estimating the real planting date of each season using the flow-out data obtained from the hydrological modelling of Shubayqa watershed using SWAT model (see Chapter 6, section 4.5).

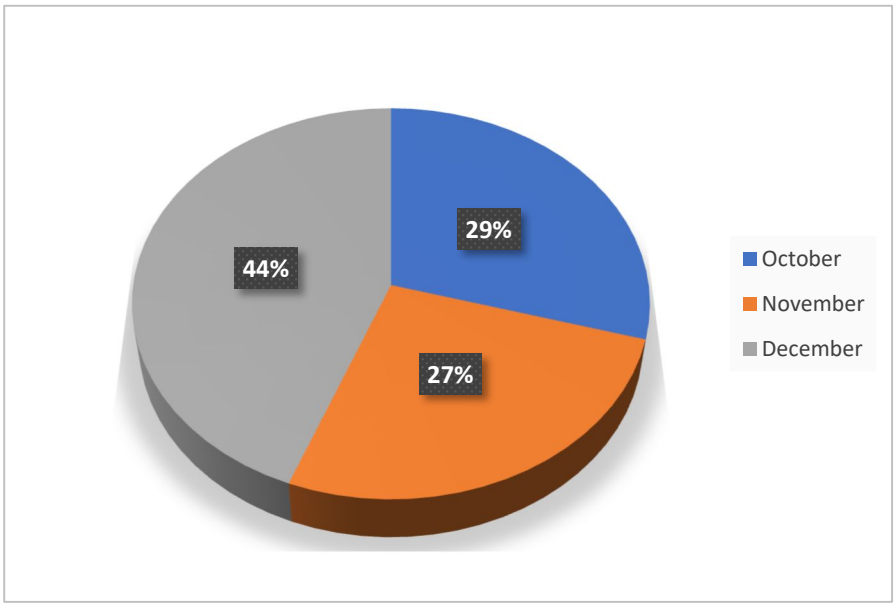

Figure 8.1: Estimated percentage of planting month for the period between 1987-2021 based on the timing of first floods simulated by the SWAT model of the Shubayqa watershed

Regarding the sowing rates, according to the survey (Chapter 3) most farmers use a dose between 80 and 100kg/ha which is approximately equivalent to 250 plants/m^2 and 240 plants/m^2 of wheat and barley respectively, based on grain unit weight of each cereal type.

According to farmers (see Chapter 3, section 3.4.2.2), tillage operations were mostly applied using chisel plough straight point tools.

Table 8.1: Seasonal simulation plan for wheat and barley cultivars with different planting dates treatments

	Cereal type	Cultivar	Planting date
Seasonal simulation run 1	Wheat	Hourani	15th October
			15th November
			15th December
		Acsad65	15th October
			15th November
			15th December
Seasonal simulation run 2	Barley	Mutah	15th October
			15th November
			15th December
		Rum	15th October
			15th November
			15th December

8.2.2. Modelling the impact of future climate change on grain yield and phenological stages of wheat and barley cultivars planted in Q'a Shubayqa

8.2.2.1. Future scenarios of climate change

For the assessment of the impact of future climate change on wheat and barley cultivars in Q'a Shubayqa, daily climate variable data were generated using the MarkSim_GCM tool which is a stochastic weather-generating platform that helps online users generate weather variable data that is bias-corrected and downscaled (Jones and Thornton, 2013). The MarkSim_GCM platform uses the well-known MarkSim application (Jones et al., 2002) working off a 30 arc-second climate surface derived from WorldClim (Hijmans et al., 2005). The MarkSim_GCM platform contains 17 GCMs from the Coupled Model Intercomparison Project phase 5 (CMIP5) (project of the World Climate Research Programme (WCRP) providing climate projections to understand past, present and future climate changes) that were considered in the IPCC fifth Assessment Report (AR5) (IPCC, 2014). The platform allows the user to select multiple GCMs for the same run and provide output files ready to be used in DSSAT.

Table 8.2: MarkSim General Circulation Models selected for this study

GCM	Source	Resolution Lat x Long °	Reference
CSIRO-Mk3.6.0	Commonwealth Scientific and Industrial Research Organisation and the Queensland Climate Change Centre of Excellence	1.875 x 1.875	(Collier et al., 2011)
HadGEM2-ES	Met Office Hadley Centre	1.2414 x 1.875	(Collins et al., 2011)
MIROC5	Japan Agency for Marine Earth Science and Technology, Atmosphere and Ocean Research Institute (The University of Tokyo), and National Institute for Environmental Studies	1.4063 x 1.4063	(Watanabe et al., 2010)
MRI-CGCM3	Meteorological Research Institute	1.125 x 1.125	(Yukimoto et al., 2012)

In this study, four GCMs were selected to generate future climate variables for the period between 2025 to 2095 (Table 8.2). The projection period was selected starting from 2025 to avoid using the same future climate data used for uncertainty analyses (see section 8.3).

Regarding GCMs, they were selected because they were already used to generate future weather data in two previous studies in Jordan that employed agricultural system models (DSSAT and APSIM) (Al-Bakri et al., 2011; Dixit et al., 2018). Regarding climate change scenarios, RCP4.5, is described by the Intergovernmental Panel on Climate Change (IPCC) as a moderate scenario representing the emission scenario that reaches its peak by 2040 and then starts to decline (IPCC, 2023). RCP8.5 is considered the most pessimistic scenario with the highest increase in temperatures and radiative forcing values globally (Meinshausen et al., 2011; Riahi et al., 2011; Thomson et al., 2011).

8.2.2.2. Projecting flood patterns using generated future climate data

The hydrological model of the Shubayqa watershed, calibrated and validated using SWAT tools (see Chapter 6), was employed to simulate daily watershed discharge using the same watershed characteristics and the generated future weather data for Jabal Druz generated from MarkSim_GCM under both RCP scenarios for the period between 2025 and 2095. The output data of discharge simulated for the period between 2027 and 2095 (first 2 years data, 2025 and 2026 are used by SWAT for warm-up period) was then re-entered into DSSAT under the irrigation option.

8.2.2.3. DSSAT simulation scenarios

The DSSAT-CERES-Wheat/barley model was implemented to simulate the impact of future climate change scenarios (RCP4.5 and RCP8.5) on wheat and barley yield for the period between 2027 to 2095. Seasonal simulation was conducted for each wheat and barley cultivar using the same configuration approach as in section 8.2.1 for the soil analysis data, cultivar genetic coefficients, tillage and initial conditions. Regarding planting date, it was fixed to be in mid-December, as December planting was dominant during the period between 1987-2021 (see Figure 8.2). Future weather data for the selected scenarios that were generated from MarkSim_GCM were imported into DSSAT. For the irrigation process, the SWAT modelled output of daily discharge for the Shubayqa watershed using future climate change data from both RCPs scenarios (see section 8.2.2.2) was used. Atmospheric CO_2 concentration levels for the selected RCPS scenarios were considered in this study. The baseline CO_2 concentration considered by the crop simulation model DSSAT was 380ppm. The future CO_2 concentration levels related to RCP4.5 and RCP8.5 were obtained from the Agricultural Intercomparison and Improvement Project (www.AgMIP.org) and were temporally partitioned into three levels (near term: 2025-2039, mid-century: 2040-2069 and end of century: 2070-2095) (Rosenzweig et al., 2018). For RCP4.5, near term CO_2= 423ppm, mid-century CO_2= 499ppm and end century CO_2= 532ppm. Regarding RCP8.5, near term CO_2= 432ppm, mid-century CO_2= 571ppm and end century CO_2= 801ppm. These CO_2 concentration levels were configured in the environmental modifications section in the DSSAT seasonal XBuild file.

8.2.3. Alternative agricultural practices to avoid yield gaps under future climate change

After simulating the impact of the studied climate change scenarios on grain yield production of wheat and barley varieties cultivated in Q'a Shubayqa, the next step is to conduct several

runs of the DSSAT model under the RCPs scenarios with implementation of alternative agricultural practices that could improve yield productivity. The choice of these alternative agricultural practices needs to consider the specific Q'a Shubayqa agricultural system and the capabilities of farmers in applying such practices. For example, we cannot ask farmers to buy and add fertilizers to their crop, because it is unsuitable to change a 100% organic agricultural system that has been adopted by local farmers over a very long period of time (about 10 thousand years ago) (Hillman et al., 2001; Ibáñez et al., 2014). In addition, during my field work and my meetings with these farmers, I concluded that it would be very hard to convince them to do such things because of the high costs and also the difficulty of transporting fertilizers to Q'a Shubayqa during the wet period. Under these circumstances, our approach is to select agricultural practices that would be easier to be apply in the near-term by farmers with minimum costs.

The first agricultural practice that will be evaluated is changing the planting time to January (mid-January). This choice was based on the fact that delayed seasonal floods have become more frequent in the last three decades so that these floods now occur mostly in December rather than October like it used to be, according to farmers statements (see Chapter 3) and the flood simulations conducted earlier in the thesis show that 44% of the planting dates were in December (see above and section 8.2.1, Figure 8.1). So, we assumed that floods would become even more delayed under climate change and a mid-January planting date is an extreme condition that may be caused by future climate change. The simulation of the wheat and barley cultivars with a delayed planting date under future climate change will allow the capability of these cultivars to adapt with the future change and to what extent they are able to adapt to be evaluated.

The second agricultural practice that will be assessed under future climate change scenarios is the addition of organic material to the cultivated lands of Q'a Shubayqa. The choice of this practice is based on several factors related to study area. The organic treatment will be the barnyard manure of local sheep where 32% of farmers are livestock owners (mainly sheep) with an estimated number of 8000 to 10000 head (see Chapter 3). In addition, during the grazing season in Q'a Shubayqa, lots of herd owners bring their livestock to the area and graze them there for 5 months at least. These conditions contribute to providing an important quantity of sheep/goat manure and make the application of organic material easier and cheaper for Q'a Shubayqa farmers. The quantity of 5000kg/ha barnyard manure will be added to the model

using crop management data interface of DSSAT (XBuild). The nutrient concentration in sheep manure will be added according to Burgess (1993) where nitrogen is 1.7%, phosphorus is 0.5% and potassium 1.2% of the added quantity.

The simulation of the grain yields using the new selected practices (January planting date and addition of organic material) will be conducted under future climate change scenarios considering the CO_2 effect for more realistic scenarios. The simulation will only include the mostly affected wheat and barley cultivars by future climate change.

8.3. Climate uncertainties in the study

In this chapter, we compare scenarios driven by observed (historical) climate data and that for future climates from several GCMs from the MarkSim_GCM platform. Before drawing conclusions from comparisons of past and future climate scenarios, from observed and simulated climate variables (rainfall and temperature), here we compare how similar these variables are over common time periods.

The first comparison was between monthly observed precipitation and simulated precipitation (using GCMs) from Jabal Druz as previous analyses (see Chapter 5 and Chapter 6) have shown its major contribution in crop growth in Q'a Shubayqa due to its role in generating seasonal floods. Correlation between observed and simulated rainfall in Jabal Druz (Figure 8.2) was acceptable (R=0.52), which demonstrates that the GCMs were, to some extent, able to predict rainfall in Jabal Druz. However, during this comparison, the range of modelled precipitation is lower than observed data and the obvious limitation of these GCMs was in predicting extreme rainfall events, where GCMs have underestimated the monthly rainfall amounts when compared to the very high monthly rainfall amounts recorded in Jabal Druz during the same months (e.g. February 2012, January 2013 and January 2019). In addition, when comparing annual average observed precipitation (569 mm) against annual average GCMs precipitation (335 mm) for the same period (2010-2020), the large difference can explain the fact that the model appears to show lower overall precipitation in the correlation plot.

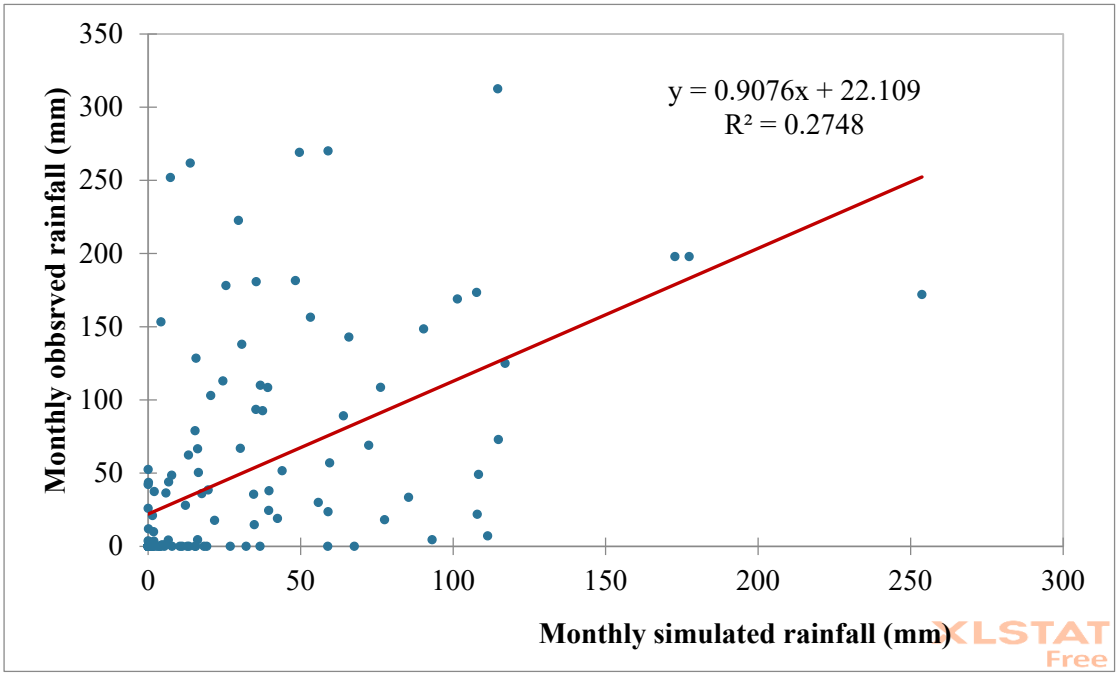

Figure 8.2: Correlation between monthly observed rainfall and MarkSim_GCM simulated monthly rainfall for the period between 2010 and 2020 of Jabal Druz area

The second comparison was between monthly observed rainfall at Safawi and simulated monthly rainfall generated from MarkSim_GCM using the same set of models employed in the previous analysis (Table 8.2) for the period between 2010 and 2020 (Figure 8,3). The correlation between observed and simulated rainfall is weak (R=0.25).

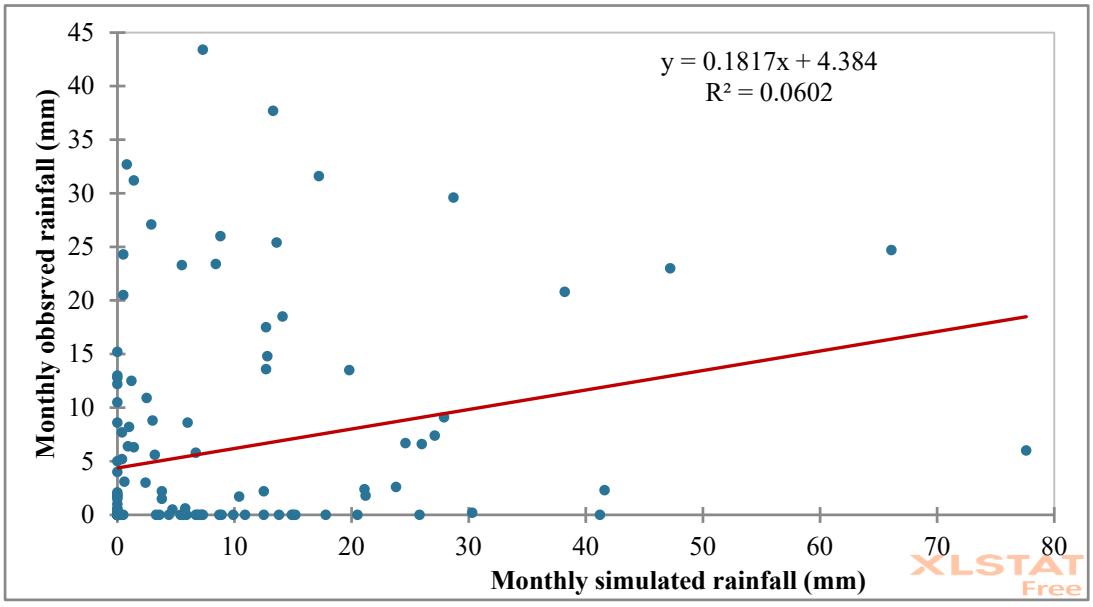

Figure 8.3: Correlation between monthly observed rainfall and MarkSim_GCM simulated monthly rainfall for the period between 2010 and 2020 of Safawi

The third comparison was between average daily observed temperatures and average simulated daily temperature for the study area over the same period (2010 to 2020) (Figure 8.4) which shows a strong correlation value of R=0.83.

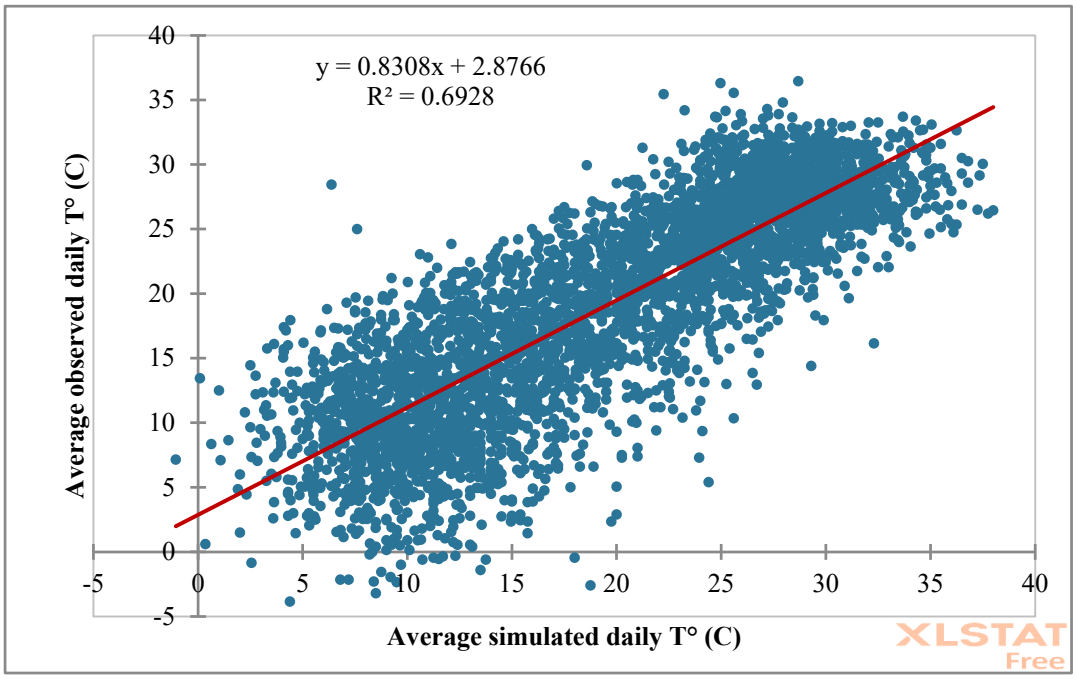

Figure 8.4: Correlation between observed daily average temperature and MarkSim_GCM simulated daily average temperature for the period between 2010-2020

These results confirm that although forecasts of daily average temperature were good, MarkSim_GCM outputs were not good at estimating rainfall in Jabal Druz and Q'a Shubayqa. The limitations of GCMs in predicting rainfall storms and amounts in arid lands (especially high rainfall amounts during extreme events) could be due to rainfall patterns in these areas, where rainstorms are very spotty, and its effectiveness varies from one area to another at local scale (Chapter 2, section 2.2.2). Additionally, these largely convective storms are sub-grid scale for almost all climate models, so they are just not simulated by GCMs (Rasp et al., 2018; W. Zhang et al., 2025). Such issues will affect DSSAT model when using MarkSIM_GCM that will immediately underestimate floods going into Q'a Shubayqa and as this water is critical for growth and development of cereals under rainfed system, MarkSIM_GCM data are not likely to produce yields at the same levels as observed climate data and will be lower than reality. This is an important point to consider when comparing future yields with present yields because future yields will automatically be lower. Under these circumstances, comparisons between baseline grain yield (based on observed precipitation data) and simulated future grain yield (based on GCMs precipitation data) from DSSAT modelling are not reasonable. However,

simulated phenology phase period using GCMs such as grain filling can be compared with baseline grain filling period because phenology is highly sensitive to temperature (Chakrabarti et al., 2013; Du et al., 2022), and comparisons between GCMs temperature and observed temperatures have shown a good correlation, which means that DSSAT would be able to simulate more realistic future grain filling period of the studied cultivars.

8.4. Results

8.4.1. Seasonal analyses of near past patterns of wheat and barley cultivars in Q'a Shubayqa

8.4.1.1. Wheat cultivars

- **Grain Yield simulations**

The historical simulation of the wheat cultivars Hourani and Acsad65 under different planting date treatments (Table 8.1) using DSSAT-CSM-CERES-Wheat, have shown an important difference in harvested grain yield. For the Hourani cultivar (Figure 8.5), October planting (treatment 1) has shown a low median value of around 704 kg/ha and a maximum yield of around 770 kg/ha, while the November planting median (treatment 2) was slightly higher with an approximate maximum yield of 900 kg/ha. December planting (treatment 3) for Hourani was much higher than both previous treatments with a median value around 884 kg/ha and 25% of the simulated yields are between 924 and 1080 kg/ha. However, yield value variability for the December planting treatment is much larger than for either the October or November treatments.

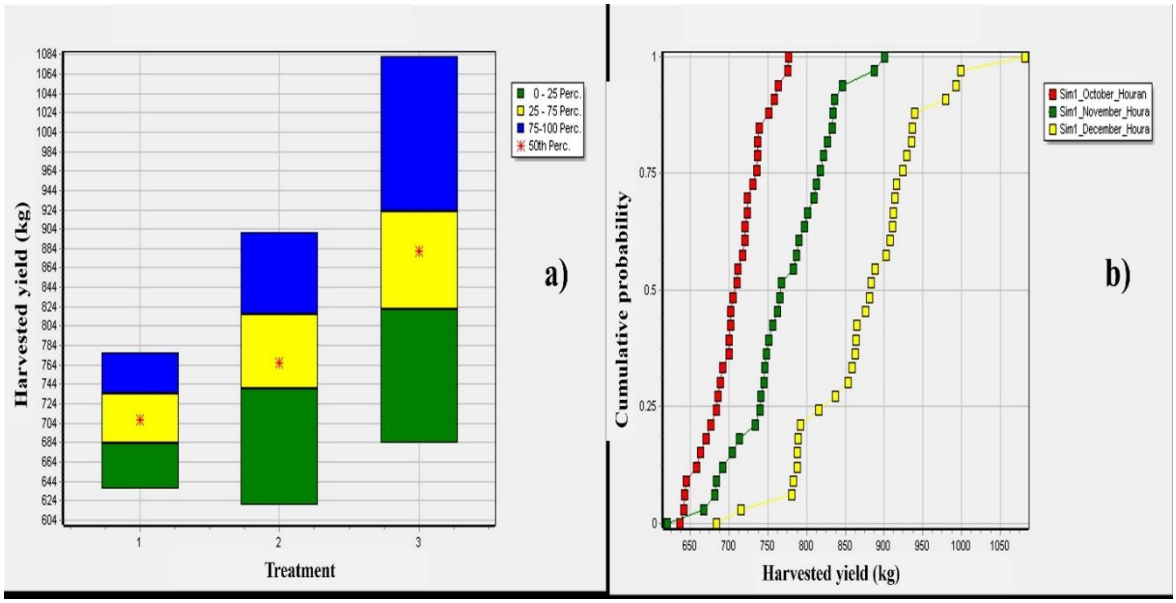

Figure 8.5: Historical simulation of Hourani grain yield (kg/ha) under different planting dates (treatment; Table 8.1) using DSSAT-CSM-CERES-Wheat: **a)** Box plot of harvested yield and **b)** Cumulative function plot of harvested yield

Regarding the grain yield simulation for Acsad65 (Figure 8.6), the median values of simulated grain yield for the period between 1987 and 2021 for the first and second treatments were very close at around 980 kg/ha, while maximum simulated harvested yields were around 1240 and 1200 kg/ha for October planting and November planting. In addition, we can notice some crossover among the distribution functions and, as a consequence, we can say that the simulation outputs in terms of grain yield of the first and second treatments tend to be more or less equal. However, the December planting has shown a median higher than either of the first two treatments with a value of 1080kg/ha, more than 25% of simulated yields are over 1160kg/ha with a maximum simulated grain yield that reaches 1420kg/ha.

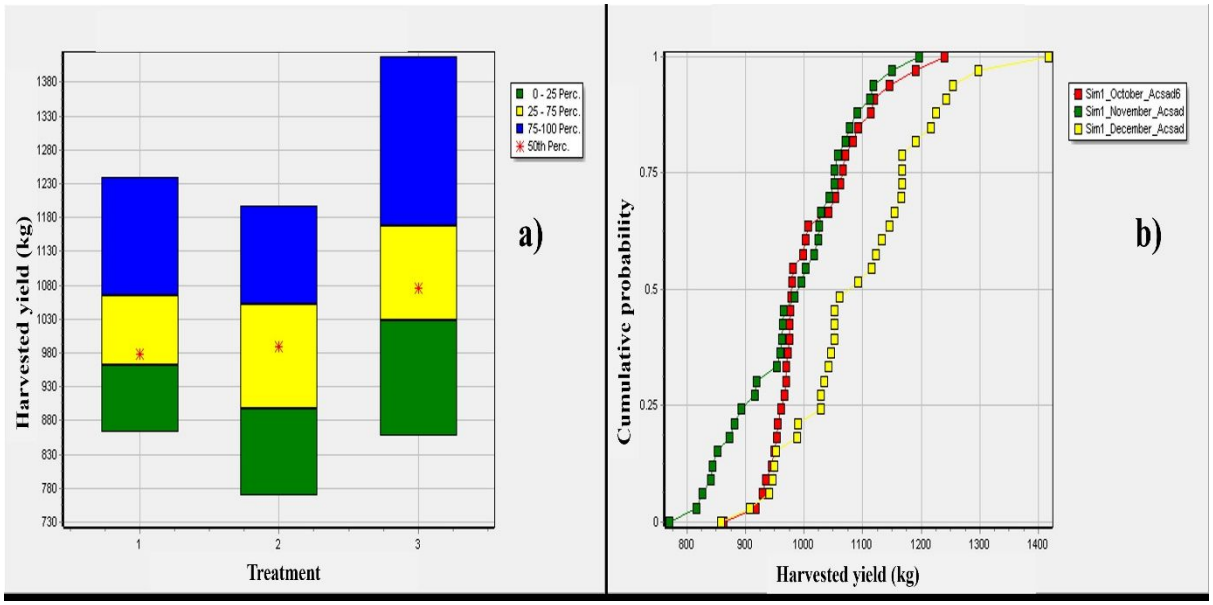

Figure 8.6: Historical simulation of Acsad65 grain yield (kg/ha) under different planting dates (treatment; Table 8.1) using DSSAT-CSM-CERES-Wheat: **a)** Box plot of harvested yield and **b)** Cumulative function plot of harvested yield

These seasonal simulation results, that represent grain yield patterns of both studied wheat cultivars in Q'a Shubayqa using DSSAT-CERES-wheat, could explain several important characteristics related to the cultivars and the model. I can conclude that grain yield of Acsad65 is higher than grain yield of Hourani even if they are planted in different dates. This difference in harvested yield is due to the genetic characteristics of both cultivars where Hourani is known as a landrace, while Acsad65 is an improved variety that is known for its high yield and its resistance to harsh weather conditions like drought. It is notable as well that the model outputs were very sensitive to the planting date variation.

Based on previous simulation results and approximate planting date estimations based on first seasonal flood dates, more realistic grain yield time series were created that would represent grain yield patterns during the historical simulation period. Figure 8.7 shows the grain yield time series of the Hourani and Acsad65 cultivars, respectively.

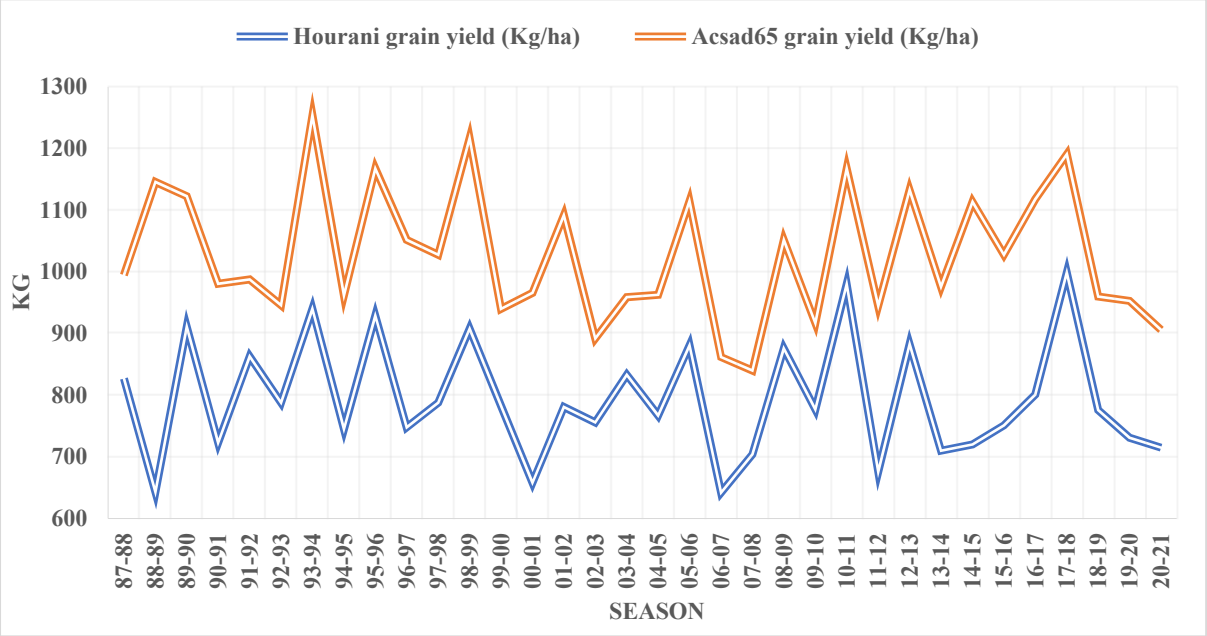

Figure 8.7: Grain yield patterns of Hourani and Acsad65 cultivars for the period between 1987-2021 in Q'a Shubayqa using DSSAT-CSM-CERES-Wheat

Time series of Hourani and Acsad65 grain yield (Figures 8.7) show an unstable pattern of grain productivity, with an inter-seasonal variation. The grain yield for Hourani can vary from 642 kg/ha (2006-2007) to 1000 kg/ha (2017-2018) and for Acsad65 from 840 kg/ha (2007-2008) to 1254 kg/ha (1993-1994). According to farmers, yield losses could be due to several environmental factors like drought, flood delay and shortage and heat waves. Invasion by pests can also cause serious damage to the crops (see Chapter 3). During these low yield seasons, farmers choose to feed the damaged crops to livestock (direct grazing) rather than harvesting (see Chapter 3). Both time series have shown an important yield decrease during the seasons 2006-2007 and 2007-2008. During the same seasons, the extremely wet days index R99p and RX5day index (annual maximum consecutive 5 days precipitation) calculated from Jabal Druz weather data were very low or null (see Chapter 4). This indicates that floods have not occurred during this period due to the absence of extreme wet days and consecutive rainy days that usually cause water runoff after soil saturation. High temperature levels represented by the high value of the daily maximum temperature index (TXx) during the season 2011-2012, have also affected grain yield for both Hourani and Acsad65 (see Chapter 4). To evaluate the accuracy of the simulated grain yield, we can also compare the observed grain yield data obtained from surveyed farmers (season 2019-2020) which were used in Chapter 7 for genetic coefficient evaluation (see Chapter 7, section 7.6.3), however it is important to consider that the observed grain yield data depend on farmers sowing rates and soil type of the cultivated land within Q'a

Shubayqa. The observed Hourani grain yield varies from 850 to 1590 kg/ha and simulated grain yield for the same season was 731 kg/ha (Figure 8.7). Regarding Acsad 65, observed grain yield varies between 1050 and 1750 kg/ha and simulated grain yield for the same season was 953 kg/ha.

❖ **Grain filling period simulation**

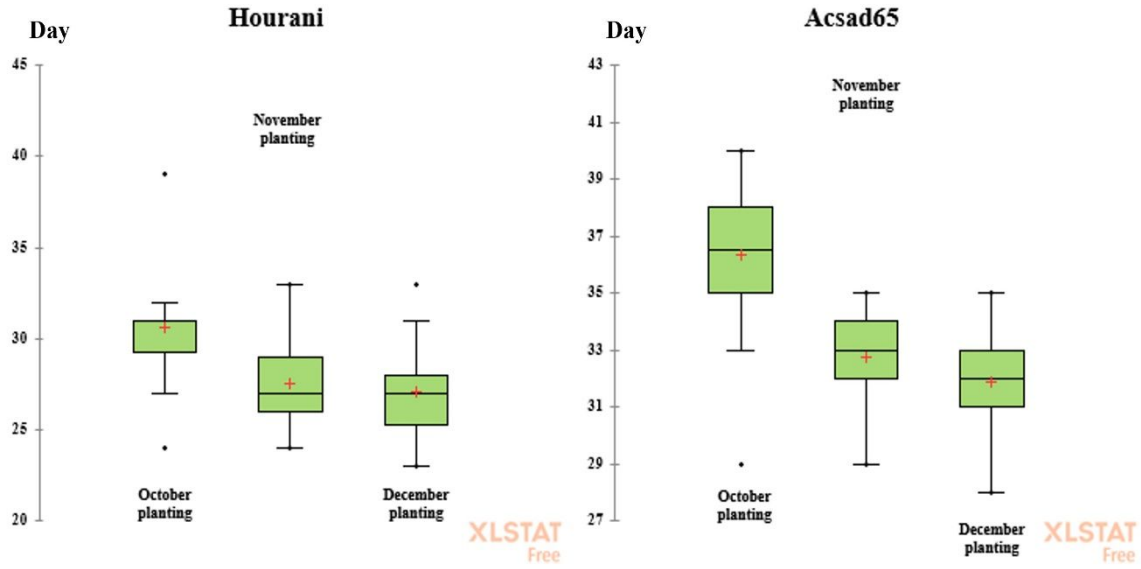

Figure 8.8: Planting date impact on grain filling period of Hourani and Acsad65 cultivars

Grain filling period seems to be sensitive to the planting date for both studied wheat cultivars as shown in Figure 8.8. For Hourani, grain filling period for November and December planting dates has shown a reduction of 3 days for November planting and 3.5 days for December planting. For Acsad65, the reduction of grain filling period for November and December planting dates is more important, with around 4 days reduction compared to the October planting date. The decrease of grain filling period for wheat will affect grain quality and relatively grain yield (See chapter 2, section 5).

To illustrate the importance of grain filling period of wheat on grain yield, a correlation between realistic grain filling periods and grain yields, extracted based on the estimated planting dates from first floods timings, was carried out for Hourani and Acsad65 cultivars (Figure 8.9).

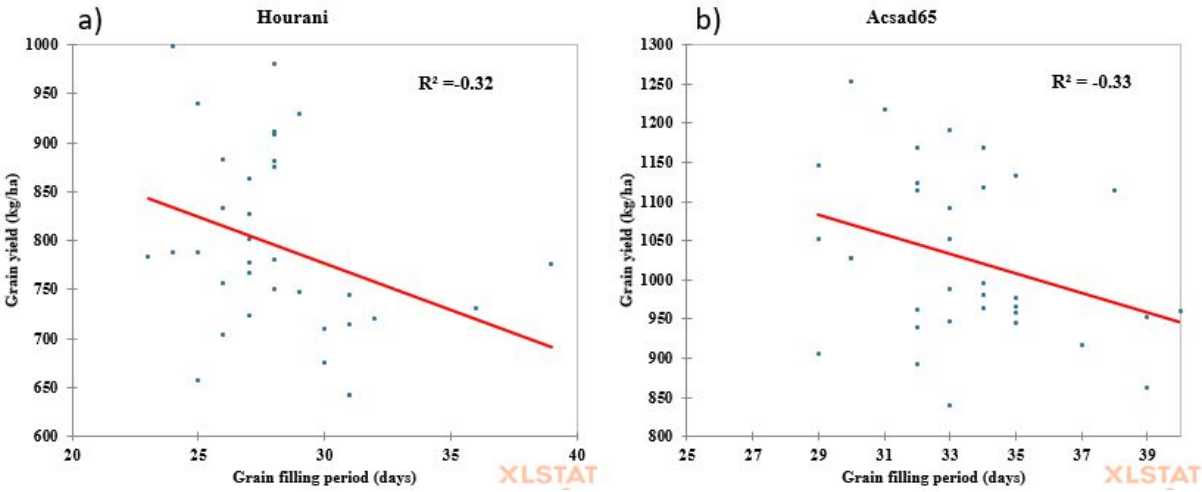

Figure 8.9: Correlation between grain yield and grain filling period of a) Hourani and b) Acsd65 wheat cultivars

Figure 8.9 shows that grain yield for both cultivars was negatively correlated (p-value<0.05) with grain filling period with R^2=-0.32 (Figure 8.9.a) and R^2=-0.33 (Figure 8.9.b), respectively for Hourani and Acsad65. Pireivatlou et al. (2011) also reported that under drought stress conditions, grain weight was negatively correlated with grain filling period, however seed number per spike was positively correlated with grain filling period.

8.4.1.2. Barley cultivars

- **Grain Yield simulations**

Long-term historical simulations of barley development and growth for Mutah and Rum cultivars under different planting dates in Q'a Shubayqa, have shown an important variation in terms of grain yield. In contrast to wheat, barley grain yield has shown higher values with earlier planting dates. For Mutah (Figure 8.10), grain yield median value for an October planting date (treatment 1) reaches 1600 kg/ha, while grain yield median value reductions were recorded at around 530 kg/ha and 600 kg/ha for November (treatment 2) and December (treatment 3) planting dates, respectively.

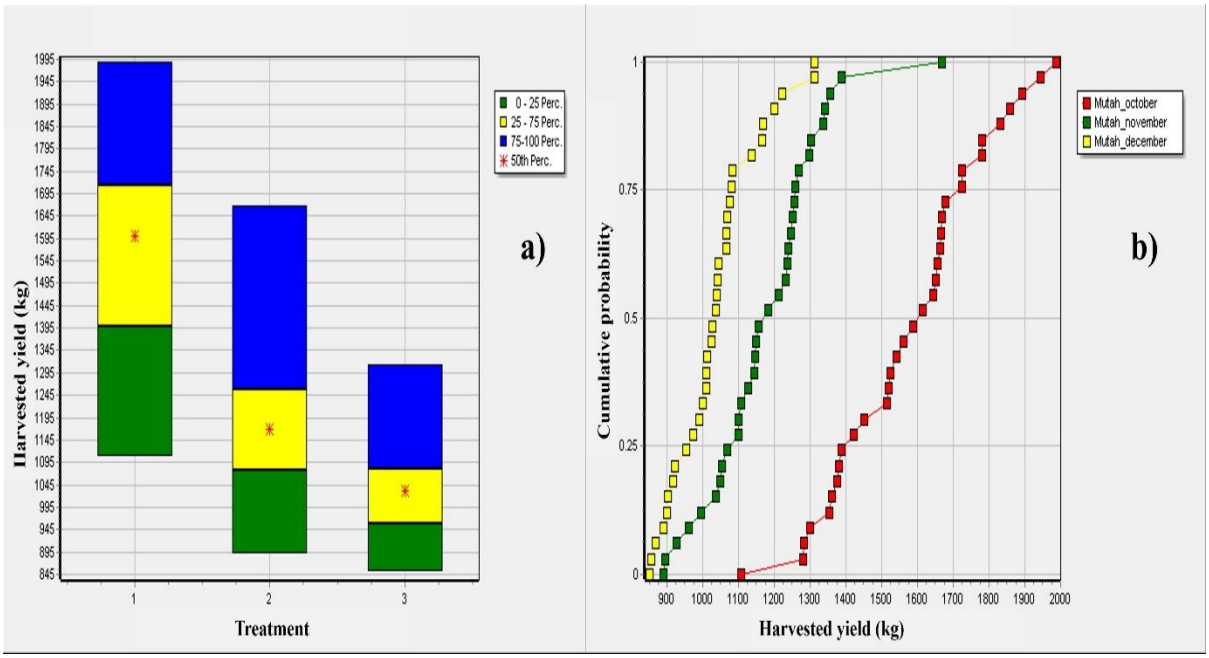

Figure 8.10: Historical simulation of Mutah grain yield (kg/ha) under different planting dates (treatment; Table 8.1) using DSSAT-CSM-CERES-Wheat: **a)** Box plot of harvested yield and **b)** Cumulative function plot of harvested yield

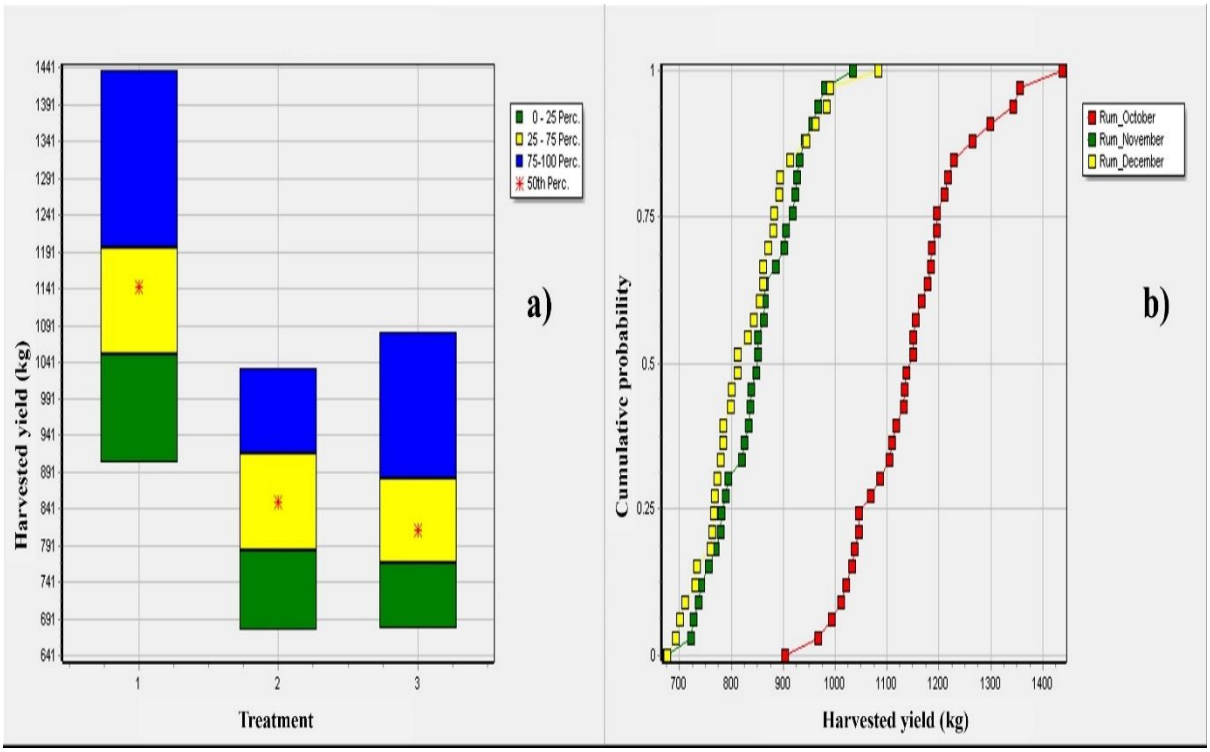

Figure 8.11: Historical simulation of Rum grain yield (kg/ha) under different planting dates (treatment; Table 8.1) using DSSAT-CSM-CERES-Wheat: **a)** Box plot of harvested yield and **b)** Cumulative function plot of harvested yield

Regarding grain yield patterns of Rum cultivars (Figure 8.11) in relation to different planting dates, the grain yield median value of October planting was around 1140 kg/ha, which is much higher than the median values of November and December planting dates. The latter have shown some crossover among the distribution functions, which means that these treatments' outputs tend to be more or less equal in terms of grain yield, with a median value around 800 kg/ha.

For both barley cultivars, planting dates seems to be an important factor that could critically affect grain production, where statistical results have shown that delayed planting dates in November and December reduce barley grain yield by around 40% and 30% for Mutah and Rum, respectively. However, farmers cannot avoid the issues of delayed planting as long as planting dates in Q'a Shubayqa mainly depend on the timing of the first seasonal floods (see Chapter 5).

Figure 8.12 represents barley grain yield patterns of Mutah and Rum cultivars planted in Q'a Shubayqa over the period between 1987 and 2021 based on realistic planting dates that were estimated according to the first seasonal floods.

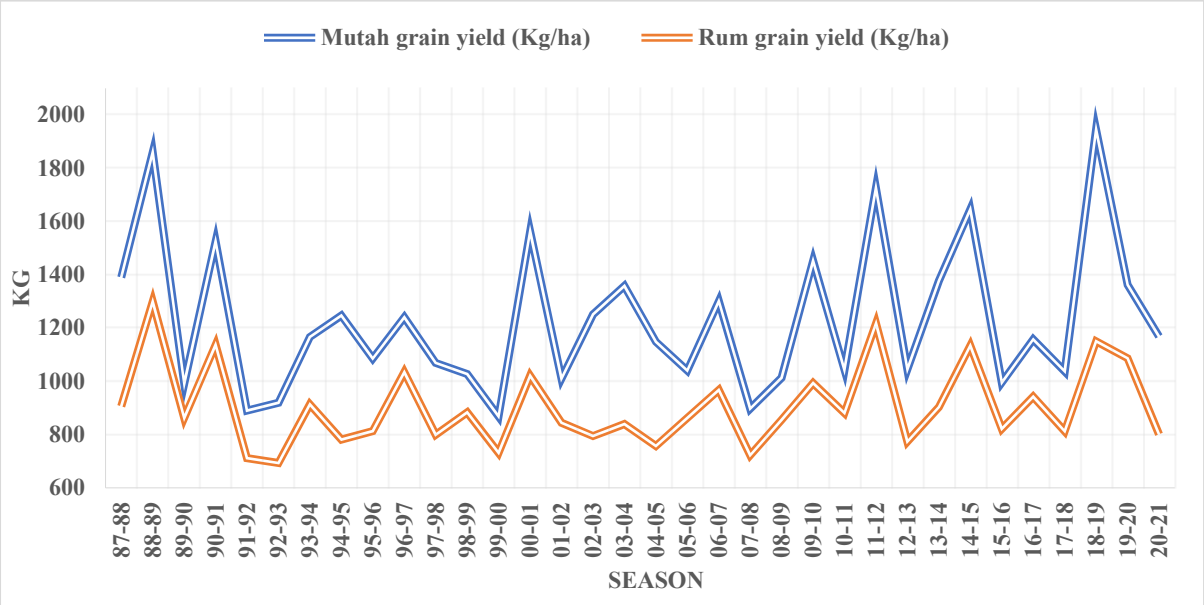

Figure 8.12: Grain yield patterns of Mutah and Rum cultivars for the period between 1987-2021 in Q'a Shubayqa using DSSAT-CSM-CERES-Barley

Grain yield reductions for Mutah and Rum cultivars during the simulation period between 1987 and 2021 were frequent. This could be due to harsh environmental conditions, for example during the seasons 1991-1992 and 1992-1993 when annual precipitation in Jabal Druz recorded the highest values during the whole studied period (see Chapter 4, Figure 4.2). Severe continuous floods could appear as a consequence of these high rainfall levels and could damage crops cultivated in Q'a Shubayqa. Farmers referred to similar situations in particular seasons and confirmed that continuous floods destroy the plants, especially when they are in the early phenological stages (see Chapter 3). In addition to the environmental factors, a delayed planting date (due to delayed first seasonal floods) is a limiting factor that could negatively affect the grain yield as shown previously. On this basis, 71 % of planting dates estimated based on the first seasonal floods during the studied period (1987-2021) were in November and December (see figure 8.1). To evaluate the accuracy of the simulated grain yield, we can also compare the observed grain yield data obtained from surveyed farmers (season 2019-2020) which were used in Chapter 7 for genetic coefficient evaluation (see Chapter 7, section 7.6.3), however it is important to consider that the observed grain yield data depend on farmers sowing rates and soil type of the cultivated land within Q'a Shubayqa. The observed Mutah grain yield varies from 1250 to 1750 kg/ha and simulated grain yield for the same season was 1362 kg/ha (Figure 8.12). Regarding Rum, observed grain yield varies between 750 and 1000 kg/ha and simulated grain yield for the same season was 1086 kg/ha.

- **Grain filling period simulation**

Grain filling period for both barley cultivars Mutah and Rum were highly affected by the different planting dates (Figure 8.13). For the Mutah cultivar, compared with October planting date, there is a reduction of 13 and 18 days of grain filling period for November and December planting dates, respectively. The decrease of grain filling period for Mutah seems to be highly affecting grain yield where the correlation between them was significant (p-value<0.05) and high (R^2= 074) (Figure 8.14).

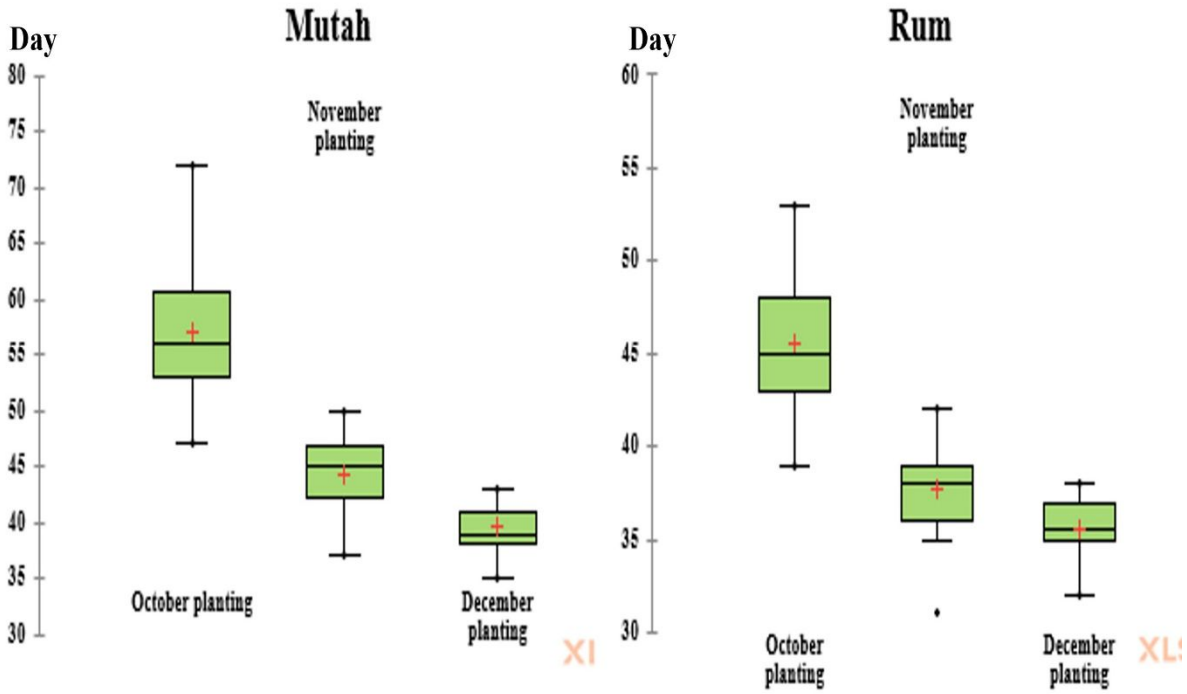

Figure 8.13: Planting date impact on grain filling period of Mutah and Rum cultivars

The reductions of grain filling period for the Rum cultivar, compared to an October planting date, were around 8 and 10 days for November and December planting dates, respectively. However, the impact of grain filling period reduction on grain yield was limited where correlation between them was low (R^2=0.22), but significant (p-value<0.05).

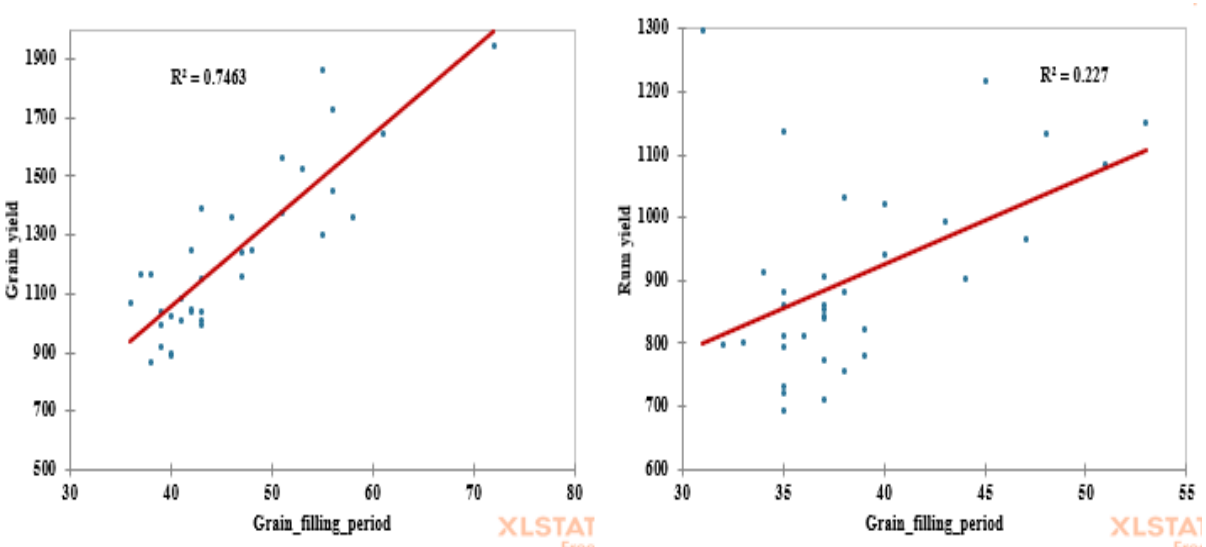

Figure 8.14: Correlation between grain yield and grain filling period of Mutah and Rum barley cultivars

These results indicate that the Rum cultivar grain filling period is less sensitive to a delayed planting date compared to the Mutah cultivar. Furthermore, the grain yield of the Mutah cultivar largely depended on grain filling period, unlike the Rum cultivar which means that planting Rum in Q'a Shubayqa, under a change of planting dates that mainly depends on the timing of the first floods, is a sustainable practice to avoid yield gaps.

8.4.2. Quantifying Future floods under different climate change scenarios

Figure 8.15 shows the changes in floods occurring in Jabal Druz and flow at Q'a Shubayqa estimated using the hydrological model (created with SWAT) of the Shubayqa watershed (Chapter 6, section 4) under two different datasets of future climate scenarios (RCP4.5 and RCP8.5). The estimated annual cumulative floods from both climate scenarios were compared with baseline floods (cumulative annal floods (mm) that flow in Q'a Shubayqa) that were estimated for the period between 1987 and 2021 using observed weather data (see Chapter 6, section 6.4.3).

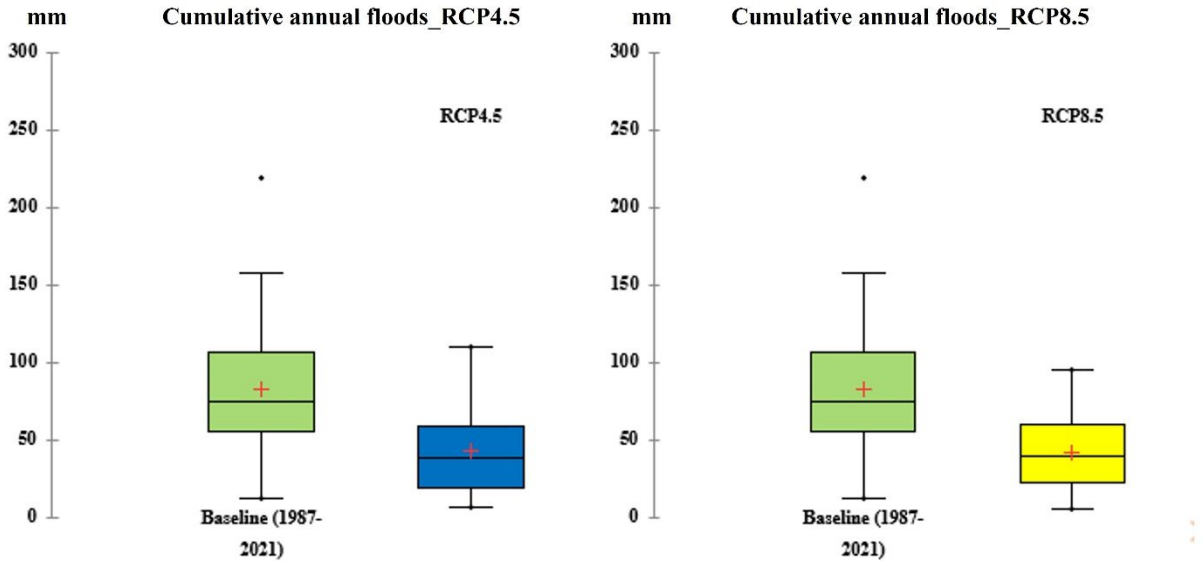

Figure 8.15: Simulated cumulative floods using SWAT model under RCP4.5 and RCP8.5 future climate scenarios (2027-2095) compared to baseline cumulative annual floods (1987-2021)

The future cumulative annual flood amounts of both RCPs scenarios driven by MarkSIM_GCM show an important decrease compared to the baseline floods. The reduction in annual cumulative floods were estimated to be 48.21% under RCP4.5 and 49.31% under RCP8.5, with a small difference of 1.1% between both scenarios. This reduction in floods that

will flow into Q'a Shubayqa is due to the GCMs that have been shown to underestimate the current precipitation in Jabal Druz (see section 8.3) assuming that this will apply in the future. The daily estimated floods under the studied RCPs scenarios as taken as irrigation water inputs to simulate the patterns of wheat and barley grain yield and grain filling period under the future changing climate in Q'a Shubayqa.

8.4.3. Seasonal analyses of future patterns of wheat and barley under different climate scenarios

8.4.3.1. Wheat cultivars

- **Grain Yield simulations**

The impact of climate change on Hourani and Acsad65 wheat cultivars during the period between 2027 and 2095 are presented in Figure 8.16 and Figure 8.17. The results were temporally partitioned into three periods (near term, mid-century and end-century) based on the different CO_2 concentration levels described in section 8.2.2.3. The simulation of wheat grain yield using DSSAT-CSM-CERES-wheat under both RCPs scenarios was conducted twice. In the first run, atmospheric CO_2 elevation (423ppm) during the three periods was included, whereas, for the second run, only changes in rainfall and temperature were considered. The comparisons between both sets of simulations should provide a clear picture of the impact of CO_2 increase on grain yield.

For Hourani, the lowest grain yields under RCP4.5 with and without the elevated CO_2 fertilization effect, was obvious during the near-term time-periods. During the mid-century time-period, Hourani grain yields show a slight improvement with an increase of 3.3% with CO_2 effect and 1.4% without CO_2 effect (Table 8.3). The gain yield kept increasing in comparison with near-term values until the end of century, but this increasing is still limited (7.8% with the CO_2 effect and 5.4% without the CO_2 effect).

Under the RCP8.5 scenario, Hourani mid-century grain yield have slightly increased by 1% without CO_2 and 4.3% with CO_2. By the end-century, Hourani grain yield have shown an important jump of 19.2% when considering CO_2 concentration. The CO_2 fertilization effect on Hourani grain yield has shown a limited effect over all time-periods of RCP4.5 scenario, however, the impact of CO_2 on Hourani grain yield was significant under RCP8.5 scenario especially when considering CO_2.

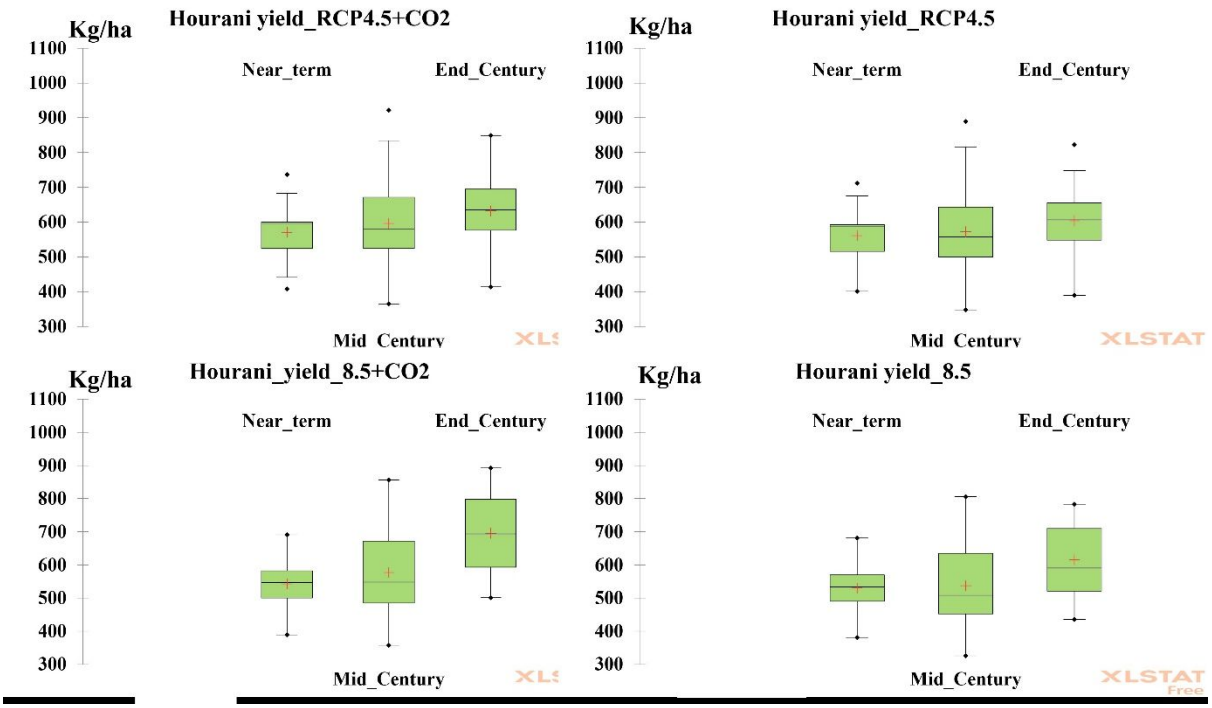

Figure 8.16: Hourani grain yield (kg/ha) simulated, under two RCP future scenarios with and without considering predicted high CO_2 concentration levels, using DSSAT

For Acsad65 simulated under RCP4.5 (Figure 8.17), the grain yield patterns have shown a limited decrease during mid-century of almost 1% in comparison with near-term grain yield with or without considering CO_2 concentrations. By the end-century period, Acsad65 grain yield was ameliorated by the effect of CO_2 with an increase of 6% in comparison with near-term grain yield. The highest impact of elevated CO_2 was observed during the end century under the RCP8.5 scenario where grain yield has increased of about 18% compared to simulated grain yields of near-term. Although still showing the effects of the increase in temperatures and the overall decrease in rainfall and flood water amounts, grain yield shows an important increase compared to grain yield simulation without the CO_2 effect, specifically during the end-century time-period due to the very high atmospheric CO_2 (801ppm). These results have shown that both studied wheat cultivars were sensitive to climate change and to the high CO_2 concentration with almost the same level of sensitivity.

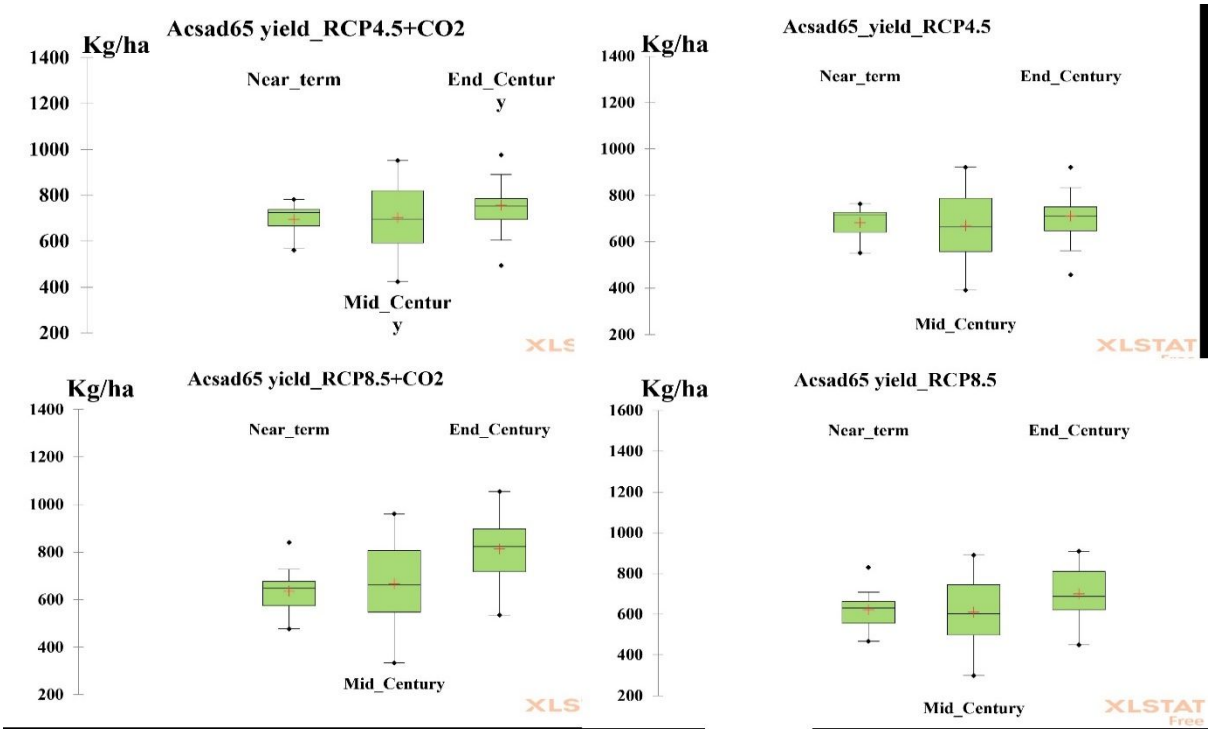

Figure 8.17: Acsad65 grain yield (kg/ha) simulated, under two RCPs future scenarios with and without considering predicted high CO_2 concentration levels, using DSSAT

❖ Grain filling period simulation

Grain filling period is an important stage of the wheat life cycle and could be affected by several environmental factors like drought and increased temperature. These factors could reduce grain weight by accelerating seed growth and by the shortening grain filling period (Akter & Rafiqul, 2017; Fahad et al., 2020). For Hourani, grain filling period simulation under the two RCPs scenarios with and without considering CO_2 effect (Figure 8.18), median values of grain filling period remain almost unchanged during all the studied time-periods compared to a recent baseline. This could be due to the characteristics of Hourani cultivars which is a landrace (see Chapter 7, section 7.5.1). Wheat landraces are known for their high levels of resistance to both biotic and abiotic stresses (Mohammadi et al., 2015).

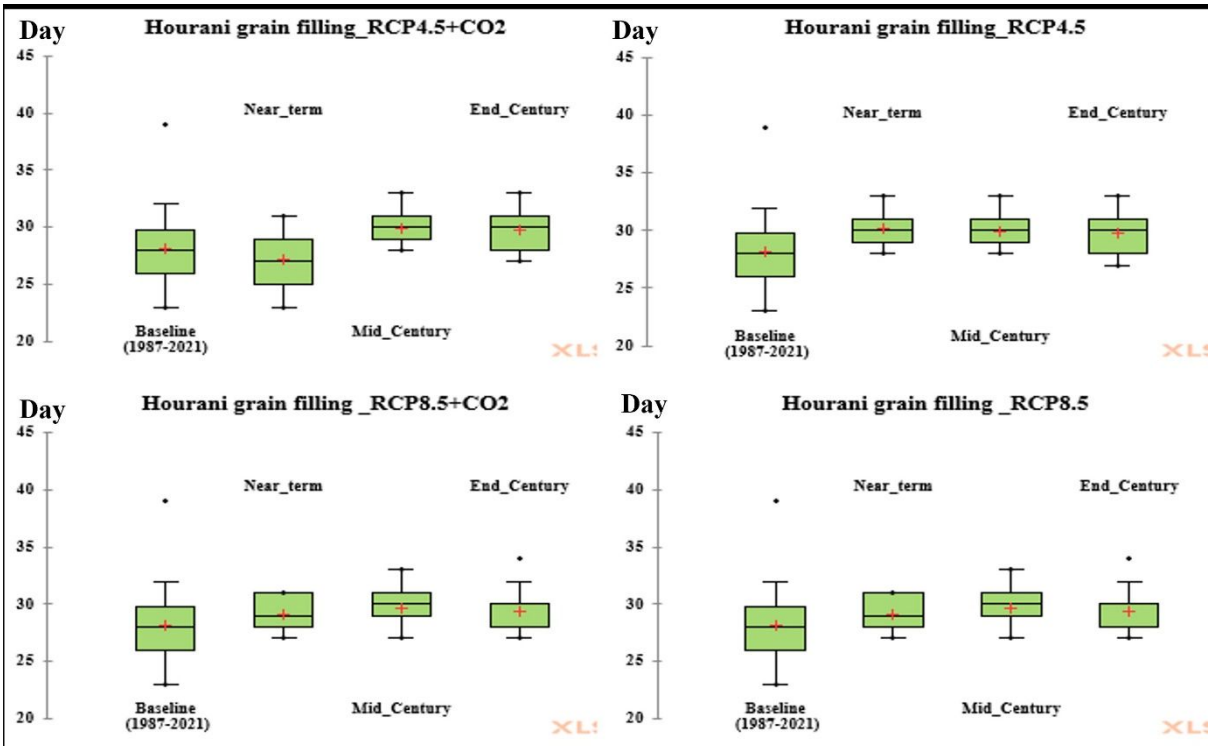

Figure 8.18: Hourani grain filling periods (days); baseline (from observed climate data) and simulated under RCP4.5 and RCP8.5 future scenarios with and without considering predicted high CO2 concentration levels.

The grain filling period of Acsad65 cultivars (Figure 8.19) was also simulated under the different RCPs scenarios with and without considering CO_2. The response of Acsad65 to the future climate change scenarios in terms of grain filling period seems to be different from Hourani. Grain filling period median values during the three time-periods and under both RCPs scenarios have decreased by approximately 2 days compared to baseline. Unlike Hourani, Acsad65 is an improved wheat variety (see chapter 7, section 7.5.1) which explains its life cycle sensitivity to climate change and relevant abiotic stresses. It is also possible that of the drop off here, between baseline and near-term simulation relates to the poor climate representation of regional rainfall.

There were no obvious changes in grain filling period for either studied wheat cultivars when CO_2 effect was included in the simulations compared to the simulations conducted without CO_2 effect.

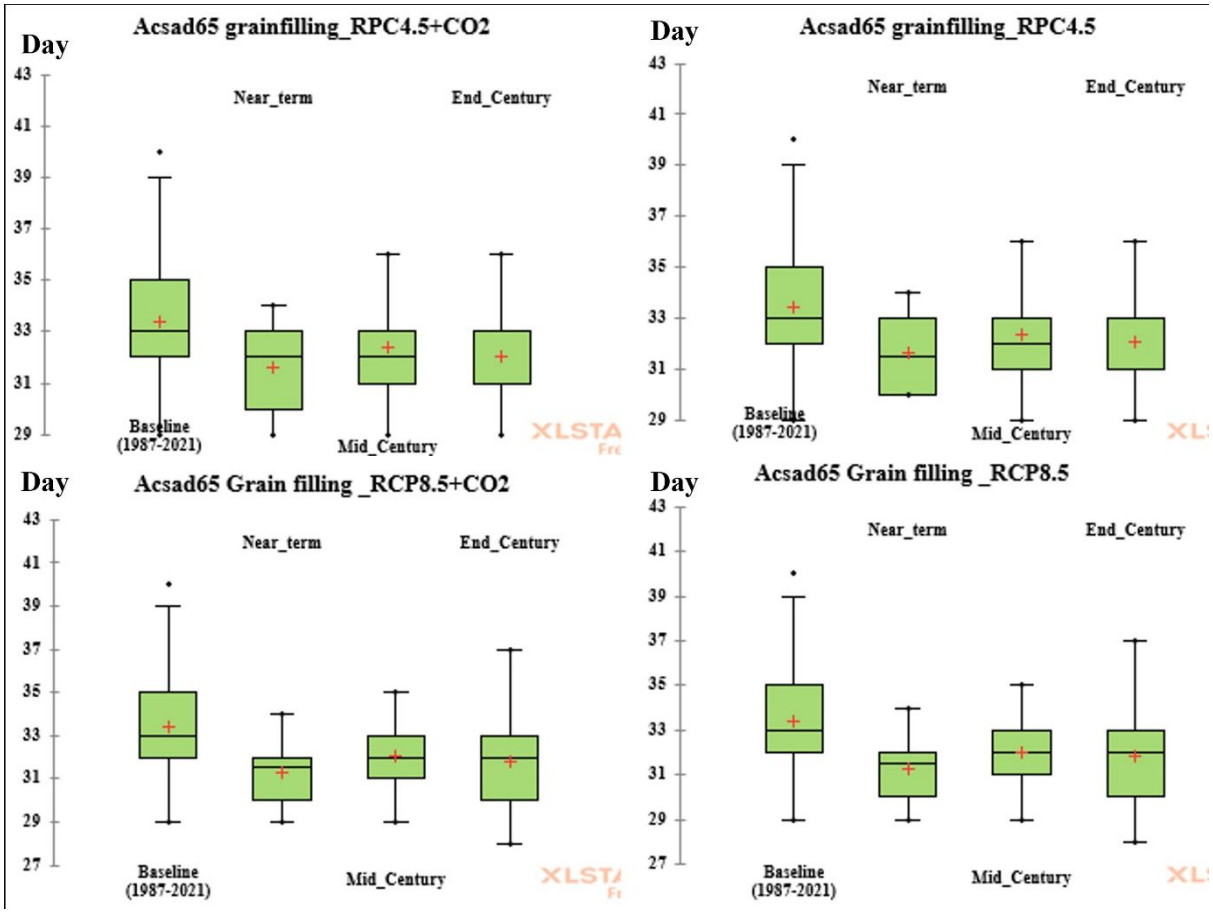

Figure 8.19: Acsad65 grain filling periods (days); baseline (from observed climate variables) and simulated under RCP4.5 and RCP8.5 future scenarios with and without considering predicted high CO_2 concentration levels

8.4.3.2. Barley cultivars

- **Grain yield simulations**

The impact of both future climate change scenarios (RCP4.5 and RCP8.5) on barley cultivars Mutah and Rum cultivated in Q'a Shubayqa are illustrated in Figure 8.20 and Figure 8.21, where average grain yield under each scenario during different time-periods, with and without considering elevated CO_2 fertilization effect, are represented.

The response of Mutah average grain yield to both RCPs scenarios considering the CO_2 effect was the same (1245kg/ha) during the near-term period, with a slight increase during mid-century of 66kg/ha under RCP8.5 (with CO_2 effect) than 24kg/ha under RCP4.5 (with CO_2 effect). A pronounced decrease in average grain yield was observed in the end-century time period for both RCPs scenarios with CO_2 effect. Mutah simulated average grain yield under the RCP scenarios without CO_2 effect has shown a very small decrease in values in the mid-

century periods compared with near-term and then a more dramatic decrease during end-century of about 418kg/ha compared to near-term grain yields. According to the grain yield patterns of Mutah represented in Figure 8.20, we can notice that even with CO_2 fertilization effect, grain yield has dramatically dropped under the effect of climate change of the end-century period for all the studied scenarios.

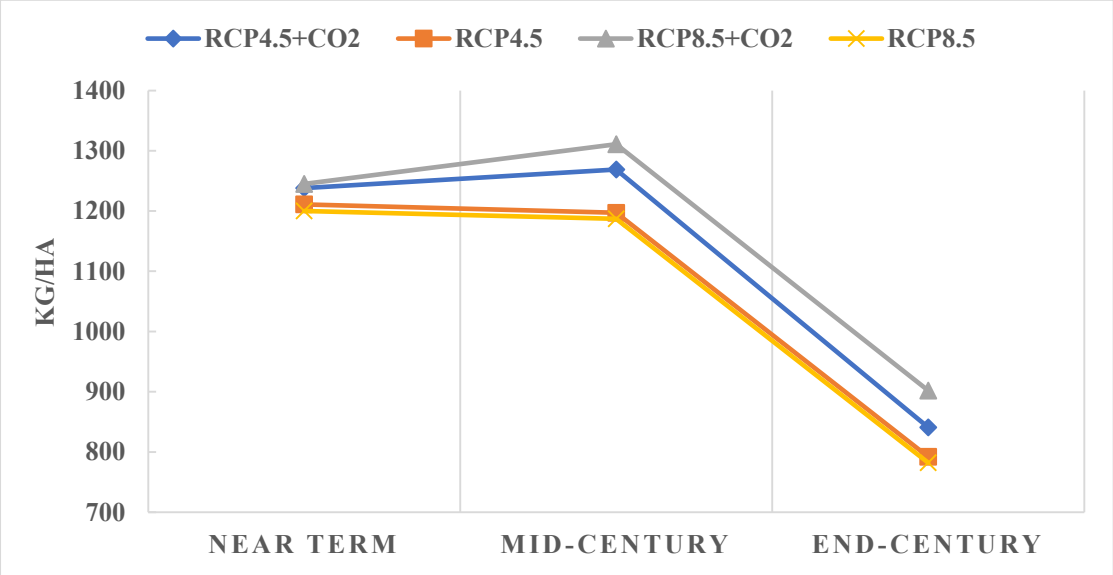

Figure 8.20: Mutah grain yield (kh/ha) patterns under RCP4.5 and RCP8.5 scenarios with and without considering CO_2 effect

Grain yield patterns of the Rum cultivar under the two studied RCP's scenarios without CO_2 effect, have shown no changes during the mid-century time period in comparing to near-term grain yield, however, the employing of CO_2 concentration have slightly improved grain yield with 37kg/ha and 72kg/ha for RCP4.5 and RCP8.5 respectively. Thereafter they keep increasing during end-century period to reach 1458kg/ha under RCP8.5 and 1353kg/ha under RCP4.5 with CO_2 effect (Figure 8.21). The fertilization effect of CO_2 was obvious on grain yield during the end-century time periods, with an increase of around 78kg/ha and 183kg/ha under RCP4.5 and RCP8.5, respectively compared to grain yield under the same scenarios without CO_2 effect.

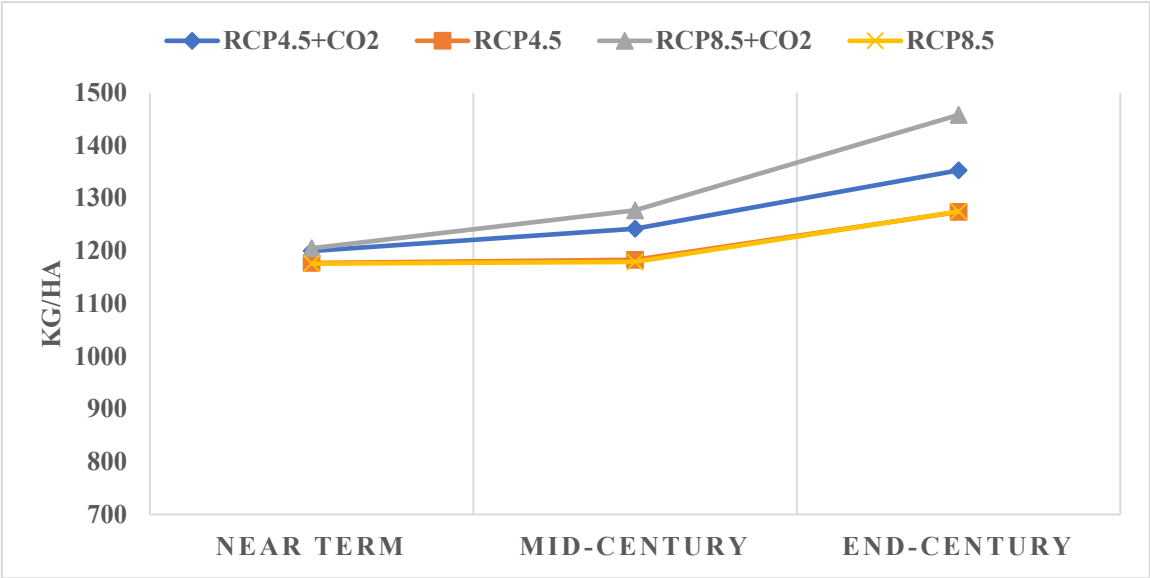

Figure 8.21: Rum grain yield (kh/ha) patterns under RCP4.5 and RCP8.5 with and without considering CO_2 effect

❖ **Grain filling period simulation**

Grain filling periods of studied barley cultivars (Mutah and Rum) have shown a decrease in the number of days compared to baseline average grain filling period simulated based on observed weather data for the period between 1987 and 2021 (Table 8.4). The reduction of grain filling period for Mutah under both RCP scenarios were 7 days, 6 days and 14 days during near term, mid-century and end-century, respectively. For the Rum cultivar, the reduction of grain filling period was constant (~4 days) throughout the whole studied period (2027-2095) under the different RCPs scenarios. There was no impact of high CO_2 levels observed on grain filling period for either Mutah and Rum cultivars over the whole projected period.

Table 8.4: Grain filling period (days) variations under different RCPs scenarios with and without CO_2 effect

Climate scenario	Mutah				Rum			
	Baseline	Near term	Mid-century	End-century	Baseline	Near term	Mid-century	End-century
RCP4.5+CO₂	46	39	39.9	32.04	38.5	34.41	35.63	34.8
RCP4.5	46	39	39.9	32.04	38.5	34.41	35.52	34.8
RCP8.5+CO₂	46	39	39.9	32.04	38.5	35.04	35.63	34.8
RCP8.5	46	39	39.9	32.04	38.5	34.41	35.63	34.8

8.4.4. Sustainable agricultural practices impact on grain yield under future climate change scenarios

The assessment of the selected agricultural practices (January planting date and organic addition) on grain yield under future climate change will be tested on the Acsad65 wheat cultivar and the Mutah barley cultivar. The latter cultivars were selected as the previous results have shown that they were more affected by climate change compared to the other studied cultivars (see section 8.3.2).

Under RCP4.5, Acsad65 grain yield was negatively impacted by a delayed planting date of mid-January, with a reduction of 117kg/ha compared to RCP4.5 with a December planting date. However, there was no observed change in the grain yield median value when simulating Acsad65 under RCP8.5 with a January planting date compared to a December planting date (Figure 8.22).

The grain yield of barley cultivar Mutah seems to be highly affected by a delayed January planting date under both RCPs scenarios (Figure 8.22), with a reduction of 215kg/ha and 266kg/ha under RCP4.5 and RCP8.5 respectively, compared to the value of grain yield with a December planting date.

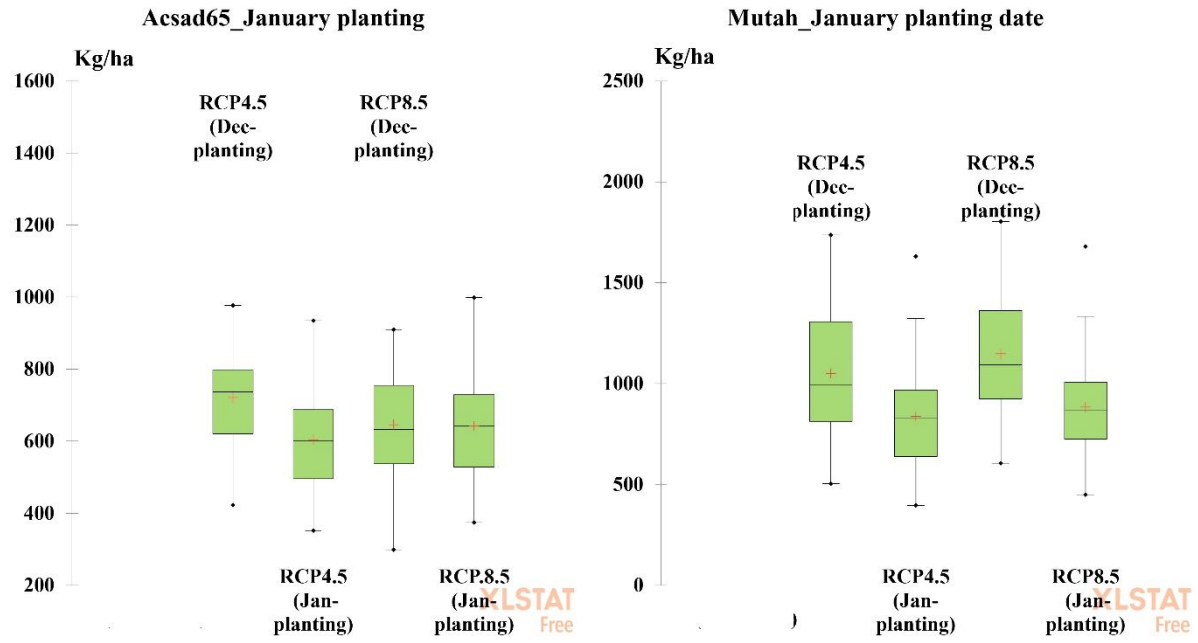

Figure 8.22: The impact of delayed planting date (mid-January) on grain yield (kg/ha) of Acsad65 and Mutah cultivars under different RCPs scenarios

Barnyard manure was applied to Mutah and Acsad65 cultivars under RCP4.5 and RCP8.5 as an agricultural practice that could improve yield productivity under future climate change. The results have shown that gain yield median value of the barley cultivar Mutah have shown an increase of 47 kg/ha when applying organic amendment under RCP4.5 compared to grain yield simulated under RCP4.5 without organic amendment (Figure 8.23). However, there was no effect of manure on grain yield of Mutah simulated under RCP8.5 compared to grain yield simulated under RCP8.5 without manure amendment.

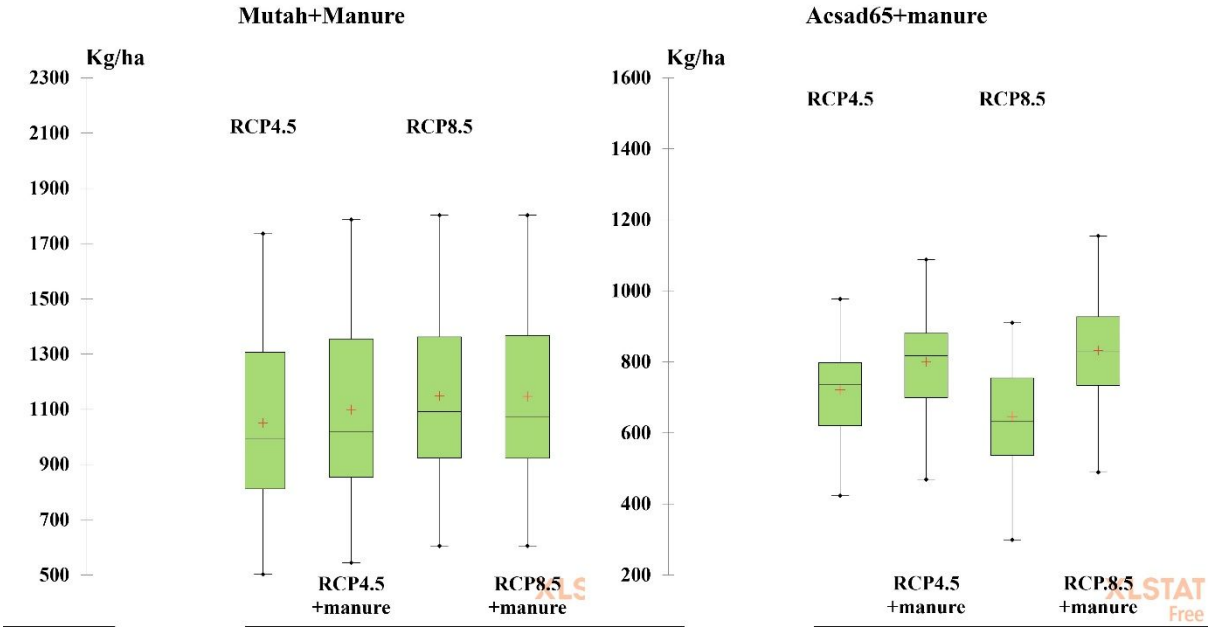

Figure 8.23: The impact of organic amendment practice on grain yield (kg/ha) of Acsad65 and Mutah cultivars under different RCPs scenarios

Acsad65 grain yield simulated under RCP4.5 with manure addition has increased by 80kg/ha compared to grain yield simulated under RCP4.5 without addition. The same reaction of the grain yield was observed when simulating Acsad65 grain yield under RCP8.5, with an important increase of 187kg/ha compared to grain yield without manure addition. This could be due to the combination of the organic matter added to the planted soil with the high atmospheric CO_2 level (801ppm) on soil quality and water holding capacity, and on the photosynthesis process.

8.5. Discussion and conclusions

The historical simulation of wheat and barley cultivars has shown that climate change has been affecting crop phenology and grain yield presented by the production gaps (falls in grain production) during several seasons of the study period (1987-2021). These notable concerns

are attributed to factors like air temperature increases (see Chapter 4) and diminishing rainfall patterns in MENA region (Luppichini et al., 2022). However, the investigation of the impact of delayed precipitation in Jabal Druz and its consequences on the timing of the first seasonal floods and planting dates in Q'a Shubayqa, which was reported by farmers (Chapter 3), has shown that delayed planting date (in December) positively affected grain yield, but not in the case of barley. Historical simulation of the studied barley cultivars yields under different planting dates have shown that grain yield and phenological stages (grain filling period) are highly sensitive to delayed planting date where both have significantly decreased. The results of a study conducted by Tita et al. (2025) on agronomic management impact on wheat yield gaps in the Mediterranean and MENA region, matches with the findings here, where they highlighted that the ideal period for planting wheat varieties in Jordan is between 1st and 15th December for maximum crop yield production. Although the planting date in Q'a Shubayqa is not optional for the farmers due to several environmental factors (primarily the timing of the seasonal floods) that prevent them from starting the cultivation season, there may therefore be a need to employ new cultivars with a shorter life cycle to adapt with these changes especially for barley.

The comparison between observed and estimated monthly rainfall in Q'a Shubayqa and Jabal Druz has shown weak correlations respectively, which indicates the limited effectiveness of MarkSim_GCM in producing reliable estimates of rainfall in such area (Drylands). Under these circumstances, although future flood-water quantity estimated based on projected rainfall in Jabal Druz using GCM outputs shows a decrease of almost 50% under both RCP scenarios in comparison with baseline, this estimate must be treated with caution. Similar findings were found by Dixit and Telleria (2015) when they studied climate models' ability to estimate rainfall in the dry areas of Northern Syria and Lebanon. They found a major difference between observed rainfall data and estimated rainfall data from MarkSim_GCM. According to them, this difference is explained by interpolated weather surfaces and/or the weather station not being close enough to the reported location which means that altitude variation at local spatial scale could affect MarkSim_GCM performance in predicting rainfall as it determines precipitation at a site from interpolated surfaces (Hartkamp et al., 2003; Semenov et al., 2013). More discussions about this difference between simulated and observed precipitation data are in section 8.3. Daily temperature predicted by MarkSim_GCM has been shown to be reliable after the good correlation obtained when comparing simulated temperature with observed temperature for a common period. Along with the predicted increasing temperature in Q'a

Shubayqa, the simulated decrease of flood water quantity would affect grain yield simulations of wheat under future RCPs scenarios where both cultivars have shown an important decrease of grain yield during the period between 2027 and 2095.

The impact of high atmospheric CO_2 concentrations on crop yields was more obvious during end-century period and mostly for the RCP8.5 scenario. The sensitivity of grain yield to the RCP scenarios relevant climate change patterns differs from cultivar to another where Hourani (wheat) and Rum seems to be more resistant to such changes. Climate change has also affected wheat phenology (grain filling period) of both studied genotypes. This is demonstrate the ability of DSSTA to detect the sensitivity of each cultivar to climate change based on its own genetic coefficients. However, the consequences of reduced grain filling period on grain yield were not similar for both cultivars due to the genetic characteristics of each cultivar. Dixit et al., (2018) have applied the APSIM crop simulation model in a dry Mediterranean climate located in Jordan to assess impact of climate change on wheat production using climate datasets derived from MarkSim_GCM and considering the same climate change scenarios (RCP4.5 and RCP8.5) employed in this study. The findings were similar to those presented here where the impact of climate variable without considering CO_2 was negative on wheat grain yield, but this adverse effect was negated when elevated CO_2 concentrations were considered in the simulation and contributed to the increase of grain yield comparing to the baseline even with a detection of a reduction of life cycle (impact of climate change on crops phenology).

For barley cultivars, the Rum cultivar has shown a much better response to climate change in terms of grain yield, especially under RCP scenarios with high CO_2 levels. However, Mutah grain yield was dramatically affected under the end century climate change scenario. Al-Bakri et al. (2011) reported that barley crop simulation under several climate change scenarios in Jordan have shown an important decrease in grain yield. However, unlike our study, they used average grain yields of multiple barley cultivars. Crop simulation really needs to be specific for each cultivar to illustrate its traits interaction with environmental changes. Under these conditions, Mutah is recommended to be cultivated in Q'a Shubayqa under future climate change. Alternative agricultural practices (delayed planting and addition of organic matter) evaluated under future climate change scenarios have shown that planting wheat and barley cultivars in mid-January has a negative impact on grain yields, but organic addition may increase grain yield under climate change scenarios when high CO_2 levels are taken into

account. These findings suggest that some adaptations to current practices may help to mitigate the impacts of climate change, although not enough to maintain yields.

It is important to conclude that the successful simulations of the impact of climate change on crops depend on several factors such as the models and tools used, the data sets' reliability and the skills and ability of the user to employ these factors according to the specificities of the studied cropping system. For this study, the main issues were related to the data used such as local precipitation and floods derived from future climate data of MarkSim _GCM. In addition, the absence of any database that contains the historical seasonal productivity of Q'a Shubayqa farming system that would allow the detailed evaluation of the model performance is one of major the limitations.

All the findings of this chapter and previous chapters will be gathered in next chapter which will presents a general discussion in relation to the aim of the thesis and a critical reflection on the limitations of the research.

Chapter 9: Discussion

This chapter reviews the previous chapters (mainly from Chapter 3 to Chapter 8) that have presented the work of this PhD towards fulfilling its aim of understanding how recent and future changing climate has and will affect agricultural system productivity in Q'a Shubayqa. The overarching themes of the work are discussed, alongside the key findings from each chapter.

The idea that cropping systems worldwide, particularly in drylands, will need to adapt as the climate changes is not new. The difficulties of providing quality analyses of how particular systems need to change are, however, significant and complicated due to multiple intervening factors and, particularly in dryland areas such as discussed here, due to the availability and quality of data. These difficulties can only be addressed once the complexity of individual systems is understood, and this has been the aim of this work.

Reviewing literature in Chapter 2 demonstrates that variations of environmental factors (climate, geomorphology, biodiversity, soil, water resources and management practices) in drylands influences the current cropping system type and productivity, for example predicted climate change patterns are estimated to vary from area to area across Jordan (MoEnv, 2009). Based on these variations, the interaction between cropping systems and patterns of changing climate will differ and affect the sustainability practices adopted, according to each individual agricultural system needs. Examples of this are presented in Chapter 3, where farming systems vary spatially within the same country (Jordan) and even within the same basin (Azraq).

It was found that the study cropping system in Q'a Shubayqa is distinctly different from surrounding cropping systems in the wider Azraq basin (Chapter 3, section 3.2.2.3). Surveys of the current farmers of Q'a Shubayqa (Chapter 3) show that this system is a chemical free, ancient, rainfed (via flooding) agricultural system where farmers adopt a cereal-based mono-cropping system based on wheat and barley; sorghum is also grown under specific flood timing conditions (see Chapter 3, section 3.4.2.2). The information and findings from this survey would have been wider and more representative if it was undertaken in normal conditions (without COVID restrictions), as I was planning to do the survey personally with a larger sample of farmers. Despite these restrictions, the survey outcomes were sufficient to describe the main components and limiting factors of the Q'a Shubayqa agricultural system.

Such mono-cropping cereal systems in dry areas typically lead to yield decline through time, due to the build-up of a series of unfavourable factors, primarily; the reduction of soil organic matter, microbial activity, soil fertility, infiltration rates and hydraulic conductivity (Liu et al., 2023; Masri & Ryan, 2006; Tekin et al., 2017; Town et al., 2022). However, according to the surveyed farmers and ongoing archaeological research (e.g. Thuesen et al., 2023), Qa Shubayqa has been, and continues to be, successfully cultivated for millennia under its mono-cropping cereal type systems, and its productivity is still stable during regular wet seasons (see Chapter 3). Despite this rare circumstance the farming system has not previously been the subject of detailed study. Based on farmers statements and soil analyses presented earlier in this thesis (see Chapter 3, section 3.3), the secret of this agricultural continuity can be shown to be due to the seasonal floods that originate in Jabal Druz in southern Syria, and flow into Q'a Shubayqa, bringing water and, potentially more importantly, soil and organic matter into the basin. The latter was confirmed when comparing organic matter values from inside and outside Q'a Shubayqa (see Chapter 3, section 3.3.2.4), where soil organic matter from inside the basin where floods flow is much higher than analysed soil from outside the basin, and even higher than the average value of soil organic matter observed in other dryland soils (Bashour et al., 2016). This flooding phenomenon therefore contributes to the regeneration of Q'a Shubayqa soils by recuperating what soils have lost (organic matter and nutrients) during previous cropping seasons.

Observed climate variables and relevant extreme indices analyses have shown that climate in Q'a Shubayqa and the surrounding area (including Jabal Druz) has been changing during the last decades (see Chapter 4, section 4.3). These changes were mainly observed as significant increasing trends of temperature and increasing trends of particular precipitation extreme indices (mainly related to heavy short rain) in Jabal Druz. Whereas wetter conditions in drylands could often be linked to more productive agricultural yields, floods, resulting from extreme rainfall events, can, however, have particular negative consequences on soil structure and aggregation, and on agricultural productivity (Rupngam & Messiga, 2024). This will be related to the floods type and properties such as frequency, velocity, depth of water and duration, also the physical properties of the watershed (e.g. Allocca et al., 2021; Gaál et al., 2012). Surveyed farmers from Q'a Shubayqa have raised this issue related to the consequences of high magnitude flash floods on the destruction of the cultivated crops and /or long period floods that cause waterlogging especially in particular areas in Q'a Shubayqa (see Chapter 3, section 3.4.2.6). This was demonstrated in the remote sensing analyses of this thesis where it

was noticed that in some particular seasons, the recorded cumulative monthly precipitation in Jabal Druz was high, but the NDVI and NDWI values during the same seasons were negligeable (see Chapter 5, section 5.4.1), likely as a result of cultivated crops being negatively affected by particularly large or intense floods.

Li et al., (2024), Rupngam & Messiga, (2024) and Trenberth, (1998) have all explained how extreme precipitation events, characterised by short periods of intense rainfall are becoming more common as the climate warms up globally. Under these circumstances, the usual advantages of seasonal floods on mono-cropping cereal system sustainability and soils restauration in Q'a Shubayqa would become limited or negative due to the climate change.

Crop yields in Q'a Shubayqa could also be impacted by climate change in ways other than increased flooding. Findings from previous studies (see Chapter 2, sections 2.5.2 and 2.5.3) have shown that the impact of climate change on precipitation patterns can vary by region, where some areas may experience more intense and frequent rainfall while others may see reductions in average precipitation leading to droughts interspersed with heavy downpours (Rupngam & Messiga, 2024). According to farmers (see Chapter 3, section 3.4.2.6) and to the analyses showing the interaction between time series of climate variables (including extreme indices), spectral indices (NDVI and NDWI), and remote sensing data like soil moisture (see Chapter 5, section 5.4.2), these changing weather patterns in the Q'a Shubayqa region are mainly long drought periods and delayed flash floods, which have been affecting farming practices, crop growth and development processes and, in consequence, wheat and barley grain yield in Q'a Shubayqa (yield gaps).

Another important climate pattern variation was noticed in Q'a Shubayqa during the last 12 years, 2010-2021 (Figure 9.1) where trends in monthly maximum value of daily maximum temperature (TXx) and annual precipitation changed from the preceding 25 years. In addition, the same period has shown important levels of NDWI value while NDVI levels were limited (see Chapter 5, Figure 5.1). This could be due to the increasing frequency of local rainfall storms in Q'a Shubayqa due to climate change as Al-Bakri et al. (2013) found that precipitation in Azraq basin (where Q'a Shubayqa geographically belong) tends to increase with 10% by 2050 under climate change impact (see Chapter 3, table 3.1). This increase of rainfall would, however, have insignificant impact on crop production in Q'a Shubayqa as the average seasonal precipitation is below 100 mm.

There remain some uncertainties around the climate changes trends and observed data used in the thesis due the often-spotty spatial characteristics of dryland climate, particularly with regard to rainfall (see Chapter 2, section 2.2.2 e.g. (Davies et al., 2016)). Q'a Shubayqa does not have its own meteorological station so the observed weather data were taken from Safawi and Ein-Al-arab meteorological stations, which are about 26 km and 51 km away from Q'a Shubayqa respectively (see Chapter 4, section 4.2.1).

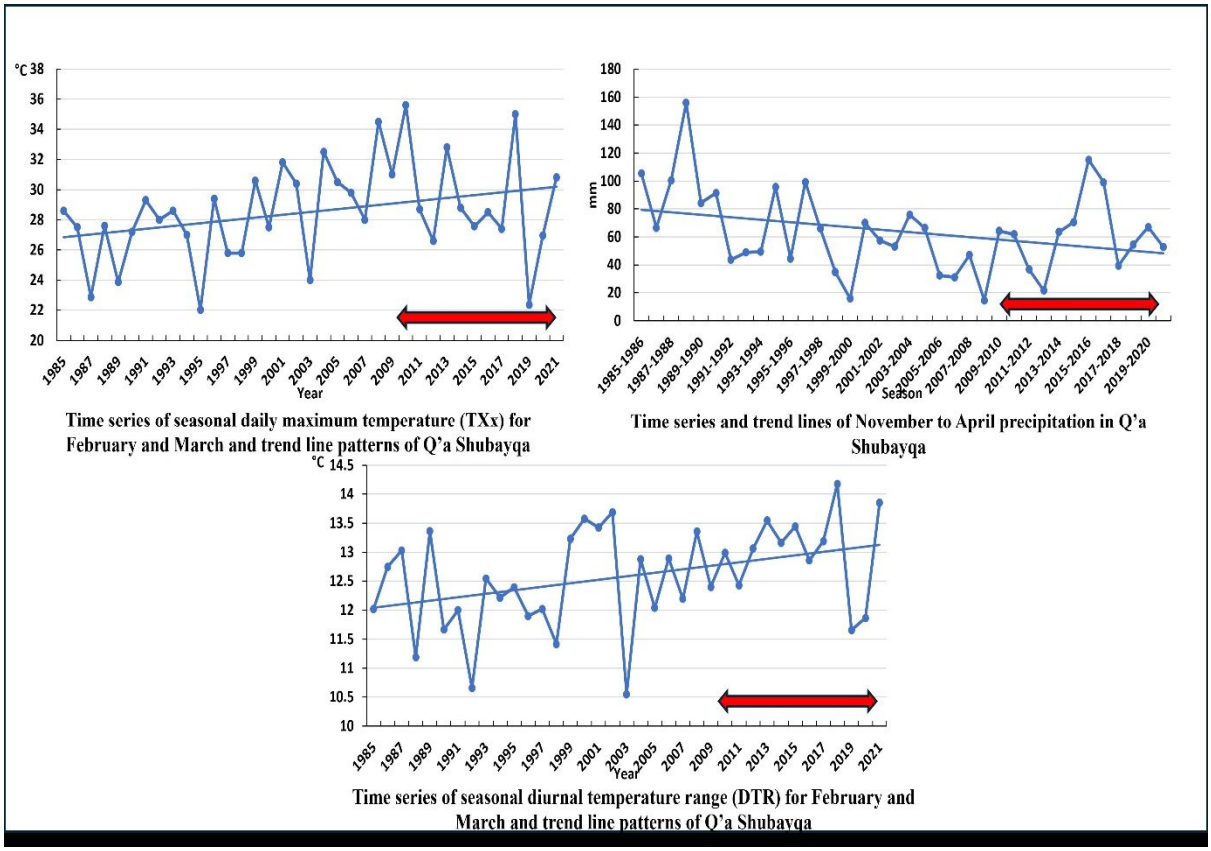

Figure 9.1: Climate variable patterns in Q'a Shubayqa between 1985-2021

Given climate change is occurring in the region and further future changes are likely to impact the Q'a Shubayqa agricultural system, models allow a representation of the system to quantify how future climate scenarios will impact crop yields. Here we review the robustness of the modelling work undertaken in the thesis.

Following to the demonstrated crucial role of seasonal Jabal druz floods in maintaining the agricultural system sustainability (see Chapter 5, section 5.4.1), the modelling of the hydrological system of the ungauged Shubayqa watershed was undertaken using a SWAT

model (see Chapter 6, section 4) to understand seasonal floods alterations in terms of timing and quantity. As discuused in Chapter 6 (section 6.2.2), SWAT has been shown to be a robust tool for watershed hydrological modelling that could be efficiently employed under several inconvenient condition such as data scarcity, trans-boundary watersheds and dryland watersheds (Dile & Srinivasan, 2014; Jajarmizadeh et al., 2017; Tobin & Bennett, 2017; Y. Wu et al., 2016). The first challenge of this process for Shubayqa was related to the absence of observed discharge data within the study watershed that would allow the direct calibration and validation of the model. The second challenge was in selecting the suitable remote sensing AET product used as an alternative to allow model calibration.

In this study, modelling limitations were detected at spatial levels when SWAT failed in estimating streamflow for particular sub-basins within Shubayqa watershed due to the scarcity or low resolution of some input data (see Chapter 6, section 6.5). Generally, analyses have shown that SWAT performed well in simulating hydrological cycle of the overall studied Q'a Shubayqa watershed when tested against remote sensing AET data for calibration and validation processes, confirming that SWAT modelling output are reliable. Similar findings were found in previous studies (Herman et al., 2018; Kunnath-Poovakka et al., 2016; Odusanya et al., 2018 and Wu et al., 2016) that were undertaken in drylands using different types of remote sensing data such as AET data and soil moisture for calibration and validation and demonstrated that SWAT performed well under these conditions.

Prior to moving to the most important step of the research related to simulating crop development and grain yield under historical and future changing climate in Q'a Shubayqa using the results from previous qualitative and quantitative analyses within DSSAT model, it was crucial (Hoogenboom, Jones, Traore, et al., 2012; L. A. Hunt & Boote, 1998) and challenging to estimate traits and characteristics of the cultivated cereal genotypes cultivated in Q'a Shubayqa. The approach adopted for the estimation of transferrable stable genetic coefficients of the cultivated varieties in Q'a Shubayqa was based on previous published research (see Chapter 7, section 7.5.2) but the details of the approach differ from one study region to another and according to users. In this study, observed field experiment phenology and grain yield data were collected from multiple areas across Jordan with different environments and different seasons, that did not include observed data from Q'a Shubayqa. According to the reviewed literature, this is the first attempt that uses observed data from field experiments undertaken in different experimental sites across Jordan and during different

seasons (see Chapter 7, Table 7.1) to estimate a generic set of genetic coefficients for the different grain types. To achieve this both genetic coefficients estimating tools provided by DSSAT (GENCALC and GLUE) were tested to see which one (or both) was able to simulate reliable genetic coefficients from this estimation approach (see Chapter 7, section 7.5.3.3). The strength of this approach is that the genetic coefficients were tested for and from a variety of environmental settings and produced modelled yield estimates (Chapter 7) that were sensible for, the independent, study site (as described in Chapter 3).

To fulfil the overall objective of the thesis, the impact of changing climate on first seasonal flood timing and in consequences on planting date was assessed by undertaking historical simulations of grain yield and grain filling period of the studied wheat and barley cultivars under potential different planting dates (see Chapter 8, section 8.4.1). The results showed that a delayed planting date seems to be advantageous on wheat grain yield and disadvantageous on barley in Q'a Shubayqa. This finding proves the ability of DSSAT in modelling the potential impact of one of the major consequences of climate change. Several previous studies (Ahmad et al., 2016; Ech-chatir et al., 2025) have shown similar results regarding DSSAT model effectiveness when applied as a decision-making tool for sowing date management of cereals considering climate change situation under arid environments.

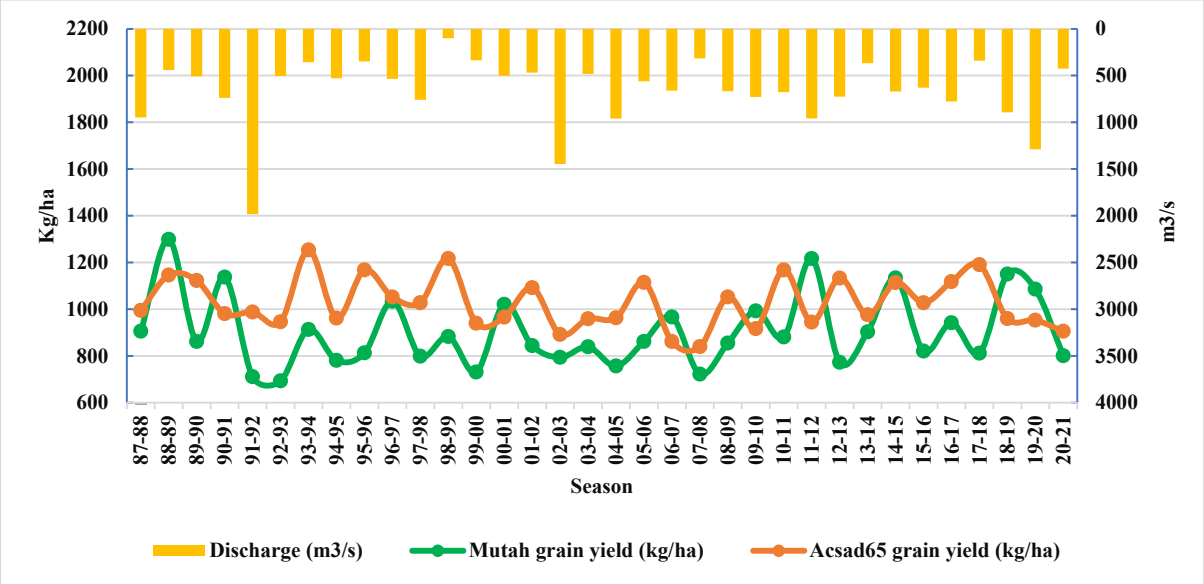

Figure 9.2: Time series representing the seasonal interaction between simulated flood discharge (from SWAT) and both wheat and barley yields for the period between 1987-2021

Grain yield of wheat and barley response to floods patterns, usually increase or decrease with floods discharge alteration based on the availability of water needed for plant growth and

productivity. The simulated grain yields during several seasons (e.g. 1991-92, 1987-88, 1998-99, 2002-03 and 2019-20; Figure 9.2) were not consistent with modelled floods discharge quantity. This is mainly related to several factors related to climate change in addition to the planting date variation that was detected by DSSAT model such as increased temperature (heat waves), waterlogging phenomena due to flash-floods, timing of floods after sowing and local precipitation. It is also noticed that the response of the two cultivated species (wheat and barley) to these climate change factors are different due to species type and the cultivar traits. The conclusion here is that DSSAT was able to detect climate change factors impact on crop growth and yield, however field experiments are still needed to determine which of these factors have the major negative impact on the agricultural system productivity.

Under modelled future climate scenarios (RCP4.5 and RCP8.5) rainfall is lower than 21st century observed rainfall, with SWAT models driven by GCM output therefore showing a resulting decrease in floods waters that reach Q'a Shubayqa. Simulated grain yields of the studied wheat and barley cultivars (except of Rum) show lower yields with this lower rainfall future and then recover through the century as climate change intensifies, because of the higher CO_2 concentrations of both scenarios (Chapter 8, section 8.4.3). Additionally, the impact of future climate change scenarios on phenology, which is more temperature related, of tested cultivars was not significant for most of them when comparing with an observed 21st Centuary baseline, except for the Acsad65 cultivar.

For this study, the uncertainty of these future climate data derived via MarkSIM was shown when comparing the current observed climate data from Q'a Shubayqa and Jabal Druz with the simulated data from the GCMs (Chapter 8, section 8.3) where correlation between compared monthly precipitation varies between acceptable and low, however correlation between compared daily average temperature was strong. This shows the ability of these GCMs in projecting appropriate temperature data better than precipitation in such drylands. Based on that, comparisons between simulated future grain yield, derived from MarkSIM data, and baseline grain yields, derived from observed data have shown a large gap.

The simulation of wheat and barley grain yield under studied RCPs scenarios and using generated climate data from MarkSIM, including alternative agricultural practices such as very delayed planting date and organic matter addition have shown that only increased organic matter can enhance grain yields under higher CO_2 concentration. In this context, several

alternative sustainable agricultural practices that may reduce the climate change impact on crops could be tested such as high temperature and drought tolerant wheat and barley cultivars and legume-based rotations. DSSAT seems to be the appropriate tool for such analyses as it has been widely employed to assess alternative sustainable agricultural practices on different crop types under changing climate conditions (Jiang et al., 2021; Lv et al., 2015; Pourebrahimi Foumani et al., n.d.; Smith et al., 2020).

- **Summary**

It can be said that the work undertaken through the chapters of this thesis fulfils, at least to a substantial degree, the objectives underlined at the start of the thesis (see Chapter 1, section 1.2). Despite the circumstances under which the survey was undertaken and the small sample of surveyed farmers, the good management of the obtained information and soil samples allowed the main characteristics of the farming system in Q'a Shubayqa to be explored and to define its main components and the most decisive limiting factors (see Chapter 3). Recent climate alterations and its impact on crop development and growth were then investigated by creating time series of the climate variable and the relevant extreme indices with remote sensing spectral indices that describe the crops situation through the time. Despite the low quality of used remote sensing data and the gaps in the observed data, the results were sufficient to prove farmers claim about the main source of water for Q'a Shubayqa crops and the fact of the changing climate in the area (see Chapter 4 and Chapter 5). The sixth chapter was dedicated to understanding the specificities of the relevant hydrological system and to quantify floods water that reaches Q'a Shubayqa. SWAT modelling linked to GIS have shown a rigorous performance in representing the studied watershed characteristics, capturing spatial variability and estimating seasonal flood patterns although the issue related to data resolution especially from Syria. The work undertaken in chapter 7 by employing DSSAT and its tools was the most important piece of the puzzle when transferrable stable genetic coefficients that represent the traits and characteristics of studied wheat and barley cultivars were developed based on a complicated approach and using limited data. This is a substantial finding of this thesis. The overall aim of the thesis was presented by the work conducted in Chapter 8 where collected information about Q'a Shubayqa agricultural system and findings from the previous chapters were gathered within DSSAT to simulate the impact of the past, current and future climate change factors on cultivated crops. Findings show that any likely increased future temperature

and/or reduced precipitation regimes are likely to be mitigated for, in terms of impact on wheat and barley yields, by increasing CO_2 in the atmosphere.

The multidisciplinary research conducted in this thesis included a thorough investigation of the agricultural system in the dryland in Q'a Shubayqa. However, additional research could be undertaken to provide further important information that would help decision makers and relevant research community to prevent the degradation of this systems resources under the future climate change and to help local farmers with mitigation strategies to remain their farming system productivity and sustainability. For example, running DSSAT using MarkSim_GCM for the period overlapping with the instrumental data to allow quantify the impact of climate model on grain yield changes. This could be done based on the key findings of this thesis.

References

Ababsa, M. (2013). Agrarian crisis, property crisis and drought in Syria (2000-2011). *Maghreb-Machrek*, *215*(1), 101–122.

Abandah, A. (1978). *long-range for casting seasonal rainfall in Jordan. Department of Metrology, Publication No*. JNWS/78/11 17 p.

Abatzoglou, J. T., Dobrowski, S. Z., Parks, S. A., & Hegewisch, K. C. (2018). TerraClimate, a high-resolution global dataset of monthly climate and climatic water balance from 1958–2015. *Scientific Data*, *5*(1), 170191. https://doi.org/10.1038/sdata.2017.191

Abbaspour, K.C. (2015). *SWAT calibration and uncertainty programs-a user manual.* Eawag (Swiss Federal Institute of Aquatic Science and Technology).

Abbaspour, K C, Johnson, C. A., & van Genuchten, M. T. (2004). Estimating Uncertain Flow and Transport Parameters Using a Sequential Uncertainty Fitting Procedure. *Vadose Zone Journal*, *3*(4), 1340–1352. https://doi.org/10.2113/3.4.1340

Abbaspour, Karim C, Faramarzi, M., Ghasemi, S. S., & Yang, H. (2009). Assessing the impact of climate change on water resources in Iran. *Water Resources Research*, *45*(10).

Abbaspour, Karim C, Vejdani, M., & Haghighat, S. (2007). *SWAT-CUP calibration and uncertainty programs for SWAT* (eds L. Oxley and D. Kulasiri (Ed.); pp. 1603–1609). Modelling and Simulation Society of Australia and New Zealand.

Abdulla, F., & Al-Badranih, L. (2000). Application of a rainfall-runoff model to three catchments in Iraq. *Hydrological Sciences Journal*, *45*(1), 13–25.

Abdulla, F., & Al-Shurafat, A. W. (2020). Rainfall-Runoff modeling for Semi-arid and trans-boundary Yarmouk River Basin. *Procedia Manufacturing*, *44*, 180–188.

Abera, E. (2019). Calibration and validation of CERES-wheat in DSSAT model for yield simulation under future climate in Adet, North Western Ethiopia. *African Journal of Agricultural Research*, *14*, 509–518. https://doi.org/10.5897/AJAR2018.13801

Abuhalaweh, N. (2017). *Student Independent Projects Environmental Studies 2017: Water scarcity in Jordan: Sustainability issues and information drought*.

Acharya, T. D., Subedi, A., & Lee, D. H. (2018). Evaluation of water indices for surface water extraction in a Landsat 8 scene of Nepal. *Sensors*, *18*(8), 2580.

Ahmad, S., Hussain, S., Fatima Ph.D, Z., Abbas, G., Rehman, A., Khan, M., Younis, H., Naz, S., Muhammad, S., Ajmal, M., Abbas, N., Akhtar, M., Rauf, A., Khan, M., Ali, Z., Hassan, M., Rizwan, M., Bajwa, R., Ajmal, A., & Hasanuzzaman, M. (2016). Application of DSSAT model for sowing date management of C4 summer cereals for fodder and grain crops under irrigated arid environment. *Pakistan Journal of Life and Social Sciences*, *14*, 104–114.

Ahmed, M. (2020). Introduction to Modern Climate Change. Andrew E. Dessler: Cambridge University Press, 2011, 252 pp, ISBN-10: 0521173159. *Science of The Total Environment*, *734*, 139397. https://doi.org/https://doi.org/10.1016/j.scitotenv.2020.139397

Ahmed, M., Hayat, R., Ahmad, M., Kheir, A., Shaheen, F. A., Raza, M. A., & Ahmad, S. (2022). Impact of Climate Change on Dryland Agricultural Systems: A Review of Current Status, Potentials, and Further Work Need. *International Journal of Plant Production*, 1–23.

Akça, M. O., Ay, A., Demirkaya, S., Dengiz, O., Karapıçak, B., Karataş, A., Namlı, A., Pacci, S., Saygın, F., Yazıcı, K., Şavşatlı, Y., & Şenol, N. D. (2023). Soil quality assessment based on hybrid computational approach with spatial multi-criteria analysis and geographical information system for sustainable tea cultivation. *The Journal of Agricultural Science*, *161*(2), 187–204. https://doi.org/DOI: 10.1017/S0021859623000138

Akter, N., & Rafiqul Islam, M. (2017). Heat stress effects and management in wheat. A review. *Agronomy for Sustainable Development*, *37*(5), 37. https://doi.org/10.1007/s13593-017-0443-9

Al-Addous, M., Bdour, M., Alnaief, M., Rabaiah, S., & Schweimanns, N. (2023). Water Resources in Jordan: A Review of Current Challenges and Future Opportunities. *Water*, *15*(21). https://doi.org/10.3390/w15213729

Al-Ajlouni, Z. I., Al-Abdallat, A. M., Al-Ghzawi, A. L. A., Ayad, J. Y., Abu Elenein, J. M., Al-Quraan, N. A., & Baenziger, P. S. (2016). Impact of Pre-Anthesis Water Deficit on Yield and Yield Components in Barley (Hordeum vulgare L.) Plants Grown under Controlled Conditions. *Agronomy*, *6*(2). https://doi.org/10.3390/agronomy6020033

Al-Ansari, N., Alibrahiem, N., Alsaman, M., & Knutsson, S. (2014). Water Demand

Management in Jordan. *Engineering*, *06*, 19–26. https://doi.org/10.4236/eng.2014.61004

Al-Bakri, J., Suleiman, A., Abdulla, F., & Ayad, J. (2011). Potential impact of climate change on rainfed agriculture of a semi-arid basin in Jordan. *Physics and Chemistry of the Earth, Parts A/B/C*, *36*(5), 125–134. https://doi.org/https://doi.org/10.1016/j.pce.2010.06.001

Al-Bakri, J. T., Salahat, M., Suleiman, A., Suifan, M., Hamdan, M. R., Khresat, S., & Kandakji, T. (2013). Impact of climate and land use changes on water and food security in jordan: Implications for transcending "the tragedy of the commons." *Sustainability*, *5*(2), 724–748.

Al-Eisawi, D. M. H. (2005). Water scarcity in relation to food security and sustainable use of biodiversity in Jordan. *Food Security under Water Scarcity in the Middle East: Problems and Solutions. CIHEAM Options Méditerranéennes: Série A. Séminaires Méditerranéens*, *65*, 239–248.

Al-Naber, M. (2016). Jordan–Azraq Basin case study. *IWMI Project Report No*.

Al-Tabini, R., Al-Khalidi, K., & Al-Shudiefat, M. (2012). Livestock, medicinal plants and rangeland viability in Jordan's Badia: through the lens of traditional and local knowledge. *Pastoralism: Research, Policy and Practice*, *2*(1), 4. https://doi.org/10.1186/2041-7136-2-4

Al Naber, M., & Molle, F. (2017). Water and sand: is groundwater-based farming in Jordan's desert sustainable? *Groundwater for Sustainable Development*, *5*, 28–37.

Ali, M. G. M., Ibrahim, M. M., El Baroudy, A., Fullen, M., Omar, E.-S. H., Ding, Z., & Kheir, A. M. S. (2020). Climate change impact and adaptation on wheat yield, water use and water use efficiency at North Nile Delta. *Frontiers of Earth Science*, *14*(3), 522–536. https://doi.org/10.1007/s11707-019-0806-4

Allison, F. E. (1973). *Soil organic matter and its role in crop production*. Elsevier.

Allouzi, S.; Al-Karadsheh, I.; Al-Hoyan, M.; Rawashdeh, I.; Al-Kaabenah, A. (2010). *Phenotypic Variation and Genetic Variation of Certified Wheat Varieties in Jordan*.

Alpert, P., Ben-Gai, T., Baharad, A., Benjamini, Y., Yekutieli, D., Colacino, M., Diodato, L., Ramis, C., Homar, V., & Romero, R. (2002). The paradoxical increase of Mediterranean extreme daily rainfall in spite of decrease in total values. *Geophysical Research Letters*,

29(11), 31.

Alqadi, M., Al Dwairi, A., Dehnavi, S., Margane, A., Raggad, M., Wreikat, M., & Chiogna, G. (2021). A Novel Method to Assess the Impact of a Government's Water Strategy on Research: A Case Study of Azraq Basin, Jordan. *Water*, *13*, 2138. https://doi.org/10.3390/w13152138

Alraggad, M., & Jasem, H. (2010). Managed aquifer recharge (MAR) through surface infiltration in the Azraq basin/Jordan. *Journal of Water Resource and Protection*, *2*(12), 1057.

Andrews, I. J. (1995). *The birds of the Hashemite Kingdom of Jordan*. IJ Andrews Midlothian.

Arnold, J G, Srinivasan, R., Muttiah, R. S., & Williams, J. R. (1998). LARGE AREA HYDROLOGIC MODELING AND ASSESSMENT PART I: MODEL DEVELOPMENT1. *JAWRA Journal of the American Water Resources Association*, *34*(1), 73–89. https://doi.org/https://doi.org/10.1111/j.1752-1688.1998.tb05961.x

Arnold, Jeffrey G, & Fohrer, N. (2005). SWAT2000: current capabilities and research opportunities in applied watershed modelling. *Hydrological Processes: An International Journal*, *19*(3), 563–572.

Arnold, Jeffrey G, Moriasi, D. N., Gassman, P. W., Abbaspour, K. C., White, M. J., Srinivasan, R., Santhi, C., Harmel, R. D., Van Griensven, A., & Van Liew, M. W. (2012). SWAT: Model use, calibration, and validation. *Transactions of the ASABE*, *55*(4), 1491–1508.

Arora, V. K., Singh, H., & Singh, B. (2007). Analyzing wheat productivity responses to climatic, irrigation and fertilizer-nitrogen regimes in a semi-arid sub-tropical environment using the CERES-Wheat model. *Agricultural Water Management*, *94*(1), 22–30. https://doi.org/https://doi.org/10.1016/j.agwat.2007.07.002

Arranz-Otaegui, A., Gonzalez Carretero, L., Ramsey, M. N., Fuller, D. Q., & Richter, T. (2018). Archaeobotanical evidence reveals the origins of bread 14,400 years ago in northeastern Jordan. *Proceedings of the National Academy of Sciences*, *115*(31), 7925–7930. https://doi.org/10.1073/pnas.1801071115

Asrar, G. Q., Fuchs, M., Kanemasu, E. T., & Hatfield, J. L. (1984). Estimating absorbed photosynthetic radiation and leaf area index from spectral reflectance in wheat 1. *Agronomy Journal*, *76*(2), 300–306.

Asseng, S., Martre, P., Maiorano, A., Rötter, R. P., O'Leary, G. J., Fitzgerald, G. J., Girousse, C., Motzo, R., Giunta, F., & Babar, M. A. (2019). Climate change impact and adaptation for wheat protein. *Global Change Biology*, *25*(1), 155–173.

Bajjali, W. (2006). Recharge mechanism and hydrochemistry evaluation of groundwater in the Nuaimeh area, Jordan, using environmental isotope techniques. *Hydrogeology Journal*, *14*(1), 180–191.

Balting, D. F., AghaKouchak, A., Lohmann, G., & Ionita, M. (2021). Northern Hemisphere drought risk in a warming climate. *Npj Climate and Atmospheric Science*, *4*(1), 61. https://doi.org/10.1038/s41612-021-00218-2

Bany Yaseen, I. (2016). *Mineralogy, petrology and Geochemistry of the Basalt flows at Ash-Shun Ash-Shamaliyya Area, North West Jordan*. *5*.

Bärlund, I., Kirkkala, T., Malve, O., & Kämäri, J. (2007). Assessing SWAT model performance in the evaluation of management actions for the implementation of the Water Framework Directive in a Finnish catchment. *Environmental Modelling & Software*, *22*, 719–724. https://doi.org/10.1016/j.envsoft.2005.12.030

Barton, R. (2013). *Know Your Garden Soil: How to Make the Most of Your Soil Type.*

Bashour, I., Al-Ouda, A., Kassam, A., Bachour, R., Jouni, K., Hansmann, B., & Estephan, C. (2016). An overview of Conservation Agriculture in the dry Mediterranean environments with a special focus on Syria and Lebanon. *AIMS Agriculture and Food*, *1*(1), 67–84.

Berry, W., Ketterings, Q., Antes, S., Page, S., Russell-Anelli, J., Rao, R., DeGloria, S. (2007). *Soil Texture*.

Bertin, N., Martre, P., Génard, M., Quilot, B., & Salon, C. (2010). Under what circumstances can process-based simulation models link genotype to phenotype for complex traits? Case-study of fruit and grain quality traits. *Journal of Experimental Botany*, *61*(4), 955–967. https://doi.org/10.1093/jxb/erp377

Black, H. I. J., & Okwakol, M. J. N. (1997). Agricultural intensification, soil biodiversity and agroecosystem function in the tropics: the role of termites. *Applied Soil Ecology*, *6*(1), 37–53.

Bocianowski, J., Niemann, J., & Nowosad, K. (2019). Genotype-by-environment interaction

for seed quality traits in interspecific cross-derived Brassica lines using additive main effects and multiplicative interaction model. *Euphytica*, *215*(1), 1–13.

Boote, K J. (1999). Concepts for calibrating crop growth models. *DSSAT Version*, *3*, 179–199.

Boote, K J, Jones, J. W., & Pickering, N. B. (1996). Potential uses and limitations of crop models. *Agronomy Journal*, *88*(5), 704–716.

Boote, K J, Kropff, M. J., & Bindraban, P. S. (2001). Physiology and modelling of traits in crop plants: implications for genetic improvement. *Agricultural Systems*, *70*(2–3), 395–420.

Boote, Kenneth J, Jones, J. W., & Hoogenboom, G. (2018). Simulation of crop growth: CROPGRO model. In *Agricultural systems modeling and simulation* (pp. 651–692). CRC Press.

Boote, Kenneth J, Porter, C., Jones, J. W., Thorburn, P. J., Kersebaum, K. C., Hoogenboom, G., White, J. W., & Hatfield, J. L. (2016). Sentinel site data for crop model improvement—definition and characterization. *Improving Modeling Tools to Assess Climate Change Effects on Crop Response*, *7*, 125–158.

Borana, s. L., & Yadav, s. K. (2018). *NDVI-based vegetation changes and Seasonal variation In Semi Arid region*.

Brooks, K. N., Ffolliott, P. F., & Magner, J. A. (2012). *Hydrology and the Management of Watersheds*. John Wiley & Sons.

Brown, L. R. (2008). *Plan B 3.0: Mobilizing to save civilization (substantially revised)*. WW Norton & Company.

Buddhaboon, C., Jintrawet, A., & Hoogenboom, G. (2018). Methodology to estimate rice genetic coefficients for the CSM-CERES-Rice model using GENCALC and GLUE genetic coefficient estimators. *The Journal of Agricultural Science*, *156*(4), 482–492. https://doi.org/10.1017/S0021859618000527

Bullard, J. E. (2005). Arid geomorphology. *Progress in Physical Geography: Earth and Environment*, *29*(1), 93–103. https://doi.org/10.1191/0309133305pp436pr

Cammarano, D., Payero, J., Basso, B., Stefanova, L., & Grace, P. (2012). Adapting wheat sowing dates to projected climate change in the Australian subtropics: analysis of crop

water use and yield. *Crop and Pasture Science*, *63*(10), 974–986. https://doi.org/10.1071/CP11324

Cattaneo, F., Di Gennaro, P., Barbanti, L., Giovannini, C., Labra, M., Moreno, B., Benitez, E., & Marzadori, C. (2014). Perennial energy cropping systems affect soil enzyme activities and bacterial community structure in a South European agricultural area. *Applied Soil Ecology*, *84*, 213–222.

Ceccato, P., Flasse, S., Tarantola, S., Jacquemoud, S., & Grégoire, J.-M. (2001). Detecting vegetation leaf water content using reflectance in the optical domain. *Remote Sensing of Environment*, *77*(1), 22–33.

Chakrabarti, B., Singh, S., Kumar, V., Harit, R., & Misra, S. (2013). Growth and yield response of wheat and chickpea crops under high temperature. *Indian Journal of Plant Physiology*, *18*. https://doi.org/10.1007/s40502-013-0002-6

Chantal Demilecamps; Wael Sartawi. (2010). *Farming In The Desert: Analysis of the agricultural situation in Azraq Basin*.

Chartzoulakis, K. S. (2005). Salinity and olive: Growth, salt tolerance, photosynthesis and yield. *Agricultural Water Management*, *78*(1), 108–121. https://doi.org/https://doi.org/10.1016/j.agwat.2005.04.025

Chen, Y., Deng, H., Li, B., Li, Z., & Xu, C. (2014). Abrupt change of temperature and precipitation extremes in the arid region of Northwest China. *Quaternary International*, *336*, 35–43.

Chytrý, M., Danihelka, J., Ermakov, N., Hájek, M., Hájková, P., Kočí, M., Kubešová, S., Lustyk, P., Otýpková, Z., & Popov, D. (2007). Plant species richness in continental southern Siberia: effects of pH and climate in the context of the species pool hypothesis. *Global Ecology and Biogeography*, *16*(5), 668–678.

Collier, M. A., Jeffrey, S. J., Rotstayn, L. D., Wong, K. K., Dravitzki, S. M., Moseneder, C., Hamalainen, C., Syktus, J. I., Suppiah, R., & Antony, J. (2011). The CSIRO-Mk3. 6.0 Atmosphere-Ocean GCM: participation in CMIP5 and data publication. *International Congress on Modelling and Simulation–MODSIM*, 2691–2697.

Collins, W. J., Bellouin, N., Doutriaux-Boucher, M., Gedney, N., Halloran, P., Hinton, T., Hughes, J., Jones, C. D., Joshi, M., Liddicoat, S., Martin, G., O'Connor, F., Rae, J., Senior,

C., Sitch, S., Totterdell, I., Wiltshire, A., & Woodward, S. (2011). Development and evaluation of an Earth-System model – HadGEM2. *Geoscientific Model Development*, *4*(4), 1051–1075. https://doi.org/10.5194/gmd-4-1051-2011

Conant, R. T., Paustian, K., & Elliott, E. T. (2001). Grassland management and conversion into grassland: effects on soil carbon. *Ecological Applications*, *11*(2), 343–355.

Contractor, S., Donat, M. G., & Alexander, L. V. (2021). Changes in observed daily precipitation over global land areas since 1950. *Journal of Climate*, *34*(1), 3–19.

Cotter, M., Asch, F., Abera, B. B., Andre Chuma, B., Senthilkumar, K., Rajaona, A., Razafindrazaka, A., Saito, K., & Stuerz, S. (2020). Creating the data basis to adapt agricultural decision support tools to new environments, land management and climate change—A case study of the RiceAdvice App. *Journal of Agronomy and Crop Science*, *206*(4), 423–432.

Courcier, R., Venot, J.-P., Molle, F., Suleiman, L., & Jridi, A. (2005). *Historical Transformations of the LowerJordan River Basin (in Jordan): Changes inWater Use and Projections (1950–2025)*. International Water Management Institute (IWMI).

CPFR. (1991). *Food from Dryland Gardens - An Ecological, Nutritional, and Social Approach to Small Scale Household Food Production*.

Cudennec, C., Leduc, C., & Koutsoyiannis, D. (2007). Dryland hydrology in Mediterranean regions—a review. *Hydrological Sciences Journal/Journal Des Sciences Hydrologiques*, *52*(6), 1077–1087.

Dahdouh, Y., & Lahbassi, O. (2018). Assessment of two loss methods for estimation of surface runoff in Zaafrania urban catchment, North-East of Algeria. *Journal of Water and Land Development*, *36*, 37–43. https://doi.org/10.2478/jwld-2018-0004

Dangol, S., Zhang, X., Liang, X.-Z., Anderson, M., Crow, W., Lee, S., Moglen, G. E., & McCarty, G. W. (2023). Multivariate Calibration of the SWAT Model Using Remotely Sensed Datasets. *Remote Sensing*, *15*(9). https://doi.org/10.3390/rs15092417

Davies, J., Barchiesi, S., Ogali, C. J., Welling, R., Dalton, J., & Laban, P. (2016). Water in drylands: Adapting to scarcity through integrated management. *IUCN: Gland, Switzerland*.

Dean, W. E. (1974). Determination of carbonate and organic matter in calcareous sediments and sedimentary rocks by loss on ignition; comparison with other methods. *Journal of Sedimentary Research*, *44*, 242–248.

Defoer, T., Budelman, A., Toulmin, C., & Carter, S. E. (2000). *Managing soil fertility in the tropics. Building common knowledge: participatory learning and action research.* Royal Tropical Institute, KIT Press.

DeFries, R. S., Townshend, J. R. G., & Hansen, M. C. (1999). Continuous fields of vegetation characteristics at the global scale at 1-km resolution. *Journal of Geophysical Research: Atmospheres*, *104*(D14), 16911–16923.

Demattê, J. A. M., Dotto, A. C., Bedin, L. G., Sayão, V. M., & e Souza, A. B. (2019). Soil analytical quality control by traditional and spectroscopy techniques: Constructing the future of a hybrid laboratory for low environmental impact. *Geoderma*, *337*, 111–121. https://doi.org/https://doi.org/10.1016/j.geoderma.2018.09.010

Demek, J., & Mapping, I. G. U. C. on G. S. and. (1972). Manual of detailed geomorphological mapping. In *TA - TT -*. Academia. https://doi.org/LK - https://worldcat.org/title/659319

Dile, Y. T., & Srinivasan, R. (2014). Evaluation of CFSR climate data for hydrologic prediction in data-scarce watersheds: an application in the Blue Nile River Basin. *JAWRA Journal of the American Water Resources Association*, *50*(5), 1226–1241. https://doi.org/https://doi.org/10.1111/jawr.12182

Dinar, A., Tieu, A., & Huynh, H. (2019). Water scarcity impacts on global food production. *Global Food Security*, *23*, 212–226. https://doi.org/https://doi.org/10.1016/j.gfs.2019.07.007

Dinpashoh, Y., Mirabbasi, R., Jhajharia, D., Abianeh, H. Z., & Mostafaeipour, A. (2014). Effect of short-term and long-term persistence on identification of temporal trends. *Journal of Hydrologic Engineering*, *19*(3), 617–625.

Dixit, P. N., & Telleria, R. (2015). Advancing the climate data driven crop-modeling studies in the dry areas of Northern Syria and Lebanon: An important first step for assessing impact of future climate. *The Science of the Total Environment*, *511*, 562–575.

Dixit, P. N., Telleria, R., Al Khatib, A. N., & Allouzi, S. F. (2018). Decadal analysis of impact of future climate on wheat production in dry Mediterranean environment: A case of

Jordan. *Science of The Total Environment*, *610–611*, 219–233. https://doi.org/https://doi.org/10.1016/j.scitotenv.2017.07.270

Djanaguiraman, M., Narayanan, S., Erdayani, E., & Prasad, P. V. V. (2020). Effects of high temperature stress during anthesis and grain filling periods on photosynthesis, lipids and grain yield in wheat. *BMC Plant Biology*, *20*(1), 268. https://doi.org/10.1186/s12870-020-02479-0

Dregne, H. E. (1976). Desertification: Symptom of a crisis. *Desertification: Process, Problems, Perspectives, Arid/Semi-Arid Natural Resources Program Seminar Papers, University of Arizona p 12-24, Sept. 1976. 6 Fig.*

Dregne, H. E. (2002). Land degradation in the drylands. *Arid Land Research and Management*, *16*(2), 99–132.

Drury, C. F., McKenney, D. J., Findlay, W. I., & Gaynor, J. D. (1993). Influence of tillage on nitrate loss in surface runoff and tile drainage. *Soil Science Society of America Journal*, *57*(3), 797–802.

DSJ. (2022). *Statistical year book*. file:///C:/Users/lgxab7/Downloads/PopulationEstimates.pdf

Du, X., Gao, Z., Sun, X., Bian, D., Ren, J., Yan, P., & Cui, Y. (2022). Increasing temperature during early spring increases winter wheat grain yield by advancing phenology and mitigating leaf senescence. *Science of The Total Environment*, *812*, 152557. https://doi.org/https://doi.org/10.1016/j.scitotenv.2021.152557

Easterling, W. E. (2011). *Guidelines for adapting agriculture to climate change*. Imperial College Press.

Ech-chatir, L., Er-Raki, S., Rodriguez, J. C., Meddich, A., & Chehbouni, A. (2025). Optimizing sowing date, fertilization, and irrigation strategies for winter wheat in Tensift Al Haouz (Morocco) using the DSSAT-CERES-wheat model. *Agricultural Water Management*, *312*, 109443. https://doi.org/https://doi.org/10.1016/j.agwat.2025.109443

Ehret, U., Gupta, H. V., Sivapalan, M., Weijs, S. V, Schymanski, S. J., Blöschl, G., Gelfan, A. N., Harman, C., Kleidon, A., & Bogaard, T. A. (2014). Advancing catchment hydrology to deal with predictions under change. *Hydrology and Earth System Sciences*, *18*(2), 649–671.

El-Naqa, A., Al-Momani, M., Kilani, S., & Hammouri, N. (2007). Groundwater deterioration of shallow groundwater aquifers due to overexploitation in northeast Jordan. *CLEAN–Soil, Air, Water*, *35*(2), 156–166.

Fahad, M., Ahmad, I., & Athar, H. (2020). Implications of 1.5 and 2.0 ºC additional warming for wheat yield using a gridded modeling approach. *Atmósfera*, *33*(4), 337–355.

FAO. (1993). *The State of Food and Agriculture. Food and Agriculture Organization of the United Nations.* https://www.fao.org/publications/card/en/c/V1790-I-EN/

FAO. (2000). *Land resource potential and constraints at regional and country levels. World Soil Resources Report No. 90.*

FAO. (2004). *Water and cereals in drylands*.

FAO. (2006). *World agriculture: towards 2030/2050. Interim Report. Global Perspective Studies Unit*.

FAO. (2011). *Organic Agriculture and Climate Change Mitigation: A Report of the Round Table on Organic Agriculture and Climate Change.*

FAO. (2013). *Smallholders and Family Farmers*. https://www.fao.org/docrep/018/ar588e/ar588e.pdf

FAO. (2018). *Assessment of Food Supply under Water Scarcity Conditions in the NENA Region Applying the Food Supply Cost Curve approach (FSCC). Jordan Case Study* (1st ed.). FAO. https://openknowledge.fao.org/handle/20.500.14283/ca1156en

FAOSTAT. (2012). *Crop production statistics*. www.%0Afaostat.fao.org

Ffolliott, P., Dawson, J.O., Fisher, J.T., Moshe, I., Fulbright, T.E., Al Musa, A, Johnson, C. & Verburg, P. (2002). Dryland environments. *Ar. Land. News.*, 52.

Fischer, R. A., Byerlee, D., & Edmeades, G. (2014). Crop yields and global food security. *ACIAR: Canberra, ACT*, 8–11.

Fischer, T., Byerlee, D., & Edmeades, G. (2012). Crop yields and food security: will yield increases continue to feed the world. *Proceedings of the 12th Australian Agronomy Conference*, 14–18.

Foster, S., & Loucks, D. P. (n.d.). *Non-renewable groundwater resources: a guidebook on*

socially-sustainable management for water-policy makers. https://unesdoc.unesco.org/notice?id=p::usmarcdef_0000146997

Fraser, E. D. G., Simelton, E., Termansen, M., Gosling, S. N., & South, A. (2013). "Vulnerability hotspots": Integrating socio-economic and hydrological models to identify where cereal production may decline in the future due to climate change induced drought. *Agricultural and Forest Meteorology*, *170*, 195–205. https://doi.org/https://doi.org/10.1016/j.agrformet.2012.04.008

FRD. (2006). *Country profile*.

Freiwan, M., & Kadioglu, M. (2008). Spatial and temporal analysis of climatological data in Jordan. *International Journal of Climatology: A Journal of the Royal Meteorological Society*, *28*(4), 521–535.

Friedrich, T., Kassam, A., and Shaxson, F. (2008). *Case study, Conservation Agriculture*.

Furtak, K., & Wolińska, A. (2023). The impact of extreme weather events as a consequence of climate change on the soil moisture and on the quality of the soil environment and agriculture – A review. *CATENA*, *231*, 107378. https://doi.org/https://doi.org/10.1016/j.catena.2023.107378

G. Arnold, J., N. Moriasi, D., W. Gassman, P., C. Abbaspour, K., J. White, M., Srinivasan, R., Santhi, C., D. Harmel, R., van Griensven, A., W. Van Liew, M., Kannan, N., & K. Jha, M. (2012). SWAT: Model Use, Calibration, and Validation. *Transactions of the ASABE*, *55*(4), 1491–1508. https://doi.org/https://doi.org/10.13031/2013.42256

Gallagher, L., Hill, C., & Martin, A. (2013). *Valuing the biodiversity of dry and sub-humid lands/CBD Technical Series*.

Gan, T. Y., Dlamini, E. M., & Biftu, G. F. (1997). Effects of model complexity and structure, data quality, and objective functions on hydrologic modeling. *Journal of Hydrology*, *192*(1–4), 81–103.

Gardi, M. W., Memic, E., Zewdu, E., & Graeff-Hönninger, S. (2022). Simulating the effect of climate change on barley yield in Ethiopia with the DSSAT-CERES-Barley model. *Agronomy Journal*, *114*(2), 1128–1145. https://doi.org/https://doi.org/10.1002/agj2.21005

Getachew, F., Bayabil, H. K., Hoogenboom, G., Kiker, G. A., Yu, Z., & Li, Y. (2023). Development of climate-smart sorghum ideotype for climate resilience in Ethiopia. *Field Crops Research*, *303*, 109135. https://doi.org/https://doi.org/10.1016/j.fcr.2023.109135

Giller, K., Delaune, T., Silva, J., Descheemaeker, K., Ven, G. W. J., Schut, A. G. T., Van Wijk, M., Hammond, J., Hochman, Z., Taulya, G., Chikowo, R., Narayanan, S., Kishore, A., Bresciani, F., Teixeira, H., Andersson, J., & Ittersum, M. (2021). The future of farming: Who will produce our food? *Food Security*, *13*. https://doi.org/10.1007/s12571-021-01184-6

Githui, F., Gitau, W., Mutua, F., & Bauwens, W. (2009). Climate change impact on SWAT simulated streamflow in western Kenya. *International Journal of Climatology: A Journal of the Royal Meteorological Society*, *29*(12), 1823–1834.

Godwin, D. (1990). *A user's guide to CERES Wheat, V2. 10* (Vol. 2). International Fertilizer Development Center.

Goward, S. N., & Dye, D. G. (1987). Evaluating North American net primary productivity with satellite observations. *Advances in Space Research*, *7*(11), 165–174.

GTZ and MWI. (2004). *National Water Master Plan*.

Guangming, Z., Siyuan, Y., & Guangxue, L. (2007). Application of satellite remote sensing to wetland research [J]. *Mar. Geol. Lett*, *23*(12), 28–33.

Gunawat, A., Sharma, D., Sharma, A., & Dubey, S. (2022). Assessment of climate change impact and potential adaptation measures on wheat yield using the DSSAT model in the semi-arid environment. *Natural Hazards*, *111*. https://doi.org/10.1007/s11069-021-05130-9

Gupta, H. V., Sorooshian, S., & Yapo, P. O. (1999). Status of automatic calibration for hydrologic models: Comparison with multilevel expert calibration. *Journal of Hydrologic Engineering*, *4*(2), 135–143.

Ha, L. T., Bastiaanssen, W. G. M., van Griensven, A., van Dijk, A. I. J. M., & Senay, G. B. (2017). SWAT-CUP for Calibration of Spatially Distributed Hydrological Processes and Ecosystem Services in a Vietnamese River Basin Using Remote Sensing. *Hydrology and Earth System Sciences Discussions*, *2017*, 1–35. https://doi.org/10.5194/hess-2017-251

Haddaway, N. R., Hedlund, K., Jackson, L. E., Kätterer, T., Lugato, E., Thomsen, I. K., Jørgensen, H. B., & Isberg, P.-E. (2017). How does tillage intensity affect soil organic carbon? A systematic review. *Environmental Evidence*, *6*(1), 1–48.

Halah, A. (2007). National Dialogue for Azraq Water Basin. *Environmental Sector Report*.

Harris, H. C. (1995). Long-term trials on soil and crop management at ICARDA. *Adv. Soil Sci*, *19*, 447–469.

Hartkamp, A. D., White, J. W., & Hoogenboom, G. (2003). Comparison of three weather generators for crop modeling: a case study for subtropical environments. *Agricultural Systems*, *76*(2), 539–560. https://doi.org/https://doi.org/10.1016/S0308-521X(01)00108-1

Hatfield, J. L., & Dold, C. (2018). Climate change impacts on corn phenology and productivity. *Corn: Production and Human Health in Changing Climate*, *95*.

Hausfather, Z. (2023). I Study Climate Change. The Data Is Telling Us Something New. *The New York Times. October*, *13*.

He, J, Dukes, M. D., Jones, J. W., Graham, W. D., & Judge, J. (2009). Applying GLUE for estimating CERES-Maize genetic and soil parameters for sweet corn production. *Transactions of the ASABE*, *52*(6), 1907–1921.

He, Jianqiang, Jones, J. W., Graham, W. D., & Dukes, M. D. (2010). Influence of likelihood function choice for estimating crop model parameters using the generalized likelihood uncertainty estimation method. *Agricultural Systems*, *103*(5), 256–264.

He, Y., Liang, H., Hu, K., Wang, H., & Hou, L. (2018). Modeling nitrogen leaching in a spring maize system under changing climate and genotype scenarios in arid Inner Mongolia, China. *Agricultural Water Management*, *210*, 316–323.

Heiri, O., Lotter, A. F., & Lemcke, G. (2001). Loss on ignition as a method for estimating organic and carbonate content in sediments: reproducibility and comparability of results. *Journal of Paleolimnology*, *25*(1), 101–110. https://doi.org/10.1023/A:1008119611481

Herman, M. R., Nejadhashemi, A. P., Abouali, M., Hernandez-Suarez, J. S., Daneshvar, F., Zhang, Z., Anderson, M. C., Sadeghi, A. M., Hain, C. R., & Sharifi, A. (2018). Evaluating the role of evapotranspiration remote sensing data in improving hydrological modeling

predictability. *Journal of Hydrology*, *556*, 39–49.

Herrero, M., Thornton, P. K., Power, B., Bogard, J. R., Remans, R., Fritz, S., Gerber, J. S., Nelson, G., See, L., & Waha, K. (2017). Farming and the geography of nutrient production for human use: a transdisciplinary analysis. *The Lancet Planetary Health*, *1*(1), e33–e42.

Hijmans, R. J., Cameron, S. E., Parra, J. L., Jones, P. G., & Jarvis, A. (2005). Very high resolution interpolated climate surfaces for global land areas. *International Journal of Climatology*, *25*(15), 1965–1978. https://doi.org/https://doi.org/10.1002/joc.1276

Hillman, G., Hedges, R., Moore, A., Colledge, S., & Pettitt, P. (2001). New evidence of Lateglacial cereal cultivation at Abu Hureyra on the Euphrates. *The Holocene*, *11*(4), 383–393.

Holling, C. S. (1973). Resilience and stability of ecological systems. *Annual Review of Ecology and Systematics*, 1–23.

Homar, V., Jansà, A., Campins, J., Genovés, A., & Ramis, C. (2007). Towards a systematic climatology of sensitivities of Mediterranean high impact weather: a contribution based on intense cyclones. *Natural Hazards and Earth System Sciences*, *7*(4), 445–454. https://doi.org/10.5194/nhess-7-445-2007

Hoogenboom, G., C.H. Porter, V. Shelia, K.J. Boote, U. Singh, W. Pavan, F.A.A. Oliveira, L.P. Moreno-Cadena, T.B. Ferreira, J.W. White, J.I. Lizaso, D.N.L. Pequeno, B.A. Kimball, P.D. Alderman, K.R. Thorp, S.V. Cuadra, M.S. Vianna, F.J. Villalobos, W.D. B, and J. W. J. (2023). *Decision Support System for Agrotechnology Transfer (DSSAT) Version 4.8.2*. DSSAT Foundation, Gainesville, Florida, USA. (www.DSSAT.net)

Hoogenboom, G., Porter, C. H., Shelia, V., Boote, K. J., Singh, U., Pavan, W., & White, J. W. (2021). Improvement and Application of Agroecosystem Models: The DSSAT Experience. *ASA, CSSA, SSSA International Annual Meeting, Salt Lake City, UT*. https://scisoc.confex.com/scisoc/2021am/meetingapp.cgi/Paper/132895

Hoogenboom, G., Jones, J. E., Wilkens, P. W., Porter, C., Boote, K. J., Hunt, L. D., Singh, U., Lizaso, J. I., White, J. W., Uryasev, O., Royce, F. S., Ogoshi, R. M., Gijsman, H. J., Tsuji, G. Y., Koo, J., Jones, J. W., Wilkens, P. W., Porter, C. H., Hunt, L. A., … Koo, J. (2012). *Decision Support System for Agrotechnology Transfer (DSSAT) Version 4.5 [CD-ROM]*. https://api.semanticscholar.org/CorpusID:68046767

Hoogenboom, G., Jones, J. W., Traore, P. C. S., & Boote, K. J. (2012). Experiments and data for model evaluation and application. *Improving Soil Fertility Recommendations in Africa Using the Decision Support System for Agrotechnology Transfer (DSSAT)*, 9–18.

Hoogenboom, G., Porter, C. H., Boote, K. J., Shelia, V., Wilkens, P. W., Singh, U., White, J. W., Asseng, S., Lizaso, J. I., & Moreno, L. P. (2019). The DSSAT crop modeling ecosystem. In *Advances in crop modelling for a sustainable agriculture* (pp. 173–216). Burleigh Dodds Science Publishing.

Hrachowitz, M., Benettin, P., Van Breukelen, B. M., Fovet, O., Howden, N. J. K., Ruiz, L., Van Der Velde, Y., & Wade, A. J. (2016). Transit times—The link between hydrology and water quality at the catchment scale. *Wiley Interdisciplinary Reviews: Water*, *3*(5), 629–657.

Huete, A. R., Liu, H. Q., Batchily, K., & van Leeuwen, W. (1997a). A comparison of vegetation indices over a global set of TM images for EOS-MODIS. *Remote Sensing of Environment*, *59*(3), 440–451. https://doi.org/https://doi.org/10.1016/S0034-4257(96)00112-5

Huete, A. R., Liu, H. Q., Batchily, K., & van Leeuwen, W. (1997b). *A comparison of vegetation indices overa global set of TM images for EOS-MODIS. Remote Sens. Environ*.

Hunt, L. A., & Boote, K. J. (1998). Data for model operation, calibration, and evaluation. In Gordon Y Tsuji, G. Hoogenboom, & P. K. Thornton (Eds.), *Understanding Options for Agricultural Production* (pp. 9–39). Springer Netherlands. https://doi.org/10.1007/978-94-017-3624-4_2

Hunt, L., Pararajasingham, S., Jones, J., Imamura, D., & Ogoshi, R. (1993). GENCALC: Software to Facilitate the Use of Crop Models for Analyzing Field Experiments. *Agronomy Journal - AGRON J*, *85*. https://doi.org/10.2134/agronj1993.00021962008500050025x

Ibáñez, J. J., González-Urquijo, J. E., & Gibaja, J. (2014). Discriminating wild vs domestic cereal harvesting micropolish through laser confocal microscopy. *Journal of Archaeological Science*, *48*, 96–103.

Ibrahim, K. M., & El-Naqa, A. R. (2018). Inverse geochemical modeling of groundwater salinization in Azraq Basin, Jordan. *Arabian Journal of Geosciences*, *11*(10), 237. https://doi.org/10.1007/s12517-018-3557-8

Ibrahim, O. M., Gaafar, A. A., Wali, A., Tawfik, M. M., & El-Nahas, M. (2016). Estimating cultivar coefficients of a spring wheat using GenCalc and GLUE in DSSAT. *Journal of Agronomy*, *15*, 130–135. https://doi.org/10.3923/ja.2016.130.135

ICCD. (2022). Convention to Combat Desertification. *Conference of the Parties Committee on Science and Technology Fifteenth Session*.

Ichii, K., Kawabata, A., & Yamaguchi, Y. (2002). Global correlation analysis for NDVI and climatic variables and NDVI trends: 1982-1990. *International Journal of Remote Sensing*, *23*(18), 3873–3878.

IFPO. (2023). *COMPREHENSIVE OVERVIEW OF THE AGRICULTURAL SECTOR IN JORDAN*. https://www.afd.fr/en/ressources/comprehensive-overview-agricultural-sector-jordan

IPCC, I. P. on C. C. (Ed.). (2023). Weather and Climate Extreme Events in a Changing Climate. In *Climate Change 2021 – The Physical Science Basis: Working Group I Contribution to the Sixth Assessment Report of the Intergovernmental Panel on Climate Change* (pp. 1513–1766). Cambridge University Press. https://doi.org/DOI: 10.1017/9781009157896.013

IPCC. (2023). *Climate Change 2023: Synthesis Report. Contribution of Working Groups I, II and III to the Sixth Assessment Report of the Intergovernmental Panel on Climate Change [Core Writing Team, H. Lee and J. Romero (eds.)]*. https://doi.org/10.59327/IPCC/AR6-9789291691647

IPCC (Intergovernmental Panel on Climate Change). (2014). *Climate change 2014: synthesis report.*

J, B. (1993). *Organic fertilizers – an introduction*.

Jacob, P., Kommuru, P., Ruchitha, R., Kuracha, H., & Taruni, T. (2023). Comparative study of MODIS, LANDSAT-8, SENTINEL-2B, and LISS-4 images for Precision farming using NDVI approach. *E3S Web of Conferences*, *405*, 1004.

Jaja, N. (2016). *Understanding the Texture of Your Soil for Agricultural Productivity*.

Jajarmizadeh, M., Harun, S., & Salarpour, M. (2012). A review on theoretical consideration and types of models in hydrology. *Journal of Environmental Science and Technology*,

5(5), 249–261.

Jajarmizadeh, M., Sidek, L. M., Harun, S., & Salarpour, M. (2017). Optimal calibration and uncertainty analysis of SWAT for an arid climate. *Air, Soil and Water Research*, *10*, 1178622117731792.

Jame, Y., & Cutforth, H. (1996). Crop growth models for decision support systems. *Canadian Journal of Plant Science*, *76*. https://doi.org/10.4141/cjps96-003

Jha, M., Pan, Z., Takle, E., & Gu, R. (2004). Impacts of climate change on streamflow in the Upper Mississippi River Basin: A regional climate model perspective. *Journal of Geophysical Research*, *109*. https://doi.org/10.1029/2003JD003686

Ji, F., Wu, Z., Huang, J., & Chassignet, E. P. (2014). Evolution of land surface air temperature trend. *Nature Climate Change*, *4*(6), 462–466. https://doi.org/10.1038/nclimate2223

Jia, K., Wei, X., Gu, X., Yao, Y., Xie, X., & Li, B. (2014). Land cover classification using Landsat 8 operational land imager data in Beijing, China. *Geocarto International*, *29*(8), 941–951.

Jiang, R., He, W., He, L., Yang, J. Y., Qian, B., Zhou, W., & He, P. (2021). Modelling adaptation strategies to reduce adverse impacts of climate change on maize cropping system in Northeast China. *Scientific Reports*, *11*(1), 810. https://doi.org/10.1038/s41598-020-79988-3

JMD. (2011). *Annual report*.

Jones, C. G., Lawton, J. H., & Shachak, M. (1994). Organisms as ecosystem engineers. In *Ecosystem management* (pp. 130–147). Springer.

Jones, J. W., Hoogenboom, G., Porter, C. H., Boote, K. J., Batchelor, W. D., Hunt, L. A., Wilkens, P. W., Singh, U., Gijsman, A. J., & Ritchie, J. T. (2003). The DSSAT cropping system model. *European Journal of Agronomy*, *18*(3–4), 235–265.

Jones, M. D., Abu-Jaber, N., AlShdaifat, A., Baird, D., Cook, B. I., Cuthbert, M. O., Dean, J. R., Djamali, M., Eastwood, W., & Fleitmann, D. (2019). 20,000 years of societal vulnerability and adaptation to climate change in southwest Asia. *Wiley Interdisciplinary Reviews: Water*, *6*(2), e1330.

Jones, M. D., Richter, T., Rollefson, G., Rowan, Y., Roe, J., Toms, P., Wood, J., Wasse, A.,

Ikram, H., Williams, M., AlShdaifat, A., Pedersen, P. N., & Esaid, W. (2021). The palaeoenvironmental potential of the eastern Jordanian desert basins (Qe'an). *Quaternary International*. https://doi.org/https://doi.org/10.1016/j.quaint.2021.06.023

Jones, P. G., & Thornton, P. K. (2013). Generating downscaled weather data from a suite of climate models for agricultural modelling applications. *Agricultural Systems*, *114*, 1–5. https://doi.org/https://doi.org/10.1016/j.agsy.2012.08.002

Jones, P. G., Thornton, P. K., Díaz, W., Wilkens, P. W., & Jones, A. L. (2002). *MarkSim: A computer tool that generates simulated weather data for crop modeling and risk Assessment: version 1 [CD-ROM]*.

Jönsson, P., & Eklundh, L. (2004). TIMESAT—a program for analyzing time-series of satellite sensor data. *Computers & Geosciences*, *30*(8), 833–845. https://doi.org/https://doi.org/10.1016/j.cageo.2004.05.006

Justice, C. O., Townshend, J. R. G., Vermote, E. F., Masuoka, E., Wolfe, R. E., Saleous, N., Roy, D. P., & Morisette, J. T. (2002). An overview of MODIS Land data processing and product status. *Remote Sensing of Environment*, *83*(1), 3–15. https://doi.org/https://doi.org/10.1016/S0034-4257(02)00084-6

Karl, T. R., Nicholls, N., & Ghazi, A. (1999). Clivar/GCOS/WMO workshop on indices and indicators for climate extremes workshop summary. In *Weather and climate extremes* (pp. 3–7). Springer.

Kent-Jones, D. W. (2023). Cereal farming. In *Encyclopedia Britannica.* https://www.britannica.com/topic/cereal-farming

Kephe, P. N., Ayisi, K. K., & Petja, B. M. (2021). Challenges and opportunities in crop simulation modelling under seasonal and projected climate change scenarios for crop production in South Africa. *Agriculture & Food Security*, *10*(1), 10. https://doi.org/10.1186/s40066-020-00283-5

Khader, B. F. Y., Yigezu, Y. A., Duwayri, M. A., Niane, A. A., & Shideed, K. (2019). Where in the value chain are we losing the most food? The case of wheat in Jordan. *Food Security*, *11*(5), 1009–1027. https://doi.org/10.1007/s12571-019-00962-7

Khaidem, J., Thounaojam, T., & Meetei, T. T. (2018). *Influence of soil pH on nutrient availability: A Review*. 707.

Khan, D. M. I. (2015). *Application of Crop Growth Simulation Models in Agriculture with special reference to Water Management Planning*. https://api.semanticscholar.org/CorpusID:212605874

Khresat, S. A., & Qudah, E. A. (2006). Formation and properties of aridic soils of Azraq Basin in northeastern Jordan. *Journal of Arid Environments*, *64*(1), 116–136. https://doi.org/https://doi.org/10.1016/j.jaridenv.2005.05.009

Khresat, S., Rawajfih, Z., Buck, B., J, B., & Monger, C. (2004). Geomorphic Features and Soil Formation of Arid Lands in Northeastern Jordan. *Archives of Agronomy and Soil Science*, *50*, 607–615. https://doi.org/10.1080/03650340400005572

Kim, C., Lee, S., Jeong, H., Jang, J., & Lee, C. (2009). Impacts and countermeasures of climate change in korean agriculture. *Korean with English Ab Stract, Seoul: Korea Rural Economic Institute (KREI)*.

Klein Tank, A. M. G., Zwiers, F. W., & Zhang, X. (2009). Guidelines on analysis of extremes in a changing climate in support of informed decisions for adaptation. WCDMP-72. *World Meteorological Organization, Geneva, Switzerland*.

Koohafkan, P. (2012). *Water and cereals in drylands*. Routledge.

Kouchi, D. H., Esmaili, K., Faridhosseini, A., Sanaeinejad, S. H., Khalili, D., & Abbaspour, K. C. (2017). Sensitivity of calibrated parameters and water resource estimates on different objective functions and optimization algorithms. *Water*, *9*(6), 384.

Kunnath-Poovakka, A., Ryu, D., Renzullo, L. J., & George, B. (2016). The efficacy of calibrating hydrologic model using remotely sensed evapotranspiration and soil moisture for streamflow prediction. *Journal of Hydrology*, *535*, 509–524.

Piper, E., J. Boote, K., & W. Jones, J. (1998). EVALUATION AND IMPROVEMENT OF CROP MODELS USING REGIONAL CULTIVAR TRIAL DATA. *Applied Engineering in Agriculture*, *14*(4), 435–446. https://doi.org/https://doi.org/10.13031/2013.19391

LADA. (2008). *Guidelines For Land Use System Mapping.Technical Report # 8*.

Laity, J. J. (2009). *Deserts and desert environments* (Vol. 3). John Wiley & Sons.

Lal, R., Delgado, J. A., Groffman, P. M., Millar, N., Dell, C., & Rotz, A. (2011). Management to mitigate and adapt to climate change. *Journal of Soil and Water Conservation*, *66*(4),

276–285.

Le, Q. B., Nkonya, E., & Mirzabaev, A. (2016). Biomass productivity-based mapping of global land degradation hotspots. *Economics of Land Degradation and Improvement–A Global Assessment for Sustainable Development*, *55*.

Leroy, P., Smits, N., Cartolaro, P., Delière, L., Goutouly, J.-P., Raynal, M., & Alonso Ugaglia, A. (2013). A bioeconomic model of downy mildew damage on grapevine for evaluation of control strategies. *Crop Protection*, *53*, 58–71. https://doi.org/https://doi.org/10.1016/j.cropro.2013.05.024

Li, J., Mao, X., Kang, S., & Barry, D. A. (2015). Modeling of hydrological processes in arid agricultural regions. *Frontiers of Agricultural Science and Engineering*, *2*(ARTICLE), 283–294.

Li, S., Liu, J., Shang, M., Jia, H., Feng, Y., Chu, Q., & Chen, F. (2019). Multi-scale assessment of winter wheat yield gaps with an integrated evaluation framework in the Huang-Huai-Hai farming region in China. *The Journal of Agricultural Science*, *157*(6), 523–536. https://doi.org/10.1017/S0021859619000856

Lin, H., Duan, X., Dong, Y., Zhong, R., Rong, L., & Huang, J. (2023). Responses of soil water-holding capacity to environmental changes in alpine ecosystems across the southern Tibetan Plateau in the past 35–40 years. *CATENA*, *222*, 106840. https://doi.org/https://doi.org/10.1016/j.catena.2022.106840

Lionello, P., Bhend, J., Buzzi, A., Della-Marta, P. M., Jansà, A., Maheras, P., Sanna, A., Trigo, I. F., & Trigo, R. M. (2005). *Cyclones in the Mediterranean Region: Climatology and Effects on the Environment*. https://api.semanticscholar.org/CorpusID:127205917

Lloyd, E. A., & Shepherd, T. G. (2020). Environmental catastrophes, climate change, and attribution. *Annals of the New York Academy of Sciences*, *1469*(1), 105–124.

López López, P., Sutanudjaja, E. H., Schellekens, J., Sterk, G., & Bierkens, M. F. P. (2017). Calibration of a large-scale hydrological model using satellite-based soil moisture and evapotranspiration products. *Hydrology and Earth System Sciences*, *21*(6), 3125–3144. https://doi.org/10.5194/hess-21-3125-2017

Lowder, S. K., Skoet, J., & Raney, T. (2016). The number, size, and distribution of farms, smallholder farms, and family farms worldwide. *World Development*, *87*, 16–29.

Lu, J., Sun, G., McNulty, S. G., & Amatya, D. M. (2005). A Comparison of Six Potential Evapotranspiration Methods for Regional Use in the Southeastern United States 1. *JAWRA Journal of the American Water Resources Association*, *41*(3), 621–633.

Lucke, B., Ziadat, F., & Taimeh, A. (2013). *The Soils of Jordan* (pp. 72–76). https://doi.org/10.4000/books.ifpo.4867

Ludwig, F., & Asseng, S. (2006). Climate change impacts on wheat production in a Mediterranean environment in Western Australia. *Agricultural Systems*, *90*(1), 159–179. https://doi.org/https://doi.org/10.1016/j.agsy.2005.12.002

Luo, L., Sheffield, J., & Wood, E. F. (2008). Towards a global drought monitoring and forecasting capability. *Climate Prediction S&T Digest*, 54.

Luppichini, M., Bini, M., Barsanti, M., Giannecchini, R., & Zanchetta, G. (2022). Seasonal rainfall trends of a key Mediterranean area in relation to large-scale atmospheric circulation: How does current global change affect the rainfall regime? *Journal of Hydrology*, *612*, 128233.

Lv, S., Yang, X., Lin, X., Liu, Z., Zhao, J., Li, K., Mu, C., Chen, X., Chen, F., & Mi, G. (2015). Yield gap simulations using ten maize cultivars commonly planted in Northeast China during the past five decades. *Agricultural and Forest Meteorology*, *205*, 1–10.

Ma, L., C. Ascough II, J., R. Ahuja, L., J. Shaffer, M., D. Hanson, J., & W. Rojas, K. (2000). ROOT ZONE WATER QUALITY MODEL SENSITIVITY ANALYSIS USING MONTE CARLO SIMULATION. *Transactions of the ASAE*, *43*(4), 883–895. https://doi.org/https://doi.org/10.13031/2013.2984

Maher, L., Macdonald, D., Allentuck, A., Martin, L., Spyrou, A., & Jones, M. (2015). Occupying wide open spaces? Late Pleistocene hunter–gatherer activities in the Eastern Levant. *Quaternary International*, *396*. https://doi.org/10.1016/j.quaint.2015.07.054

Maldonado, I., Rodriguez, G., & Castillo, D. (2015). Determination of genetic coefficients of three spring wheat varieties under a Mediterranean environment applying the DSSAT model. *Chilean Journal of Agricultural Research*, *75*, 412–424. https://doi.org/10.4067/S0718-58392015000500006

Malik, W., & Dechmi, F. (2019). DSSAT modelling for best irrigation management practices assessment under Mediterranean conditions. *Agricultural Water Management*, *216*, 27–

43. https://doi.org/https://doi.org/10.1016/j.agwat.2019.01.017

Mavromatis, T., Boote, K. J., Jones, J. W., Wilkerson, G. G., & Hoogenboom, G. (2002). Repeatability of model genetic coefficients derived from soybean performance trials across different states. *Crop Science*, *42*(1), 76–89.

Mazoyer, M., & Roudart, L. (2006). *A history of world agriculture: from the neolithic age to the current crisis*. NYU Press.

McFeeters, S. K. (1996). The use of the Normalized Difference Water Index (NDWI) in the delineation of open water features. *International Journal of Remote Sensing*, *17*(7), 1425–1432.

Médail, F. (2008). Mediterranean. In S. E. Jørgensen & B. D. Fath (Eds.), *Encyclopedia of Ecology* (pp. 2296–2308). Academic Press. https://doi.org/https://doi.org/10.1016/B978-008045405-4.00348-7

Meinshausen, M., Smith, S. J., Calvin, K., Daniel, J. S., Kainuma, M. L. T., Lamarque, J.-F., Matsumoto, K., Montzka, S. A., Raper, S. C. B., Riahi, K., Thomson, A., Velders, G. J. M., & van Vuuren, D. P. P. (2011). The RCP greenhouse gas concentrations and their extensions from 1765 to 2300. *Climatic Change*, *109*(1), 213. https://doi.org/10.1007/s10584-011-0156-z

Mengistu, A. G., van Rensburg, L. D., & Woyessa, Y. E. (2019). Techniques for calibration and validation of SWAT model in data scarce arid and semi-arid catchments in South Africa. *Journal of Hydrology: Regional Studies*, *25*, 100621.

Mereu, V., Gallo, A., & Spano, D. (2019). Optimizing Genetic Parameters of CSM-CERES Wheat and CSM-CERES Maize for Durum Wheat, Common Wheat, and Maize in Italy. *Agronomy*, *9*, 665. https://doi.org/10.3390/agronomy9100665

Meroni, M., Fasbender, D., Rembold, F., Atzberger, C., & Klisch, A. (2019). Near real-time vegetation anomaly detection with MODIS NDVI: Timeliness vs. accuracy and effect of anomaly computation options. *Remote Sensing of Environment*, *221*, 508–521. https://doi.org/10.1016/j.rse.2018.11.041

Metternicht, G., Davies, J., Ogali, C., & Laban, P. (2015). *Homing in on the range: enabling investments for sustainable land management*.

Michael, T. P., Salome, P. A., Hannah, J. Y., Spencer, T. R., Sharp, E. L., McPeek, M. A., Alonso, J. M., Ecker, J. R., & McClung, C. R. (2003). Enhanced fitness conferred by naturally occurring variation in the circadian clock. *Science*, *302*(5647), 1049–1053.

Miralles, D. G., De Jeu, R. A. M., Gash, J. H., Holmes, T. R. H., & Dolman, A. J. (2011). Magnitude and variability of land evaporation and its components at the global scale. *Hydrology and Earth System Sciences*, *15*(3), 967–981. https://doi.org/10.5194/hess-15-967-2011

Miralles, D. G., Holmes, T. R. H., De Jeu, R. A. M., Gash, J. H., Meesters, A. G. C. A., & Dolman, A. J. (2011). Global land-surface evaporation estimated from satellite-based observations. *Hydrology and Earth System Sciences*, *15*(2), 453–469. https://doi.org/10.5194/hess-15-453-2011

MIRRA. (2019). *Realizing Sustainable Agriculture and Efficient Water Management in the Azraq Basin in Jordan through the Adaptation and Integration of Proven Technology and Community Partnership*. https://mirra-jo.org/realizing-sustainable-agriculture-in-azraq/#:~:text=Realizing Sustainable Agriculture In Azraq - MIRRA&text=Introduce the use of drip,decrease the stress ground water.

MoA. (1995). *The soils of Jordan, Report of the National Soil Map and Land Use Project*.

MoA. (2008). *Annual report*.

MoA. (2010). *Annual report*.

MoEnv (Ministry of Environment). (2009). *Jordan's Second National Communication to the UNFCCC*.

Mohammadi, R., Sadeghzadeh, B., Ahmadi, H., Bahrami, N., & Amri, A. (2015). Field evaluation of durum wheat landraces for prevailing abiotic and biotic stresses in highland rainfed regions of Iran. *The Crop Journal*, *3*(5), 423–433. https://doi.org/https://doi.org/10.1016/j.cj.2015.03.008

Molden, D., Oweis, T. Y., Pasquale, S., Kijne, J. W., Hanjra, M. A., Bindraban, P. S., Bouman, B. A. M., Mahoo, H. F., Silva, P., & Upadhyaya, A. (2007). *Pathways for increasing agricultural water productivity*.

Momany, Y. (2001). Focus on Seed Programs The Seed Industry in Jordan. *Lebanon:*

International Center for Agricultural Research in the Dry Areas (ICARDA).

Moriasi, D. N., Arnold, J. G., Van Liew, M. W., Bingner, R. L., Harmel, R. D., & Veith, T. L. (2007). Model evaluation guidelines for systematic quantification of accuracy in watershed simulations. *Transactions of the ASABE*, *50*(3), 885–900.

Mortimore, M., & Adams, W. M. (1999). *Working the Sahel: environment and society in northern Nigeria.* Routledge.

Mu, Q., Heinsch, F. A., Zhao, M., & Running, S. W. (2007). Development of a global evapotranspiration algorithm based on MODIS and global meteorology data. *Remote Sensing of Environment*, *111*(4), 519–536. https://doi.org/https://doi.org/10.1016/j.rse.2007.04.015

Mu, Q., Zhao, M., & Running, S. W. (2011). Improvements to a MODIS global terrestrial evapotranspiration algorithm. *Remote Sensing of Environment*, *115*(8), 1781–1800. https://doi.org/https://doi.org/10.1016/j.rse.2011.02.019

Muñoz Sabater, J. (2019). *ERA5-Land monthly averaged data from 1981 to present*. https://doi.org/https://doi.org/10.24381/cds.68d2bb30

MWI. (2010). *Annual report*.

MWI. (2013). *Annual report*.

MWI. (2023). *National Water Strategy 2023 - 2040*. https://www.mwi.gov.jo/EBV4.0/Root_Storage/AR/EB_Ticker/National_Water_Strategy_2023-2040_Summary-English_-ver2.pdf

Myung, I. J. (2003). Tutorial on maximum likelihood estimation. *Journal of Mathematical Psychology*, *47*(1), 90–100.

Nair, S. S., King, K. W., Witter, J. D., Sohngen, B. L., & Fausey, N. R. (2011). Importance of crop yield in calibrating watershed water quality simulation tools 1. *JAWRA Journal of the American Water Resources Association*, *47*(6), 1285–1297.

Nash, J. E., & Sutcliffe, J. V. (1970). River flow forecasting through conceptual models part I—A discussion of principles. *Journal of Hydrology*, *10*(3), 282–290.

Nations, U. (2019). *World Population Prospects: The 2019 Revision. New York: United Nations Department of Economic and Social Affairs, Population Division.*

Nazco, R., Villegas, D., Ammar, K., Peña, R. J., Moragues, M., & Royo, C. (2012). Can Mediterranean durum wheat landraces contribute to improved grain quality attributes in modern cultivars? *Euphytica*, *185*, 1–17.

Ndomba, P., Mtalo, F., & Killingtveit, Å. (2005). *The Suitability of SWAT Model in Sediment Yield Modeling for Ungauged Catchments. A Case of Simiyu River Subcatchment, Tanzania*.

Neitsch, S.L.; Arnold, J.G.; Kiniry, J.R.; Williams, J. R. (2011). Soil and Water Assessment Tool Theoretical Documentation Version 2009. *Texas Water Resources Institute*, *2009*. https://hdl.handle.net/1969.1/128050

Neitsch, S., Arnold, J., Kinry, J. R., & Williams, J. R. (2011). Soil and water assessment tool theoretical documentation. *Version*.

Neitsch, S. L., Arnold, J. G., Kiniry, J. R., Srinivasan, R., & Williams, J. R. (2004). Soil and water assessment tool input/output file documentation, version 2005. *US Department of Agriculture-Agricultural Research Service, Grassland Soil and Water Research Laboratory, Temple, TX*.

Neitsch, S. L., Arnold, J. G., Kiniry, J. R., Williams, J. R., & King, K. W. (2002). Soil and water assessment tool—theoretical documentation (ver. 2000). *Texas Water Resources Institute, College Station, TX*, *458*.

Nikou, M., & Mavromatis, T. (2023). Demonstrating the Use of the Yield-Gap Concept on Crop Model Calibration in Data-Poor Regions: An Application to CERES-Wheat Crop Model in Greece. *Land*, *12*(7). https://doi.org/10.3390/land12071372

Odusanya, A., Mehdi-Schulz, B., Schürz, C., Adebayo Olubukola, O., Awokola, O., Awomeso, J., Adejuwon, J., & Karsten, S. (2018). Multi-site calibration and validation of SWAT with satellite-based evapotranspiration in a data sparse catchment in southwestern Nigeria. *Hydrology and Earth System Sciences Discussions*, 1–37. https://doi.org/10.5194/hess-2018-170

Okello, M., Lamo, J., Ochwo-Ssemakula, M., & Onyilo, F. (2021). Challenges and innovations in achieving zero hunger and environmental sustainability through the lens of sub-Saharan Africa. *Outlook on Agriculture*, *50*(2), 141–147. https://doi.org/10.1177/0030727020975778

Paine, R. T. (1966). Food web complexity and species diversity. *The American Naturalist*, *100*(910), 65–75.

Palacios-Orueta, A., Khanna, S., Litago, J., Whiting, M., & Ustin, S. (2005). *Assessment of NDVI and NDWI spectral indices using MODIS time series analysis and development of a new spectral index based on MODIS shortwave infrared bands*. https://doi.org/10.13140/2.1.1305.4400

Palmer, A. R., & Bennett, J. E. (2013). Degradation of communal rangelands in South Africa: towards an improved understanding to inform policy. *African Journal of Range & Forage Science*, *30*(1–2), 57–63.

Palosuo, T., Kersebaum, K. C., Angulo, C., Hlavinka, P., Moriondo, M., Olesen, J. E., Patil, R. H., Ruget, F., Rumbaur, C., & Takáč, J. (2011). Simulation of winter wheat yield and its variability in different climates of Europe: A comparison of eight crop growth models. *European Journal of Agronomy*, *35*(3), 103–114.

Parry, M. L., Canziani, O. F., Palutikof, J. P., Van Der Linden, P. J., & Hanson, C. E. (2007). IPCC, 2007: climate change 2007: impacts, adaptation and vulnerability. Contribution of working group II to the fourth assessment report of the intergovernmental panel on climate change. *Cambridge Uni-Versity Press, Cambridge, UK*.

Peterson, G. A. (2018). Dryland Farming☆. In *Reference Module in Earth Systems and Environmental Sciences*. Elsevier. https://doi.org/https://doi.org/10.1016/B978-0-12-409548-9.11401-0

Peterson, G., Unger, P., Payne, W., Anderson, R., & Baumhardt, R. L. (2006). *Dryland Agriculture Research Issues*. https://doi.org/10.2134/agronmonogr23.2ed.c22

Peterson, G., Unger, P., Payne, W., Ryan, J., De Pauw, E., Gomez, H., & Mrabet, R. (2006). Drylands of the Mediterranean Zone: Biophysical Resources and Cropping Systems. In *Proceedings of the International Dryland Agriculture Conference*. https://doi.org/10.2134/agronmonogr23.2ed.c15

Peterson, T. C., Zhang, X., Brunet-India, M., & Vázquez-Aguirre, J. L. (2008). Changes in North American extremes derived from daily weather data. *Journal of Geophysical Research: Atmospheres*, *113*(D7).

Peterson, T., Folland, C., Gruza, G., Hogg, W., Mokssit, A., & Plummer, N. (2001). *Report on*

the activities of the working group on climate change detection and related rapporteurs. Citeseer.

Pireivatlou, A. S., Aliyev, R., & Lalehloo, B. S. (2011). *GRAIN FILLING RATE AND DURATION IN BREAD WHEAT UNDER IRRIGATED AND DROUGHT STRESSED CONDITIONS*. https://api.semanticscholar.org/CorpusID:56011022

Portmann, R. W., Solomon, S., & Hegerl, G. C. (2009). Spatial and seasonal patterns in climate change, temperatures, and precipitation across the United States. *Proceedings of the National Academy of Sciences of the United States of America*, *106*(18), 7324–7329. https://doi.org/10.1073/pnas.0808533106

Pourebrahimi Foumani, M., Xinhua, Y., Joshua S., F., & and Yang, C.-E. (n.d.). Simulation modeling of cotton yield responses to management strategies under climate change: insights from DSSAT. *Journal of Plant Nutrition*, 1–15. https://doi.org/10.1080/01904167.2025.2462702

Power, J. F., & Prasad, R. (1997). *Soil fertility management for sustainable agriculture*. CRC press.

Powlson, D. S., Stirling, C. M., Jat, M. L., Gerard, B. G., Palm, C. A., Sanchez, P. A., & Cassman, K. G. (2014). Limited potential of no-till agriculture for climate change mitigation. *Nature Climate Change*, *4*(8), 678–683.

Prakasa Rao, E. V. S., & Kavi, P. (2000). Nitrates, agriculture and environment. *Curr Sci*, *79*.

Pretty, J., & Bharucha, Z. P. (2014). Sustainable intensification in agricultural systems. *Annals of Botany*, *114*(8), 1571–1596.

Priestley, C. H. B., & TAYLOR, R. J. (1972). On the assessment of surface heat flux and evaporation using large-scale parameters. *Monthly Weather Review*, *100*(2), 81–92.

Prince, S. D. (1991). Satellite remote sensing of primary production: comparison of results for Sahelian grasslands 1981-1988. *International Journal of Remote Sensing*, *12*(6), 1301–1311.

Qi, Z., Kang, G., Chu, C., Qiu, Y., Xu, Z., & Wang, Y. (2017). Comparison of SWAT and GWLF model simulation performance in humid south and semi-arid north of China. *Water*, *9*(8), 567.

Quideau, S. A. (2002). Organic matter accumulation. *Encyclopedia of Soil Science*, *26*, 1–4.

Rafiei Emam, A., Kappas, M., Hoang Khanh Nguyen, L., & Renchin, T. (2016). Hydrological Modeling in an Ungauged Basin of Central Vietnam Using SWAT Model. *Hydrology and Earth System Sciences Discussions*, *2016*, 1–33. https://doi.org/10.5194/hess-2016-44

Rajib, M. A., Merwade, V., & Yu, Z. (2016). Multi-objective calibration of a hydrologic model using spatially distributed remotely sensed/in-situ soil moisture. *Journal of Hydrology*, *536*, 192–207.

Rasp, S., Pritchard, M. S., & Gentine, P. (2018). Deep learning to represent subgrid processes in climate models. *Proceedings of the National Academy of Sciences*, *115*(39), 9684–9689. https://doi.org/10.1073/pnas.1810286115

Rawajfih, Z., Khresat, S. A., & Buck, B. (2005). Arid soils of the Badia region of northeastern Jordan: Potential use for sustainable agriculture. *Archives of Agronomy and Soil Science*, *51*(1), 25–32.

Razaq, M., Zhang, P., Shen, H.-L., & Salahuddin. (2017). Influence of nitrogen and phosphorous on the growth and root morphology of Acer mono. *PloS One*, *12*(2), e0171321. https://doi.org/10.1371/journal.pone.0171321

Refsgaard, J. C. (1997). Parameterisation, calibration and validation of distributed hydrological models. *Journal of Hydrology*, *198*(1–4), 69–97.

Reichl, J. P. C., Western, A. W., McIntyre, N. R., & Chiew, F. H. S. (2009). Optimization of a similarity measure for estimating ungauged streamflow. *Water Resources Research*, *45*(10).

Reilly, J. M., & Schimmelpfennig, D. (1999). Agricultural impact assessment, vulnerability, and the scope for adaptation. *Climatic Change*, *43*(4), 745–788.

Reynolds, J. F., Smith, D. M. S., Lambin, E. F., Turner, B. L. 2nd, Mortimore, M., Batterbury, S. P. J., Downing, T. E., Dowlatabadi, H., Fernández, R. J., Herrick, J. E., Huber-Sannwald, E., Jiang, H., Leemans, R., Lynam, T., Maestre, F. T., Ayarza, M., & Walker, B. (2007). Global desertification: building a science for dryland development. *Science (New York, N.Y.)*, *316*(5826), 847–851. https://doi.org/10.1126/science.1131634

Riahi, K., Rao, S., Krey, V., Cho, C., Chirkov, V., Fischer, G., Kindermann, G., Nakicenovic,

N., & Rafaj, P. (2011). RCP 8.5—A scenario of comparatively high greenhouse gas emissions. *Climatic Change*, *109*, 33–57.

Rice, C. W. (2002). Organic matter and nutrient dynamics. *Encyclopedia of Soil Science*, *2*, 1180–1183.

Richter, T., Arranz-Otaegui, A., Yeomans, L., & Boaretto, E. (2017). High resolution AMS dates from Shubayqa 1, northeast Jordan reveal complex origins of Late Epipalaeolithic Natufian in the Levant. *Scientific Reports*, *7*(1), 1–10.

Riebe, P. E. (2018). *Water Abstractions and Nature Conservation in Northern Jordan under a MARISCO Perspective*. Hochschule für nachhaltige Entwicklung Eberswalde, Fachber. 1.

Ritchie, J., & Otter, S. (1985). Description and performance of CERES-Wheat: A user-oriented wheat yield model. *USDA-ARS, ARS-38*, *38*.

Rosenzweig, C., Antle, J. M., Ruane, A. C., Jones, J. W., H., & J. L., Boote, K. J., ... Mutter, C. Z. (2018). *Protocols for AgMIP regional integrated assessments: Version 7.0. New ork, NY: Columbia University, Agricultural Model Intercomparison and Improvement Project (AgMIP)*. https://agmip.org/wp-content/uploads/2018/08/AgMIP-Protocols-for-Regional-Integrated-Assessment-v7-0-20180218-1-ilovepdf-compressed.pdf

Rupngam, T., & Messiga, A. J. (2024). Unraveling the Interactions between Flooding Dynamics and Agricultural Productivity in a Changing Climate. *Sustainability*, *16*(14). https://doi.org/10.3390/su16146141

Saba, M., Al-Naber, G., & Mohawesh, Y. (2010). *Analysis of Jordan vegetation cover dynamics using MODIS/NDVI from 2000 to 2009*.

Safriel, U., Adeel, Z., Niemeijer, D., Puigdefabregas, J., White, R., Lal, R., Winslow, M., Ziedler, J., Prince, S., & Archer, E. (2005). Dryland systems. In *Ecosystems and Human Well-being: Current State and Trends.: Findings of the Condition and Trends Working Group* (pp. 623–662). Island Press.

Salameh, E., & Bannayan, H. (1993). Water resources of Jordan. *Future and Future Potentials: Amman, Jordan, Friedrich Ebert Stiftung*.

Salvacion, A. (2011). *Simulating Impact of Climate Change in Crop Productivity Using Future Climate Projections and DSSAT Crop Simulation Models GUIDE MODULE*.

https://doi.org/10.13140/2.1.2647.4563

Samberg, L. H., Gerber, J. S., Ramankutty, N., Herrero, M., & West, P. C. (2016). Subnational distribution of average farm size and smallholder contributions to global food production. *Environmental Research Letters*, *11*(12), 124010.

Santra, P., & Chkraborty, A. (2011). ANALYSIS OF SEASONAL AND ANNUAL CHANGE OF VEGETATION IN THE INDIAN THAR DESERT USING MODIS DATA. *The International Archives of the Photogrammetry, Remote Sensing and Spatial Information Sciences*, *XXXVIII-8/*, 175–178. https://doi.org/10.5194/isprsarchives-XXXVIII-8-W20-175-2011

Schimel, D. S., Asner, G. P., & Moorcroft, P. (2013). Observing changing ecological diversity in the Anthropocene. *Frontiers in Ecology and the Environment*, *11*(3), 129–137.

Schmidt, G. L., Jenkerson, C. B., Masek, J., Vermote, E., & Gao, F. (2013). Landsat ecosystem disturbance adaptive processing system (LEDAPS) algorithm description. *U.S. Geol. Surv. Open File Rep.*, *1057*.

Schober, P., Boer, C., & Schwarte, L. (2018). Correlation Coefficients: Appropriate Use and Interpretation. *Anesthesia & Analgesia*, *126*, 1. https://doi.org/10.1213/ANE.0000000000002864

Schwilch, G., Liniger, H. P., & Hurni, H. (2014). Sustainable land management (SLM) practices in drylands: how do they address desertification threats? *Environmental Management*, *54*(5), 983–1004.

Semenov, Pilkington-Bennett, S., & Calanca, P. (2013). Validation of ELPIS 1980-2010 baseline scenarios using the observed European Climate Assessment data set. *Climate Research*, *57*(1), 1–9. https://www.int-res.com/abstracts/cr/v57/n1/p1-9/

Shachak, M., & Pickett, S. T. A. (1997). Linking ecological understanding and application: patchiness in a dryland system. In *The ecological basis of conservation* (pp. 108–119). Springer.

Shah, N. H., & Paulsen, G. M. (2003). Interaction of drought and high temperature on photosynthesis and grain-filling of wheat. *Plant and Soil*, *257*(1), 219–226.

Shahbaz, M., & Sunna, B. (1998). Integrated studies of the Azraq Basin in Jordan. *Proceedings*

RMRS., *13*, 149.

Shaxson, F., Kassam, A. H., Friedrich, T., Boddey, B., & Adekunle, A. (2008). Underpinning conservation agriculture's benefits: the roots of soil health and function. *Main Background Document for the Workshop on Investing in Sustainable Crop Intensification: The Case for Improving Soil Health*, 22–24.

Sheng, T. (1990). Watershed management field manual. *FAO Conservation Guide*, *13*(6), 148.

Shrestha, M. K., Recknagel, F., Frizenschaf, J., & Meyer, W. (2016). Assessing SWAT models based on single and multi-site calibration for the simulation of flow and nutrient loads in the semi-arid Onkaparinga catchment in South Australia. *Agricultural Water Management*, *175*, 61–71.

Si, Z., Zain, M., Li, S., Liu, J., Liang, Y., Gao, Y., & Duan, A. (2021). Optimizing nitrogen application for drip-irrigated winter wheat using the DSSAT-CERES-Wheat model. *Agricultural Water Management*, *244*, 106592. https://doi.org/https://doi.org/10.1016/j.agwat.2020.106592

Sinclair, T. R., & Rufty, T. W. (2012). Nitrogen and water resources commonly limit crop yield increases, not necessarily plant genetics. *Global Food Security*, *1*(2), 94–98.

Sinnathamby, S., Douglas-Mankin, K. R., & Craige, C. (2017). Field-scale calibration of crop-yield parameters in the Soil and Water Assessment Tool (SWAT). *Agricultural Water Management*, *180*, 61–69.

Smith, W., Grant, B., Qi, Z., He, W., Qian, B., Jing, Q., VanderZaag, A., Drury, C. F., Luce, M. S., & Wagner-Riddle, C. (2020). Towards an improved methodology for modelling climate change impacts on cropping systems in cool climates. *Science of the Total Environment*, *728*, 138845.

Soldevilla, M., Martin-Lammerding, D., Tenorio, J. L., Walter, I., Quemada, M., & Lizaso, J. (2013). Simulating improved combinations tillage-rotation under dryland conditions. *Spanish Journal of Agricultural Research*, *11*, 820. https://doi.org/10.5424/sjar/2013113-3747

Soltanian, F. K., Abbasi, M., & Bakhtyari, H. R. R. (2019). Flood monitoring using Ndwi and Mndwi spectral indices: A case study of Aghqala flood-2019, Golestan Province, Iran. *The International Archives of Photogrammetry, Remote Sensing and Spatial Information*

Sciences, *42*, 605–607.

Spinoni, J., Naumann, G., Carrao, H., Barbosa, P., & Vogt, J. (2014). World drought frequency, duration, and severity for 1951–2010. *International Journal of Climatology*, *34*(8), 2792–2804.

Stewart, B. A. B. T.-R. M. in F. S. (2016). *Dryland Farming*. Elsevier. https://doi.org/https://doi.org/10.1016/B978-0-08-100596-5.02937-1

Stewart, B. A., & Thapa, S. (2016). Dryland farming: concept, origin and brief history. In *Innovations in Dryland Agriculture* (pp. 3–29). Springer.

Stirzaker, R. J., Passioura, J. B., & Wilms, Y. (1996). Soil structure and plant growth: Impact of bulk density and biopores. *Plant and Soil*, *185*(1), 151–162. http://www.jstor.org/stable/42949803

Sunoj, V. S. J., Prasad, P. V. V., Ciampitti, I. A., & Maswada, H. F. (2020). Narrowing Diurnal Temperature Amplitude Alters Carbon Tradeoff and Reduces Growth in C(4) Crop Sorghum. *Frontiers in Plant Science*, *11*, 1262. https://doi.org/10.3389/fpls.2020.01262

Swain, J. B., & Patra, K. C. (2017). Streamflow estimation in ungauged catchments using regionalization techniques. *Journal of Hydrology*, *554*, 420–433.

Tabari, H. (2020). Climate change impact on flood and extreme precipitation increases with water availability. *Scientific Reports*, *10*(1), 1–10.

Tabari, H., Marofi, S., Aeini, A., Talaee, P. H., & Mohammadi, K. (2011). Trend analysis of reference evapotranspiration in the western half of Iran. *Agricultural and Forest Meteorology*, *151*(2), 128–136.

Tan, K. H. (1994). Environmental soil science, Marcel Decker. *Inc., New York, Basel, Hong Kong*.

Tarawneh, Q., & Kadıoğlu, M. (2003). An analysis of precipitation climatology in Jordan. *Theoretical and Applied Climatology*, *74*, 123–136.

Tarawneh, Q. Y. (2022). Monitoring Climate Change in Jordan and its Impact on Agriculture. *The Arab World Geographer*, *25*(4), 230–247.

Tate III, R. L. (1987). *Soil organic matter. Biological and ecological effects.*

Te Chow, V. (2010). *Applied Hydrology*. Tata McGraw-Hill Education. https://books.google.co.uk/books?id=RRwidSsBJrEC

Theng, B. K. G. (1987). Clay-humic interactions and soil aggregate stability. *Soil Structure and Aggregate Stability, Pp. 32â€“73. Proc. Institute of Irrigation and Salinity Research. Tatura, Australia*.

Thompson, M., Gamage, D., Hirotsu, N., Martin, A., & Seneweera, S. (2017). Effects of elevated carbon dioxide on photosynthesis and carbon partitioning: a perspective on root sugar sensing and hormonal crosstalk. *Frontiers in Physiology*, 578.

Thomson, A. M., Calvin, K. V, Smith, S. J., Kyle, G. P., Volke, A., Patel, P., Delgado-Arias, S., Bond-Lamberty, B., Wise, M. A., & Clarke, L. E. (2011). RCP4. 5: a pathway for stabilization of radiative forcing by 2100. *Climatic Change*, *109*, 77–94.

Thuesen, M. B., Alarashi, H., Ruter, A., & Richter, T. (2023). Nascent craft specialization in the Pre-Pottery Neolithic A? Bead making at Shubayqa 6 (northeast Jordan). *PLOS ONE*, *18*(12), 1–27. https://doi.org/10.1371/journal.pone.0292954

Tian, F., Lü, Y. H., Fu, B. J., Yang, Y. H., Qiu, G., Zang, C., & Zhang, L. (2016). Effects of ecological engineering on water balance under two different vegetation scenarios in the Qilian Mountain, northwestern China. *Journal of Hydrology: Regional Studies*, *5*, 324–335.

Timsina, J. (2007). *Procedures for evaluating crop models and datasets intended for model applications*. *28*, 1–13.

Tita, D., Mahdi, K., Devkota, K. P., & Devkota, M. (2025). Climate change and agronomic management: Addressing wheat yield gaps and sustainability challenges in the Mediterranean and MENA regions. *Agricultural Systems*, *224*, 104242. https://doi.org/https://doi.org/10.1016/j.agsy.2024.104242

Tobin, K. J., & Bennett, M. E. (2017). Constraining SWAT calibration with remotely sensed evapotranspiration data. *JAWRA Journal of the American Water Resources Association*, *53*(3), 593–604.

Trigo, I. F. (2006). Climatology and interannual variability of storm-tracks in the Euro-Atlantic sector: a comparison between ERA-40 and NCEP/NCAR reanalyses. *Climate Dynamics*, *26*(2), 127–143. https://doi.org/10.1007/s00382-005-0065-9

Tsikerdekis, M. (2013). The effects of perceived anonymity and anonymity states on conformity and groupthink in online communities: A Wikipedia study. *Journal of the American Society for Information Science and Technology*, *64*(5), 1001–1015. https://doi.org/https://doi.org/10.1002/asi.22795

Tsuji, Gordon Yukio, & Balas, S. (1993). *The IBSNAT decade: Ten years of endeavor at the frontier of science and technology*.

Tucker, C. J. (1980). Remote sensing of leaf water content in the near infrared. *Remote Sensing of Environment*, *10*(1), 23–32.

UN. (2015). *Transforming our World: The 2030 Agenda for Sustainable Development*.

UNCCD. (1994). *Article 2 of the Text of the United Nations Convention to Combat Desertification*. http://www.unccd.int/Lists/ Site Document Library/convention Text/conv-eng.pdf.

UNCCD. (2011a). *Drylands. Global Land Outlook, Chapter 12*.

UNCCD. (2011b). *Global Drylands: A UN Systems-Wide Report. Committee for the Review of the Implementation of the Convention 9th session, Bonn February 21-25, 2011. ICCD/CRIC(9)/CRP.1*.

UNCCD. (2012). *Desertification Land Degradation and Drought (DLDD) – Some global facts and figures. Information sheet from the UNCCD.*

UNDESA. (2017). *World Population Prospects: The 2017 Revision, Key Findings and Advance Tables.*

Valerio, F., Godinho, S., Marques, A. T., Crispim-Mendes, T., Pita, R., & Silva, J. P. (2024). GEE_xtract: High-quality remote sensing data preparation and extraction for multiple spatio-temporal ecological scaling. *Ecological Informatics*, *80*, 102502. https://doi.org/https://doi.org/10.1016/j.ecoinf.2024.102502

Van Dijk, M., Morley, T., van Loon, M., Reidsma, P., Tesfaye, K., & van Ittersum, M. K. (2020). Reducing the maize yield gap in Ethiopia: Decomposition and policy simulation. *Agricultural Systems*, *183*, 102828.

Van Ittersum, M. K., Cassman, K. G., Grassini, P., Wolf, J., Tittonell, P., & Hochman, Z. (2013). Yield gap analysis with local to global relevance—a review. *Field Crops*

Research, *143*, 4–17.

Velastegui-Montoya, A., Montalván-Burbano, N., Carrión-Mero, P., Rivera-Torres, H., Sadeck, L., & Adami, M. (2023). Google Earth Engine: A Global Analysis and Future Trends. *Remote Sensing*, *15*(14). https://doi.org/10.3390/rs15143675

Vingiani, S., Di Iorio, E., Colombo, C., & Terribile, F. (2018). Integrated study of red Mediterranean soils from southern Italy. *Catena*, *168*, 129–140.

Vörösmarty, C. J., Douglas, E. M., Green, P. A., & Revenga, C. (2005). Geospatial Indicators of Emerging Water Stress: An Application to Africa. *AMBIO: A Journal of the Human Environment*, *34*(3), 230–236. https://doi.org/10.1579/0044-7447-34.3.230

Wallace, J., Behn, G., & Furby, S. (2006). Vegetation condition assessment and monitoring from sequences of satellite imagery. *Ecological Management & Restoration*, *7*, S31–S36.

Wallach, D., & Goffinet, B. (1989). Mean squared error of prediction as a criterion for evaluating and comparing system models. *Ecological Modelling*, *44*(3–4), 299–306.

Wang, T., Kou, X., Xiong, Y., Mou, P., Wu, J., & Ge, J. (2010). Temporal and spatial patterns of NDVI and their relationship to precipitation in the Loess Plateau of China. *International Journal of Remote Sensing*, *31*(7), 1943–1958. https://doi.org/10.1080/01431160902929263

Wang, X., M. Melesse, A., & Yang, W. (2006). Influences of Potential Evapotranspiration Estimation Methods on SWAT's Hydrologic Simulation in a Northwestern Minnesota Watershed. *Transactions of the ASABE*, *49*(6), 1755–1771. https://doi.org/https://doi.org/10.13031/2013.22297

Wardlow, B. D., Egbert, S. L., & Kastens, J. H. (2007). Analysis of time-series MODIS 250 m vegetation index data for crop classification in the U.S. Central Great Plains. *Remote Sensing of Environment*, *108*(3), 290–310. https://doi.org/https://doi.org/10.1016/j.rse.2006.11.021

Wartenburger, R., Hirschi, M., Donat, M. G., Greve, P., Pitman, A. J., & Seneviratne, S. I. (2017). *Changes in regional climate extremes as a function of global mean temperature: an interactive plotting framework. Geoscientific Model Development, 10, 3609–3634, doi: 10.5194*. gmd-2017-33.

Watanabe, M., Suzuki, T., O'ishi, R., Komuro, Y., Watanabe, S., Emori, S., Takemura, T., Chikira, M., Ogura, T., Sekiguchi, M., Takata, K., Yamazaki, D., Yokohata, T., Nozawa, T., Hasumi, H., Tatebe, H., & Kimoto, M. (2010). Improved Climate Simulation by MIROC5: Mean States, Variability, and Climate Sensitivity. *Journal of Climate*, *23*(23), 6312–6335. https://doi.org/https://doi.org/10.1175/2010JCLI3679.1

Webb, N. P., Marshall, N. A., Stringer, L. C., Reed, M. S., Chappell, A., & Herrick, J. E. (2017). Land degradation and climate change: building climate resilience in agriculture. *Frontiers in Ecology and the Environment*, *15*(8), 450–459.

Weier, J., & Herring, D. (2019). Measuring vegetation (NDVI & EVI). 2000. *NASA Earth Observatory. Dispinível Em: Http://Earthobservatory. Nasa. Gov/Features/MeasuringVegetation/, Site Consultado A*, *15*.

West, B. G. (1970). Soil Survey in the Baqa 'a Valley. *Unpublished Report. Ministry of Agriculture of Jordan. Amman*.

Williams, J. D., Long, D. S., & Reardon, C. L. (2020). Productivity and water use efficiency of intensified dryland cropping systems under low precipitation in Pacific Northwest, USA. *Field Crops Research*, *254*, 107787.

Williams, P. F., & Rust, B. R. (1969). The sedimentology of a braided river. *Journal of Sedimentary Research*, *39*(2), 649–679.

Winchell, M., Srinivasan, R., Di Luzio, M., and Arnold, J. G. (2013). *Arcswat Interface for SWAT2012: User's Guide* (1–464). https://vdocuments.site/reader/full/arcswat-documentation-2012

World Bank. (2018). *World Development Indicators, customized data generated at http://databank.worldbank.org/data/reports.aspx?source=world-development-indicators.* http://databank.worldbank.org/data/reports.aspx?source=world-development-indicators.

Woźniak, A., & Soroka, M. (2015). Structure of weed communities occurring in crop rotation and monoculture of cereals. *International Journal of Plant Production*, *9*(3).

Wu, X., Hao, Z., Tang, Q., Singh, V. P., Zhang, X., & Hao, F. (2021). Projected increase in compound dry and hot events over global land areas. *International Journal of Climatology*, *41*(1), 393–403.

Wu, Y., Li, C., Zhang, C., Shi, X., Bourque, C. P.-A., & Zhao, S. (2016). Evaluation of the applicability of the SWAT model in an arid piedmont plain oasis. *Water Science and Technology*, *73*(6), 1341–1348.

Xu, C. (2002). WASMOD–The water and snow balance modeling system. *Mathematical Models of Small Watershed Hydrology and Applications*, 555–590.

Xue, Q., Rudd, J. C., Liu, S., Jessup, K. E., Devkota, R. N., & Mahan, J. R. (2014). Yield determination and water-use efficiency of wheat under water-limited conditions in the US Southern High Plains. *Crop Science*, *54*(1), 34–47.

Yang, Z., Li, Y., Li, P., Zhang, F., & Thomas, B. W. (2016). Effect of difference between day and night temperature on tomato (Lycopersicon esculentum Mill.) root activity and low molecular weight organic acid secretion. *Soil Science and Plant Nutrition*, *62*(5–6), 423–431.

Yukimoto, S., Adachi, Y., Hosaka, M., Sakami, T., Yoshimura, H., Hirabara, M., Tanaka, T., Shindo, E., Tsujino, H., Deushi, M., Mizuta, R., Yabu, S., Obata, A., Nakano, H., Koshiro, T., Ose, T., & Kitoh, A. (2012). A New Global Climate Model of the Meteorological Research Institute: MRI-CGCM3 ^|^mdash;Model Description and Basic Performance^|^mdash; *Journal of the Meteorological Society of Japan*, *90A*, 23–64. https://doi.org/10.2151/jmsj.2012-A02

Zhang, L., Jin, X., He, C., Zhang, B., Zhang, X., Li, J., Zhao, C., Tian, J., & DeMarchi, C. (2016). Comparison of SWAT and DLBRM for hydrological modeling of a mountainous watershed in arid northwest China. *Journal of Hydrologic Engineering*, *21*(5), 4016007.

Zhang, W., Wang, H., Zhang, X., Peng, Y., Liu, Z., Wang, D., Zhang, D., Han, C., Zhao, Y., & Zhong, J. (2025). Investigating the impact of subgrid-scale aerosol-cloud interaction on mesoscale meteorology prediction. *EGUsphere*, *2025*, 1–34.

Zhang, X., Aguilar, E., Sensoy, S., Melkonyan, H., Tagiyeva, U., Ahmed, N., Kutaladze, N., Rahimzadeh, F., Taghipour, A., & Hantosh, T. H. (2005). Trends in Middle East climate extreme indices from 1950 to 2003. *Journal of Geophysical Research: Atmospheres*, *110*(D22).

Zhang, X., & Yang, F. (2004). RClimDex (1.0) user manual. *Climate Research Branch Environment Canada*, *22*, 13–14.

Zhang, Y., Zhang, L., Hou, J., Gu, J., & Huang, C. (2017). Development of an evapotranspiration data assimilation technique for streamflow estimates: a case study in a semi-arid region. *Sustainability*, *9*(10), 1658.

Zhao, C., Liu, B., Piao, S., Wang, X., Lobell, D. B., Huang, Y., Huang, M., Yao, Y., Bassu, S., & Ciais, P. (2017). Temperature increase reduces global yields of major crops in four independent estimates. *Proceedings of the National Academy of Sciences*, *114*(35), 9326–9331.

Appendices

Appendix A

1. Survey background

The survey (questionnaire) was meant to be done in May or June 2020 during field work, but due to COVID-19 and travel restrictions, field work was cancelled. To avoid delay a solution was to collaborate with someone who has good knowledge of this area and the local people. My supervisors nominated Khalid Al-Masaeed. Khalid is originally from the Jordanian north Badia, and he is employed as an engineer in the north Badia research centre (Safawi) responsible for providing facilities and accompanying visiting researchers during their field work in the area. Khalid also has experience of such projects and of collecting similar data. Currently, Khalid is a PhD student at the University of Jordan. Before conducting the survey, risk assessment and research ethics forms were completed and approved by the School of Geography.

The questionnaire was designed to be semi-structured including open-ended questions, so that both quantitative and qualitative information could be gathered, also to explore participant thoughts, feelings and beliefs about the investigated topic. The questionnaire contained six main sets of questions. Each set was dedicated to a specific field: General information about the participant farmers, crop production, soil and water resources, livestock and rangelands, and climate change**.** At the top of the questionnaire sheet, information was provided about the aims of this survey. To enhance farmers reponses rate, it was mentionned that questionnaire was anonymous and the research project is sponsored by a University for research purposes only. Usually, declarations like promise of anonymity and studies sponsored by universities, yielded higher accurate responses rates (Tsikerdekis, 2013). Questionning was done through personal interviews. There were no specifications when selecting the participants, the only condition was to be a farmer who is currently using a land in Q'a Shubayqa to produce crops. The only obstacle was how to reach farmers due to the lack of any formal records indicating their names, contact numbers or addresses. The idea was for Khaled to contact farmers of the area who already had a personal relationship with him. Then, these farmers should get him in touch with their neighbouring farmers in the area. According this method, 25 participant farmers were listed and they accepted to be interviewed.

2. Survey components

- General information: this section contained standard questions such as the farmer's name, age, type of farming system (only crop production or mixed with livestock), land tenure situation (owner or tenant), any second job besides farming, place of residence and frequency of visits to the cultivated land during the season. The latter three questions could provide a clear idea about the importance of this land and the cultivated crops to the owner from an economic and cultural perspective. Farmers were asked to locate their land on a map of the Q'a and to give the land area in hectares.
- Farming background and agricultural practices: in this section, questions were dedicated to collect more details about the farming system in Q'a Shubayqa and the reason behind adopting such agricultural practices. Besides that, the questions set were designed based on the required input data for the agricultural system model DSSAT. The collected information would be used later as input data to run DSSAT. This section included questions about the type of farming system (rainfed or irrigated), tillage timing and tools used for preparing the seedbed. In addition, questions were about practices such as sowing rates and timing, the harvesting period, and any adopted crop rotation.
- Crop production: Questions in this section were designed to fit with data required for DSSAT model calibration process. The questions were about the type of cultivated crops and varieties names, reasons for cultivating such crops, harvested grain yield and plant biomass, and any types and amounts of fertilizers, pesticides, and herbicides applied during the season.
- Soil and water resources: In this section, questions were dedicated to investigating the farmers point of view regarding the natural resources' situation in Q'a Shubayqa. We asked farmers what they thought about soil quality, also if they or someone else, had conducted any soil analysis for research purposes. Another question was about any practices applied by farmers to improve soil quality. Regarding water, the questions were mainly about the main water sources for the cultivated land, and if there was availability shortage of these resources and the reason behind that.
- Livestock and rangelands: The questions set in this part of the questionnaire were dedicated to herd-owner farmers. It included questions such as livestock type, number of head, grazing period and if they noticed changes in vegetation cover in the surrounding rangelands. Farmers were asked about their own perspective regarding the impact of livestock on crop productivity in their lands.

- Climate change impact on the farming system: in this final section of the questionnaire, we tried to ask farmers questions about weather changes and at what point these changes have affected the farming practices and crop productivity of the agricultural system. The questions were designed to make farmers report the changes they have experienced and noticed during the last few decades due to climate alterations. Farmers answers would allow understanding of the impact of climate change on the agricultural system and its components and to build an overview idea about that before conducting long-term climate variables analysis. The first questions were about the source of weather information they rely on and the traditional practices they use to predict weather conditions. The rest of the questions were about any long-term alteration in climate variables they had noticed and the type of these alterations. We asked farmers to evaluate these weather changes from their own perspective (extreme changes, moderate changes or few changes) and to specify what were the most significant changes in terms of climate variability and its severity level. Regarding the impact of climate change on agricultural patterns, we asked farmers to rate the vulnerability of their practices to these weather alterations and extreme climate events. The last question was about how farmers have managed to adapt with the climate changes and extreme events and what type of practices they have adopted or adjusted to cope with these changes.

3. Survey analyses

Descriptive statistics were applied using Excel to analyse farmers responses, and to provide an idea about the distribution of collected data. This should outline the nature of the studied farming system, the main factors that could affect it and the main components of the existing system. The descriptive statistics would also show the difference between farmers in terms of management, perspectives and patterns. Based on the latter, a classification process was applied to the farmers land using mapping tools in ArcMap (ArcGis) to represent spatial distribution of grain yield and local classification of Q'a Shubayqa regions according to farmers descriptions. In this process, the Ordinary Kriging spatial interpolation method within ArcMap was performed to create geostatistical maps from the output data of the survey. Kriging is a type of spatial interpolation that estimates values at unknown points based on values at known points.

4. Questionnaire format

Survey questions list

Thank you for agreeing to take part in this survey, which forms part of a research project from the University of Nottingham, UK in collaboration with the CBRL. The project looks to model agricultural systems in the Badia of Jordan to consider how the region might change in the future and how it might have changed in the past. The outputs from this research will allow us to suggest adaptation strategies which may help farmers cope with these changes and to enhance their farm productivity.

The answers to these questions will be used in the PhD thesis of Ali Ben Mustapha, which will be publicly available once complete, and may be used in academic papers written by the project team, which includes myself, Khalid Al-Masaeed. If you would like to see the outcomes of this research please provide your details at the end of the survey, and we will provide these to you when they are complete (an initial report should be available within one year).

All data collected will be stored in accordance with the requirements of the GDPR Act 2018. We will keep the data for 7 years after the submission of the PhD thesis. Then, all hard copies of data collection tools and data which enable the identification of individual participants will be destroyed.

If there are any questions you do not want to answer that if ok, and you can stop, and/or withdraw your questions from the survey at any time. All response on this questionnaire will be anonymised (unless subject to specific agreement) and not shared with any other people.

For more details, please do not hesitate to get in touch with Ali Ben Mustapha by email (ali.benmustapha@nottingham.ac.uk) or by telephone (00447404945634). Or supervisors Prof. Matthew Jones (matthew.jones@nottingham.ac.uk) and Prof. Sarah Metcalfe (sarah.metcalfe@nottingham.ac.uk).

I have read and understood the information above and give permission for the data I provide in this questionnaire to be used for the purposes described.

Signature: …….

Personal information

1. What's your name please?

……

2. How old are you?

……

3. Where do you live? How often do you visit your field per season?

……

Farming Background

1. What type of farming you do?

……

2. Do you have any other occupation besides farming?

……

3. What is the situation of land tenure (owner/tenant/ect)?

……

Section A: Crop production

1. How do you prepare the soil for cultivation and what tools used for that?

   ……

   ……

2. What are the main crops cultivated on your land?

   ……

   ……

3. What are the optimal dates for sowing and harvesting?

Crop type	Sowing date	Harvesting date

4. What are the varieties names of the cultivated crops?

Crop type	Variety

5. What three criteria are important to you when choosing the type of cultivated crop?

RANK from 1= most important to 3=least important]

1-

2-

3-

1= High yielding; 2=Fast growth; 3= Animal produce more milk; 4=Disease/pest tolerant; 5= Easy to harvest and feed to animal; 6=Availability/cost of seed/planting material; 7= climate tolerant; 8=Other (specify)

6. Do you use your own conserved seeds? If no, where do you get your seeds from?

……
……
……

7. Do you adopt any specific crop rotation system in your farm?

☐ Yes

☐ No

8. If yes, please specify?

Crop/Fallow	Soil occupation period

9. Do you apply any fertilizers/pesticides/herbicides?

☐ Fertilizers

☐ Pesticides

☐ Herbicides

……
……

If you apply fertilizers, could you please state its type and quantity per season?

……
……

10. What are the main criteria that could push you to decide that harvesting the yield is not profitable and converting it to grazing field for your livestock is more gainful?

……
……

Section B: Soil

1. Have you or anyone else made any soil analysis before for your farm?

☐ Yes

☐ No

2. If yes, could you please describe the results of the analysis, and how long ago the analysis was carried out?

……
……

3. How do you manage the manure produced by your livestock?

- ☐ Apply directly on soil
- ☐ Collect under shade
- ☐ Collect uncovered in the open
- ☐ Compost it
- ☐ Sell to others

Section C: Water resource

1. What is the main source of water for this farm?

- ☐ Rainfall
- ☐ Wells
- ☐ Water harvesting catchments
- ☐ Floods water
- ☐ Other …….

2. Which techniques do you use for water and moisture conservation in your land?

- ☐ Irrigation scheduling
- ☐ Planting drought-tolerant crops
- ☐ Rotational grazing (Reduce water runoff)
- ☐ Using compost and manure

☐ Other …….

3. Have you noticed any change of rainfall and flood frequency in these last years?

☐ Yes

☐ No

Do you think it may be other factors that have affected water availability? If yes, please identify them?
……
……

Section D: Livestock and Rangelands

1. What type and number of livestock do you own?

Livestock	Selected type	Number
Sheep		
Goat		
Camel		

2. Would you say that the impact of livestock on your crop production system is?

☐ Positive

☐ Negative

3. Specify please, how it's positive or negative impact.
……
……
…….

4. Which months of the year you let your herd graze the field?

Jul	Aug	Sep	Oct	Nov	Dec	Jan	Feb	Mar	Apr	May	Jun	

5. Have you seen changes in vegetation cover and vegetation type in range land during the last ten years?

☐ Yes

☐ No

If yes, please describe these changes?
……
……..

Section E: Weather change

1. Where do you usually get information about the weather from?

……
……

2. Do you use any traditional methods (indicators) to estimate coming weather condition?

☐ Yes

☐ No

3. If yes, please describe the method or the indicator?

……
……

4. Have you observed any long-term changes in seasonal weather variable (particularly temperature, rainfall, floods and frost)?

☐ Yes

☐ No

5. If yes, indicate what have been the changes?

☐ Increased temperature

☐ Decreased temperature

☐ Increased in number of rainfall events

☐ Increased in rainfall intensity

☐ Decreased in number of rainfall events

☐ Decreased in rainfall intensity

☐ Increased in frost period

☐ Decreased in frost period

☐ Fast decreasing of soil moisture (high evaporation)

☐ delay in seasonal Flood timing

6. How do you evaluate these changes?

☐ Extreme changes

☐ Many changes

☐ Some changes

☐ Few changes

☐ I don't know

7. What have you observed to be the main effects/impacts (negative) of these long-term changes in terms of climate variables over the last 10 years? Please specify the period or the year of each effect/impact?

   Rank: on a scale of 1-4, where 1 = Extremely severe (disastrous), 2 = Severe, 3 = Significant, 4 = Irrelevant.

Effect (Negative impact)	**Selected factors**	**RANK** (ORDER OF SEVERITY)	**Period / Year**
Changed timing of rains			
Abrupt change in season/ changes in growing season			
Reduced cropping (growing) season			
Increased frequency of drought and crop failure			
Increased frequency of floods and crop destructions			
Increased frequency of frost periods			
Increased frequency of heat waves			
Pests invasion			
Prevalence of disease			
Erosion			
Death of livestock			
Disappearance of vegetation cover for grazing			

8. How do you consider the vulnerability of your farm activities (Ploughing, sowing, harvesting..) toward the following factors?

RANK: on scale of 1 to 3 where 1 = Extremely vulnerable, 2 = Vulnerable, 3 = Not vulnerable

Incidence	**Vulnerability**
Increased temperature	
Decreased rainfall	
Floods	
Droughts	
Changed timing of rains	
Increased frost period	

9. After tough unproductive seasons, is farming remained your primary activity?

……
……

10. Have you made any changes/adjustments in your farming practices in response to climate change and variability over the last 10 years? If so, please indicate below what adjustments you have made.

- [ ] Changing sowing and planting dates
- [ ] Using different crop varieties and crop types
- [ ] Implement soil conservation techniques
- [ ] Mixed cropping
- [ ] Searching for new water resources
- [ ] Using herbicides, fungicides and fertilisers
- [ ] Sold livestock
- [ ] Employ new crop rotation
- [ ] Fallow land
- [ ] Reducing tillage
- [ ] Other……..

Appendix B

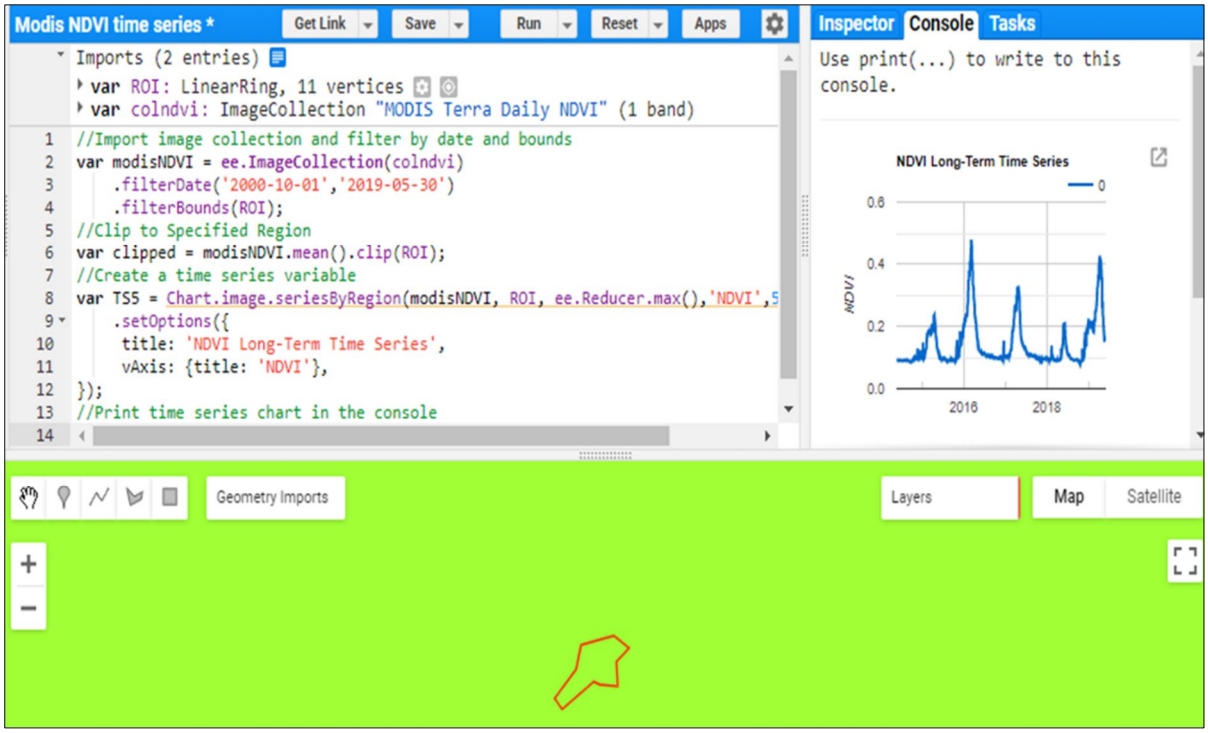

Figure 1: GEE code editor script for NDVI time series using MODIS daily dataset

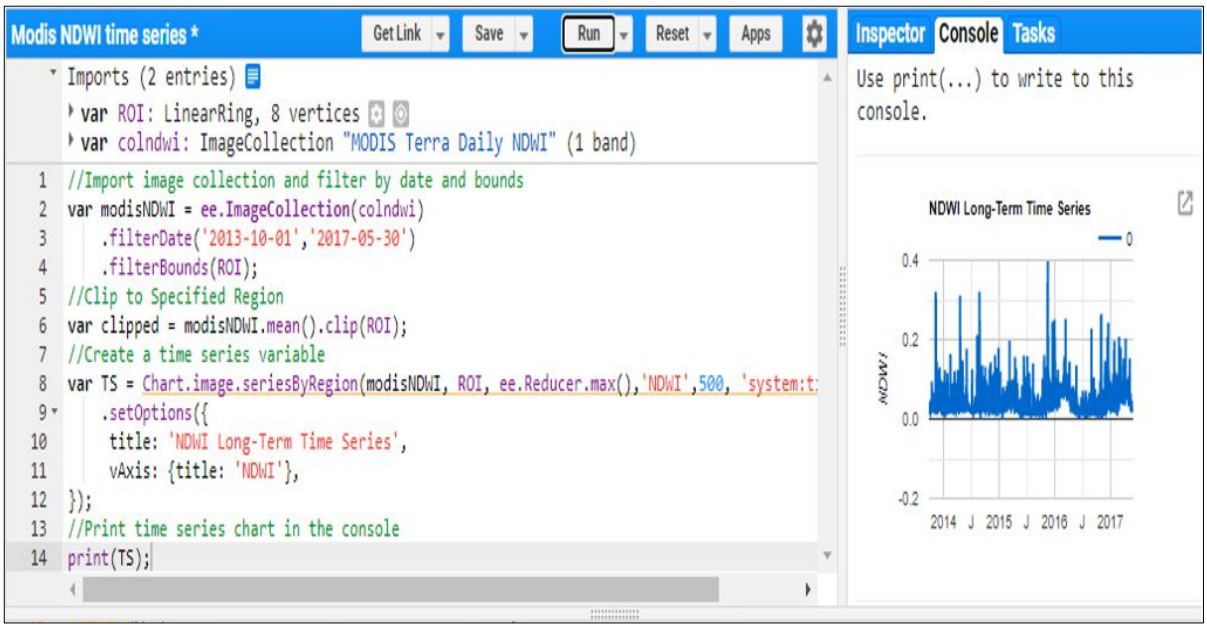

Figure 2: GEE code editor script for NDWI time series using MODIS daily dataset

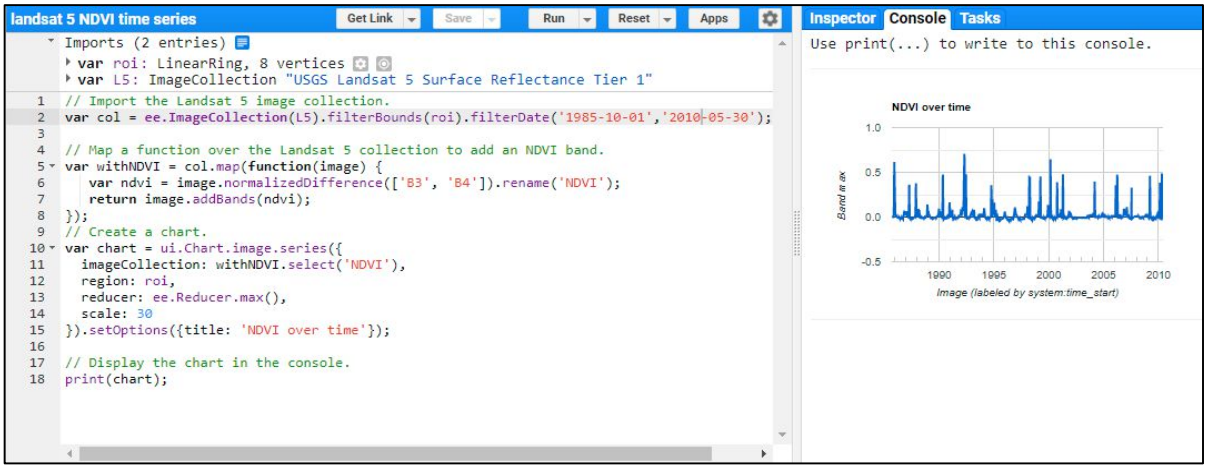

Figure 3: GEE code editor script for NDVI time series using Landsat 5 dataset

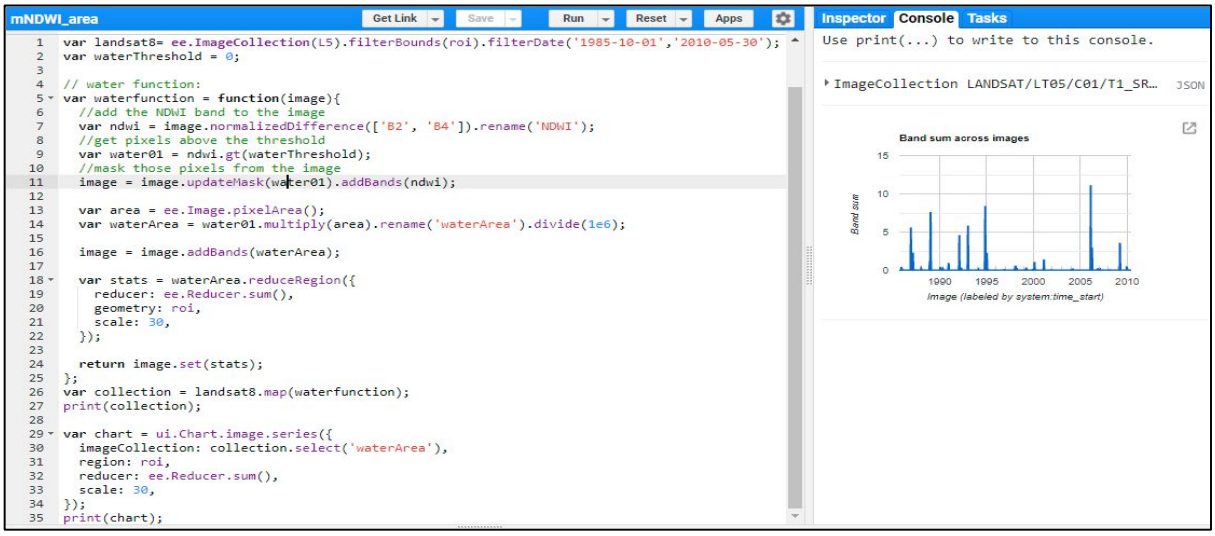

Figure 4: GEE code editor script for NDWI time series using Landsat 5 dataset

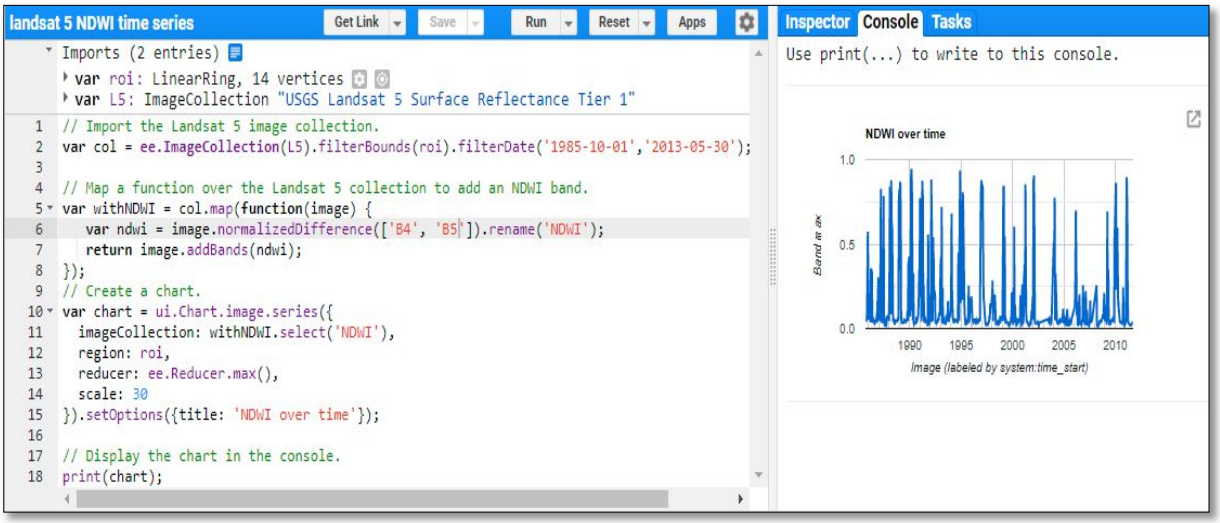

Figure 5: GEE code editor script for flood water diffusion area time series using Landsat 5 dataset

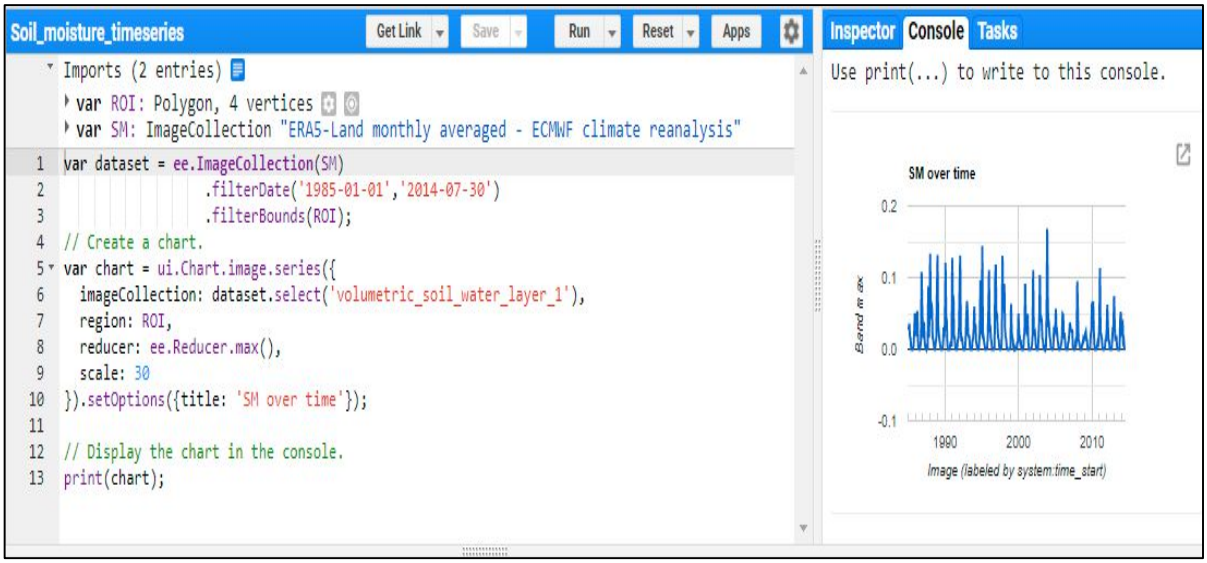

Figure 6: GEE code editor script for volumetric soil water time series using ERA5-Land dataset

Appendix C

Table: Parameters of the sensitivity analysis related to Evapotranspiration.

No.	Parameter	Unit	Description	Minimum	Maximum
1	**r__CN2.mgt**	DIM	Initial SCS runoff curve number for moisture condition II	-20%	20%
2	**v__ALPHA_BF.gw**	day	Baseflow alpha factor	0	1
3	**a__GW_DELAY.gw**	day	Groundwater delay time	-10	10
4	**a__GWQMN.gw**	mm	Threshold depth of water in the shallow aquifer required for return flow to occur	-1000	1000
5	**v__SFTMP.bsn**	ºC	Snowfall temperature	-5	5
6	**v__SMTMP.bsn**	ºC	Snow melt base temperature	-3	3
7	**v__SMFMX.bsn**	mm H2O/ºC-day	Melt factor on snow on June	1.4	6.9
8	**v__SMFMN.bsn**	mm H2O/ºC-day	Melt factor on snow on December	1.4	6.9
9	**v__TIMP.bsn**	DIM	Snowpack temperature lag factor	0.01	1
10	**r__SOL_AWC().sol**	mm mm-1	Available water capacity of the soil layer	-25%	25%
11	**v__ESCO.bsn**	DIM	Soil evaporation compensation factor	0.01	1
12	**v__EPCO.bsn**	DIM	Plant uptake compensation factor	0.01	1
13	**v__ESCO.hru**	DIM	Soil evaporation compensation factor	0.01	1
14	**v__EPCO.hru**	DIM	Plant uptake compensation factor	0.01	1
15	**v__SURLAG.bsn**	day	Surface runoff lag coefficient	0	20
16	**v__OV_N.hru**	DIM	Manning's "n" value for overland flow	0.008	0.48
17	**v__GW_REVAP.gw**	DIM	Groundwater "revap" coefficient	0.02	0.2

18	**v__REVAPMN.gw**	mm	Threshold depth of water in the shallow aquifer for “revap”	0	1000
19	**v__RCHRG_DP.gw**	DM	Deep aquifer percolation fraction	0	1
20	**v__CNCOEF.bsn**	DM	Plant ET curve number coefficient	0.5	2
21	**v__SOL_CRK.sol**	DM	Maximum crack volume of the soil profile expressed as a fraction of the total soil volume	0	1
22	**v__SOL_BD().so**	Mg/m3	Moisture Bulk density	1.1	1.9
23	**v__FFCB.bsn**	DM	Initial soil water storage	0	1
24	**v__CANMX.hru**	MM	Maximum canopy storage	0	100
25	**r__SOL_K().sol**	mm h-1	Saturated hydraulic conductivity	-25%	25%
26	**r__SOL_ZMX.sol**	mm	Maximum rooting depth of soil profile	-50%	50%

DM: *dimensionless. v: replace, r: relative and a: add ➔Methods of variation*